Glia-to-interneuron conversion in the postnatal mouse cerebral cortex

Beltran Arranz, Ana

Awarding institution:
King's College London

Glia-to-interneuron conversion in the postnatal mouse cerebral cortex

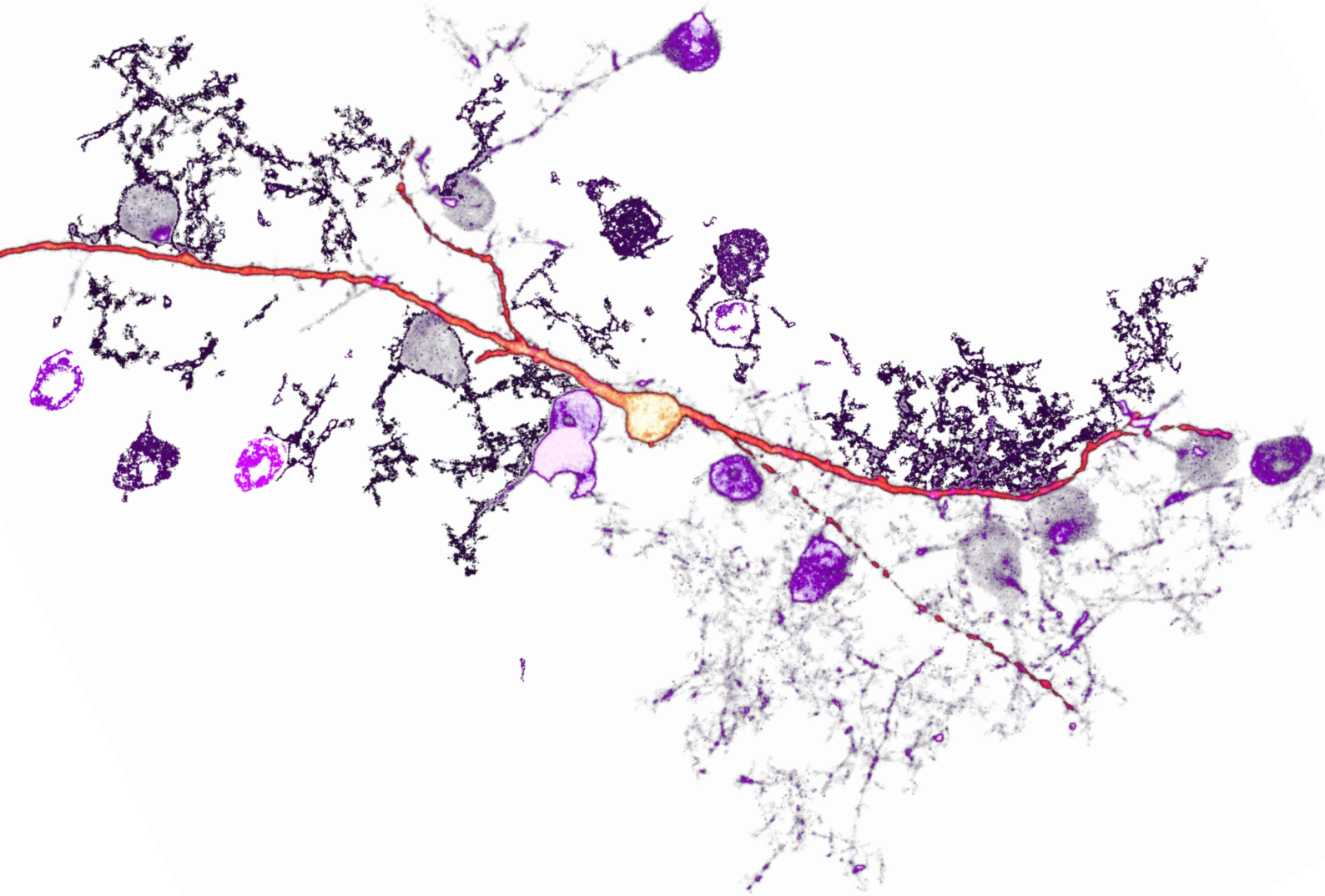

Ana Beltrán Arranz

A thesis for the degree of Doctor of Philosophy
London, May 2023

Centre for Developmental Neurobiology

KING'S College LONDON

Abstract

Interneurons modulate and synchronise local network activity, which is essential for establishing balance of excitatory-inhibitory activity in the brain. Defects among distinct interneuron populations are associated with numerous neuropsychiatric disorders. Engineering induced neurons (iNs) from other resident brain cells emerges as an innovative strategy to replace lost or dysfunctional neurons and restore function in brain regions devoid of intrinsic regenerative capacity. In this study, I aimed at generating glia-derived interneuron-like cells in the postnatal mouse cerebral cortex via transcription factor-mediated lineage reprogramming.

Here, I showed that Ascl1SA6, a phospho-site mutant form of Ascl1 in which six serine-proline sites subject to phosphorylation were mutated, exhibited enhanced neurogenic activity during *in vivo* glia-to-neuron conversion. In addition, co-expression of Ascl1SA6 together with other reprogramming factors, such as Bcl2 or Dlx2, boosted the reprogramming efficiency and generated a remarkable proportion of GABAergic-like iNs. A fraction of Ascl1SA6 and Bcl2-derived iNs acquired hallmarks of parvalbumin (PV) interneurons, such as the expression of PV interneuron-specific markers as well as acquisition of fast-spiking firing properties. Using robust fate-mapping strategies, I unambiguously demonstrated that iNs originated from glial cells, with astrocytes being the main starting cell population from which iNs were generated. Finally, I found that PV-like iNs were missing some morphological and molecular features of mature endogenous PV interneurons. Aiming at promoting iNs maturation, I developed a strategy to selectively activate iNs upon inducible chemogenetic stimulation, opening new avenues to study activity-dependent modulation of iNs during lineage reprogramming.

Taken together, this study sheds light on the molecular cues and regulatory mechanisms necessary to induce glial fate switch towards an interneuron identity in the postnatal mouse cerebral cortex. Hence, this work provides solid basis for future work aiming at replacing dysfunctional fast-spiking PV interneurons as an innovative therapeutic approach to treat neuropsychiatric disorders.

Acknowledgements

This journey that I have travelled during the last four years has been full of challenges, enriching experiences, learning, personal growth and self-improvement. This chapter is now coming to an end and when I look back I can only thank all the people who have accompanied me in one way or another during this exciting stage of my life.

I am extremely grateful to my PhD supervisor Prof. Benedikt Berninger for giving me the opportunity to develop this beautiful project in his laboratory. I can't thank you enough for sharing your passion for science with me, for the advice and discussions throughout my project, and your constant trust and support. It has been truly inspiring and enjoyable to work next to you and learn from your scientific and philosophic way of thinking. I am also deeply thankful for all the scientific exchange opportunities that you have provided me with, which have allowed me to meet great scientists from all over the world.

I would also like to thank my second supervisor Prof. Juan Burrone for his advice, especially on the early stages of my PhD thesis, as well as my Thesis Committee members Prof. Beatriz Rico and Prof. Vincenzo de Paola for their support and guidance throughout the entire development of my PhD project.

The members of the Berninger lab have made my experience so much more enjoyable and fun over the past years and I wanted to thank you all for creating a fantastic environment to grow as a scientist. Thanks Laia for being my PhD soulmate and sharing this journey with me from beginning to end. I would not have survived without our long conversations about science, future and, especially, gossips. Emilio, thanks for being my sports mate, for all the stupid jokes and laughs and for always willing to join any plan. I am very thankful to Alexis, for being supportive and always offering help with a smile, I also have enjoyed a lot our little trips. To Jero and Andrea, thanks for making the lab a super fun place to work. I laughed a lot with both of you over these years and I wanted to thank you for always being happy to help. A special thanks to Sophie and Nico, for giving me very useful advice and guidance over my PhD journey and for sharing part of this exciting project with me. Thank you Errin for being my office neighbour and sharing with me so many fun moments. Thank you Youran for all the support and hugs you gave me when I needed them. Sydney, thanks for all the science discussions and for teaching me the real Londoner English. Finally, I am extremely grateful to Nancy for the amazing technical and also personal support.

También quiero agradecer el apoyo de todos mis amigos más cercanos en España. Gracias a los de siempre porque, a pesar del tiempo y la distancia, siempre me hacéis sentir en casa cuando vuelvo a Madrid. A vosotros, Miki, Pablo, Mireya e Isa, gracias por seguir a mi lado después de todos estos años, por darme apoyo, por darme confianza en mí misma para conseguir lo que me propongo y por todos los momentos vividos juntos. Gracias también a mis bioquímicas, las pichonas, por haber empezado juntas la vida científica hace muchos años. Mil gracias por compartir siempre nuestras experiencias en la ciencia, por los consejos y por el apoyo. A pesar de haber estado cada una en un sitio distinto del mundo, siempre me he sentido muy cerca de vosotras.

Por último, quiero terminar dando las gracias a lo más importante que tengo, mi familia. Hoy no estaría escribiendo esto si no fuera por vosotros. Mamá y papá, gracias por estar a mi lado contra viento y marea, gracias por caminar conmigo de la mano cuando el viento soplaba a favor pero, sobre todo, por darme vuestra fuerza cuando el viento soplaba en contra. Gracias por apoyarme en todas las etapas del camino, que no ha sido siempre sencillo. Gracias por enseñarme a no rendirme, a seguir luchando y por haberme apoyado siempre para conseguir todo esto. Antonio y Teresa, gracias por haber sido mi pequeña familia en Londres y por haberme acogido y arropado siempre que lo he necesitado. Antonio, gracias por ser un ejemplo a seguir para mí desde pequeños, siempre te he seguido a todas partes y he admirado tu curiosidad insaciable pero, sobre todo, lo buena persona y hermano que eres. Muchas gracias a mi tía Blanca, por haberme apoyado siempre en mis decisiones y darme fuerzas para seguir siempre avanzando en mi camino. Tatán, gracias por enseñarme los valores de la perseverancia, el esfuerzo y la dedicación, que me han acompañado durante toda mi vida y doctorado. Gracias a mis abuelas que, aunque se hayan quedado en distintas partes de mi camino, siempre me han dado mucho amor y sé que hoy estarían orgullosas de mí. Y a ti, Pedro, gracias por ser mi apoyo diario, por calmar el estrés de mis peores días y celebrar conmigo mis pequeños y grandes logros. Gracias por elegir acompañarme en este camino.

Esta tesis también es vuestra.

Table of contents

Abstract……..……2

Acknowledgements……..……..3

Table of contents…….……5

List of figures…….....9

List of abbreviations……..12

Introduction…….....16

1. Organisation of the mammalian cerebral cortex…….....18
   - 1.1. Developmental origin of cellular diversity in the cerebral cortex……19
     - 1.1.1. Neurogenesis in the cerebral cortex……19
     - 1.1.2. Gliogenesis in the cerebral cortex……...22
   - 1.2. Interneuron diversity in the cerebral cortex……24
   - 1.3. Molecular mechanisms underlying interneuron diversity in the cerebral cortex……27
     - 1.3.1. Spatial patterning and neurogenesis within the ventral telencephalon……28
     - 1.3.2. Post-translational regulation of the proneural transcription factor Ascl1……30
     - 1.3.3. Regional specification of MGE-derived interneurons……32
   - 1.4. Activity-dependent regulation of wiring and maturation of interneurons into cortical networks……33
   - 1.5. Cortical interneurons in health and disease……35

2. Regeneration of the Central Nervous System (CNS)……..……..38
   - 2.1. Limited intrinsic regeneration capacity of the mammalian CNS……..38
   - 2.2. Cell replacement strategies in the CNS……..40

2.3. Direct lineage reprogramming for brain repair……41

2.3.1. Glial cells as starting cell population for direct neuronal reprogramming……42

2.3.2. *In vitro* direct neuronal reprogramming……..……44

2.3.3. *In vivo* direct neuronal reprogramming……..……47

2.3.4. Direct neuronal reprogramming in the postnatal mouse cerebral cortex……...50

Objectives……54

Materials & Methods……55

Results……72

Chapter I. *In vivo* reprogramming of cortical postnatal glia into parvalbumin-like iNs by forced expression of Ascl1SA6 and Bcl2……73

1.1 Proliferation of glial cells and lack of neurogenesis within the postnatal mouse cerebral cortex……74

1.2 Retroviral targeting of proliferating glia in the postnatal mouse cerebral cortex……..76

1.3 *In vivo* reprogramming of cortical postnatal glia by forced expression of Ascl1: effect of different phosphorylation states……78

1.4 *In vivo* reprogramming of cortical postnatal glia by forced co-expression of Ascl1 and Bcl2……82

1.5 Overexpression of Ascl1SA6 and Bcl2 instructs cortical postnatal glia to reprogram into PV interneuron-like iNs……90

1.6 Ascl1SA6 and Bcl2-derived iNs acquire expression of hallmark genes from fast-spiking parvalbumin interneurons……95

1.7 In vivo reprogramming of cortical postnatal glia using a tri-cistronic retroviral vector……98

1.8 Fate-mapping experiments unveil a predominant astrocytic origin of glia-derived iNs by forced co-expression of Ascl1SA6 and Bcl2…..98
1.9 Tri-cistronic vector encoding for Ascl1-Bcl2 generates GABAergic iNs that lack PV specification properties……110

Chapter II. *In vivo* glia-to-interneuron conversion in the postnatal mouse cortex by forced expression of Ascl1SA6 and Dlx2……..113

2.1 Ascl1SA6 and Bcl2-derived iNs exhibit ectopic mRNA expression of Ascl1 and lack endogenous Dlx2 mRNA expression……...114
2.2 Ascl1SA6 and Dlx2 synergise to convert cortical postnatal glia into NeuN-expressing iNs……114
2.3 Forced co-expression of Ascl1SA6 and Dlx2 generates GABAergic iNs that do not acquire any subtype-specific identity……119
2.4 Tri-cistronic vector co-expressing Ascl1SA6 and Dlx2 yields a high number of NeuN-expressing iNs……..122
2.5 Fate-mapping experiments reveal astroglial origin of Ascl1-Dlx2-derived iNs……..124
2.6 A low number of Ascl1SA6-Dlx2-derived iNs acquire GABAergic identity……...127

Chapter III. Modulation of induced neurons activity through chemogenetic-mediated stimulation…….....130

3.1 Establishing a model for activation of iNs through chemogenetic-mediated stimulation……...131
3.2 Ascl1SA6 and Bcl2-derived iNs can be specifically activated through DREADD-mediated stimulation……132

3.3 Chemogenetic activation of Ascl1SA6 and Bcl2-derived iNs does not influence their expression levels of PV……..……135

Discussion……140

1. Demonstrating authenticity of glia-to-neuron conversion *in vivo*……143
2. Impact of different cell types as source for neuronal reprogramming……..146
   2.1 Astroglia as a starting cell population for neuronal reprogramming in the postnatal mouse cerebral cortex……..……146
   2.2 NG2 glia as a starting cell population for neuronal reprogramming in the postnatal mouse cerebral cortex……148
3. Role of phosphorylation in Ascl1-mediated neuronal reprogramming of postnatal glia in the mouse cortex……..…150
4. Role of Bcl2 in glia-to-neuron conversion in the mouse postnatal cortex…….153
5. Fate specification of glia-derived iNs into neuronal subtypes……..155
6. Differences in reprogramming outcome using single retroviral vectors or a tri-cistronic retroviral vector……...158
7. Impact of environment and extrinsic inputs on neuronal reprogramming…….160
   7.1 Impact of distinct brain areas on neuronal reprogramming……160
   7.2 Impact of injury-mediated signalling on neuronal reprogramming……161
   7.3 Impact of activity during neuronal reprogramming……..162
8. Limitations and challenges on glia-to-neuron conversion in the postnatal mouse cortex……...165
9. Future directions and clinical translation of neuronal reprogramming……..167

Conclusions…….....170

Disclosure statement……..…171

References……..…172

List of figures and tables

Introduction

Table 1.1. GABAergic neuron diversity in the cortex.

Table 1.2. Summary of published studies recapitulating direct lineage reprogramming of resident brain cells into iNs *in vitro*.

Table 1.3. Summary of published studies recapitulating direct lineage reprogramming of resident brain cells into iNs *in vivo*.

Figure 1.1. Timeline of the main events underlying neurogenesis and gliogenesis in the cerebral mouse cortex.

Figure 1.2. Structure and phosphorylation of the proneural transcription factor Ascl1.

Figure 1.3. Electrophysiological properties of co-transduced cells with Ascl1 or Ascl1SA6 and Bcl2.

Figure 1.4. Glia-to-neuron conversion in the postnatal mouse cerebral cortex.

Materials & Methods

Table 2.1. Details of the primers, the expected size of PCR products and the PCR programmes used for genotyping transgenic mouse lines.

Table 2.2. Original plasmids and primers used to amplify genes of interest for cloning of tri-cistronic vectors.

Table 2.3. List of retroviral constructs used for direct lineage reprogramming.

Figure 2.1. Maps of retroviral constructs used for direct lineage reprogramming.

Results

Figure 3.1. Proliferation of glial cells and lack of neurogenesis in the postnatal mouse cerebral cortex.

Figure 3.2. MMLV retroviruses specifically transduce glial cells in the postnatal mouse cerebral cortex.

Figure 3.3. Forced expression of Ascl1 fails to drive neuronal reprogramming whereas Ascl1SA6 shows moderate glia-to-neuron conversion in the postnatal mouse cerebral cortex.

Figure 3.4. Forced co-expression of Ascl1SA6 and Bcl2 drives glia-to-neuron conversion with high efficiency in the postnatal mouse cerebral cortex.

Figure 3.5. Co-transduced cells with Ascl1 or Ascl1SA6 and Bcl2 do not retain astroglial identity.

Figure 3.6. Most of co-transduced cells with Ascl1 and Bcl2 show oligodendroglial identity.

Figure 3.7. Forced co-expression of Ascl1SA6 and Bcl2 converts cortical postnatal glia into GABA and PV-expressing iNs.

Figure 3.8. Ascl1SA6 and Bcl2-iNs display differences in PV expression levels, soma size and layer distribution in the mouse cortex compared to endogenous PV neurons.

Figure 3.9. Ascl1SA6 and Bcl2-iNs acquire expression of of Kv3.1 and Syt2 at mRNA level.

Figure 3.10. Tri-cistronic vector encoding for Ascl1SA6-Bcl2 yields high glia-to-neuron conversion rate in the postnatal mouse cerebral cortex.

Figure 3.11. EdU incorporation in Ascl1SA6-Bcl2-derived iNs reveals their origin from proliferating glial cells.

Figure 3.12. Fate-mapping experiments reveal that most Ascl1SA6-Bcl2-derived iNs have an astroglial origin.

Figure 3.13. Fate-mapping experiments reveal that few Ascl1SA6-Bcl2-derived iNs originate from OPCs.

Figure 3.14. Fate-mapping experiments reveal the glial origin of cells targeted by control retroviruses in the mouse cerebral cortex.

Figure 3.15. Tri-cistronic vector encoding for Ascl1SA6-Bcl2 generates iNs that expressed GABA but lack specific features of fast-spiking PV interneurons.

Figure 3.16. Ascl1SA6 and Bcl2-derived iNs exhibit ectopic overexpression of Ascl1 but lack Dlx2 expression at the mRNA level.

Figure 3.17. Forced expression of Dlx2 generates some Dcx-expressing iNs.

Figure 3.18. Forced co-expression of Ascl1SA6 and Dlx2 drives conversion of postnatal glial cells into NeuN-expressing iNs.

Figure 3.19. Forced co-expression of Ascl1SA6 and Dlx2 generates GABA-expressing iNs that do not differentiate into interneuron-specific subtypes.

Figure 3.20. Ascl1SA6 and Dlx2-derived iNs express Kv3.1 mRNA but do not display a high-frequency firing pattern.

Figure 3.21. Tri-cistronic vector encoding for Ascl1SA6-Bcl2 drives efficient glia-to-neuron conversion in the postnatal mouse cortex.

Figure 3.22. Fate-mapping experiments reveal glial origin of Ascl1SA6-Bcl2-derived iNs.

Figure 3.23. Transduced cells with Ascl1SA6-Dlx2 retroviral vector instructs conversion of glia into some GABAergic-like iNs that do not acquire PV identity.

Figure 3.24. Activation of iNs through chemogenetic-mediated stimulation.

Figure 3.25. PV expression levels of iNs do not change upon DREADD-mediated activation.

Discussion

Figure 4.1. Graphical summary of main findings

Figure 4.2. Influence of Ascl1 phosphorylation in glia-to-neuron conversion in the postnatal mouse cerebral cortex.

Figure 4.3. Role of Bcl2 in direct lineage reprogramming.

Figure 4.4. Factors influencing direct lineage reprogramming.

List of Abbreviations

6-OHDA:	6-hydroxydopamine
AAV:	Adeno-Associated Virus
AKT:	Protein Kinase B
Aldh1l1:	Aldehyde Dehydrogenase 1 Family Member L1 Locus
Ascl1:	Achaete-Scute Complex-Like 1
ASD:	Autism Spectrum Disorder
ATACseq:	Transposase-Accessible Chromatin sequencing
ATP:	Adenosin Triphosphate
BBB:	Blood Brain Barrier
Bcl2:	B-Cell Leukemia/Lymphoma 2
BDNF:	Brain-Derived Neurotrophic Factor
bHLH:	Basic Helix Loop Helix
BMP:	Bone Morphogenetic Proteins
BrdU:	Bromodeoxyuridine
bRGC:	Basal Radial Glia Cell
CAG:	Chicken β-Actin Promoter
CB:	Calbindin
CCK:	Cholecystokinin
Cdk:	Cyclin-dependent Kinase
CGE:	Caudal Ganglionic Eminence
ChIP:	Chromatin Immunoprecipitation
CMV:	Cytomegalovirus
CNO:	Clozapine-N-Oxide
CNS:	Central Nervous System
CR:	Calretinin
DAT:	Dopamine Transporter
DCX:	Doublecortin

DLX1/2: Distal-Less Homeobox1/2 Genes

DEPC: Diethyl pyrocarbonate

DG: Dentate Gyrus

DMSO: Dimethyl Sulfoxide

DPI: Days Post-Injection

DREADDs: Designer Receptors Exclusively Activated by Designer Drugs

E: Embryonic day

EDTA: Ethylenediaminetetraacetic acid

EdU: 5-Ethynyl-2'-Deoxyuridine

ERα: Estrogen Receptor-alpha

ERK: Extracellular signal-regulated kinases

FBS: Fetal Bovine Serum

FGF: Fibroblast Growth Factor

GABA: γ-Amino Butyric Acid

GAD67: Glutamate decarboxylase 1

GFAP: Glial Fibrillary Acidic Protein

GFP: Green Fluorescence Protein

Gli: Glioma-Associated Oncogene Family Zinc Finger

hESCs: Human Embryonic Stem Cells

Htr3a: Serotonin Receptor 3A

IEG: Immediate Early Gene

iNs: Induced Neurons

iPSCs: Induced Pluripotent Stem Cells

IRES: Internal Ribosome Entry Sites

KA: Kainic acid

L: Layer

LGE: Lateral Ganglionic Eminence

Lhx6: LIM Homeodomain Factor

LTR: Long Terminal Repeat

MeCP2: Methyl-CpG-binding Protein 2

MEFs: Mouse Embryonic Fibroblasts

MGE: Medial Ganglionic Eminence

MMLV: Moloney Murine Leukemia Virus

MZ: Marginal Zone

Neurog2: Neurogenin-2

NG2: Nerve/Glial antigen 2

NMDA: N-methyl-D-aspartate

NPY: Neuropeptide Y

NSCs: Neural Stem Cells

Olig2: Oligodendrocyte Transcription Factor 2

OPCs: Oligodendrocyte Progenitor Cells

P: Postnatal day

PB: Phosphate Buffer

PBS: Phosphate Buffered Saline

PDGFRA: Platelet-Derived Growth Factor Receptor Alpha

PFA: Paraformaldehyde

PI3K: Phosphatidylinositol 3-Kinase

POA: Preoptic Area

POH: Preoptic Hypothalamic Region

Ppargc1a: Peroxisome proliferator-activated receptor gamma coactivator 1-alpha

Prx-2: Peroxiredoxin-2

PV: Parvalbumin

RFP: Red Fluorescence Protein

RGCs: Radial Glial Cells

RMS: Rostral Migratory Stream

ROI: Region Of Interest

ROS: Reactive Oxygen Species

RTK: Receptor Tyrosine Kinases

SCI:	Spinal Cord Injury
sEPSCs:	Spontaneous Excitatory Post-Synaptic Currents
SHH:	Sonic Hedgehog
Sp8:	Specificity Protein 8
SST:	Somatostatin
SVZ:	Subventricular Zone
SWI:	Stab-wound Injury
Syt2:	Synaptotagmin 2
TAPs:	Transit Amplifying Progenitors
TBS-5:	Tris-Buffered Saline 5
TdT:	Terminal Deoxynucleotidyl Transferase
TH:	Tyrosine Hydroxylase
TUNEL:	Terminal Deoxynucleotidyl Transferase dUTP Nick-End Labelling
Vgat:	Vesicular GABA Transporter
VIP:	Vasoactive Intestinal Peptide
VSV-G:	Vesicular Stomatitis Virus-Glycoprotein
VZ:	Ventricular Zone
WNT:	Wingless-Related Integration Site
WPRE:	Woodchuck Hepatitis Virus Posttranscriptional Regulatory Element

INTRODUCTION

Preface

Brain function is tightly regulated by the interplay between excitatory activity of principal neurons and inhibitory signalling from locally projecting interneurons. Interneurons shape local network activity to establish balance of excitatory-inhibitory activity in the brain (Tremblay et al., 2016). Interneuron dysfunction has been associated with numerous neurological disorders, such as epilepsy, schizophrenia or autism spectrum disorder (ASD). Chronic disorders or acute injury resulting in degeneration and loss of neurons are devastating because the adult mammalian central nervous system (CNS) lacks intrinsic capacity to regenerate lost or dysfunctional neurons.

In response to this therapeutic need, regenerative medicine has focused on developing cell-based replacement therapies to restore lost functions and correct neurological deficits. Classical cell replacement strategies, such as transplantation of stem cell-derived progenitors or neurons, still face major hurdles of cell availability, risk of tumorigenesis and immune rejection by the host tissue (Lindvall, 2012). An innovative approach towards achieving neuronal restoration is to induce fate conversion of resident brain cells into induced neurons (iNs) by direct lineage reprogramming (Barker et al., 2018; Heinrich et al., 2015). This innovative strategy consists of assigning neuronal identity to terminally differentiated brain resident cells by selective expression of key neurogenic reprogramming factors. Although significant progress in the field has shown efficient conversion of mouse and human cells into iNs *in vitro* (Berninger et al., 2007; Heinrich et al., 2010; Karow et al., 2012), demonstrating efficient subtype-specific lineage reprogramming *in vivo* remains a challenge within the murine CNS. Ongoing research is now focused on demonstrating the authenticity of *in vivo* lineage reprogramming aiming at the generation iNs that acquire the desired neuronal identity and functionally integrate within the endogenous neuronal networks.

The goal of this PhD thesis was to generate glia-derived induced interneurons in the postnatal mouse cortex via transcription factor-mediated lineage reprogramming. The motivation of this research was to expand our understanding on the molecular cues necessary to induce glial fate switch towards an interneuron identity in the cerebral cortex. Investigating glia-to-interneuron conversion in the postnatal cortex may open new avenues for neuronal restoration in the context of different neurodevelopmental disorders. To this end, it is necessary to step back and learn the molecular mechanisms underlying interneurons specification, migration and integration in the endogenous developing cortex.

"*Unfortunately, nature seems unaware of our intellectual need for convenience and unity, and very often takes delight in complication and diversity*" (Ramon y Cajal, 1906)

1. Organisation of the mammalian cerebral cortex

The cerebral cortex is comprised by billions of interconnected neurons responsible for supporting higher order cognitive functions in the brain, such as sensory information processing, coordination of motor activities, decision-making and consciousness (Harris & Mrsic-Flogel, 2013). During evolution, the cerebral cortex has progressively expanded to become the largest area of the brain due to an immense increase in the number of neurons and functional areas, which is directly correlated with an increase in neuronal diversity (Finlay & Darlington, 1995).

The enormous diversity of neuronal subtypes in the cerebral cortex was highlighted for the first time more than a century ago by Santiago Ramón y Cajal, when he described the existence of many morphologically diverse neurons in the cerebral cortex (Ramón y Cajal, 1909). However, after several decades of research dedicated to the description of the cellular diversity in the cerebral cortex, the number of distinct neuronal subclasses remains to be elucidated. A combination of histological, anatomical, and electrophysiological strategies has provided a classification of the major neuronal subpopulations based on their expression of specific biochemical markers, morphology and functional properties (Molyneaux et al., 2007). However, the emergence of single-cell sequencing technologies has rapidly increased the discovery of novel neuronal cell types based on their transcriptomic profile (Gouwens et al., 2020; Johnson et al., 2015; Tasic et al., 2016; Zeisel et al., 2015; M. Zhang et al., 2021). Besides the broad diversity of neuronal subtypes in the cerebral cortex, this brain region also comprises by various types of glial cells that closely interact with neurons and play essential roles in physiological conditions and disease. Once neurogenesis is over, astrocytes and oligodendrocyte progenitor cells (OPCs) populate the cerebral cortex and undergo local division to populate this region. Recently, several studies exploiting sequencing strategies have also identified a great diversity of astrocytes and OPCs subtypes, not only throughout different brain regions but also accross layers of the cerebral cortex (Batiuk et al., 2020; Bayraktar et al., 2015; Hilscher et al., 2022; S. Marques et al., 2016).

In this section, I will describe the current knowledge about the origin and development of the main cell types that reside in the mammalian cerebral cortex with a special focus on GABAergic neurogenesis.

1.1. Developmental origin of cellular diversity in the cerebral cortex

1.1.1. Neurogenesis in the cerebral cortex

The cerebral cortex comprises two main types of neurons: glutamatergic excitatory pyramidal neurons, which mostly exhibit long-range projections, and inhibitory interneurons that project locally. Pyramidal neurons account for approximately 80% of cortical neurons in the rodent brain and use mainly glutamate to transmit neural activity to postsynaptic targets. These neurons connect local and distal targets throughout different cortical and subcortical regions, brainstem and spinal cord (Han et al., 2018), representing the main information processing units of the cortical circuitry. There are plenty of different pyramidal cell types in the cortex, which are defined primarily by their connectivity patterns (Harris & Mrsic-Flogel, 2013). However, the diversity in pyramidal neuron subclasses has been recently expanded by a recent study that integrates morphological, electrophysiological and transcriptomic features to define distinct met-types in the cortex (Gouwens et al., 2020).

Inhibitory interneurons represent around 20% of neurons in the rodent cortex and release γ-amino butyric acid (GABA) to exert precise spatiotemporal control over pyramidal neurons excitatory activity and network dynamics. Comparative studies have revealed differences in the neuronal composition of the cortex across species, for instance, a 2.5-fold increase in the interneuron fraction has been found in the primate cortex compared to the rodent (Bakken et al., 2021; Loomba et al., 2022). Although GABAergic interneurons only account for a small fraction of cortical neurons, they play highly diverse roles in modulating and synchronising local network activity, which are essential for establishing balance of excitatory-inhibitory activity in the cortex (Tremblay et al., 2016). Under exceptional circumstances, certain subtypes of interneurons can generate excitatory depolarising activity, which is believed to play key roles during homeostasis of developing cortical circuits (Ben-Ari, 2002; Pan-Vazquez et al., 2020). This heterogeneity of functions correlates with an astonishing variety of interneuron subtypes, which provides cortical networks with the necessary dynamism to perform

complex operations during information processing in the cortex (Kepecs & Fishell, 2014). Remarkably, different subtypes of cortical interneurons differentially express biochemical markers, acquire unique morphologies and laminar distribution within the cortex, and display distinctive electrophysiological firing patterns (Bartolini et al., 2013; Gouwens et al., 2020). Moreover, similar interneuron populations with similar molecular profiles have been identified in different cortical areas and are conserved among mammalian and reptile brains, although their proportion and diversity differ across species (Tosches et al., 2018).

Pyramidal neurons and interneurons are generated from two different regions of the embryonic telencephalon. Whereas pyramidal cells arise from progenitor cells located in the dorsal telencephalon (or pallium), interneurons are born in the ventral telencephalon (or subpallium) (Fig. 1.1). The ventral telencephalon is further subdivided in regions that give rise to distinct interneuron subclasses. Most of cortical parvalbumin (PV) and somatostatin (SST) interneurons are originated in the medial ganglion eminence (MGE) (Butt et al., 2005; Fogarty et al., 2007; Miyoshi et al., 2010), although some of these subtypes have been also found to arise from the preoptic area (POA) as well (D. Gelman et al., 2011; D. M. Gelman et al., 2009). On the other hand, the majority of cortical serotonin receptor 3A (Htr3a) interneurons are derived from the caudal ganglionic eminence (CGE) together with the preoptic hypothalamic region (POH) (Fogarty et al., 2007; López-Bendito et al., 2004; Miyoshi et al., 2010; Nery et al., 2002; Niquille et al., 2018; Rubin et al., 2010). Finally, the lateral ganglionic eminence (LGE) gives rise to striatal GABAergic projection interneurons and most of the interneurons destined to olfactory bulb (Deacon et al., 1994; Wichterle et al., 1999, 2001). In both dorsal and ventral telencephalic regions, the germinal zone is divided in two areas: the ventricular zone (VZ) adjacent to the ventricles and populated by apical progenitors, also known as radial glial cells (RGCs), and the sub-ventricular zone (SVZ) located immediately next to the VZ and where basal progenitors, also known as intermediate progenitor cells, reside (Haubensak et al., 2004; Noctor et al., 2004; Pilz et al., 2013). During neurogenesis in the rodent brain, apical progenitors undergo self-renewing asymmetric division to generate another apical progenitor and a basal progenitor or a postmitotic neuron, whereas basal progenitors produce two postmitotic neurons by terminal symmetric neurogenic division (Haubensak et al., 2004; Noctor et al., 2004). In contrast, apical progenitors from primates and other gyrencephalic species generate a second type of progenitor, known as basal radial glia cells (bRGCs), which delaminates from the VZ but retains the pial contact and multipotent properties characteristic from RGCs (Hansen et al., 2010a; Reillo et al., 2011).

Importantly, bRGCs are abundant in gyrencephalic brains but rarely found in lysencephalic brains, and the retention of their pial contact has been suggested to be important for the process of gyrification during development (Borrell & Reillo, 2012). Although the progenitor diversity has been extensively explored in the dorsal telencephalon, it remains to be properly described in the many zones of the ventral telencephalon, where it has been suggested that basal progenitors may undergo multiple rounds of division (Pilz et al., 2013).

The first neurons that exit the proliferative zone initially form a structure called the preplate. Then, the first wave of migrating projection neurons divides the preplate into two separate regions, the marginal zone and the subplate. These migrating neurons start to generate a new region in the developing cortex between the marginal zone and the subplate, the cortical plate, from which mature cortical layers will be formed. Interestingly, the cortical layers are generated "inside-out", with late-born neurons progressively migrating past the early-born neurons to populate the superficial layers (Angevine & Sidman, 1961; Rakic, 1974). Pyramidal neurons are generated locally and use the basal process from RGCs to migrate radially towards the pial surface. In contrast, interneurons travel long distances to populate the cortical plate through a process known as tangential migration (Marín & Rubenstein, 2001) (Fig 1.1). Moreover, interneurons instead of using basal processes from RGCs to help them migrate towards the cortical plate, they are guided to migrate in organised cortical streams thanks to a combination of chemoattractant and chemorepulsive cues (Marín et al., 2013). For instance, chemoattractant molecules such as Neuregulin-1, Neurotrophin-4 and brain-derived neurotrophic factor (BDNF) are simultaneously expressed along the interneuron migratory path towards the cortex, to which interneurons are responsive through the expression of ErbB4 and TrkB receptors (Flames et al., 2004; Polleux et al., 2002). The chemokine Cxcl12 is expressed in the marginal zone and intermediate zone as well as in the subplate to a lesser extent, while migrating interneurons express the Cxcl12 chemokine receptors Cxcr4 and Cxcr7. This signalling pathway plays an important role in restricting interneuron migration in defined streams towards the cortical plate (López-Bendito et al., 2008; Sánchez-Alcañiz et al., 2011; Stumm et al., 2003; Tiveron et al., 2006). In addition, the migratory interneuron switch from tangential to radial mode is controlled by Cxcl12 signalling, which enhances branching of interneuron leading processes and slows down their tangential migration rate (Lysko et al., 2011; Y. Wang et al., 2011). Cxcl12 is also released by blood vessels, which acts as a chemoattractant to both interneurons and first-wave OPCs and contributes to their migration in separate and defined paths (López-Bendito

et al., 2008; Tiveron et al., 2006; Tsai et al., 2016). At the cellular level, interneuron migration is tightly orchestrated by unidirectional contact repulsion exerted from first-wave OPCs through PlexinA3-Semaphorin6a/6b signalling (Lepiemme et al., 2022). As interneurons migrate through the developing cortical plate, their primary cilia sense the concentration gradient of Shh, which acts as a guidance cue by helping them to migrate and integrate into the correct cortical layers (Baudoin et al., 2012; Higginbotham et al., 2012). Interneurons also distribute in an "inside-out" manner guided by pyramidal neurons through the expression of attractive chemokines such as Neuregulin-3 (Bartolini et al., 2017; Rymar & Sadikot, 2007).

1.1.2. Gliogenesis in the cerebral cortex

At postnatal stages, once RGCs have generated and guided newly born neurons to populate the cortical plate, these progenitors undergo a transcriptional and morphological switch and shift from producing neurons to glia (Kriegstein & Alvarez-Buylla, 2009). This gliogenic switch is regulated by a combination of intrinsic and extrinsic molecular cues that supress neuron generation while promoting glia production. The JAK/STAT signalling pathway promotes astrocytic differentiation by phosphorylation of STAT proteins, which results in the STAT-mediated transcription of astrocytic-related genes (F. He et al., 2005). RGCs that will differentiate into astrocytes detach from the ventricle and migrate towards the cortical plate (Noctor et al., 2008). Once they reach the developing cortex, astrocytes proliferate locally and undergo symmetric division to populate the cortex until the third postnatal week (W. P. Ge et al., 2012) (Fig.1.1). Astrocytes generated throughout postnatal development mature and integrate into the cortical circuit by coupling with surrounding astrocytes by gap-junction connections (W. P. Ge et al., 2012).

In contrast, oligodendrocytes originate in multiple waves over postnatal development from RGCs located both in the ventral and dorsal telencephalon (Fig.1.1). The first wave of cortical oligodendrocytes arises from Nkx2.1-expressing progenitor cells located in the MGE of the ventral telencephalon around embryonic day 12.5 (E12.5) and reach the cortex around embryonic day 15 (E15) in the mouse (Pringle & Richardson, 1993; Spassky et al., 1998; Tekki-Kessaris et al., 2001). A fraction of these MGE-derived oligodendrocytes originates from a common pool of progenitor cells that also give rise to GABAergic neurons (He et al., 2001; Nery et al., 2001), where the

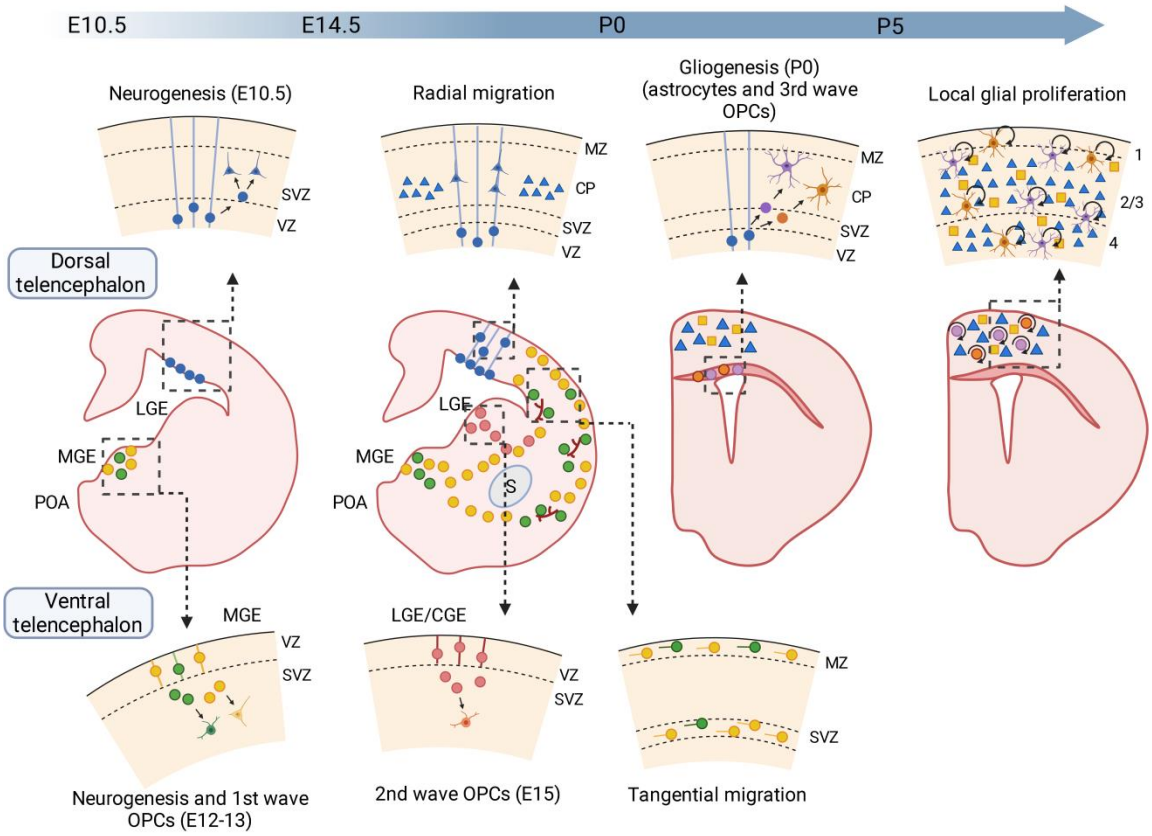

Figure 1.1. Timeline of the main events underlying neurogenesis and gliogenesis in the mouse cerebral cortex. Pyramidal cells are generated in the dorsal telencephalon by progenitors populating the ventricular zone (VZ) and subventricular zone (SVZ) and migrate radially to populate the cortical plate (CP) in an "inside-out" manner. Interneurons and first-wave oligodendrocyte progenitors (OPCs) are originated from progenitors in the medial ganglionic eminence (MGE) of the ventral telencephalon. They migrate tangentially in streams along the marginal zone (MZ) and SVZ following chemoattractive and chemorepulsive cues to reach the CP. Second-wave OPCs originate later from progenitors located in the VZ and SVZ regions of the CGE/LGE. After birth, astroglia and third-wave OPCs are generated from dorsal progenitors and migrate radially along progenitor processes to populate the cortex, where they undergo local proliferation over the first postnatal weeks. CGE, Caudal Ganglionic Eminence; CP, Cortical Plate; LGE, Lateral Ganglionic Eminence; MZ, Marginal Zone; MGE, Medial Ganglionic Eminence; OPCs, Oligodendrocyte Progenitor Cells; POA, Preoptic Area; S, Striatum; SVZ, Subventricular Zone; VZ, Ventricular Zone. Adapted from (Lim et al., 2018).

interplay between specific transcription factors regulates the neuron-to-oligodendrocyte switch (Petryniak et al., 2007). As previously mentioned, it has been recently discovered that this population of early-generated OPCs contribute to guide interneuron migrations towards the dorsal telencephalon by unidirectional contact repulsion (Lepiemme et al., 2022). A second wave of oligodendrocytes is produced by Gsh2-expressing progenitors located in the CGE and LGE around E15, from where they migrate to the dorsal cortex (Kessaris et al., 2005). After birth, a third wave of oligodendrocytes arises from Emx1-expressing precursors in the dorsal telencephalon (Gorski et al., 2002; Kessaris et al., 2005). Interestingly, the majority of MGE-derived oligodendrocytes are depleted during postnatal development, thus most of the oligodendrocytes populating the adult cortex are originated from progenitors located in the CGE/LGE as well as the dorsal telencephalon (Kessaris et al., 2005).

Unlike neurons and other types of glial cells, microglia originate from primitive myeloid progenitors present in the embryonic yolk sac (Ginhoux et al., 2010; Kierdorf et al., 2013). During early embryogenesis, around E8.5 in mice and during the third week of gestation in humans, these progenitor cells migrate into the developing CNS, where they colonise the brain and spinal cord and differentiate into microglia (Swinnen et al., 2013; Verney et al., 2010). These specialised type of macrophages act as resident immune cells in the CNS by contributing to immune surveillance and homeostasis maintenance. Their unique developmental origin sets them apart from other immune cells, as they maintain a distinct self-renewal capacity throughout life (D. Hashimoto et al., 2013).

1.2. Interneuron diversity in the cerebral cortex

Cortical interneurons represent a large and diverse population of neurons that display distinct biochemical, anatomical, electrophysiological and connectivity features (Gouwens et al., 2020; Lim et al., 2018; Tremblay et al., 2016; Wamsley & Fishell, 2017). Most cortical interneurons can be classified into three cardinal subclasses based on the expression of neurochemical markers: PV and somatostatin SST-positive interneurons represent the two most abundant subpopulations, and Htr3a-positive interneurons accounts for the minority group (Rudy et al., 2011).

PV interneurons represent the most abundant subpopulation of cortical interneurons, accounting for around 40% of total number of interneurons in the cortex. PV interneurons display a fast-spiking firing pattern, which allows them to rapidly regulate and coordinate the activity of cortical networks (Hu et al., 2014), supporting the generation of gamma-oscillations (Cardin et al., 2009; Sohal et al., 2009). The expression of PV, a Ca2+ binding protein that acts as buffer to regulate intracellular Ca2+ transients, is essential to sustain high-frequency firing activity of PV interneurons (Caillard et al., 2000). PV interneurons play critical roles in cortical activity, which are essential for sensory processing (Wood et al., 2017). In addition, these interneurons exhibit a high degree of plasticity, providing them with the ability to modulate learning and memory consolidation (Dehorter et al., 2015; Donato et al., 2013, 2015). The essential functions that PV interneurons play in regulating circuitry activity generate a high energy demand, which is provided by the presence of a large number of mitochondria in these neurons (Gulyás et al., 2006). In terms of PV interneurons diversity, this subpopulation can be further subdivided into three classes based on their morphological characteristics: basket cells, chandelier cells and translaminar neurons. PV-expressing basket cells are the main subtype of PV interneurons and innervate the soma and proximal dendrites of pyramidal cells through characteristic dense axonal arbours that acquire basket-like structures (Buhl et al., 1995; Hu et al., 2014). They are distributed throughout layers 2 to 6 (L2-6) of the cortex, being preferentially present in L4, and normally innervate pyramidal cells located within the same cortical layer (Hu et al., 2014; Jiang et al., 2015; Tremblay et al., 2016). Chandelier cells are the second most common subtype of PV interneurons in the cortex, and they are named after the singular chandelier-like arborisation of their axons (Somogyi, 1977; Somogyi et al., 1982). They form synapses onto the axon initial segment of excitatory neurons and are particularly abundant in L2/3, L5 and L6 of the cortex (Taniguchi et al., 2013). Although a fraction of chandelier cells does not express detectable levels of PV, these cells are still considered part of this subclass due to the important similarities with PV-expressing interneurons. Lastly, translaminar cells represent a small population of PV interneurons located in the L6 of the cortex which innervate pyramidal cells across all cortical layers (Bortone et al., 2014).

The second largest subtype of cortical interneurons is characterised by the expression of the neuropeptide SST, which represents approximately 30% of the total number of cortical inhibitory interneurons. Unlike PV cells, SST interneurons target the distal dendrites of pyramidal neurons (De Lima & Morrison, 1989; Dennison-Cavanagh et al., 1993; Kawaguchi & Kubota, 1996, 1997), allowing them to control the dendritic

integration of synaptic inputs. SST interneurons display heterogeneous firing patterns, typically exhibiting adapting non-fast spiking or intrinsic-burst-spiking properties. They are distributed throughout L2-6 of the cortex, being particularly abundant in L5, and they mediate inhibitory feedback in cortical circuits (Y. Ma et al., 2006; Xu et al., 2013). Based on their morphological properties, SST interneurons have been classified into two major subclasses: Martinotti and non-Martinotti cells (Y. Ma et al., 2006; McGarry et al., 2010; Nigro et al., 2018). Martinotti cells are the most abundant subtype and they are particularly abundant in L5, from where they extend a characteristic columnar axonal arborisation to L1. In contrast, non-Martinotti cells are mostly located in L4, where they project locally onto PV interneurons, regulating disinhibition of pyramidal neurons in the cortex (Xu et al., 2013).

The Htr3a-expressing interneurons represent a very heterogeneous group in terms of morphological and electrophysiological properties, and account for the majority of cortical interneurons located in superficial layers. Neurogliaform cells and single-bouquet cells express Reelin and are particularly present in L1, where they regulate sensory processing by innervating the apical dendrites of pyramidal neurons (Ibrahim et al., 2021; S. H. Lee et al., 2010; Schuman et al., 2019). Cholecystokinin (CCK)-expressing basket cells innervate the soma and proximal dendrites of pyramidal cells and can be further divided into two subgroups depending on their expression of the vasoactive intestinal peptide (VIP) and layer distribution (M. He et al., 2016). Bipolar cells often co-express VIP and the calcium-binding protein calretinin (CR), and they are enriched in the supragranular layers of the cortex. They selectively target PV and SST interneurons supporting network disinhibition (Dávid et al., 2007; Prönneke et al., 2015; Walker et al., 2016). Lastly, multipolar cells express neuropeptide Y (NPY) and are particularly abundant between layers 1 and 2 (D. M. Gelman et al., 2009; Miyoshi et al., 2010).

These main classes of cortical interneurons have been described over the last decades by a combination of strategies that collected morphological, genetic and functional properties. However, in recent years, the number of interneuron subtypes identified has increased with the emergence of single-cell RNA sequencing technologies, suggesting the presence of up to 60 different interneuron subtypes (Tasic et al., 2018; Zeisel et al., 2015). A more recent study that integrates the transcriptomic signature of cortical interneurons together with their morphological and electrophysiological properties has recently identified up to 28 distinct met-types (Gouwens et al., 2020). These interesting findings have shed light on the idea that

cortical interneurons comprise a diverse group of cells responsible for coordinating network activity at multiple levels. However, it still remains to be elucidated how and when cortical interneurons are specified during development and which are the mechanisms underlying these processes at the molecular level.

Interneuron classes	Interneuron subclasses	Selective marker expression	Layer preference	Developmental region of origin
Parvalbumin (PV)	Basket cells	PV+	L2-6	MGE/POA
	Chandelier cells	PV+/PV-	L2/3, L4, L5	
	Translaminar cells	PV+	L6	
Somatostatin (SST)	Martinotti cells	SST+/CR+/CB+	L5	MGE/POA
	Non-Martinotti cells	SST+	L4	
Serotonin receptor 3A (Htr3a)	Neurogliaform cells	Htr3a+/Reelin+	L1	POH
	Multipolar cells	Htr3a+/NPY+	L1/2	POH
	Single-bouquet cells	Htr3a+/Reelin+	L1	CGE
	Basket cells	Htr3a+/CCK+/VIP+	L2/3	CGE
		Htr3a+/CCK+	L5/6	
	Bipolar cells	VIP+	L2/3	

Table 1.1. GABAergic neuron diversity in the cortex. Summary of the main interneuron classes and subclasses, including their specific marker expression, preferential cortical layer distribution and developmental region of origin. CB, Calbindin; CCK, Cholecystokinin; CGE, Caudal Ganglionic Eminence; CR, Calretinin; Htr3a, Serotonin Receptor 3A; LGE, Lateral Ganglionic Eminence; MGE, Medial Ganglionic Eminence; NPY, Neuropeptide-Y; POA, Preoptic Area; POH, Preoptic Hypothalamic Region; PV, Parvalbumin; SST, Somatostatin; VIP, Vasoactive Intestinal Peptide.

1.3. Molecular mechanisms underlying interneuron diversity in the cerebral cortex

As previously described, the cortical interneuron subpopulations described above originate from different regions of the ventral telencephalon. The MGE gives rise to most of cortical PV and SST interneurons (Butt et al., 2005; Fogarty et al., 2007; Miyoshi et al., 2010), although some of these subtypes have been reported to come

from the POA as well (D. Gelman et al., 2011; D. M. Gelman et al., 2009). On the other hand, the majority of cortical Htr3a interneurons are derived from the CGE together with the POH (Fogarty et al., 2007; López-Bendito et al., 2004; Miyoshi et al., 2010; Nery et al., 2002; Niquille et al., 2018; Rubin et al., 2010). The specification of distinct interneuron subclasses is tightly regulated by molecular cues that dictate the acquisition of a certain identity. During early development, specific regions of the telencephalon are delineated through a complex interaction involving morphogen signalling gradients and the coordinated expression of transcription factors, which will be further described in the following sub-sections. Importantly, the distinct regional developmental origins influence the specification and wiring properties as well as the laminar distribution of cortical interneurons in the adult brain (Batista-Brito & Fishell, 2009).

1.3.1. Spatial patterning and neurogenesis within the ventral telencephalon

Interneurons born in the ventral telencephalon travel a long way before they settle and mature in the cerebral cortex. How early an interneuron is fully committed to become one subtype or another along this journey remains a fundamental question. Transcriptomic studies have recently suggested that cortical interneuron diversity is established during early stages of development (Mayer et al., 2018; Mi et al., 2018). Thus, the molecular mechanisms taking place in the regions where interneurons originate during early development are essential to determine the fate specification of these cells.

During embryonic development, the interplay between morphogen signalling gradients and the combinatorial expression of transcription factors segregates the telencephalon in defined regions (Schuurmans & Guillemot, 2002). Secretion of Wingless-related integration site (Wnt) and Bone morphogenetic proteins (BMPs) in the dorsal telencephalon opposed to Shh signalling from the ventral telencephalon establish the axial patterning in a gradient-dependent manner. The ventral telencephalon identity is also defined by the interplay between Shh and Fibroblast Growth Factor (FGF) signalling. Together they act as a repressor of the transcription factor family Glioma-Associated Oncogene Family Zinc Finger (Gli) to define the dorso-ventral boundaries (Hébert & Fishell, 2008).

These initial patterning events results in the expression of core transcription factors that contributes to further define the identity of the ventral telencephalon. Early expression of transcription factors plays a crucial role in orchestrating the dynamics of gene regulatory networks during interneuron specification. In particular, the expression of basic helix loop helix (bHLH) transcription factors is essential to promote specification of neuronal cells during development (Bertrand et al., 2002) (Fig 1.2A). Whereas the bHLH transcription factor Neurogenin-2 (Neurog2) is expressed in the dorsal telencephalon and is involved in differentiation of cortical excitatory neurons, Achaete-scute complex-like 1 (Ascl1) is highly expressed in the ventral telencephalon and plays crucial roles in the specification of interneurons during embryonic neurogenesis (Casarosa et al., 1999a; Fode et al., 2000; Guillemot & Joyner, 1993; Nieto et al., 2001). Importantly, Ascl1 also is expressed in the radial glia of the developing human cortex, suggesting that its role is conserved in human embryonic neurogenesis (Hansen et al., 2010b). Ascl1 is known to be a pioneer transcription factor, as it is able to bind both open and closed chromatin regions, promoting chromatin accessibility at its target sites during neurogenesis (Raposo et al., 2015). Opposed to its essential function in neuronal differentiation and cell cycle exit, Ascl1 also promotes cell proliferation of neural progenitors by activating target genes involved in cell division, such as CyclinD1 (Castro et al., 2011; Urbán et al., 2016). It has been suggested that fluctuating levels of Ascl1 expression promote progenitor proliferation, whereas steady and high levels induce neuronal differentiation (Imayoshi et al., 2013). Moreover, Ascl1 plays a critical role in gliogenesis during development, where it interacts with the Oligodendrocyte transcription factor (Olig2) to orchestrate generation of OPCs in the ventral telencephalon (Parras et al., 2004, 2007). At postnatal stages, Ascl1 is also expressed by progenitors in the SVZ and is required for the formation of OPCs (Nakatani et al., 2013; Parras et al., 2007).

Ascl1 directly regulates the expression of its downstream targets Distal-less homeobox1 and 2 genes (Dlx1 and 2), two transcription factors essential for cortical interneuron development (Castro et al., 2011; Poitras et al., 2007). Dlx1/2 are co-expressed in the proliferative regions of the ventral telencephalon, and act as pan-GABAergic interneuron regulators (Alzu'bi & Clowry, 2019; Cobos et al., 2005; Long et al., 2009). They are essential for the survival and differentiation of inhibitory interneurons in the forebrain and their ablation leads to severe defects in interneuron formation, maturation and survival (Anderson et al., 1997; Cobos et al., 2005). In addition, Dlx1/2 downregulate the expression of Olig2 to orchestrate the balance between neurogenesis and oligodendrogenesis from common precursors from the

ventral telencephalon (Petryniak et al., 2007). The interplay between these genes regulates the size of the interneuron population. In addition, Dlx1/2 are also essential for the tangential migration of interneurons towards the cortex by restraining their axon and neurite outgrowth (Cobos et al., 2007; Colasante et al., 2008; Le et al., 2007).

1.3.2. Post-translational regulation of the proneural transcription factor Ascl1

The proneural activity of bHLH transcription factors, such as Ascl1, is not only determined by their ability to induce neuronal differentiation, but also by their activation of the Notch/Delta signalling pathway. When bHLH transcription factors are expressed in a progenitor cell, they transactivate the expression of Delta, which binds to Notch ligands in neighbouring cells. Subsequently, Notch initiates a signalling cascade that results in the expression of Hes genes, which in turn supresses the expression of bHLH genes (Castro et al., 2006). Thanks to this process known as "lateral inhibition", bHLH transcription factors confine their expression to a restricted number of neural progenitor cells and regulate the generation of neurons.

Importantly, the specification of neurons during development is not only modulated by transcriptional programmes, but it is also highly influenced by post-translational mechanisms. In particular, single or multi-site phosphorylation of bHLH transcription factors, including Ascl1, has been shown to regulate multiple aspects of their activity (Ali et al., 2014; Hand et al., 2005; Hindley et al., 2012; H. Li et al., 2011; Quan et al., 2016). Murine Ascl1 contains six conserved serine-proline residues, which are subjected to phosphorylation by proline-directed kinases (Fig 1.2B). During cell division, increased levels of cyclins drive higher Cyclin-dependent kinases (Cdk) activity, which results in phosphorylation of SP sites of Ascl1 (Fig 1.2C). The phosphorylation of these sites by Cdk2 during *Xenopus laevis* development keeps progenitor cells in proliferative state and hinders neurogenesis (Ali et al., 2014; Wylie et al., 2015). Interestingly, when phosphorylation is hampered by mutating all six serine-proline sites into alanine residues promotes neurogenic activity both *in vivo* and *in vitro* and confers resistance to lateral inhibition and cell cycle regulation mediated by CyclinA/Cdk2 activity (Ali et al., 2014). Indeed, wildtype Ascl1 fails to drive neuronal differentiation in a *Xenopus laevis* developmental model of neuroblastoma, whereas the phospho-site mutant Ascl1 restores neurogenesis (Wylie et al., 2015).

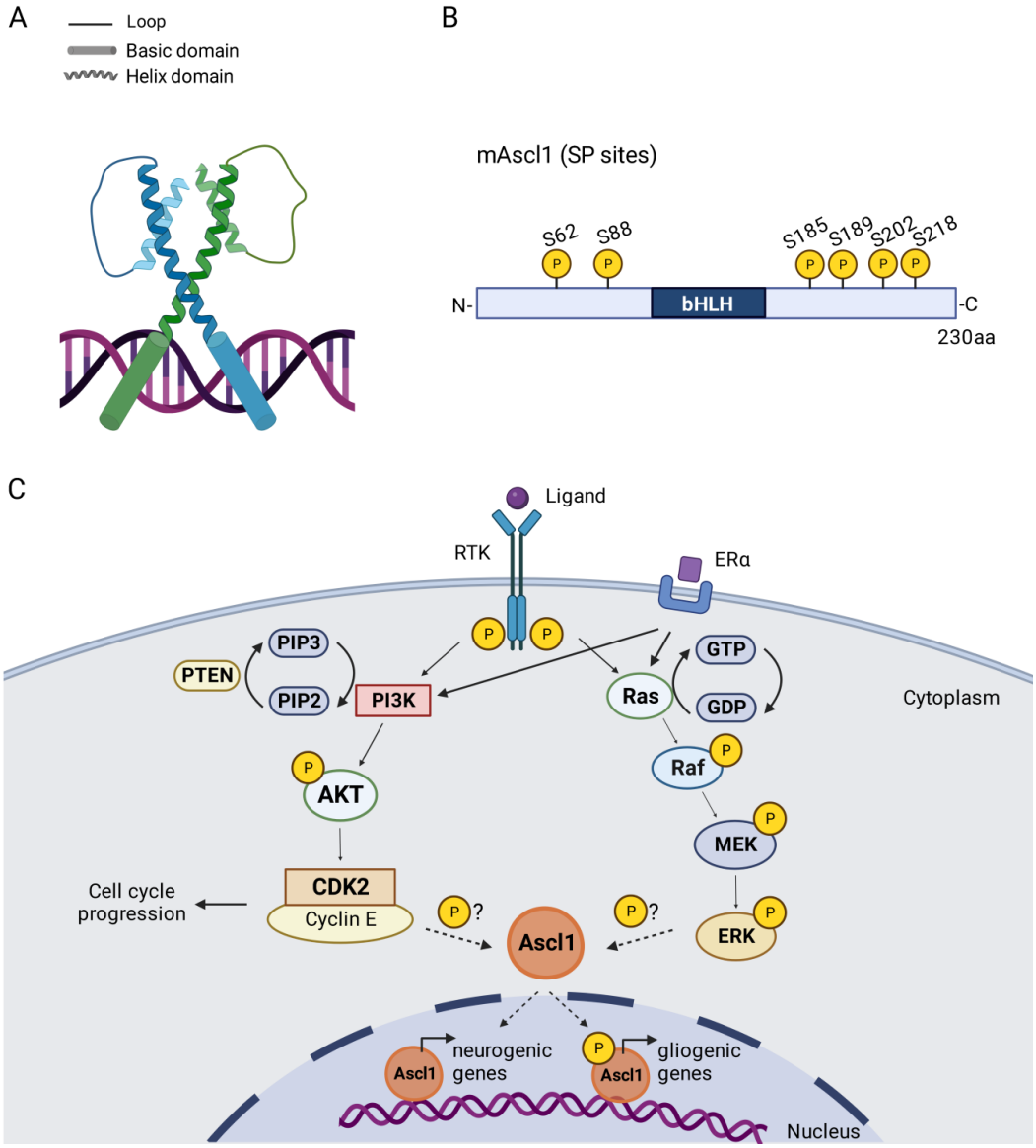

Figure 1.2. Structure and phosphorylation of the proneural transcription factor Ascl1. (A) Structure of the basic helix-loop-helix (bHLH) transcription factors, such as Ascl1. (B) Schematic representation of mouse Ascl1 serine-proline (SP) sites subject to phosphorylation. (C) Activation of receptor tyrosine kinases (RTKs) leads to activation of phosphorylation of phosphatidylinositol 3-kinase (PI3K), which results in protein kinase B (AKT) phosphorylation. Active AKT regulates cell cycle progression by activating Cyclin-dependent kinase 2 (Cdk2) activity, which in turn can phosphorylate the SP sites of Ascl1 (Ali et al., 2014). In addition, RTKs and Estrogen Receptor alpha (ERα) can also activate the RAS/Extracellular signal-regulated kinases (ERK) signalling pathway, which can result in Ascl1 phosphorylation. Depending on the activation levels of this pathway, Ascl1 will either activate a glionenic or neurogenic transcriptional programme in the cell nucleus (Li et al., 2014). AKT, Protein Kinase B; bHLH, basic Helix-Loop-Helix; Cdk2, Cyclin-dependent kinase; ERα, Estrogen Receptor alpha; ERK, Extracellular signal-regulated kinases; PI3K, Phosphatidylinositol 3-Kinase; RTK, Receptor Tyrosine Kinases.

Another relevant regulatory mechanism that controls Ascl1 neurogenic potential and specification properties is the RAS/Extracellular signal-regulated kinases (ERK) signalling pathway. This pathway directly influences Ascl1 fate specification properties in mouse cortical progenitors by a dosage-dependent RAS/ERK activity (Fig 1.2C). Mechanistically, elevated levels of RAS activity drive ERK-mediated phosphorylation of Ascl1 and induces gliogenesis, while exposure to low levels of RAS activation reduces Ascl1 phosphorylation and promotes neurogenesis towards a GABAergic lineage (S. Li et al., 2014). Upon increased levels of RAS activity, Ascl1 activates the gliogenic differentiation programme via transactivation of Sox9 whereas reduced levels of the signalling pathway lead to activation of the neurogenic programme via Dlx1/2 expression. However, the phospho-site mutant Ascl1 is not influenced by different levels of RAS/ERK activity (S. Li et al., 2014).

1.3.3. Regional specification of MGE-derived interneurons

All the aforementioned signalling gradients and transcription factors contribute to segregate the identity of the ventral telencephalon from the dorsal regions. However, the ganglionic eminences and the preoptic region are also organised in distinct spatial domains that give rise to non-overlapping interneuron subclasses. This interneuron diversity is similarly achieved by the differential expression of transcription factors across the different regions of the ventral telencephalon.

The progenitor cells located in the MGE, which give rise to PV and SST interneurons, are characterised by the expression of the transcription factor Nkx2.1. The specific deletion of this gene converts the MGE into a structure with properties from the CGE and LGE regions and impairs the generation of MGE-derived interneurons (Butt et al., 2008; Sussel et al., 1999). Nkx2.1 not only represses neighbouring cell fates, but it also is essential for the activation of a transcriptional programme that induces the generation of MGE-derived cortical interneurons. The LIM homeodomain factor (*Lhx6*) is a direct downstream target of Nkx2.1 and it is expressed in post-mitotic MGE-derived interneurons across development and adulthood. Lhx6 ensures that postmitotic neurons acquire an MGE-derived interneuron identity by inhibiting the expression of the Specificity Protein 8 (*Sp8*), a gene specifically expressed in CDE and LGE-derived interneurons (T. Ma et al., 2012; Vogt et al., 2014). Sox6 acts downstream of Lhx6 in the developing ventral telencephalon and supresses

the expression of progenitor genes, such as Ascl1, thus segregating the pre- and postmitotic transcriptional programmes in the MGE (Batista-Brito & Fishell, 2009).

Taken together, intrinsic transcriptional programmes must cooperate with environmental signals to tightly define the specification and differentiation of the multiple interneuron subtypes that will later populate the cortex.

1.4. Activity-dependent regulation of wiring and maturation of interneurons into cortical networks

Postmitotic interneurons must travel a great distance before arriving and settling in the cerebral cortex. It is believed that interneurons are already committed to a specific cell identity when they reach their final laminar positions in the cortex. However, recent research has found that when interneurons interact with neighbouring cells within developing cortical networks, they unfold molecular programmes that enable them to fully acquire their final identity (Lim et al., 2018; Wamsley & Fishell, 2017).

Once interneurons and pyramidal neurons populate the cerebral cortex, they undergo a process of programmed cell death that takes place within a specific window of early postnatal development (Southwell et al., 2012; Wong et al., 2018). This refinement process sculpts the neural networks in an activity-dependent manner to control the final number of cells that the cortical circuit must contain for proper functioning (Denaxa et al., 2018; Priya et al., 2018). Interneurons that show lower activity during the time window of programmed cell death are more likely to be eliminated through activity-dependent PTEN inhibition regulated by pyramidal neurons (Wong et al., 2018). Since pyramidal neurons directly control interneuron activity, it has been suggested that these two populations have developed this regulatory mechanism to match their numbers and maintain a proper excitatory-inhibitory balance in the cortex. Besides the role that interactions between interneurons and pyramidal neurons play in postnatal programmed cell death, the formation of GABAergic synapses between interneurons and OPCs also regulate their mutual survival during postnatal development. Interneurons and first-wave OPCs sharing the same embryonic origin display preferential synaptic connectivity and survival rates compared to those with low levels of connectivity (Orduz et al., 2019).

Neural activity and sensory experience not only modulate programmed cell death but also have an important effect on the assembly of cortical networks. Apart from regulating the survival of MGE-derived interneurons during early postnatal development, neuronal activity also controls the morphological development and laminar distribution of specific types of interneurons (Babij & De Marco Garcia, 2016; De Marco García et al., 2011). Indeed, disruption of the thalamocortical activity leads to morphological defects in neurogliaform interneurons (De Marco García et al., 2015). Neuronal activity also seems to play important roles in remodelling synaptic connections of PV basket interneurons by modulating certain components of their perineuronal nets (Favuzzi et al., 2017). In addition, the plasticity and intrinsic properties of this interneuron population have been shown to be also dynamically regulated by experience (Donato et al., 2013, 2015). These observations support the idea that dynamic adaptation of interneurons in response to activity changes and experience is essential to carry out high cognitive functions, such as learning and memory.

These activity-dependent mechanisms are, at least, partially mediated by the activation of transcriptional programmes. For instance, the activation of the transcription factor Dlx1 has been shown to be crucial for maturation of certain interneuron subtypes (Cobos et al., 2005; De Marco García et al., 2011). Neuronal activity also induces the expression of the immediate early gene (IEG) *Npas4* specifically in SST interneurons to control the formation of excitatory synapses onto these cells (Spiegel et al., 2014). However, neuronal activation promotes a completely different response in VIP interneurons, by driving the formation of inhibitory synapses onto these neurons (Mardinly et al., 2016). Moreover, neuronal activity also regulates the expression as well as subcellular location of the Etv1 transcription factor in PV interneurons (Dehorter et al., 2015). *Etv1* activation results in Kv1.1 expression, a potassium channel required for the delayed firing of these interneurons, conferring them the ability to adapt to activity changes by tuning their excitability (Goldberg et al., 2008). Altogether, these observations indicate that neuronal activity modulates the connectivity patterns and intrinsic properties of cortical interneurons through the activation of transcriptional programmes that seem to be cell type-specific.

Cortical network maturation also involves the formation of specific connections between neurons and the establishment of functional networks. Microglia have recently emerged as key regulators in the process of synaptogenesis, including the formation of inhibitory synapses. In particular, microglia promote the establishment and

maintenance of axo-axonic synapses between chandelier cells and the axon initial segment of pyramidal neurons in the cortex by forming tripartite interactions with these cell types (Gallo et al., 2022). During cortical development, there is an overproduction of neuronal synapses, creating a surplus of connections that will subsequently undergo through a process called synaptic pruning, where weaker connections are eliminated while stronger connections are reinforced. In this context, microglia also play a crucial role in the refinement of cortical networks by engulfing and eliminating excess synapses, which is essential for fine-tuning the connectivity of neuronal networks (Paolicelli et al., 2011; Schafer et al., 2012; Stevens et al., 2007). Although most work has been focused on excitatory synapses pruning, it has been more recently reported that microglia expressing GABA receptors selectively interact with inhibitory synapses during postnatal development and shape their connectivity without impacting excitatory synapses (Favuzzi et al., 2021). Overall, microglia actively influence synaptic strength and neuronal excitability, ultimately shaping the functional connectivity and activity patterns within cortical networks.

Altogether, intrinsic and extrinsic mechanisms taking place during brain development play crucial roles on the ability of interneurons to connect to the right neuronal targets and acquire their mature identity.

1.5. Cortical interneurons in health and disease

Defects in interneuron development and correct functioning have been implicated in multiple neurological and psychiatric disorders, behavioural diseases and intellectual disabilities (Marín, 2012). Such impairments are associated with the disruption of the excitatory-inhibitory balance leading to pathological hyperexcitability in brain circuits.

Epilepsy is characterised by spontaneous recurrent epileptic seizures which can result from a decreased number of interneurons or a reduced inhibitory activity within brain networks. This disorder can manifest at any age and a substantial fraction of epileptic disorders carry strong genetic determinants. For instance, impaired migration of interneurons caused by a mutation in the *Arx* gene reduces GABA-mediated inhibition in cortical networks and causes seizures (Friocourt et al., 2008). Likewise, decreased number of interneurons in mice lacking *Dlx1/2* expression, two transcription factors essential for the production and survival of interneurons, causes epileptic

seizures in these animals (Cobos et al., 2005). In addition, reduced excitability of PV interneurons caused by mutations in the gene *Scn1A* encoding for the Nav1.1 sodium channel has severe implications in generating epileptic seizures during childhood (Cheah et al., 2012). However, another leading cause of epilepsy arises as a consequence of brain injury or stroke.

Besides epilepsy, which is the most well-characterised disorder linked to network hyperexcitability, more subtle perturbations in the excitatory-inhibitory balance have been also implicated in multiple psychiatric disorders. Patients suffering from schizophrenia exhibit disruptions in the inhibitory network, mainly in the prefrontal cortex. Several lines of evidence have pointed at defects on PV interneurons as one of the possible causes underlying impairments on the working memory of schizophrenia patients. For instance, decreased expression of Glutamate decarboxylase 1 (GAD67) and N-methyl-D-aspartate (NMDA) receptor has been found in PV interneurons of schizophrenic patients (Akbarian et al., 1995; Belforte et al., 2010; T. Hashimoto et al., 2003; Korotkova et al., 2010). In addition, alterations on Erbb4-Nrg1 signalling pathway, which is involved in PV interneuron wiring, have been repeatedly associated with development of schizophrenic behaviours (Harrison & Law, 2006; Mei & Xiong, 2008).

The pathophysiology of schizophrenia seems to be very specific to impairments in a particular interneuron subtype. However, other neurodevelopmental disorders like autism might result from general disruptions of the inhibitory activity in the brain. Rett's syndrome, an autism spectrum disorder (ASD), is caused by mutations in the gene encoding methyl-CpG-binding protein 2 (*MeCP2*) (Amir et al., 1999) and its ablation in GABAergic neurons specifically recapitulates the cognitive and motor dysfunctions characteristic from this disorder (Chao et al., 2010). Other lines of evidence have also supported GABAergic deficits in autism, for instance, depletion of *Shank3* gene (Durand et al., 2007; Moessner et al., 2007). This gene is involved in the formation of excitatory synapses onto GABAergic neurons and *Shank3-null* mutant mice exhibit abnormal social interactions and behaviour (Peça et al., 2011).

Lastly, general disruption of inhibitory circuits also contributes to intellectual disabilities observed in several neurodevelopmental disorders. For instance, patients suffering from fragile X-syndrome or Down's syndrome have notable defects in GABAergic cortical and hippocampal circuits respectively (Belichenko et al., 2009;

Kleschevnicov et al., 2004; Olmos-Serrano et al., 2010; Selby et al., 2007), although the exact mechanisms underlying inhibitory disruption still remain unclear.

Over the past decades, a wide range of neurological and psychiatric disorders have been found to be directly associated to disruptions in interneuron development, connectivity and maturation by altering the correct functioning of inhibitory networks. Our increased understanding on how impaired inhibitory activity is involved in the development of these disorders has not been accompanied by advances in therapeutic strategies to treat these conditions. Therefore, it is of great importance to find novel strategies and technologies that would allow the correction or replacement of impaired interneuron function.

"In adult centers the nerve paths are something fixed, ended, immutable. Everything may die, nothing may be regenerated. It is key for the science of the future to change, if possible, this decree" (Ramon y Cajal, 1928)

2. Regeneration of the Central Nervous System

Acute injury or chronic disorders affecting the human CNS are dreadful because of its very limited endogenous regenerative capacity to restore lost neurons. Thus, acute injury or chronic neurodegenerative disorders are linked to irreversible loss of neurons, which ultimately results in permanent functional impairments and neurological disabilities. Over the last decades, remarkable advances have been made in preclinical research to understand the mechanisms underlying neuronal dysfunction and loss in various CNS disorders. However, this progress has so far not been translated into effective therapies and further research is needed to develop novel relevant strategies in the field of regenerative medicine.

2.1. Limited intrinsic regeneration capacity of the mammalian CNS

Less than a century ago, it was widely accepted by the scientific community that no new neurons could be generated after birth. It was believed that following embryonic development the structural composition of neurons within the brain remained unchanged. However, the first detection of newly generated neurons in the postnatal mammalian brain in the early 1960 (Altman, 1962) shed light on the idea that the adult brain might exhibit more plasticity than previously thought. Over the next decades, Altman's findings were corroborated by several studies providing evidence for the existence of adult neurogenesis mainly in two regions: the SVZ of the lateral ventricles (Reynolds & Weiss, 1992; Richards et al., 1992) and in the dentate gyrus (DG) of the hippocampus (Gage et al., 1995; Palmer et al., 1997). Later on, low levels of neurogenesis were also reported in other brain regions, including the hypothalamus, amygdala, *substantia nigra* or cortex (Bernier et al., 2002; Gould et al., 1999; Kokoeva et al., 2005; Zhao et al., 2003).

Neurogenesis in the adult brain occurs through the division of neural stem cells in the neurogenic niches and their subsequent migration, maturation and integration in the network. In the SVZ, newborn neurons migrate throughout the rostral migratory

stream (RMS) and give rise to GABAergic and dopaminergic neurons that integrate into the olfactory bulb (Lois & Alvarez-Buylla, 1994), whereas newly generated glutamatergic neurons in the DG migrate short distances to integrate into the granule cell layer of the hippocampus (Markakis & Gage, 1999). Integration of newly generated neurons in the existing neural network has been linked to important functional implications linked to brain plasticity, such as odour discrimination time in the olfactory bulb (Breton-Provencher et al., 2009) or pattern separation in the hippocampus (Aimone et al., 2010).

Given that newborn neurons in the adult brain can functionally integrate in the neuronal circuitry, extensive research has focused on exploiting the brain's endogenous potential to generate new neurons. Many studies have investigated the intrinsic and extrinsic cues that regulate neural stem cells activation for regenerative purposes. Interestingly, it has been shown that neurogenesis can be stimulated in the adult brain upon injury (Llorens-Bobadilla et al., 2015; B. L. Marques et al., 2019) and neuroblasts derived from the SVZ can migrate towards the injured site and eventually differentiate into mature neurons (Jin et al., 2003; Yamashita et al., 2006). These important findings opened up new doors for therapeutic strategies to replace lost neurons. However, many challenges still lie ahead before finding a clinical application. First, adult neurogenesis remains restricted to defined regions in the adult mammalian brain, limiting its regenerative potential for other brain areas. Even if neuroblast migration towards the injured site can occur during brain damage, it is usually not accompanied by a functional recovery of lost functions. In addition, a progressive decline in adult neurogenesis has been directly associated with aging of the mammalian brain, which hinders a possible clinical application in age-related diseases. Finally, it is still a controversy whether adult neurogenesis also takes places in the human brain and whether it is regulated by the same molecular mechanisms (Kempermann et al., 2018; Moreno-Jiménez et al., 2021; Paredes et al., 2018; Sorrells et al., 2018), questioning whether these strategies could be used for repairing the human brain.

Taken together, unveiling the molecular mechanisms and functional implications of adult neurogenesis can contribute to understand how newborn neurons can integrate in mature neural circuits for potential regenerative applications. However, the intrinsic regenerative capacity of the adult brain remains very limited and it is crucial to find alternative strategies to replace lost neurons.

2.2. Cell replacement strategies in the CNS

Given the limited intrinsic regenerative potential of the CNS, cell replacement therapies have been extensively explored as an attractive alternative for brain repair. Over the past decades, multiple cell transplantation approaches have provided proof-of-principle evidence that grafted stem cell-derived neurons or progenitors can replace lost neurons in diseased brains, re-innervate damaged areas, release neurotransmitters and show partial functional recovery in some patients (Lindvall & Kokaia, 2010). Remarkably, landmark experiments conducted in the 90s showed that dopaminergic neurons derived from human foetuses were successfully transplanted into the striatum of Parkinson's Disease patients (Spencer et al., 1992), providing proof-of-concept for the viability of this strategy. More recently, research has focused on the use of human embryonic stem cells (hESCs) or induced pluripotent stem cells (iPSCs). These cells can be easily expanded *in vitro*, solving the issue of cell availability. Currently, iPSCs are the most common cell source used, since autologous transplantation prevents a possible immune rejection while also avoiding the ethical concerns raised by the use of human blastocysts. Because iPSCs can potentially differentiate into any cell type, they are a promising source for treating a wide range of neurological disorders where different cell populations are affected. Indeed, ongoing phase I/II clinical trials using patient-derived iPSCs are being conducted in patients with Parkinson's Disease (BRT-DA01) and retinal diseases, such as age-related macular degeneration (NCT04339764, NCT02286089 and NCT03178149) or retinitis pigmentosa (NCT03963154).

Multiple studies have successfully transplanted iPSCs-derived neurons in diseased animal models without any worrying side effects (Brot et al., 2022; Hallett et al., 2015; Nori et al., 2011; Yoon et al., 2020). However, several concerns emerge when using cell replacement therapies, the most alarming being the high risk of tumour formation. Although grafted cells undergo rigorous sorting processes prior to transplantation, undifferentiated cells may still be present and generate tumours. It is also possible that transplanted cells undergo dedifferentiation once grafted in the host tissue and become tumorigenic. Therefore, it is essential to ensure the homogeneity and stability of cells prior to transplantation.

In conclusion, pre-clinical studies have clearly indicated that cell-replacement approaches have a promising potential to treat numerous neurological disorders. However, these classical transplantation approaches still face major obstacles that

prevent their translation into clinically effective therapies (Lindvall, 2012). Thus, it is urgent to develop novel therapeutic approaches to address these unmet clinical needs.

2.3. Direct lineage reprogramming for brain repair

Cell identity of differentiated cells was initially defined as constant and irreversible (Waddington, 1957). Waddington's model suggested that cell lineage specification is like a marble rolling down a hill, where it encounters different bifurcations and has to choose which path to take until it reaches the end of the valley (Waddington, 1957). This metaphor makes reference of how cells coming from a pluripotent state make irreversible fate choices until they become differentiated cells (Amamoto & Arlotta, 2014; Waddington, 1957). A few years later, Gurdon challenged this model by demonstrating that transferring the nucleus of a differentiated tadpole gut cell into enucleated eggs could successfully give rise to adult frogs (Gurdon, 1962). This finding indicated that differentiated cells might be able to revert their identity and return to pluripotency. Based on this idea, the landmark study from Takashi and Yamanaka demonstrated that differentiated fibroblasts from adult mice could be successfully reprogrammed into iPSCs by ectopic expression of the transcription factors Oct3/4, Sox2, c-Myc and Klf4 (Takahashi & Yamanaka, 2006).

In parallel to these findings, another line of research demonstrated that terminally differentiated cells could be directly converted into other somatic cell types by ectopic expression of the bHLH transcription factor MyoD (Tapscott et al., 1988). This study showed that overexpression of MyoD1 could directly reprogram cultured mouse embryonic fibroblast into myocytes without undergoing through a pluripotent state (Tapscott et al., 1988). More recently, it has been shown that directly reprogrammed cells retain age-associated epigenetic signatures in fibroblast-derived human neurons (Mertens et al., 2015), opening new avenues for modelling epigenetic aging of neurodegenerative diseases and developing drug discovery platforms. However, using fibroblasts as a cell source for generating iNs has very limited potential for brain repair strategies, as they are only available at the perivascular space, meninges and choroid plexus of the brain (Dani et al., 2021; Vanlandewijck et al., 2018). For this reason, efforts have largely sought to find suitable alternative cell populations for the generation of directly reprogrammed iNs. In this context, glial cells emerged as an attractive option based on the idea that progenitors that give rise to neurons during development belong to the glial lineage – the RGCs. Based on this

idea, different lines of research started to investigate whether the potential of RGCs to generate neurons during reprogramming was retained by other cells of glial lineage, such as astrocytes or OPCs, in the postnatal and adult brain.

2.3.1. Glial cells as starting cell population for direct neuronal reprogramming

Finding the cell type that is the most suitable to undergo conversion into iNs is one of the main crucial milestones for *in vivo* reprogramming. The starting cell population of choice not only needs to be available at the right place, but it can also highly influence the conversion outcome. It is very likely that the gene expression profile and epigenetic signature of the source cell type will impose a specific molecular context in which the reprogramming factors have to operate. Additionally, it is also important to take into account that reprograming of brain resident glial cells into iNs may be accompanied by a partial depletion of the converted glial cell population. Hence, depending on the specific physiological role played by the source cell type targeted for reprogramming, this partial depletion could be beneficial and act in synergy with iNs to promote functional rescue or, on the opposite side, be detrimental and act against the therapeutic potential of iNs.

Astrocytes share a common progenitor with neurons – the RGCs. During cortical development, RGCs first generate neurons during embryonic stages (~E11-E17) followed by generation of astrocytes and subsequently OPCs that will continue locally expanding in postnatal stages to populate the cortex (Kriegstein & Alvarez-Buylla, 2009). Interestingly, RGCs possess molecular and cytological hallmarks of the astroglial lineage and exhibit a gene expression profile similar to astrocytes (Akimoto et al., 1993; Götz & Barde, 2005; Hartfuss et al., 2001). Moreover, over the past decade, several studies have indicated that neural stem cells (NSCs) in the adult brain could be considered a specialised type of astrocytes. In fact, they have demonstrated that when NSCs remain in quiescent state, their transcriptomic profile shares many similarities with that of astrocytes (Cebrian-Silla et al., 2021; Hartfuss et al., 2001; Zywitza et al., 2018). Remarkably, some recent studies have suggested that astrocytes entail a latent neurogenic programme that can be activated upon injury (Magnusson et al., 2014, 2020). Even more strikingly, cortical and striatal astrocytes have been suggested to be able to generate neuroblasts under an excitotoxic disease model in the absence of reprogramming factors (Nato et al., 2015; Yang et al., 2023). These data raise the

question of whether astrocytes may be dormant NSCs that can activate their stemness properties upon different situations of injury or disease, thus suggesting that they could potentially have the appropriate intrinsic context for their conversion into neurons. In this context, it is also important considering that astrocytes comprise a very heterogenous cell population. For many years, astrocyte classification was limited to morphological differences: fibrous astrocytes that reside in the white matter and protoplasmic astrocytes found in the grey matter of brain. More recently, RNA-sequencing profiling has revealed a great heterogeneity in the astrocyte population, even within the same brain regions (Batiuk et al., 2020). Interestingly, cortical astrocytes also display layer-specfic morphological and molecular features, which underlie layer-specific interaction between astrocytes and neurons (Bayraktar et al., 2015; Lanjakornsiripan et al., 2018). This diversity in the astrocyte population suggests that astrocytes within distinct cortical regions or layers may possess unique molecular contexts that could directly impact their susceptibility to reprogramming.

As an alternative to astroglia, OPCs emerge as a very attractive cell source for neuronal reprogramming due to their extensive self-renewal capability (Dimou et al., 2008), as it would bypass the potential risk of disrupting tissue homeostasis. Indeed, OPCs has been shown to be able to proliferate during the adulthood in physiological conditions (Hughes et al., 2013; Nishiyama et al., 2009), which would bring a great advantage for specifically targeting this cell population at different stages. Additionally, it is now well described that OPCs receive excitatory and inhibitory inputs from neurons in all brain regions (Bergles et al., 2000; Lin & Bergles, 2004; Orduz et al., 2015). Thus, the machinery required to establish synaptic contacts would be already in place, potentially facilitating the integration of newly generated iNs in the host circuitry. In response to acute injury in the cerebral cortex, OPCs react not only by rapidly migrating towards the injured site (Dimou & Götz, 2014) but also by fast and massive proliferation, which can increase approximately 90-times compared to their baseline proliferation in physiological conditions (Simon et al., 2011). Therefore, the homeostatic capacity of OPCs together with their close functional interaction with neurons during development and adult brain, suggest that using OPCs for neuronal reprogramming could bring advantages compared to other cell types.

Besides astrocytes and OPCs, microglia might also be considered as a potential candidate for generation of iNs. Microglia could be an interesting cell population to target in an injury context due to their intrinsic ability to migrate to the lesioned area. However, it is not known whether partially depleting the pool of microglia could help to control an exacerbated inflammatory response or, on the contrary, result

detrimental for regenerative purposes. In addition, microglia are derived from a different lineage to neurons, the myeloid lineage, which could impose certain barriers for instructing their conversion into iNs.

2.3.2. *In vitro* direct neuronal reprogramming

Pioneering work from the Götz lab showed for the first time that non-neurogenic astrocytes derived from the postnatal mouse cerebral cortex could be successfully converted into iNs via retrovirus-mediated expression of the transcription factor Pax6 (Heins et al., 2002) or the proneural transcription factors Neurog2 or Ascl1 (Berninger et al., 2007). Later on, another study demonstrated that the expression of the neurogenic fate determinants Neurog2 or Ascl1 together with Dlx2 could instruct postnatal astroglia to mature into iNs that established functional synapses and acquired neuronal subtype-specific identities (Heinrich et al., 2010). Importantly, differentiation into a specific phenotype could be regulated by the transcription factors employed: whereas Neurog2 instructed cortical astrocytes to convert into glutamatergic iNs, forced expression of Dlx2 induced a GABAergic identity (Heinrich et al., 2010, 2011). Employing fate-mapping approaches, this study could also reliably demonstrate conversion of lineage-traced cortical astrocytes into iNs. Later work showed that overexpression of alternative proneural transcription factors, such as NeuroD1, could also convert postnatal astrocytes into glutamatergic iNs (Guo et al., 2014) or combined expression of NeuroD4 and Insm1 (Masserdotti et al., 2015). In addition, postnatal astroglia could also be instructed to generate alternative neuronal fates, such as midbrain dopaminergic iNs, by forced co-expression of Ascl1, Lmx1b and Nurr1 (Addis et al., 2011). Besides achieving successful reprogramming of cortical astrocytes *in vitro*, further studies also demonstrated that Nerve/Glial antigen 2 (NG2) cells isolated from the postnatal mouse cerebral cortex could be reprogrammed into both glutamatergic and GABAergic iNs via overexpression of NeuroD1 (Guo et al., 2014). Interestingly, recent work also claimed that microglia, a glial cell type from a non-neural lineage, could also successfully reprogram into functional subtype-specific iNs (Matsuda et al., 2019).

From a translational point of view, an important question is whether the human brain also contains cells susceptible to lineage conversion. To address this question, pioneering work showed that pericytes isolated from cortical tissue of adult human patients could be instructed to generate human iNs by combined expression of Ascl1

and Sox2 (Karow et al., 2012, 2018). Whereas the majority of iNs acquired a forebrain GABAergic identity, a subset of Ascl1/Sox2-derived iNs activated a glutamatergic genetic programme. Interestingly, this line of work also showed that iNs undergo a transient neural stem cell-like programme during the process of direct conversion (Karow et al., 2018). These findings shed light on the possibility to use human cells for brain repair by identifying pericytes as novel candidates for lineage conversion. Later on, astrocytes isolated from human foetal cortex were successfully reprogrammed into human iNs after their transplantation in rat brains, providing proof-of-concept for conversion of human astrocytes into iNs within an *in vivo* context (Torper et al., 2013). Later studies corroborated that human foetal astrocytes could be reprogrammed into iNs *in vitro* by forced expression of alternative transcription factors, such as of NeuroD1 (Guo et al., 2014), or NeuroD4 alone or co-expressed with Insm1, Prox1 or Sox11 (Masserdotti et al., 2015). Generating human iNs that differentiate into distinct neuronal subtypes is crucial to develop therapies for neuronal diseases where a specific neuronal subpopulation is lost, as it is the case for Parkinson's disease. A combination of the transcription factors NeuroD1/Ascl1/Lmx1a together with the micro-RNA miR-218 and small molecules successfully converted human foetal astrocytes into dopaminergic iNs (Rivetti Di Val Cervo et al., 2017).

Besides the use of transcription factors to induce neuronal reprogramming, several groups have also succeeded converting human astrocytes into iNs using only a cocktail of small molecules. This strategy could be appealing for future clinical applications, as it would circumvent the use of retrovirus for transcription factor expression and avoid an invasive surgery to target the desired region. One study identified a combination of nine small molecules capable of converting human foetal astrocytes, but not mouse astrocytes, into iNs *in vitro* (L. Zhang et al., 2015). The selected compounds worked to block glial signalling, enhance neuronal differentiation pathways, increase survival and promote chromatin plasticity. Human astrocytes-derived iNs survived long-term in culture, acquired properties of glutamatergic neurons and were capable of network formation. In a posterior publication, the authors showed that combination of just four of the aforementioned molecules was sufficient to generate iNs at even greater efficiencies, which acquired glutamatergic or GABAergic identity depending on whether the astrocytes were of cortical or midbrain origin respectively (Yin et al., 2019). However, the selected chemical cocktail failed to induce neuronal conversion in the mouse brain *in vivo* (Yin et al., 2019; L. Zhang et al., 2015). One possible barrier that hinders glia-to-neuron conversion using small molecules is to keep them at a steady concentration in the brain. In addition, some of the challenges to

address during chemical reprogramming are to avoid off-target reprogramming after systemic administration of the small molecules and ascertain that prolonged exposure to chemicals on brain resident cells does not produce detrimental side-effects.

Altogether, these data showed that both mouse and human non-neuronal cells can be efficiently converted into functional and subtype-specific iNs *in vitro* by transcription factor-mediated expression or treatment with small molecules.

Brain region	Source cell	Species	Viral vector	Reprogramming factors	Phenotype	Reference
Cortex	Astrocytes	Mouse	RV	Pax6	Tuj1	(Heins et al., 2002)
Cortex	Astrocytes	Mouse	RV	Neurog2	Tuj1, Tbr1	(Berninger et al., 2007)
				Ascl1	Tuj1	
Cortex	Astrocytes	Mouse	RV	Neurog2	Glutamatergic	(Heinrich et al., 2010,)
				Dlx2 or Dlx2+Ascl1	GABAergic	
Cortex	Astrocytes	Mouse	LV	Ascl1+Lmx1b+Nurr1	Dopaminergic	(Addis et al., 2011)
Cortex	Astrocytes and OPCs	Mouse, human	RV	NeuroD1	Glutamatergic	(Guo et al., 2014)
Cortex	Astrocytes	Mouse, human	RV	NeuroD4 NeuroD4+Insm1 NeuroD4+Prox1	Glutamatergic/Tuj1	(Masserdotti et al., 2015)
Cortex	Microglia	Mouse	LV	NeuroD1	Glutamatergic and GABAergic	(Matsuda et al., 2019)
Cortex	Pericytes	Human	RV	Ascl1+Sox2	Glutamatergic and GABAergic	(Karow et al., 2012, 2018)
Cortex	Foetal astrocytes	Human	LV	Ascl1+Brn2a+Myt1l	hNCAM	(Torper et al., 2013)
-	Foetal astrocytes	Human	LV	NeuroD1+Ascl1+Lmx1a (+miR-218 and small molecules)	Dopaminergic neurons	(Rivetti Di Val Cervo et al., 2017)

Table 1.2. Summary of published studies recapitulating direct lineage reprogramming of resident brain cells into iNs *in vitro*. hNCAM, Human Neural Cell Adhesion Molecule; LV, Lentivirus; RV, Retrovirus, Tbr-1, T-Brain 1; Tuj1, Class III Beta-Tubulin.

2.3.3. *In vivo* direct neuronal reprogramming

Based on the successful studies demonstrating neuronal reprogramming *in vitro*, the quest for promoting neurogenesis *in vivo* rapidly became a main goal. Many studies sought to take advantage of retroviruses to target reactive glial cells that usually accompany acute brain injury and many neurological diseases (Dimou & Götz, 2014; Robel et al., 2011). Inhibition of Olig2 function or induction of Pax6 expression in reactive proliferative cells upon stab-wound injury promoted the generation of immature Dcx-expressing iNs in the adult mouse cerebral cortex (Buffo et al., 2005). Later studies demonstrated that retroviral-driven expression of Neurog2, but not Ascl1, was also able to induce Dcx-positive cells in the adult neocortex and striatum after stab-wound injury (Grande et al., 2013). At that time, the identity of cells that were targeted and successfully reprogrammed into iNs still remained unclear. Employing a genetic fate-mapping approach, it was shown a year later that proliferating OPCs could be instructed to convert into Dcx-expressing iNs by forced co-expression of Ascl1 and Sox2 in the adult mouse cortex upon stab-wound injury (Heinrich et al., 2014). Intriguingly, reactive cortical OPCs could also be converted into iNs by single expression of the transcription factor Sox2, regardless of its role in maintaining self-renewal of the neural stem cell pool. So far, only a small subset of iNs was able to mature and acquire expression of mature and subtype-specific neuronal markers (Heinrich et al., 2014). Using a retroviral construct encoding NeuroD1 under the control of glial fibrillary acidic protein (GFAP) or NG2 promoter, reactive astrocytes or OPCs in the stab-injured cortex or in an Alzheimer's disease mouse model could be converted into functional iNs that acquired neuronal subtype-specific identities (Guo et al., 2014). Further studies showed that combining expression of Neurog2 and B-Cell Leukemia/Lymphoma 2 (Bcl2) in glial cells induced their conversion into NeuN-positive iNs following cortical stab injury (Gascón et al., 2016). Interestingly, an additional treatment with vitamin D receptor ligand or vitamin E promoted iNs maturation into Ctip2-expressing cells (Gascón et al., 2016). More recently, another study showed that reactive glia can be instructed to reprogram into GABAergic-like iNs in the epileptic hippocampus by retroviral-mediated expression of Ascl1 and Dlx2 (Lentini et al., 2021). Importantly, glia-derived iNs were able to integrate into the hippocampal network and reduced epileptic seizures (Lentini et al., 2021).

In parallel, another line of work sought to achieve neuronal reprogramming using non-proliferative glial cells. Employing Cre-recombinase lentivirus encoding Ascl1, Brn2a and Myt1l, astrocytes reprogrammed towards a neuronal identity in the

striatum of GFAP-Cre mice (Torper et al., 2013). The same group showed later that directing the expression of Ascl1, Lmx1a and Nurr1 to striatal OPCs using Cre-recombinase adeno-associated virus (AAV) vectors induced their conversion into glutamatergic and GABAergic iNs (Torper et al., 2015). Additional studies reported that lentiviral-mediated expression of Sox2 was sufficient to convert adult mouse quiescent striatal astrocytes into Ascl1-expressing neural progenitor which subsequently acquired neuroblast identity and expressed Dcx (Niu et al., 2013, 2015)

Given the successful conversion outcomes achieved using lentiviral and AAV recombinant systems to deliver reprogramming factors in the desired cell type, many other studies continued employing this strategy to induce glia-to-neuron conversion in injury and disease models. Using a mouse model of Parkinson's disease, Tet-regulated lentiviruses encoding Ascl1, NeuroD1, Lmx1a and miR-218 induced the appearance of dopaminergic iNs in the lesioned striatum of GFAP-tTa mice (Rivetti Di Val Cervo et al., 2017). These iNs acquired the expression of midbrain markers, such as tyrosine hydroxylase (TH) or dopamine transporter (DAT). Although few of them displayed electrophysiological properties characteristic of this population, the authors reported improved motor functions in lesioned mice. However, a parallel study using the same animal model reported the spontaneous appearance of TH+ neurons in the lesioned striatum, casting doubt on the actual origin of these cells (Pereira et al., 2017). In the same study, the authors used Cre recombinase-dependent AAV vectors to convert OPCs into fast-spiking interneurons in the lesioned striatum. Intriguingly, iNs were strongly committed to an interneuron identity regardless of the combination of proneural factors (Neurog2, Ascl1, NeuroD1) and dopaminergic fate determinants (Nurr1, FoxA2, Lmx1a, En1) employed (Pereira et al., 2017). Later on, injecting FLEx switch AAV vectors encoding Neurog2 and Nurr1 in the stab-injured cortex, the Götz lab managed to convert both quiescent and proliferating cortical astrocytes into glutamatergic iNs that acquired hallmark layer-specific identities according to their laminar position (Mattugini et al., 2019). Using the same vectors but solely encoding the single transcription factor NeuroD1, the Chen lab claimed to achieve very efficient cortical and striatal astrocyte-to-neuron conversion in multiple models of ischemic injury and neurodegenerative disease mouse models (Chen et al., 2020b; Puls et al., 2020; Tang et al., 2021). Remarkably, these studies reported regeneration of lost neurons and functional recovery of lost functions, even in a model of adult non-human primates (L. J. Ge et al., 2020).

Brain region	Source cell	Injury model	Viral vector	Reprogramming factors	Phenotype	Reference
Cortex	Reactive glia	SWI	RV	Pax6 or Olig2 repression	Dcx	(Buffo et al., 2005)
Cortex, striatum	Reactive glia	SWI/ ischemia	RV	Neurog2	Dcx	(Grande et al., 2013)
Cortex	Reactive OPCs	SWI	RV	Ascl1+Sox2	Dcx	(Heinrich et al., 2014)
Cortex	Reactive astrocytes & OPCs	SWI/ Alzheimer's	RV	NeuroD1	Tuj1, NeuN	(Guo et al., 2014)
Cortex	Reactive glia	SWI	RV	Neurog2+Bcl2	NeuN	(Gascón et al., 2016)
Hippocampus	Reactive glia	KA	RV	Ascl1+Dlx2	GABAergic	(Lentini et al., 2021)
Striatum	Astrocytes	-	LV	Ascl1+Brn2a+Myt1l	NeuN	(Torper et al., 2013)
Striatum	OPCs	-	AAV	Ascl1+Lmx1a+Nurr1	Glutamatergic, GABAergic	(Torper et al., 2015)
Striatum	Astrocytes	-	LV	Sox2	Dcx	(Niu et al., 2013, 2015)
Striatum	Astrocytes	6-OHDA	LV	Ascl1+NeuroD1+Lmx1a (+miR-218)	Dopaminergic	(Rivetti Di Val Cervo et al., 2017)
Striatum	OPCs	6-OHDA (+/-)	AAV	Ascl1/Neurog2+Lmx1a+Nurr1; Ascl1+Neurog2+Nurr1; Neurog2+NeuroD1; Ascl1+FoxA2+Lmx1a+En1	GABAergic	(Pereira et al., 2017)
Cortex	Astrocytes	SWI	AAV	Neurog2+Nurr1	Glutamatergic	(Mattugini et al., 2019)
Cortex, striatum	Astrocytes	Ischemia, SCI, stroke	AAV	NeuroD1	Glutamatergic	(Chen et al., 2020a; L. J. Ge et al., 2020; Puls et al., 2020; Tang et al., 2021)

Table 1.3. Summary of published studies recapitulating direct lineage reprogramming of resident brain cells into iNs *in vivo*. 6-OHDA, 6-hydroxydopamine; AVV, Adeno-Associated Virus; KA, Kainic Acid; LV, Lentivirus; OPCs, Oligodendrocyte Progenitor Cells; RV, Retrovirus; SCI, Spinal Cord Injury; SWI, Stab-wound Injury, Tuj1, Class III Beta-Tubulin.

These astonishing results would mean a huge advance towards the application of direct lineage reprogramming as a therapeutic strategy for brain repair. However, recent studies have raised serious scepticism about the glial origin of the putative iNs due to the use of genetic tools employed to target transgene expression specifically to glial cells (L. L. Wang et al., 2021a). In this report, the Zhang lab tested various AAV-based strategies previously used to claim efficient *in vivo* glia-to-neuron conversion. First, the authors investigated whether putative iNs originated from proliferating reactive astrocytes in the adult injured brain had incorporated the nucleoside analogue bromodeoxyuridine (BrdU). However, they could not find any evidence for this, hence demonstrating that putative iNs do not derive from cells that were proliferating prior reprogramming. Interestingly, the Chen lab fought back this argument by reporting that BrdU incorporation inhibited the process of glia-to-neuron conversion (T. Wang et al., 2022). Second, the Zhang lab showed the absence of immature phenotypes or intermediate neuronal states expressing Dcx, suggesting that the process of glia-to-neuron conversion, if authentic, occurs without undergoing through immature neuronal states. Third, the authors used robust fate-mapping strategies to achieve irreversible labelling of astrocytes in the Aldh1l1-CreERT2 mouse line crossed with the R26R-YFP reporter mouse line. The putative reprogrammed neurons did not express the reporter gene from the mouse line, strongly indicating that they do not derive from astrocytes. Finally, this study also used a retrograde labelling strategy to trace endogenous neurons, which revealed that this population was the cell source for the alleged iNs. Overall, this work indicates that AAV vectors lose glial specificity over time and gradually induce reporter expression in endogenous neurons.

Taken together, numerous studies have provided proof-of-principle evidence for direct neuronal reprogramming *in vivo*. However, it is crucial to demonstrate the authenticity of fate switch during lineage conversion by developing the correct tools.

2.3.4. Direct neuronal reprogramming in the postnatal mouse cerebral cortex

Many of the aforementioned studies exploited the heightened cellular plasticity of glial cells acquired during proliferation after inducing an injury. Glial cells do not proliferate in the adult brain, or they do it at very low rates, during physiological conditions (Buffo et al., 2005; Burns et al., 2009). Exploring direct lineage reprogramming in injury or disease models is essential to develop therapies to restore neuronal loss following a lesion. However, it is similarly important to study how fate switch takes place in the

healthy brain to fully understand the basis of neuronal reprogramming. Over the past few years, our laboratory and collaborators have developed a model to investigate direct neuronal reprogramming taking advantage of the potentially enhanced plasticity of glial cells during physiological proliferation in the postnatal cortex. As previously described at the beginning of this section, neurogenesis takes place during embryonic cortical development whereas glial cells expand by local division in the cortex during the first postnatal weeks (Clavreul et al., 2019; W. P. Ge et al., 2012). Given that retroviruses can only transduce cells undergoing division, retrovirus-mediated delivery of reprogramming factors in the postnatal cortex would specifically target proliferating glial cells. Retroviruses specifically integrate their genome into proliferating cells as they can only access the chromatin in cells whose nuclear envelope is dissembled.

Using this strategy, recent work showed that retrovirus encoding Neurog2 and Bcl2 instructed proliferating postnatal glia to convert into iNs that acquired region-specific identities in the cortex (Herrero-Navarro et al., 2021). In addition, this study observed that the majority of cells targeted with retrovirus in the postnatal cortex were astrocytes. Work from our laboratory using the same model corroborated that retrovirus predominantly targeted astroglia and additionally showed that the remaining transduced cells accounted for Sox10-positive oligodendrocytes (Galante et al., 2022). In both studies, control retrovirus did not transduce any cells expressing neuronal markers, providing robust evidence for the reliability of the model. Interestingly, retrovirus-mediated expression of Ascl1 failed to convert postnatal glia into iNs in the cortex, but enhanced OPCs proliferation (Galante et al., 2022).

Unpublished data from our laboratory has shown through whole-cell patch-clamp electrophysiological recordings (performed by Dr. Nicolas Marichal) that postnatal proliferating glia co-transduced with Ascl1 and Bcl2 only had the ability to generate a single small spike in response to a sustained depolarisation at 12dpi (Fig. 1.3A, E). In sharp contrast, co-transduced cells with Ascl1SA6, a phospho-site mutant of Ascl1, together with Bcl2 were able to fire well-developed action potentials repetitively in response to depolarisation (Fig. 1.3B, E). Remarkably, half of the recorded cells exhibited a sustained high-frequency firing reaching values up to 150 Hz (Fig. 1.3B, E), a distinctive feature of cortical fast-spiking interneurons (Hu et al., 2014). Additionally, voltage-clamp recordings showed that most cells co-transduced with Ascl1 or Ascl1SA6 together with Bcl2 exhibited spontaneous excitatory postsynaptic currents (sESPC) (Fig. 1.3C-D), suggesting their integration in the local pre-existing neuronal circuitry. However, frequency and amplitude of sESPC was higher in iNs generated by overexpression of Ascl1SA6 and Bcl2 (Fig. 1.3F).

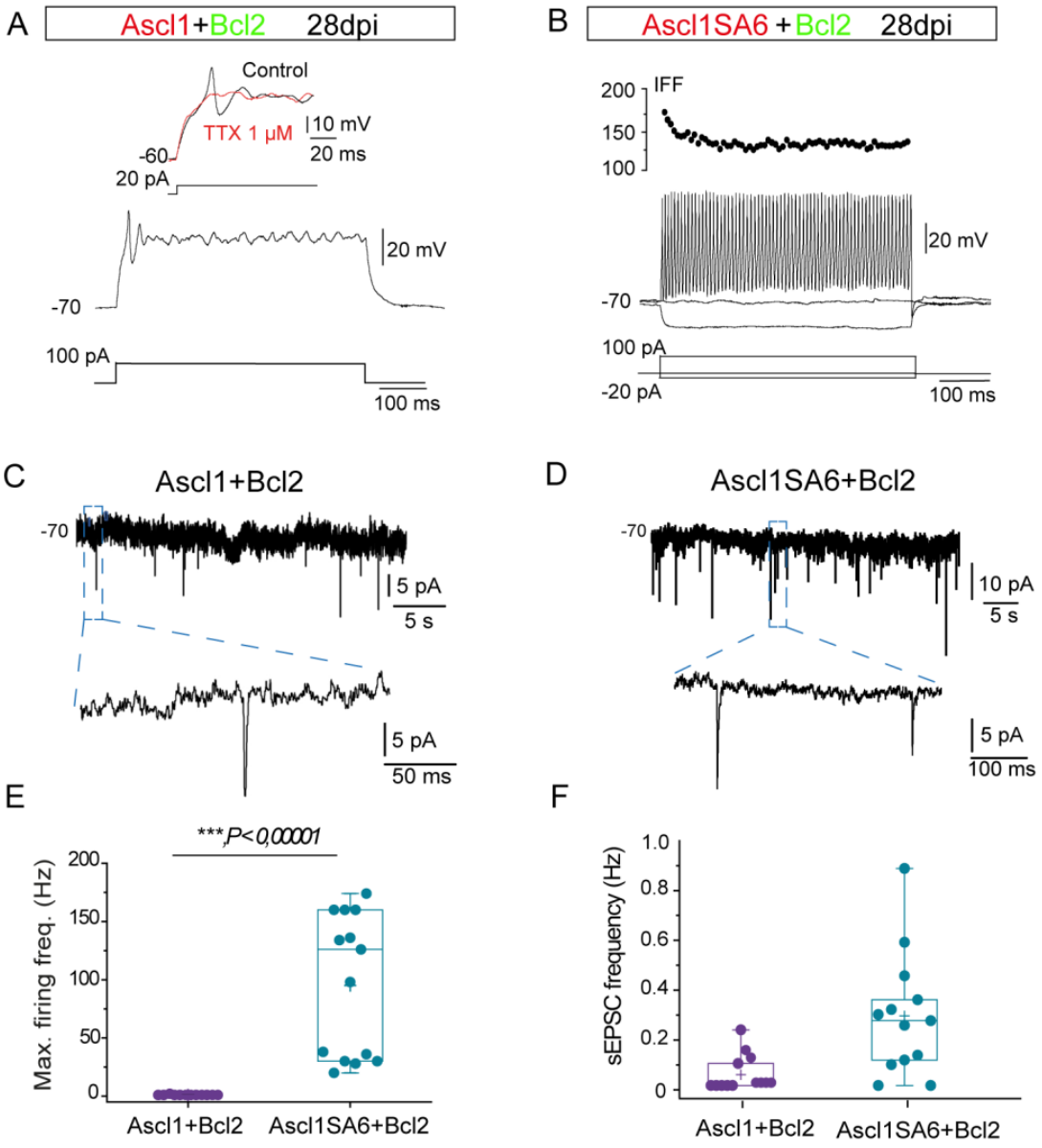

Figure 1.3. Electrophysiological properties of co-transduced cells with Ascl1 or Ascl1SA6 and Bcl2. (A) Current-clamp recording of a cell co-transduced with Ascl1+Bcl2 showing the generation of a single small spike in response to depolarisation. (B) Current-clamp recording of a cell co-transduced with Ascl1SA6+Bcl2 exhibiting high-frequency firing in response to depolarisation. (C) Voltage-clamp recording of a cell co-transduced with Ascl1SA6+Bcl2 exhibiting sESPC. (D) Voltage-clamp recording of a cell co-transduced with Ascl1SA6+Bcl2 exhibiting sESPC. (E) Graph showing the maximum firing frequency (Hz) of recorded cells co-transduced with Ascl1+Bcl2 or Ascl1SA6+Bcl2. (F) Graph showing sESPC frequency (Hz) of recorded cells co-transduced with Ascl1+Bcl2 or Ascl1SA6+Bcl2.

Based on these exciting findings as a starting point for my thesis, I have exploited the postnatal mouse cortex model as a robust experimental model to study glia-to-interneuron conversion (Fig. 1.4). Given the evidences suggesting that Ascl1SA6 and Bcl2 synergise to convert postnatal glia into functional fast-spiking iNs, I further investigated whether the combinatorial expression of these reprogramming factors generate distinct subclasses of interneuron-like iNs. Additionally, I have explored other candidate reprogramming factors and strategies to improve glia-to-interneuron conversion in the postnatal mouse cortex.

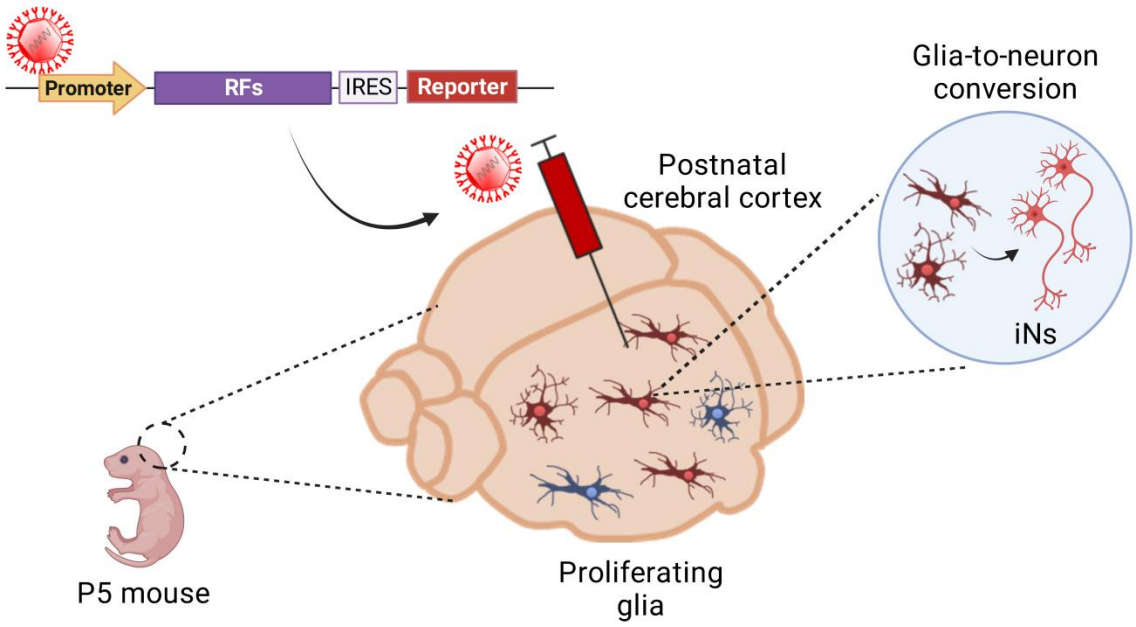

Figure 1.4. Glia-to-neuron conversion in the postnatal mouse cerebral cortex. Retroviruses encoding for candidate reprogramming factors are injected in the postnatal mouse cerebral cortex. Given that the postnatal cortex is devoid of physiological neurogenesis and only glial cells undergo local proliferation, retroviruses will specifically transduce dividing glia. Transduced glial cells will overexpress the selected reprogramming factors and may eventually convert into induced neurons (iNs).

Objectives

Engineering iNs from other resident brain cells emerges as an innovative approach towards achieving neuronal restoration in brain regions devoid of intrinsic regenerative capacity. Since pioneering *in vitro* studies (Berninger et al., 2007; Heinrich et al., 2010; Heins et al., 2002), considerable progress in the field has provided proof-of-principle evidence for the conversion of various resident glial cell types into iNs in different brain regions *in vivo* (Gascón et al., 2016; Grande et al., 2013; Heinrich et al., 2014; Herrero-Navarro et al., 2021; Lentini et al., 2021). However, demonstrating authentic and efficient generation of functional subtype-specific iNs *in vivo* remains a main challenge.

In the present work, I aimed to address these questions in the context of the postnatal mouse cortex as an experimental model to study glia-to-neuron conversion *in vivo*. The main goals of my PhD thesis are the following:

Aim 1. Generate glia-derived induced interneurons via transcription factor-mediated lineage reprogramming in the postnatal mouse cerebral cortex. Retroviruses encoding candidate genes that play an important role for interneuron specification during development were injected in the postnatal day 5 (P5) mouse cortex in order to specifically target proliferative glial cells. The successful conversion of glial cells into interneuron-like iNs was analysed by the acquisition and analysis of subtype-specific neuronal markers.

Aim 2. Demonstrate the authenticity of glial origin during *in vivo* lineage reprogramming. Robust fate-mapping strategies were used to demonstrate the proliferative glial origin of iNs in the postnatal mouse cerebral cortex.

Aim 3. Investigate chemogenetic-mediated stimulation of iNs. Selective chemogenetic activation of iNs expressing hM3Dq was used to study activity-dependent modulation of iNs during lineage conversion.

MATERIALS & METHODS

1. Mice

All animal procedures were approved by the ethical committee of King's College London and conducted under Home Office personal and project licenses (project license number PD025E9BC) following the UK Animals (Scientific Procedures) 1986 Act. Mice were maintained under standard, temperature controlled, laboratory conditions, and kept on a 12:12 light/dark cycle and received food and water *ad libitum*. Mice were housed in groups of up to five littermates per cage after weaning.

Male and female C57BL/6J were purchased from Charles River Laboratories (Walden, UK) and bred in house. To assess the acquisition of an interneuron-like phenotype by reprogrammed cells, mice in which the expression of Cre recombinase is driven by Vesicular GABA transporter (Vgat) promoter (Vgat-Cre, JAX028862) (Vong et al., 2011) (provided by Prof. Oscar Marin) were crossed with an EGFP reporter mouse line (RCE-floxed, JAX032037) (Sousa et al., 2009) to generate double transgenic mice (Vgat-Cre/RCE). For fate-mapping experiments, mice in which the expression of Cre recombinase is driven by mouse GFAP promoter (mGFAP-Cre, JAX024098) (Gregorian et al., 2009) or in which tamoxifen-inducible Cre recombinase is driven by the aldehyde dehydrogenase 1 family member L1 locus (Aldh1l1) (Aldh1l1-Cre/ERT2, JAX031008) (Srinivasan et al., 2016) or the mouse NG2 promoter (NG2-CreERTM, JAX008538) (Zhu et al., 2011) were crossed with the aforementioned EGFP reporter mouse line (RCE-floxed, JAX032037) (Sousa et al., 2009) to generate double transgenic mice (GFAP-Cre/RCE, Aldh1l1-CreERT2/RCE or NG2-CreERTM/RCE).

Both male and female mice were used in all experiments. Injection of retroviruses in the postnatal mouse cortex was performed from P4 to P6. For histological analyses, mouse ages range from P17 to P33.

1.1 Tamoxifen administration

In the Cre-inducible transgenic mice lines Aldh1l1-Cre/ERT2/RCE or NG2-CreERTM/RCE, tamoxifen was administered to conditionally allow the expression of EGFP in astrocytes and OPCs during postnatal development respectively. Tamoxifen (ApexBio Technology, #B5965) was dissolved in corn oil (Sigma-Aldrich, #C8267) at 37°C with constant agitation at a final concentration of 6mg/ml. A dose of 150mg/kg of tamoxifen was administered via subcutaneous injection into postnatal NG2-iCreERT2/GFP mouse pups at the ages of P2 and P5, and into postnatal Aldh1l1-Cre/ERT2 daily from P2 to P5.

1.2 Genotyping

When required, genotyping of the litter was performed prior to the experimental procedure to cull off mice of unwanted genotype. Mouse genomic DNA was extracted from tail biopsies (pups <P10) or ear (mice >P10) biopsies. The tissue was digested in 75 µl of 1X Lysis Buffer (250mM NaOH, Sigma-Aldrich #S5881 and 0.2mM ethylenediaminetetraacetic acid, EDTA, Sigma-Aldrich #E8008) and heated at 95ºC for 1 hour while shaking in a ThermoMixer. Then, 75 µl of 1X Neutralisation Buffer (0.4M Trizma® hydrochloride, HCl, Sigma-Aldrich # T15760) was added to the solution and centrifuged at maximum in a microfuge for 1 minute to remove the undissolved component.

A standard PCR programme was used to amplify the allele of interest for each transgenic mouse line (Table 2.1). To this end, 1 µl of extracted genomic DNA was added to each 19 µl of PCR reaction mixture containing 1X PCRBIO Taq Mix Red (Taq DNA Polymerase, 6mM MgCl2, 2mM dNTPs, enhancers, stabilisers, and red dye) (PCRBiosystems, #PB10.23) and specific forward and reverse primers at a concentration of 10 µM each to target the allele of interest. The PCR reaction was carried out in a thermocycling PCR machine with heated lid (Eppendorf nexus X2). The primer sequences, the expected size of DNA bands and the PCR programmes used for genotyping each transgenic mouse line are reported in Table 2.1.

Finally, PCR products were run in an electrophoresis chamber (Bio Rad, Sub-Cell GT Cell) at 100V in a 2-3% agarose gel to separate and detect the amplified DNA sequences of interest. The agarose gel was made in 1X Tris-acetate-EDTA (TAE) from a 50X stock solution containing 50mM EDTA disodium salt (Sigma-Aldrich E5134), 2M Tris (Invitrogen 15504-020), and 1M acetic acid (Sigma-Aldrich ARK2183). Then, 1X SYBRTM Safe DNA Gel Stain (ThermoFisher S33102) was added to label the DNA fragments on the agarose gel. The bands were then visualised using the SyngeneTM NuGenius Gel Documentation System.

Transgenic mouse line	Targeted allele	Primers (5'-3')	Length of PCR product	PCR programme
Aldh1l1-CreERT2/RCE	Aldh1l1	**F**: GGCAAACGGACAGAAGCA **R**: CTTCAACAGGTGCCTTCCA	198 bp	94°C 2 Min Denature 94°C 20 Sec Denature 60°C 15 Sec **X10** Anneal 68°C 10 Sec Extend 94°C 15 Sec Denature 60°C 15 Sec **X28** Anneal 72°C 10 Sec Extend 72°C 2 Min Extend
mGFAP-Cre/RCE	mGFAP	**F**:TCCATAAAGGCCCTGACATC **R**:TGCGAACCTCATCACTCGT	400 bp	94°C 2 Min Denature 94°C 30 Sec Denature 65°C 45 Sec **X10** Anneal 68°C 45 Sec Extend 94°C 30 Sec Denature 60°C 45 Sec **X28** Anneal 72°C 45 Sec Extend 72°C 10 Min Extend
NG2-iCreEsr1/RCE	Cre	**F**:TCCATAAAGGCCCTGACATC **R**:TGCGAACCTCATCACTCGT	100 bp	94°C 2 Min Denature 94°C 15 Sec Denature 65°C 15 Sec **X10** Anneal 68°C 30 Sec Extend 94°C 15 Sec Denature 60°C 15 Sec **X28** Anneal 72°C 30 Sec Extend 72°C 2 Min Extend

Table 2.1. Details of the primers, the expected size of PCR products and the PCR programmes used for genotyping transgenic mouse lines.

2. Generation of plasmids and retroviral particles

2.1 Plasmid cloning

For the expression of neurogenic transcription factors in astroglial cells, we used self-inactivating retroviral vectors based on the Moloney Murine Leukemia Virus (MMLV), which contain a deletion of the U3 region to hamper the viral promoter and enhancer activity in their 3′ long terminal repeat (LTR) (Naviaux et al., 1996). After the first viral replication, the deletion in the U3 region of the 3'LTR self-inactivates the promoter activity of the 5'LTR, which reduces the potential risk of activation of neighbouring genes and offers the possibility to choose the promoter for driving transgene expression. Expression of the genes of interest (Ascl1, Acl1SA6, Dlx2 or DREADD) was driven under control of an internal CAG promoter, which contains the chicken β-actin promoter with the cytomegalovirus (CMV) early enhancer element and a large synthetic intron optimized for strong and long-term expression. The genes of interest were linked to a fluorescence reporter (either GFP or DsRed) located downstream an internal ribosome entry site (IRES) allowing for simultaneous reporter gene expression as previously described (Heinrich et al., 2011) (Fig. 2.1). To enhance viral gene expression, a Woodchuck Hepatitis Virus Posttranscriptional Regulatory Element (WPRE) was located downstream the reporter gene sequence. As a negative control, glial cells were transduced with a virus encoding only DsRed downstream an IRES site driven by the same CAG promoter described above. Generation of pCAG-IRES-DsRed, pCAG-Ascl1-IRES-DsRed, pCAG-Ascl1SA6-IRES-DsRed and pCAG-hM3Dq-IRES-GFP retroviral constructs was performed by previous lab members. The retroviral constructs pCAG-Dlx2-IRES-DsRed and pCAG-Ascl1-P2A-Dlx2-IRES-DsRed were a kind gift of Prof. Christophe Heinrich (Heinrich et al., 2011; Lentini et al., 2021). The retroviral construct for the expression of human Bcl2 (5'LTR-hBcl2-IRES-GFP) was a kind gift of Prof. Sergio Gascón (Gascón et al., 2016) and contains a 5'LTR that functions as a promoter for the gene of interest.

To generate the tri-cistronic retroviral vectors pCAG-Ascl1-T2A-Bcl2-IRES-DsRed and pCAG-Ascl1SA6-T2A-Bcl2-IRES-DsRed, I synthesised a fusion sequence containing both reprogramming factors flanked by restriction enzyme cutting sites and linked by a T2A region. First, I separately amplified *Ascl1* and *Ascl1SA6* sequences by PCR from single plasmids encoding these genes. *Ascl1* and *Ascl1SA6* genes were amplified using a forward primer with a flanking sequence containing the restriction enzyme site KpnI and a reverse primer lacking the STOP codon of the *Ascl1* and

Ascl1SA6 genes (Table 2.2). *Bcl2* gene was amplified together with a T2 sequence using a tri-cistronic already available in the lab encoding *Neurog2* and *Bcl2* genes that were linked by a T2A region (pCAG-Neurog2-T2A-Bcl2-IRES-DsRed). To this end, I used a forward primer binding to the beginning of a GSG linker region flanking the T2A sequence and a reverse primer with an overhanging sequence containing the restriction enzyme site XhoI (Table 2.2). The *Ascl1* and *Ascl1SA6* reverse primer and the (GSG)T2A-*Bcl2* forward primer contained overlapping sequences. Subsequently, the PCR products were purified by electrophoresis using the Monarch DNA Gel Extraction Kit (New Englad Biolabs, #T1020S). Then, I carried a fusion PCR to link both fragments using Q5 High-Fidelity DNA Polymerase (New Englad Biolabs, #M0491). The PCR products were inserted in the multiple cloning site of the pENTRY1A Dual Selection plasmid (Thermo Fisher Scientific, #A10462) using the KpnI and XhoI restriction enzyme sites. Finally, the donor vector containing attL and attB sites allowed recombination between the pENTRY1A vector and the destination vector by Gateway LR Clonase II catalysis (Thermo Fisher Scientific, #11791020). This resulted in the insertion of the genes of interest in the destination vector, allowing polycistronic expression of the reprogramming factors together with DsRed downstream of IRES under control of the CAG promoter (Fig. 2.1).

Original plasmid used	Targeted sequence	Primers
pCAG-Ascl1-IRES-DsRed	Ascl1	F: cagtcgactggatccggtacATGGAGAGCTCTGGCAAG R: ctccgcttccGAACCAGTTGGTAAAGTCC
pCAG-Ascl1SA6-IRES-DsRed	Ascl1SA6	F: cagtcgactggatccggtacATGGAGAGCTCTGGCAAG R: ctccgcttccGAACCAGTTGGTAAAGTCC
pCAG-Neurog2-T2A-Bcl2-IRES-DsRed	(GSG)T2A-Bcl2	F: caactggttcGGAAGCGGAGAGGGCAGA R: gaaagctgggtctagatatcTCACTTGTGGCCCAGATAGG

Table 2.2. Original plasmids and primers used to amplify genes of interest for cloning of tri-cistronic vectors.

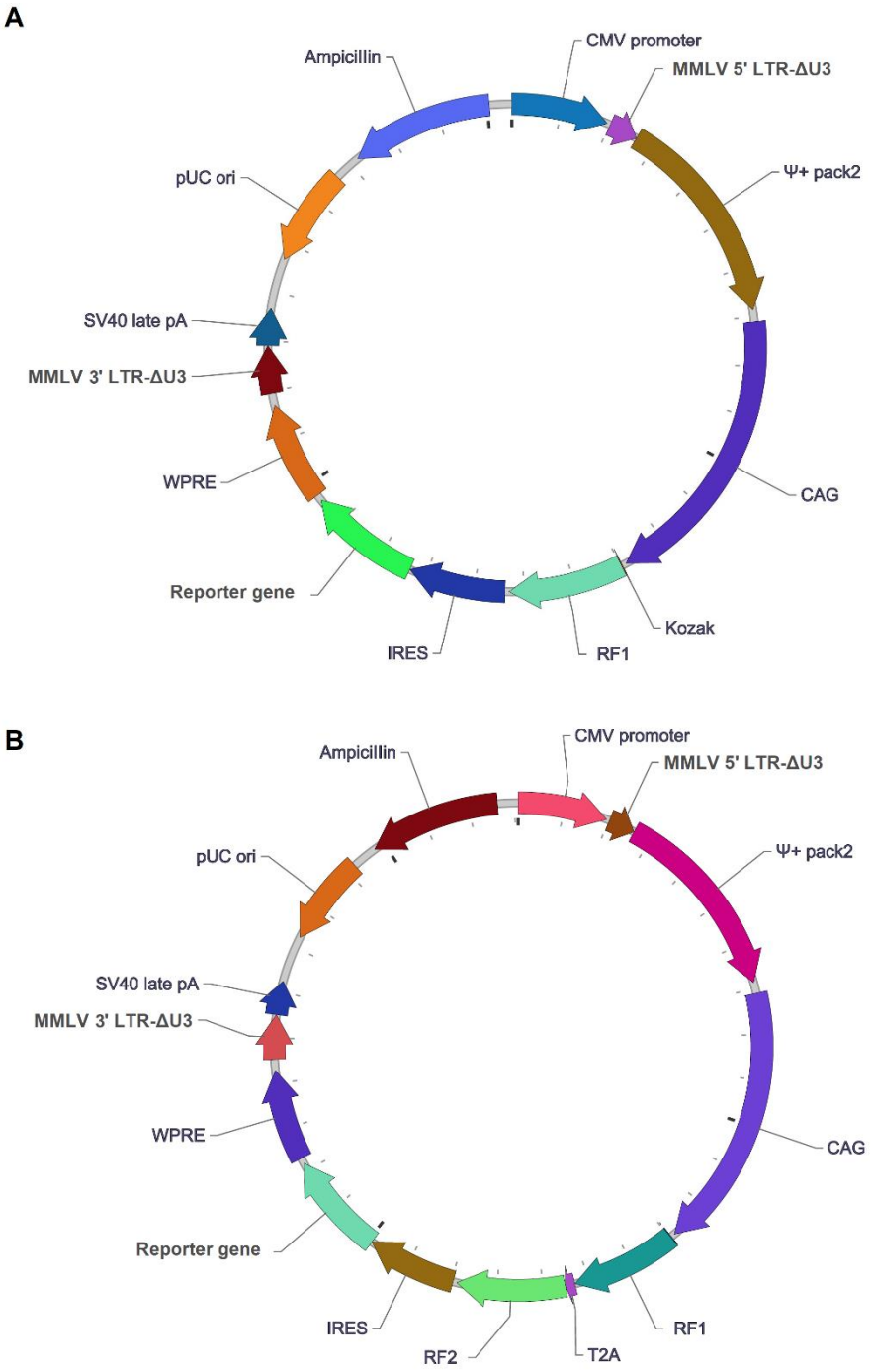

Figure 2.1. Maps of retroviral constructs used for direct lineage reprogramming. (A) Expression of reprogramming factors was driven under control of an internal CAG promoter, which contains the chicken β-actin promoter with the cytomegalovirus early enhancer element and a synthetic intron optimized for strong and long-term expression. The genes of interest were linked to a fluorescence reporter (either GFP or DsRed) located downstream an IRES sequence allowing for simultaneous reporter gene expression. (B) Polycistronic retroviral vectors allowed for expression of multiple reprogramming factors linked by the self-cleavage T2A region. CAG, Chicken β-actin Promoter; CMV, cytomegalovirus; IRES, Internal Ribosome Entry Site; MMLV, Moloney Murine Leukemia Virus; RF, reprogramming factor; WPRE, Woodchuck Hepatitis Virus Posttranscriptional Regulatory Element.

Retroviral construct	Insert size (bp)	Viral titre
CAG-IRES-DsRed	No insert (control)	6.58E+07
CAG-Ascl1-IRES-DsRed	696	8.28E+06
CAG-Ascl1SA6-IRES-DsRed	696	5.87E+08
CAG-Ascl1-T2A-Bcl2-DsRed	1476	6.71E+07
CAG-Ascl1SA6-T2A-Bcl2-DsRed	1476	7.97E+07
5'LTR-Bcl2-IRES-GFP	720	2.97E+06
5'LTR-Bcl2-IRES-Cre	720	1.13E+06
CAG-Dlx2-IRES-GFP	978	2.03E+07
CAG-Ascl1-T2A-Dlx2-DsRed	1755	1.11E+06
CAG-Ascl1SA6-T2A-Dlx2-DsRed	1755	1.85E+07
CAG-hM3Dq-IRES-GFP	1781	4.91E+06

Table 2.3. List of retroviral constructs used for direct lineage reprogramming, including the insert size and the viral titres.

2.2 Preparation of DNA plasmids for retroviral production.

A competent strain of *Escherichia coli*, named as DH5*alpha*, was transformed with purified DNA plasmid and plated in LB agar (Thermo Fisher Scientific #22700025) containing 100µg/ml Ampicillin (Sigma-Aldrich #A5354). Positive colonies were inoculated in LB medium (Sigma-Aldrich #G5516) for 12-16h at 37°C while shaking for amplification. To isolate the expression plasmids, bacterial suspensions were first pelleted by centrifugation and, subsequently, the plasmid DNA was extracted and purified via anion-exchange column chromatography using the commercial kit PureLink™ HiPure Plasmid DNA Maxiprep kit (Thermo Fisher Scientific, #K210007) according to the manufacturers' instructions, which allows the preparation of high-quality and high-purity DNA. The DNA concentration was measured using a NanoDrop™ 2000/2000c (ND-2000). To confirm the correct insertion of the gene of interest, all plasmids were sent to sequence by GeneWiz. The primers used for sequencing were the following: 5'-CGTGTGACCGGCGGCTCTA-3', 5'-CCAGTCAATCTTTCACAA-3', 5'-CCTCACATTGCCAAAAGACG-3' and 5'-TGGCTCTCCTCAAGCGTATT-3'.

2.3 Production of retroviral particles

Retrovirus were used to transduce proliferating glial cells in the postnatal mouse cortex due to their ability to integrate their viral genome into dividing cells only. Retrovirus lack the pre-integration complex and nuclear import system required to access the nucleus and mediate the integration of the viral genome into the host cell genome. For this reason, retrovirus require a nuclear envelope disassembly, which only occurs during cell division, to access the host genome (Roe et al., 1993). For retrovirus particle production, we used VSV-G (Vesicular Stomatitis Virus-Glycoprotein)-pseudotyped gamma-retroviral vectors as described in previous studies from our laboratory (Galante et al., 2022). Retroviral particles were produced using a CAG-driven MMLV (Moloney Murine Leukemia Virus)-based retroviral expression plasmid, and a stable packaging cell line 293GPG, named 1F8, expressing MLV gag-pol and VSV-G under Tet-off control (Ory et al., 1996). 1F8 cells were cultured in Growth Medium containing DMEM/F12 (Thermo Fisher Scientific #21331020), 10% Fetal Bovine Serum (FBS) (Thermo Fisher Scientific #10106-169) and 1X Glutamine (Thermo Fisher Scientific #25030024) supplemented with the following antibiotics: Puromycin (2µg/ml) for selection of the integrated VSV-G gene and the transactivator tetR/VP16; G418 Sulfate (Geneticin; 0.3 mg/ml) for selection of the MLV genome *(gag-pol*) and Tetracyclin (2µg/ml) for inhibition of the VSV-G gene. Cells were kept in culture at 37°C with 5% CO2 and passaged via trypsinisation and resuspension when at 70-80% confluency.

For retroviral production, 1F8 cells were seeded at ~10^7 cells/plate in Plating Medium containing DMEM (Thermo Fisher Scientific #11960), 10% FBS (Thermo Fisher Scientific #10106-169), 1X Glutamine (Thermo Fisher Scientific #25030024); 1X NEAA (Thermo Fisher Scientific #11140050); 1X Na-Pyruvate (Thermo Fisher Scientific #11360070) supplemented with 0.5 µg/ml Tetracycline. The following day, the Plating Medium was replaced with fresh medium lacking Tetracycline antibiotic to allow VSV-G expression. Subsequently, 1F8 cells were transfected with 125 µg of plasmid DNA and 1mg/ml polyethylenimine (PEI) (Sigma-Aldrich, #408727) diluted in Opti-MEM (Thermo Fisher Scientific, #10149832). After three days, retroviral particles were harvested by collecting and filtering the supernatant with 0.45 µm low-protein-binding PVDF syringe filters (StarLab E4780-1451). 1F8 cells were supplemented with fresh medium. Harvested supernatants were collected in Ultra-Clear tube (Beckman Coulter 344058) and 300 µl of 60% Optiprep were added to the bottom of the tube to concentrate the viral particles. Then, the solution was centrifuged at 24000 rpm for 2

hours at 4°C using the swinging-bucket rotor SW 32 Ti (Beckman Coulter 369694) in an ultracentrifuge (Beckman Coulter, Max-XP). The supernatant was discarded and the pellet was supplemented with 30ml of Tris-buffered saline 5 (TBS-5) (1M Tris/HCl, pH7.8; 5M NaCl; 1M KCl; 1M Mg2Cl) and centrifuged again using the same settings. Finally, the supernatant was discarded and the pellet containing the retroviral particles was re-suspended in 100 µ of TBS-5 and stored at -80ºC until use. The same harvesting procedure was repeated two and four days after. Viral titres used for experiments were typically in the range of 10^{6-8} transducing units/mL.

3. Retroviral injections in the postnatal cortex.

P5 pups were deeply anesthetized with an intraperitoneal injection of 0.5mg/Kg body weight Medetomidin + 5mg/Kg body weight Midazolam + 0.025mg/Kg body weight Fentanyl. In addition, an anaesthetic cutaneous cream containing lidocaine and prilocaine (EMLA cream; #PL39699/0088) was applied on the skin region where the incision was going to be made. Once the mice were in deep anaesthesia and had lost the paw reflexes, the head was fixed in the stereotaxic frame using the blunt end of the ear bars. A small incision was made on the skin with a surgical blade and a small hole on the skull was carefully opened with the tip of a needle. Then, a retroviral solution containing the construct of interest was injected in the cerebral cortex using glass capillaries (Fisher Scientific UK, #9600105), which were pulled with a micropipette puller. The coordinates of reference used for injection were the following: +3 mm rostrocaudal from lambda, +/-0.5 mm mesolateral from the midline and -0.5 mm ventral. The cortical area injected with the retroviral solution comprised the anterior cingulate, the primary and secondary motor and the retrosplenial cortical areas. Each pup received a total volume of 0.8-1µl of retroviral suspension injected in the cortex. After injection, the glass capillary was left inside the cortex for 5 additional minutes to allow diffusion of the viral solution and then was carefully retracted. The wound was closed with Vetbond surgical glue (#1469SB) and anaesthesia was antagonised via intraperitoneal injection of 2.5mg/kg body weight Atipamezol, 0.5mg/Kg body weight Flumazenil and 0.1mg/Kg body weight Buprenorphin. Pups were left in a warm incubator at 37°C to recover before reuniting them to the mother. The recovery state was daily checked for three days after the surgery.

4. Drugs administration.

4.1 Clozapine-N-oxide (CNO) administration.

CNO (Bio-Techne, #4936/10) was dissolved in NaCl 0.9% (Sigma-Aldrich, #S7653) and Dimethyl sulfoxide 0.25% (DMSO, Sigma-Aldrich, #D5879) at a final concentration of 0.5ml/ml. For experiments that required DREADDs activation, CNO was injected intraperitoneally at a dose of 5mg/kg of body weight into P13 mice for 10 days with a break of 2 days after the first 5 days. Three days after the last dose, mice were injected with the last dose of CNO and subsequently perfused after 1h for tissue processing. For control groups, P13 mice were injected with vehicle (NaCl 0.9%) instead of CNO during the same time periods.

4.2 5-ethynyl-2'-deoxyuridine (EdU) administration

EdU (Thermo Fisher Scientific, #A10044) was dissolved in 1X PBS (Oxoid, #BR0014G) at a final concentration of 5mg/ml. EdU at a dose of 50mg/kg of body weight was administered via intraperitoneal injection into postnatal mouse pups at the age of P5 to allow labelling of proliferating cells in the cortex at the time of the retroviral injection.

5. Histology

5.1 Tissue preparation

Mice were lethally anesthetised with a solution of 150 mg/kg Ketamine and 1 mg/kg Medetomidine diluted in NaCl 0.9% by intraperitoneal injection, and transcardially perfused with NaCl 0.9% solution (Sigma-Aldrich, #S7653) followed by 4% paraformaldehyde (PFA) (Sigma-Aldrich, #441244) in 0.1M Phosphate Buffer (PB) solution (30 mM Na2HPO4·12H2O (Sigma-Aldrich, #71663); 33 mM NaH2PO4·2H2O (Sigma-Aldrich, #71500) pH 7.4). The brains were removed from the skull and post-fixed in 4% PFA overnight at 4ºC. The brains were then sliced in coronal sections of 40µm on a vibratome (Leica #VT1000S), collected in a cryoprotective solution (20% glucose (Sigma-Aldrich, #G8270), 40% ethylene glycol (Sigma-Aldrich, #324558), 0.025% Sodium Azide (Severn Biotech Ltd., #40-2010-01), in 0.5M PB (15mM Na2HPO4·12H2O (Sigma-Aldrich, #71663); 16mM NaH2PO4·2H2O (Sigma-Aldrich, #71500; pH 7.4) and stored at -20ºC.

5.2 Immunohistochemistry

Sections were used for immunohistochemistry using a free-floating procedure. Free-floating sections were washed three times in 1X phosphate-buffered saline (PBS; Oxoid, #BR0014G) for 15 minutes each and were then incubated in a blocking solution containing 0.3% Triton X-100 (Sigma-Aldrich, #T9284); 5% goat (Sigma-Aldrich, #G9023) and/or donkey serum (Sigma-Aldrich, #D9663) depending on the secondary antibody host species; 1x PBS for 1h and 30min. Slices were then incubated with primary antibodies diluted in blocking solution for 2h at room temperature followed by an overnight incubation at 4ºC. The following primary antibodies were used: anti-Red Fluorescence Protein (RFP, rabbit, 1:500, Rockland, #600401379), anti-mCherry (chicken, 1:500, Encor Bio, #CPCA-mCherry), anti-Green Fluorescence Protein (GFP, chicken, 1:1000, AvesLabs, #GFP-1020), anti-Green Fluorescence Protein (GFP, goat, 1:1000, Abcam, #ab5450), anti-Sox9 (mouse IgG1, 1:500 , eBioscience, #GMPR9), anti-Sox10 (goat, 1:300 , R&D Systems, #AF2864), anti-Doublecortin (DCX, guinea pig, 1:500, Merck Millipore, #AB2253), anti-NeuN (mouse IgG1, 1:500, Merck Millipore, #MAB377), anti-Gamma-aminobutyric acid (GABA, rabbit, 1:300, Sigma-Aldrich, #A2052), anti-Parvalbumin (PV, guinea pig, 1:1000, Synaptic Systems, #195004), anti-Somatostatin (SST, rat IgGb2, 1:200, Merck Millipore, #MAB354), anti-Vasointestinal peptide (VIP, rabbit,1:1000, ImmunoStar, # 20077), anti-c-Fos (guinea pig, 1:250, Synaptic Systems, #226004). The next day, after washing the brain sections three times in PBS for 15 minutes each, they were incubated with appropriate species-specific, fluorochrome-conjugated secondary antibodies for 1h and 30 min in the dark at room temperature, followed by three washes of 15min with 1X PBS. The following secondary antibodies were used: anti-chicken Alexa Fluor 488 (donkey, 1:300, Jackson Immunoresearch, #703545155), anti-goat Alexa Fluor 488 (donkey, 1:300, Abcam, #ab150129), anti-mouse-IgG1 Alexa Fluor 488 (goat, 1:300, Thermo Fisher Scientific, #A21121), anti-rabbit Alexa Fluor 488 (donkey, 1:300, Thermo Fisher Scientific, #A21206), anti-chicken Cy3 (donkey, 1:500, Jackson Immunoresearch, #703165155), anti-rabbit Alexa Fluor 568 (goat, 1:500, Thermo Fisher Scientific, #A11011), anti-mouse-IgG Alexa Fluor 568 (goat, 1:500, Invitrogen, Thermo Fisher Scientific, #A11004), anti-guinea pig Cy5 (donkey, 1:500, Jackson Immunoresearch, #706175148), anti-mouse-IgG1 Alexa Fluor 647 (goat, 1:500, Thermo Fisher Scientific, #A21240), anti-rabbit Alexa Fluor 647 (donkey, 1:500, Thermo Fisher Scientific, #A31573). For mounting, slices were washed two times during 15min with 0.1M PB solution and mounted onto glass slides (#N/A143), air-dried, and covered with cover-glasses with a mounting medium (Mowiol, Generon, #17951-500).

For EdU signal detection, the Click-iT™ EdU Cell Proliferation commercial kit (Thermo Fisher Scientific, #C10340) was used following manufacturer's standard protocols. Briefly, the immunohistochemistry was carried out as described above with an additional incubation of the EdU detection cocktail for 2h at RT. After washing with 1X PBS three times for 15min, the immunohistochemistry protocol was continued as previously described.

5.3 Single-molecule fluorescent in situ hybridisation (smFISH)

All solutions for single-molecule fluorescent *in situ* hybridisation were prepared in RNase-free Diethyl pyrocarbonate (DEPC)-treated water Sigma-Aldrich, #D5758). Mice were perfused as described above. Brains were postfixed overnight at 4ºC and sectioned on 40 µm coronal slices using a vibratome (Leica #VT1000S). RNA ISH was carried out using the RNAscope Multiplex Fluorescent v2 assay (ACDBio #323110), according to manufacturer's protocol. Briefly, brain slices were washed in 0.1M PB, mounted onto SuperFrost Plus slides (Thermo Fisher Scientific, Waltham, MA, USA) and then left to dry overnight. The following day, brain sections were dried 60min at 60ºC, rinsed with water and dehydrated with 50%, 70% and 100% EtOH, for 5min each. Brain slices were incubated with hydrogen peroxide for 10min at RT, washed with water, and then incubated with RNAscope Multiplex FL v2 Target Retrieval Solution for 10min at 90ºC. The sections were washed again in water and dipped in 100% ethanol. A hydrophobic barrier was drawn around the slices and left to dry. The slices were treated with Protease III for 15min at 40ºC, washed with water, and hybridised with the probe against the mRNA transcript of interest or control probes for 2h at 40ºC. The following probes were used: Mm-Sst-C3 (#404631-C3), Mm-Kcnc1-C1 (#564521-C1), Mm-Syt2-C3 (#493691-C3), Mm-Ascl1-C2 (#313291-C2), Mm-Dlx2-C3 (#555951-C3). Signal amplification and development was carried out with RNAscope Multiplex FL v2 HRP for each specific channel and using the following fluorophore dyes: Opal520 (#FP1487A), Opal570 (#FP1488A) or Opal690 (#FP1487A) fluorophore, as described in the manufacturer's instructions.

Following HRP signal development, brain slices were subjected to immunohistochemistry generally as described previously, but with a few alterations. Brain sections washed three times for 15 min with 1X PBS, permeabilized with 0.25% Triton-X100; 1X PBS for 20min at RT, and then incubated in blocking solution: 0.3% Triton-X100; 5% BSA; 10% serum; 1X PBS for 2h at RT. Slices were incubated with primary antibodies diluted in antibody solution: 0.3% Triton-X100; 1% BSA; 5% serum;

1X PBS overnight at 4ºC. The following primary antibodies were used: anti-GFP (chicken, 1:200, AvesLabs, #GFP-1020) and anti-RFP (rabbit, 1:100, Rockland, #600401379). After three washing steps with 1X PBS, brain slices were incubated in blocking solution for 2h at RT and then incubated with Alexa Fluor secondary antibodies diluted in antibody solution for 2h at RT. The following secondary antibodies were used: anti-chicken Alexa Fluor 488 (donkey, 1:200, Jackson Immunoresearch, #703545155) and anti-rabbit Alexa Fluor 568 (goat, 1:250, Thermo Fisher Scientific, #A11011).Slices were washed three time with 1X PBS, incubated with 5µM DAPI dissolved in 1X PBS for 5 min at RT and washed twice with PB 0.1M, prior to be mounted in Prolong™ Gold Antifade Mountant (Thermo Fisher Scientific, #P36930) and then covered with cover-glasses.

6. Image acquisition and image analysis

Images were acquired with the laser-scanning confocal microscope Zeiss LSM 800 confocal microscope (Carl Zeiss Microscopy, Jena, Germany) equipped with four solid-state lasers (405, 488, 561, and 633 nm) at a 20X (NA 0.8) or 40X (NA 1.3) objectives (Centre for Developmental Neurobiology, King's College London). Serial Z-stacks spaced at 0.5–1.5 mm distance were acquired to image the whole thickness of the brain sections. Z-stacks of digital images were captured for quantifications using the ZEN software (Zeiss). For the figures, maximum intensity projections from the Z-stacks were generated using the function provided by the software. Cell quantifications were performed by analysing the Z-stacks using ZEN software or ImageJ 1.51v software (National Institute of Health, USA). Cell counts for immunostainings were done by navigating through the Z-stacks of confocal images, allowing the accurate visualisation of the cells of interest. All figures were designed in Adobe Illustrator 26.5 and schematic illustrations were created using BioRender.

Determination of reprogramming efficiency. To determine the number of iNs, we counted for each mouse the total number of GFP+ and/or DsRed+ transduced cells and the number of GFP+ and/or DsRed+ cells expressing neuronal markers (Dcx, NeuN). The number of iNs was expressed as a percentage of the total number of transduced GFP+ and/or DsRed+ cells (i.e., reprogramming efficiency). For each retroviral combination, three independent mice were quantified, and values are given as mean percentages ± SD.

Phenotype of glia-derived iNs. To determine the phenotype of glia-derived iNs, we counted the number of reporter-positive (DsRed+) cells expressing neurochemical markers from the interneuronal lineage (GABA, PV, SST or VIP). For each experiment, this number was expressed as a percentage of the total number of DsRed+ cells. In addition, to further characterise iNs, we used Vgat-Cre/EGFP mice, from which glia-derived GABAergic iNs will turn on GFP expression under control of the Vgat promoter). We counted the number of DsRed+ cells and the number of GFP+/DsRed+ cells. For each mouse, the number of GFP+/DsRed+ cells (i.e., GABAergic-like iNs) was expressed as a percentage of the total number of DsRed+ cells. For each condition, three independent experiments were quantified and values are given as mean percentages ± SD.

Glial origin of iNs. To determine the glial origin of iNs, we used Aldh1l1-Cre/ERT2 or NG2-iCreERT2/GFP transgenic mice lines, from which astrocytes or OPCs-derived iNs respectively will turn on GFP expression. For fate-mapping experiments, we counted the number of 1) DsRed/GFP/Dcx or NeuN-triple-positive cells (i.e., fate-mapped iNs); 2) DsRed/Dcx or DsRed/NeuN-double positive cells (i.e., non-fate-mapped iNs); 3) DsRed/GFP-double positive transduced cells (i.e., fate-mapped glia) and 4) RFP only positive transduced cells (non-fate-mapped glia). For each mouse line and condition (Ascl1SA6-Bcl2 or Ascl1SA6-Dlx2), three independent mice were analysed and quantified. Cells in each group are expressed as a percentage of the total number of DsRed-positive transduced cells ± SD.

Proliferating cells in the cortex. To identify cells undergoing proliferation in the cortex at specific time points, we counted the number of cells that incorporated EdU and expressed the reporter gene DsRed for iNs or neurochemical markers for endogenous neurons and glia (Dcx, Sox9, Sox10). The number of proliferative cells was expressed as a percentage of the total number of transduced DsRed+ cells for iNs or EdU+ cells for endogenous neurons and glia. For each experiment, three independent mice were quantified, and data are represented as mean percentages ± SD.

Soma size. For each mouse, the surface and circularity of PV+ endogenous neurons or iNs soma (μm^2) was measured using ImageJ 1.51v software (National Institute of Health, USA). A region of interest (ROI) was drawn around the soma of cells of interest, using the PV signal for PV+ endogenous neurons or the DsRed reporter signal in the case of iNs. Three independent mice were quantified and data are expressed as mean surface (μm^2 ± SEM) or circularity index.

Layer distribution analysis. To assess distribution of PV-expressing iNs across the cortex, we counted the number of GFP+ and DsRed+ transduced cells that acquired PV expression throughout superficial (layer I) or deep cortical layers (layer II-layer VI). For each mouse, the number of GFP+/DsRed+/PV+ cells was expressed as a percentage of the total number of GFP+/DsRed+ cells within a specific layer. Three independent mice were quantified and values are given as mean percentages ± SD.

PV intensity levels. To determine PV intensity levels, the contour of PV+ endogenous neurons or iNs was used to draw a region of interest (ROI) in ImageJ 1.51v software (National Institute of Health, USA). The three Z-stacks with the highest mean intensity within the ROIs (raw intensity/area in pixels) were used to calculate the mean PV intensity for each cell. The background was subtracted from each image. Only neurons whose entire soma was within the microscope images were counted for the analysis. Immunostainings of brain sections were performed at the same time and under the same conditions. Image acquisition was taken under the same settings, in such a way that the pixels within the ROI were not saturated. Three to five independent mice were quantified and data are expressed as mean percentages ± SD.

SmFISH analysis. For mRNA particle analysis, the DsRed reporter signal from transduced cells or the DAPI+ nuclei from endogenous neurons was used to draw a ROI. The number of mRNA transcripts was manually counted by navigating through the Z-stacks of confocal images obtained with a 40X (NA 1.3) objective and spaced at 0.5-0.75 mm distance. Given that high-magnification images provided high resolution in these analyses, the expression of mRNA particles was reliably detected. The number of mRNA transcripts was expressed as total number of dots per DsRed+ cell. For each experiment, three independent mice were quantified and values are given as total number of mRNA particles per retroviral combination.

Determination of DREADDs-mediated activation of iNs. To determine activation of iNs through DREADDs-mediated stimulation, we counted the number of double reporter-positive cells (GFP+/DsRed+) or single reporter-positive cells (GFP+ or DsRed+) expressing the immediate early gene (IEG) c-Fos. For each experiment, this number was expressed as a percentage of the total number of double or single-reporter positive cells. Five independent mice were analysed and data are expressed as mean percentages ± SD. To correlate network activation levels at the site of the retroviral injection with activation of iNs, we counted the number of cells expressing c-Fos over all DAPI+ nuclei in the cortical regions around iNs using a Python script written by Gabriel Emilio Herrera Oropeza, a PhD student from our group. For each condition

(either CNO or vehicle-treated), five independent mice were quantified and data are expressed as mean percentages ± SD for each animal.

7. Statistical analysis

Statistical analysis was performed using GraphPad Prism 9 (GraphPad, San Diego, CA, USA). The normality of distribution was assessed using Shapiro-Wilk test. The significance of the differences between two groups was analysed by *t-test* for independent samples with normal distribution. The significance of differences between multiple experimental groups was assessed using one-way ANOVA followed by Tukey's multiple comparisons *post hoc* test or two-way ANOVA followed by Bonferroni's multiple comparisons *post hoc* test. For non-normally distributed data, the significance of differences between multiple experimental groups was assessed using Kruskal-Wallis test followed by Dunn's multiple comparisons *post hoc* test. The significance of the differences between two cumulative frequency distributions was analysed using non-parametric Kolgomorov-Smirnov test. The statistical tests, the number of independent experiments (n) and the number of cells analysed are reported in the figure legends. Data are represented as means ± SD. Statistical significance was considered when p-values < 0.05.

RESULTS

CHAPTER I.

In vivo reprogramming of cortical postnatal glia into parvalbumin-like iNs by forced expression of Ascl1SA6 and Bcl2

1.1. Proliferation of glial cells and lack of neurogenesis within the postnatal mouse cerebral cortex.

During embryonic stages of cortical development, neurons are generated first followed by gliogenesis and local expansion of glial cells during the early postnatal weeks (Clavreul et al., 2019; Kriegstein & Alvarez-Buylla, 2009). Local proliferation of glial cells and lack of neurogenesis during postnatal stages makes the cortex a suitable region for retroviral delivery aiming at inducing reprogramming of non-neurogenic glial cells (Galante et al., 2022; W. P. Ge et al., 2012). To characterise the postnatal mouse cerebral cortex as a reliable experimental model to study glia-to-neuron conversion, I first aimed to study the temporal profiles of proliferation of the different glial cell types within the postnatal cortex to identify appropriate cell targets for conversion. To this end, mice were injected intraperitoneally with 5-ethynyl-2'-deoxyuridine (EdU), a thymidine analogue which is incorporated in the DNA of cells during cell division (Buck et al., 2008). To monitor the proliferating cells at the time of the retroviral injection, EdU was injected intraperitoneally at postnatal day 5 (P5) and sacrificed 4 hours later (Fig. 3.1A). In order to identify which glial cell types were proliferating at this age, brain coronal sections were labelled against EdU in combination with specific glial markers for astrocytes and oligodendrocyte lineage cells.

Using Sox9 as an astrocyte-specific nuclear marker (Klum et al., 2018; Martini et al., 2013; Stolt et al., 2003), I observed that more than half of the cells proliferating in the mouse cerebral cortex at P5 were astrocytes (56.1 ± 3.0% of Sox9+/EdU+ cells; Fig. 3.1C-D), in agreement with previous published data showing that local division of cortical astrocytes is the major source for astroglia generation (W. P. Ge et al., 2012). Next, I used Sox10 as a transcription factor expressed in OPCs and oligodendrocytes (Kuhlbrodt et al., 1998; Stolt et al., 2003). Quantifications revealed that nearly the remaining population of proliferating cells corresponded to the oligodendrocyte lineage (38.7 ± 3.4% of Sox10+/EdU+ cells; Fig. 3.1C, E).

Importantly, neurogenesis cessation in the cortex after birth has been previously described in several studies (Kriegstein & Alvarez-Buylla, 2009). This issue is of crucial importance when considering inducing *in vivo* reprogramming of glial cells into iNs using a retroviral strategy, as it is critical to avoid targeting proliferating cells with neurogenic potential by the retrovirus at the same time as non-neurogenic glial cells.

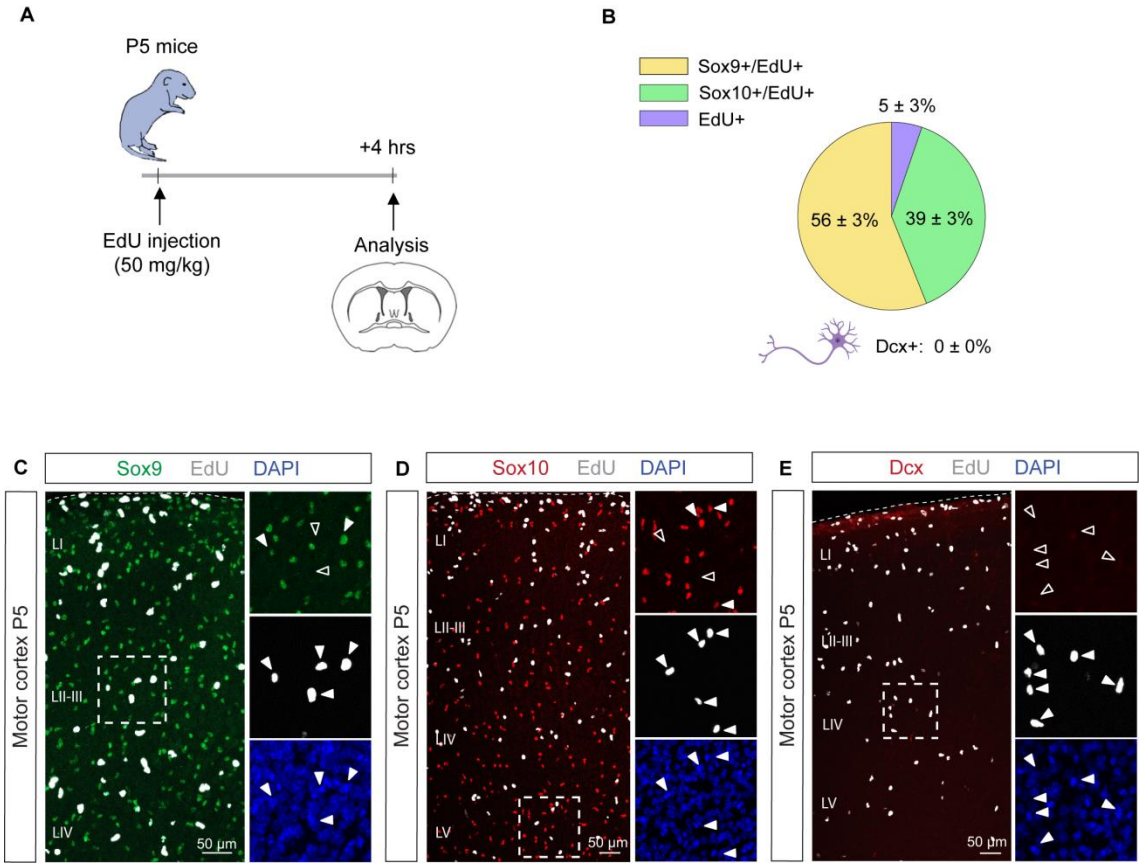

Figure 3.1. Proliferation of glial cells and lack of neurogenesis in the postnatal mouse cerebral cortex. (A) Schematic representation of experimental design. P5 mice received an intraperitoneal injection of EdU (50mg/kg) and were sacrificed 4 hours later to identify cells undergoing division at this age. (B) Pie chart showing relative numbers of proliferating cells that have incorporated EdU and express Sox9, Sox10 or Dcx in P5 mice; n = 3 mice (1550 cells) for Sox9, n = 3 mice (804 cells) for Sox10 and n = 3 mice (1550 cells) for Dcx. (C-E) Confocal images depicting incorporation of EdU in Sox9+ (C, in green), Sox10+ (D, in red) or Dcx+ cells (E, in red) in the P5 cerebral cortex.

Thus, I next examined whether cells expressing the immature neuronal marker Dcx were newly generated in the postnatal mouse cerebral cortex at the moment of the retroviral injection using the same EdU treatment described above. Importantly, I did not find any proliferating cells immunoreactive to Dcx (0.0 ± 0.0% of Dcx+/EdU+ cells; Fig. 3.1C, F).

Altogether, these data suggest that the postnatal mouse cerebral cortex is devoid of neurogenesis whereas both astroglia and OPCs keep proliferating at this age, making them good candidates for retroviral delivery of reprogramming factors.

1.2. Retroviral targeting of proliferating glia in the postnatal mouse cerebral cortex.

In the light of the considerable number of proliferating glial cells in the postnatal mouse cerebral cortex and in agreement with previous data reporting dividing glia as potential cell targets by retrovirus (Galante et al., 2022; W. P. Ge et al., 2012) I reasoned that using a retroviral delivery system would be a relevant strategy to force expression of reprogramming factors specifically in dividing glial cells.

To identify which glial population could serve as a source for neuronal reprogramming and whether a specific glial subtype could be preferentially targeted by retrovirus in the postnatal cerebral cortex, mice received an intracortical injection of a control retroviral vector encoding the reporter gene DsRed but none reprogramming factors at P5 (Fig. 3.2A). Transduced cells were then characterised 28 days post retrovirus injection (dpi) by immunostaining for DsRed in combination with glial markers. I found that the majority of transduced cells were immunoreactive for the astroglial marker Sox9 (67.5 ± 3.9% of Sox9+/DsRed+ cells; Fig. 3.2B-C), whereas most of the remaining transduced cells expressed the oligodendroglial marker Sox10 (34.9 ± 3.7% of Sox10+/DsRed+ cells; Fig. 3.2B-C). These results are consistent with previous work from our laboratory demonstrating that control retrovirus injected in the mouse cerebral cortex at the same age (P5) specifically transduces similar proportions of astroglial and olidendroglial cells when analysed at 3 dpi (Galante et al., 2022). Importantly, the data at 28dpi confirms that the number of transduced cells does not significantly change at longer time points post-injection.

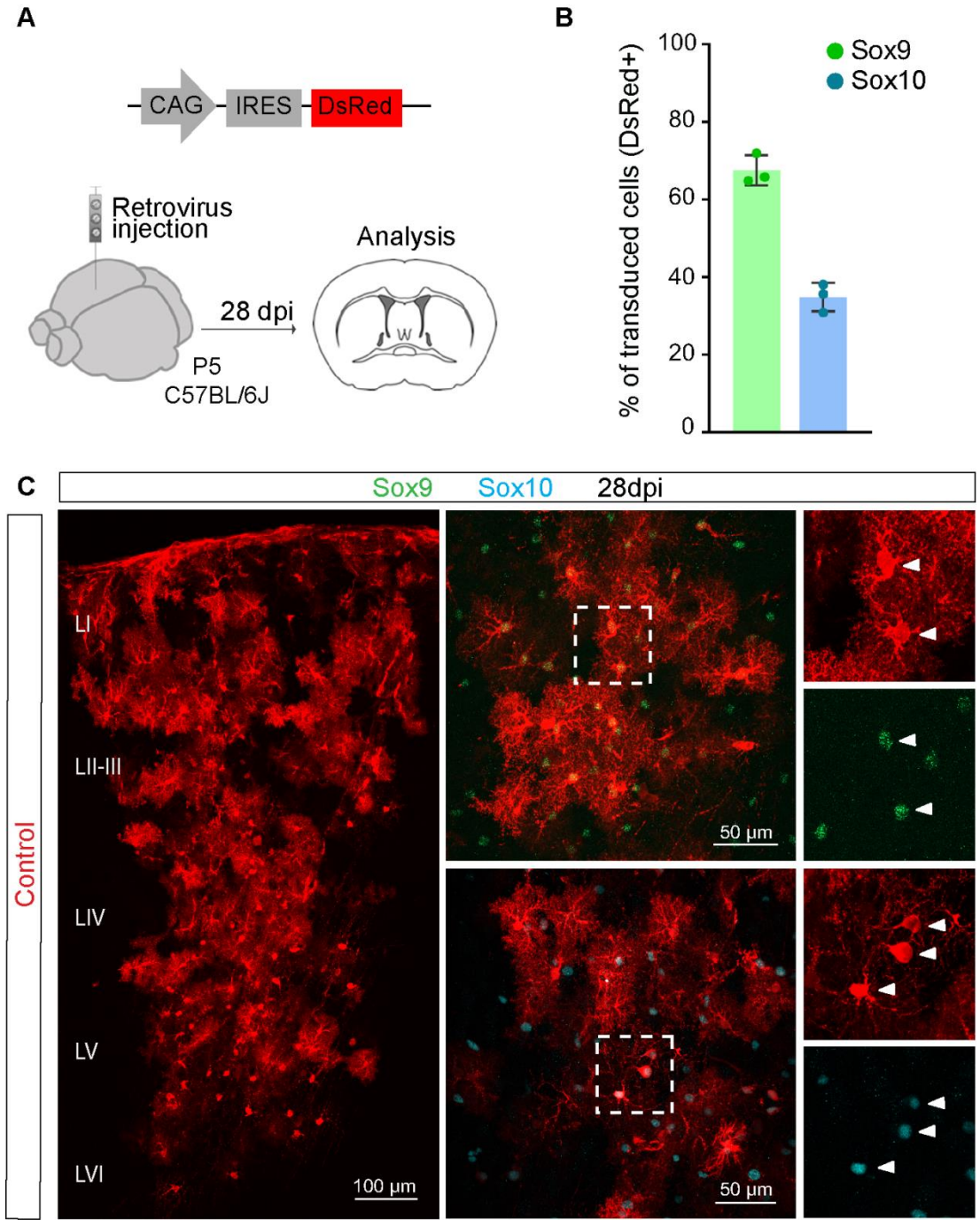

Figure 3.2. MMLV retroviruses specifically transduce glial cells in the postnatal mouse cerebral cortex. (A) Schematic representation of experimental design. Control retrovirus encoding only for the DsRed reporter gene (pCAG-IRES-DsRed) was injected in the mouse cerebral cortex at P5 and the identity of transduced cells was analysed at 28 dpi. (B) Bar graph showing the relative number of astroglial (Sox9+) and oligodendroglial (Sox10+) cells among transduced cells; n = 3 (1118 cells) for Sox9 and n = 3 (1240 cells) for Sox10. (C) Confocal images depicting transduced cells (in red) co-expressing Sox9 (in green, upper insets) or Sox10 (in cyan, lower insets).

1.3. *In vivo* reprogramming of cortical postnatal glia by forced expression of Ascl1: effect of different phosphorylation states.

Next, to investigate whether cortical proliferative glial cells, most likely astrocytes and OPCs, could be converted into iNs, I used a retrovirus strategy to overexpress key neurogenic transcription factors in glial cells at P5. For control, mice were again injected with a control retrovirus encoding DsRed. The occurrence and efficiency of glia-to-neuron conversion were assessed by immunostaining of cortical sections for the DsRed reporter gene and the neuronal markers Dcx and NeuN at 28 dpi (Fig. 3.3A).

Following injection of the control retrovirus, none of the transduced cells acquired the expression of Dcx or NeuN at 28dpi (0.0 ± 0.0% of Dcx+/DsRed+; 0.0 ± 0.0% of NeuN+/DsRed+ cells; Fig. 3.3C-D), in agreement with previous work in our laboratory at earlier time points (Galante et al., 2022). These data rule out the possibilities that the control vector induces a switch in cell fate or that endogenous neurons get labelled at later time points.

Based on the growing understanding of transcriptional programs orchestrating neuronal differentiation during development, I selected Ascl1 as a candidate reprogramming factor, which has been reported to play a major role in specification of GABAergic lineage during development (Casarosa et al., 1999b; Fode et al., 2000; Horton et al., 1999). In addition, previous work from our laboratory showed that Ascl1 can reprogram cultured postnatal astroglia into neurons *in vitro* (Berninger et al., 2007; Heinrich et al., 2010). To examine the ability of Ascl1 to reprogram proliferating glia into iNs *in vivo*, a retroviral vector containing the murine Ascl1 sequence was injected in the postnatal cerebral cortex. Despite a massive number of DsRed+ transduced cells throughout the cortex, only very few displayed neuronal morphology and none of them expressed the neuronal marker NeuN at 28 dpi (0.0 ± 0.0% of NeuN+/DsRed+ cells; Fig. 3.3C, E). The inefficient neurogenic activity of Ascl1 in the postnatal cerebral cortex is consistent with recent results from our laboratory (Galante et al., 2022), showing that Ascl1 induces OPCs proliferation but fails to drive glia-to-neuron conversion in the postnatal cerebral cortex at 12 dpi. Strikingly, in contrast to what it was described in this study at earlier time points (Galante et al., 2022), I found that a large proportion of transduced cells acquired the expression of the marker Dcx at 28dpi (69.8 ± 2.6% of Dcx+/DsRed+ cells; Fig. 3.3C, E), in spite of retaining their glial morphology. Of note, Dcx expression levels in transduced cells were lower than Dcx expression from putative newborn neurons found in the dentate gyrus of the hippocampus within the same brains (Fig. 3.3B).

Previous studies have shown that post-translational modifications can regulate the fate specification properties of Ascl1 (Ali et al., 2014). Remarkably, phosphorylation of Ascl1 has been shown to hamper its neurogenic potential and promote a proliferative glial program instead (S. Li et al., 2014). These studies have suggested that the phosphorylation state of Ascl1 may influence its fate specification properties by driving different chromatin-remodelling modifications and promoting Ascl1 binding to additional genomic targets (Ali et al., 2014; S. Li et al., 2014). Alternatively, it could also be possible that phosphorylation of Ascl1 might affect the protein stability and therefore influence its neurogenic potential. To examine the effect of Ascl1 phosphorylation on glia-to-neuron conversion, I injected in the postnatal cerebral cortex a retroviral vector encoding a phospho-site mutant form of Ascl1, namely Ascl1SA6, in which all conserved six serine-proline sites subject to phosphorylation were mutated to alanine. Interestingly, a significant fraction of transduced cells by Ascl1SA6 expressed the mature neuronal marker NeuN (35.2 ± 12.9% of NeuN+/DsRed+ cells; Fig. 3.3C, F). In addition, most of these NeuN-expressing iNs exhibited conspicuous neuronal morphology. Interestingly, DsRed+ transduced cells that acquired the expression of the immature neuronal marker Dcx also remained with glial-like morphology (10.5 ± 9.2% Dcx+/DsRed+; Fig. 3.3C, F), but this cell population was smaller in comparison to Ascl1-transduced cells.

Intriguingly, the number of DsRed+ transduced cells found at the site of the retroviral injection was significantly lower when injecting the retroviral construct encoding Ascl1SA6 compared to Ascl1 (Fig. 3.3C, F, low-magnification images). Given that ectopic expression of Ascl1 enhances OPCs proliferation (Galante et al., 2022), it cannot be firmly concluded that finding a lower number of cells transduced with Ascl1SA6 is due to cell death and additional assays should be performed to confirm this hypothesis. However, consistent with this theory, there have been a study reporting that a major limitation of neuronal reprogramming is cell death during the process of fate conversion (Gascón et al., 2016).

Altogether, these data suggest that the phospho-site mutant Ascl1SA6 is more potent in inducing neuronal reprogramming of proliferative postnatal cortical glia compared to wildtype Ascl1. These data also suggest that Ascl1 is, at least, being partially phosphorylated in the context of *in vivo* neuronal reprogramming.

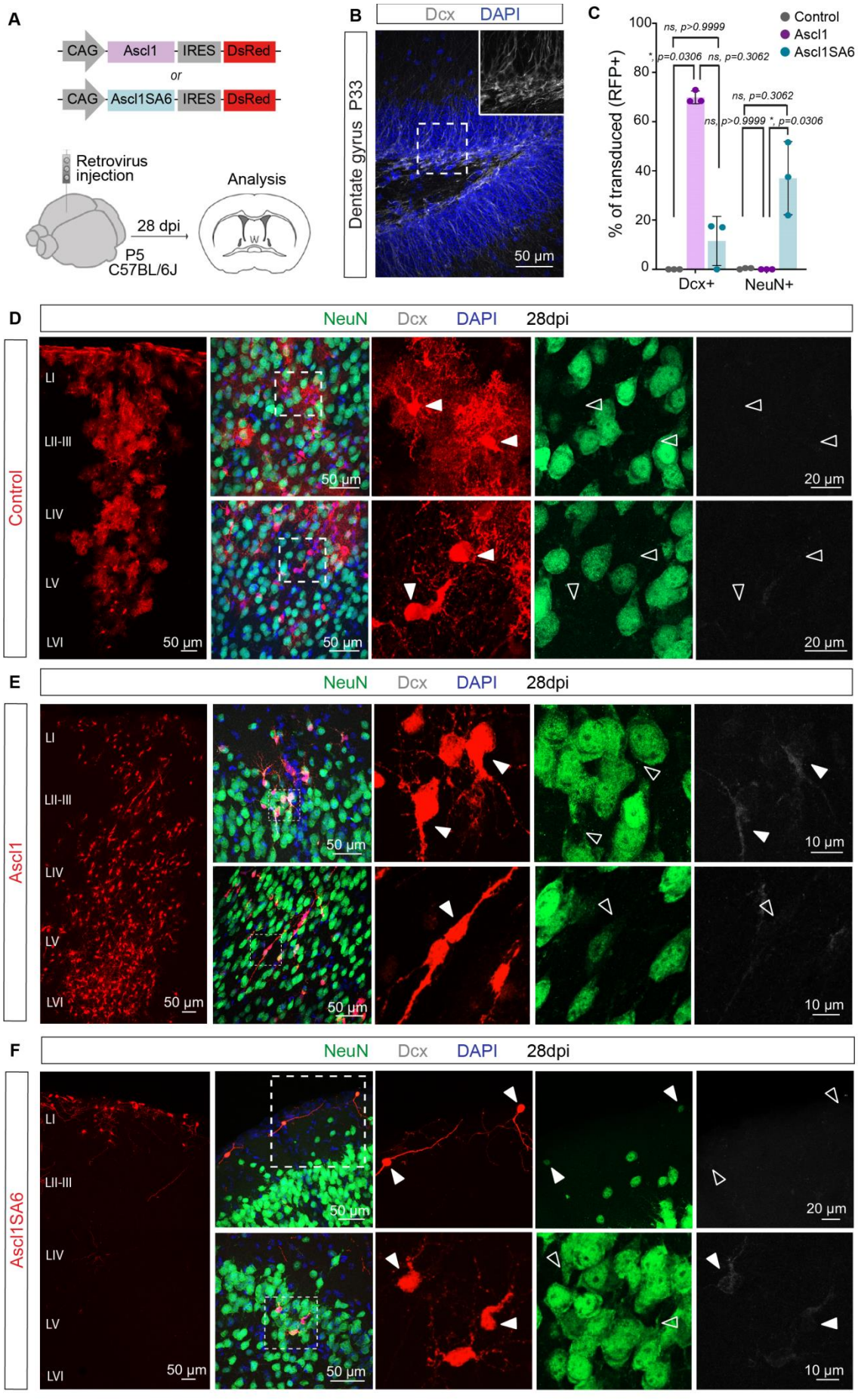
A
CAG
Ascl1
IRES
DsRed
or
CAG
Ascl1SA6
IRES
DsRed
Retrovirus injection
28 dpi
P5
C57BL/6J
Analysis
B
Dcx
DAPI
Dentate gyrus P33
50 µm
C
Control
Ascl1
Ascl1SA6
% of transduced (RFP+)
ns, p>0.9999
*, p=0.0306
ns, p=0.3062
ns, p=0.3062
ns, p>0.9999
*, p=0.0306
Dcx+
NeuN+
D
NeuN
Dcx
DAPI
28dpi
Control
LI
LII-III
LIV
LV
LVI
50 µm
20 µm
E
Ascl1
10 µm
F
Ascl1SA6

Figure 3.3. Forced expression of Ascl1 fails to drive neuronal reprogramming whereas Ascl1SA6 shows moderate glia-to-neuron conversion in the postnatal mouse cerebral cortex. (A) Schematic representation of experimental design. Retrovirus encoding Ascl1 (pCAG-Ascl1-DsRed) or Ascl1SA6 (pCAG-Ascl1SA6-DsRed) were injected in the mouse cerebral cortex at P5, and the reprogramming efficiency was analysed at 28dpi. (B) Confocal image depicting Dcx-expressing putative newborn neurons in the dentate gyrus of the hippocampus in P33 mice. (C) Quantification of the percentage of transduced cells expressing Dcx or NeuN at 28dpi. Data shown as mean ± SD. Kruskal-Wallis test followed by Dunn's multiple comparisons *post hoc* test, * P=0.0306 for Dcx expression in Ascl1-transduced cells vs control, P=0.3062 (ns) for Dcx expression in Ascl1-transduced cells vs Ascl1SA6-transduced cells, P>0.9999 (ns) for Dcx expression in control vs Ascl1SA6-transduced cells, * P=0.0306 for NeuN expression in Ascl1SA6-transduced cells vs Ascl1-transduced cells, P>0.9999 (ns) for NeuN expression in control vs Ascl1-transduced cells, P=0.3062 (ns) for NeuN expression in control vs Ascl1SA6-transduced cells, n = 3 mice (590 cells) for control, n = 3 mice (572 cells) for Ascl1, n = 3 mice (152 cells) for Ascl1SA6. (D-F) Low-magnification confocal images depicting transduced cells at cortical site of injection (left insets). Confocal images depicting Dcx (in white) and NeuN (in green) expression in cells transduced with control retrovirus (D), Ascl1-encoding retrovirus (E) or Ascl1SA6-encoding retrovirus (F). Empty arrows indicate marker-negative cells.

1.4. *In vivo* reprogramming of cortical postnatal glia by forced co-expression of Ascl1SA6 and Bcl2.

Based on my previous results showing moderate reprogramming efficiency (35.2 ± 12.9% of NeuN+/DsRed+ cells; Fig. 3.3C, F) and low number of iNs by forced expression of Ascl1SA6, I explored strategies to improve glia-to-neuron conversion. Previous studies have shown that Bcl2 increases reprogramming efficiency by acting as a pro-survival factor (Gascón et al., 2016). Thus, I reasoned that combined expression of Ascl1 or Ascl1SA6 together with Bcl2 may improve neuronal conversion efficiency and promote iNs survival (Fig 3.4A). Interestingly, I found that forced co-expression of Ascl1 and Bcl2 induced the generation of a small population of NeuN-expressing iNs (4.5 ± 3.6% of NeuN+/GFP+/DsRed+ cells; Fig. 3.4B-C), whereas the majority of co-transduced cells remained with glial-like morphology and lacked expression of neuronal markers (Fig. 3.4C). Strikingly, combined expression of Ascl1SA6 and Bcl2 instructed postnatal glial cells to generate a significantly higher proportion of iNs, evidenced by the acquisition of neuronal-like morphology and the expression of the neuronal marker NeuN (80.7 ± 3.5% of NeuN+/GFP+/DsRed+ cells; Fig. 3.4B, D). In contrast to forced expression of Ascl1SA6 alone, most of co-transduced cells with Ascl1SA6 and Bcl2 converted into NeuN-expressing iNs.

Since iNs are putatively originated from glial cells, I next investigated whether iNs generated by forced expression of Ascl1 or Ascl1SA6 together with Bcl2 still retained any hallmark gene expression from glial cells (Fig. 3.5A). As evidenced by immunostainings performed against the astroglial marker Sox9, I found very few co-transduced cells with Ascl1 and Bcl2 that retained an astroglial identity at 28 dpi (0.7 ± 0.6% of Sox9+/GFP+/DsRed+ cells; Fig. 3.5B, C). Similarly, I did not find any co-transduced cells with Ascl1SA6 and Bcl2 that expressed the astroglial marker Sox9 (0.0 ± 0.0% of Sox9+/GFP+/DsRed+ cells; Fig. 3.5B, D). Additionally, I also evaluated whether single-transduced cells with Ascl1, Ascl1SA6 or Bcl2 within the same brains retained a glial identity. Interestingly, very few cells transduced with Ascl1 (2.0 ± 1.8% of Sox9+/DsRed+ cells; Fig. 3.5B, C) or Ascl1SA6 (10.0 ± 17.3% of Sox9+/DsRed+ cells; Fig. 3.5B,D) expressed the astroglial marker Sox9 at 28 dpi, evidencing that ectopic expression of these transcription factors elicits important changes in the genetic landscape of targeted cells. As an internal control, I also evaluated whether single-transduced cells with Bcl2, which has been shown to not act as a reprogramming factor on its own (Gascón et al., 2016), retained expression of Sox9. In this case, Bcl2-transduced cells remained with glial-like morphology and a relevant number of these cells retained the expression of the astroglial marker Sox9.

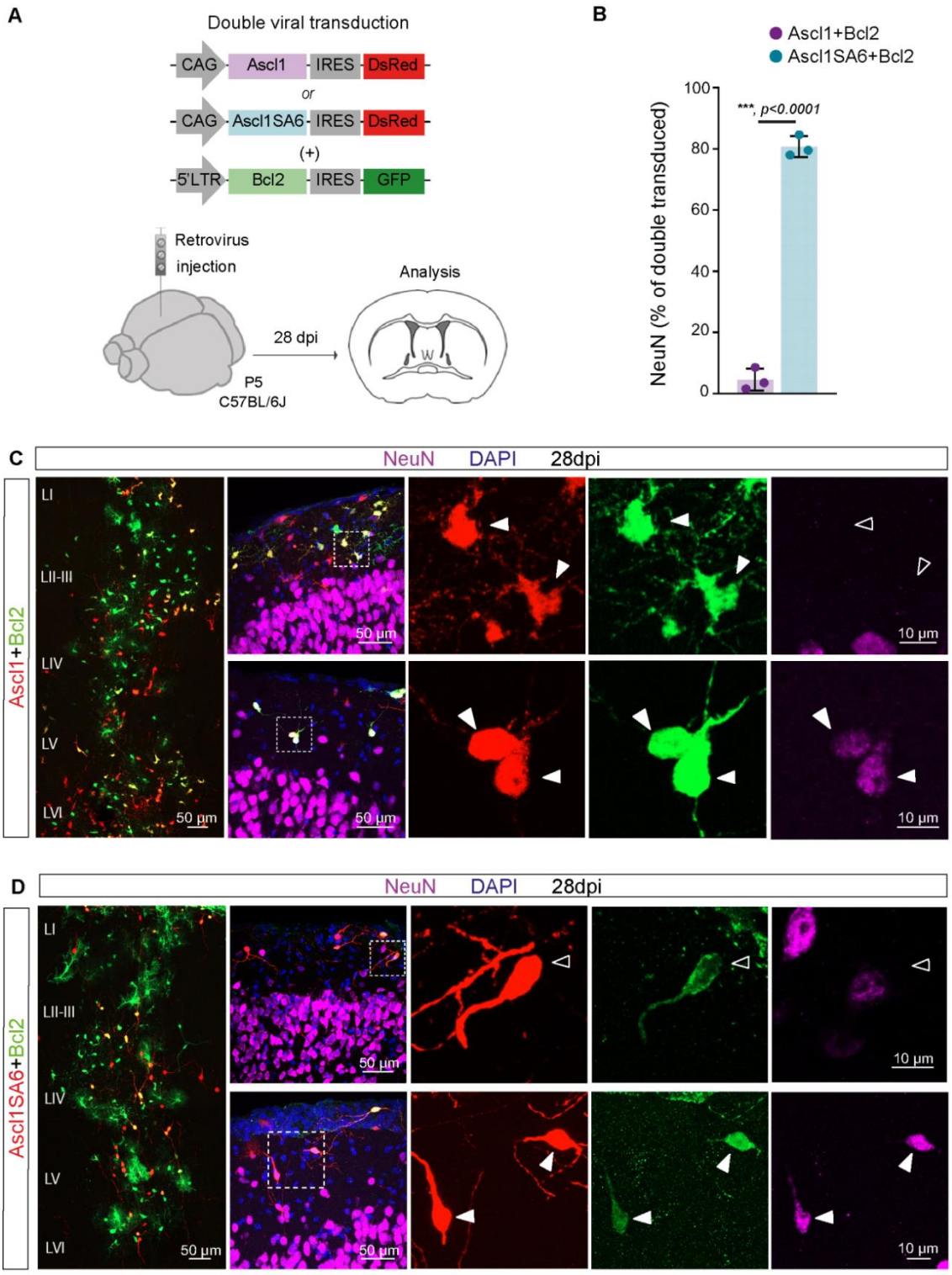
A
Double viral transduction
CAG
Ascl1
IRES
DsRed
or
CAG
Ascl1SA6
IRES
DsRed
(+)
5'LTR
Bcl2
IRES
GFP
Retrovirus injection
28 dpi
P5
C57BL/6J
Analysis
B
Ascl1+Bcl2
Ascl1SA6+Bcl2
NeuN (% of double transduced)
***, p<0.0001
C
NeuN
DAPI
28dpi
Ascl1+Bcl2
LI
LII-III
LIV
LV
LVI
50 µm
10 µm
D
NeuN
DAPI
28dpi
Ascl1SA6+Bcl2
LI
LII-III
LIV
LV
LVI
50 µm
10 µm

Figure 3.4. Forced co-expression of Ascl1SA6 and Bcl2 drives glia-to-neuron conversion with high efficiency in the postnatal mouse cerebral cortex. (A) Schematic representation of experimental design. Retroviral constructs encoding for Ascl1 (pCAG-Ascl1-DsRed) or Ascl1SA6 (pCAG-Ascl1SA6-DsRed) together with Bcl2 (5'LTR-Bcl2-GFP) were injected in the mouse cerebral cortex at P5, and the reprogramming efficiency was analysed at 28dpi. (B) Quantification of the percentage of double-transduced cells expressing NeuN at 28dpi. Data shown as mean ± SD. Two-tailed Student's unpaired t-test, *** $P<0.0001$, n = 3 mice (499 cells) for Ascl1 + Bcl2, n = 3 mice (157 cells) for Ascl1SA6 + Bcl2. (C-D) Low-magnification confocal images showing Ascl1 (C) or Ascl1SA6 (D) and Bcl2-transduced cells at the site of injection (left insets). Confocal images depicting NeuN expression (in violet) in Ascl1 (C) or Ascl1SA6 (D) and Bcl2-transduced cells at 28dpi. Empty arrows indicate marker-negative cells.

However, the number of Bcl2-transduced cells expressing Sox9 was significantly higher in the brains were Bcl2 was co-injected with Ascl1SA6 (62.0 ± 6.9% of Sox9+/GFP+; Fig. 3.5B-C) compared to those in which Blc2 expression was combined with Ascl1 (18.5 ± 12.2% of Sox9+/GFP+; Fig. 3.5B, D).

Given that the previous results suggest that retroviruses injected in the postnatal mouse cerebral cortex also target a significant number of OPCs (Fig. 3.2), I next decided to investigate whether co-transduced cells with Ascl1 or Ascl1SA6 together with Bcl2 expressed the oligodendroglial marker Sox10 (Fig 3.6A). In line with the results showing that co-transduced cells with Ascl1SA6 and Bcl2 do not retain an astroglial identity, I found very few of these cells that expressed the oligodendroglial marker Sox10 (2.1 ± 2.7% of Sox10+/ GFP+/DsRed+; Fig. 3.6B, D). However, in sharp contrast, I found that the vast majority of cells co-transduced with Ascl1 and Bcl2 expressed Sox10 (93.6 ± 6.1% of Sox10+/GFP+/DsRed+; Fig. 3.6B-C). Similarly, I found that whereas none of the single-transduced cells with Ascl1SA6 retained an oligodendroglial identity (0.0 ± 0.0% of Sox10+/DsRed+ cells; Fig. 3.6B, D), most of the cells transduced with Ascl1 expressed Sox10 (93.2 ± 1.9% of Sox10+/DsRed+; Fig. 3.6B-C). These data are in line with the previous results from our laboratory demonstrating that ectopic expression of Ascl1 enhances OPCs proliferation (Galante et al., 2022). Interestingly, I could observe that about a third of Bcl2-transduced cells expressed Sox10 in the brains where Bcl2 was co-injected with Ascl1SA6 (29.7 ± 15.0% of Sox10+/GFP+; Fig. 3.6B, D), corresponding with the remaining number of cells that did not expressed the astroglial marker Sox9. Remarkably, the majority of single-transduced cells with Bcl2 when injected together with Ascl1 showed an oligodendroglial identity evidenced by the expression of Sox10 (85.6 ± 7.2% of Sox10+/GFP+; Fig. 3.6B-C).

Taken together, these data demonstrate that Ascl1SA6 and Bcl2 synergise to induce very efficient neuronal reprogramming in the postnatal cerebral cortex. In contrast, cells co-transduced with Ascl1 and Bcl2 rarely acquire a neuronal phenotype but, instead, the majority of this cell population show an oligodendroglial identity.

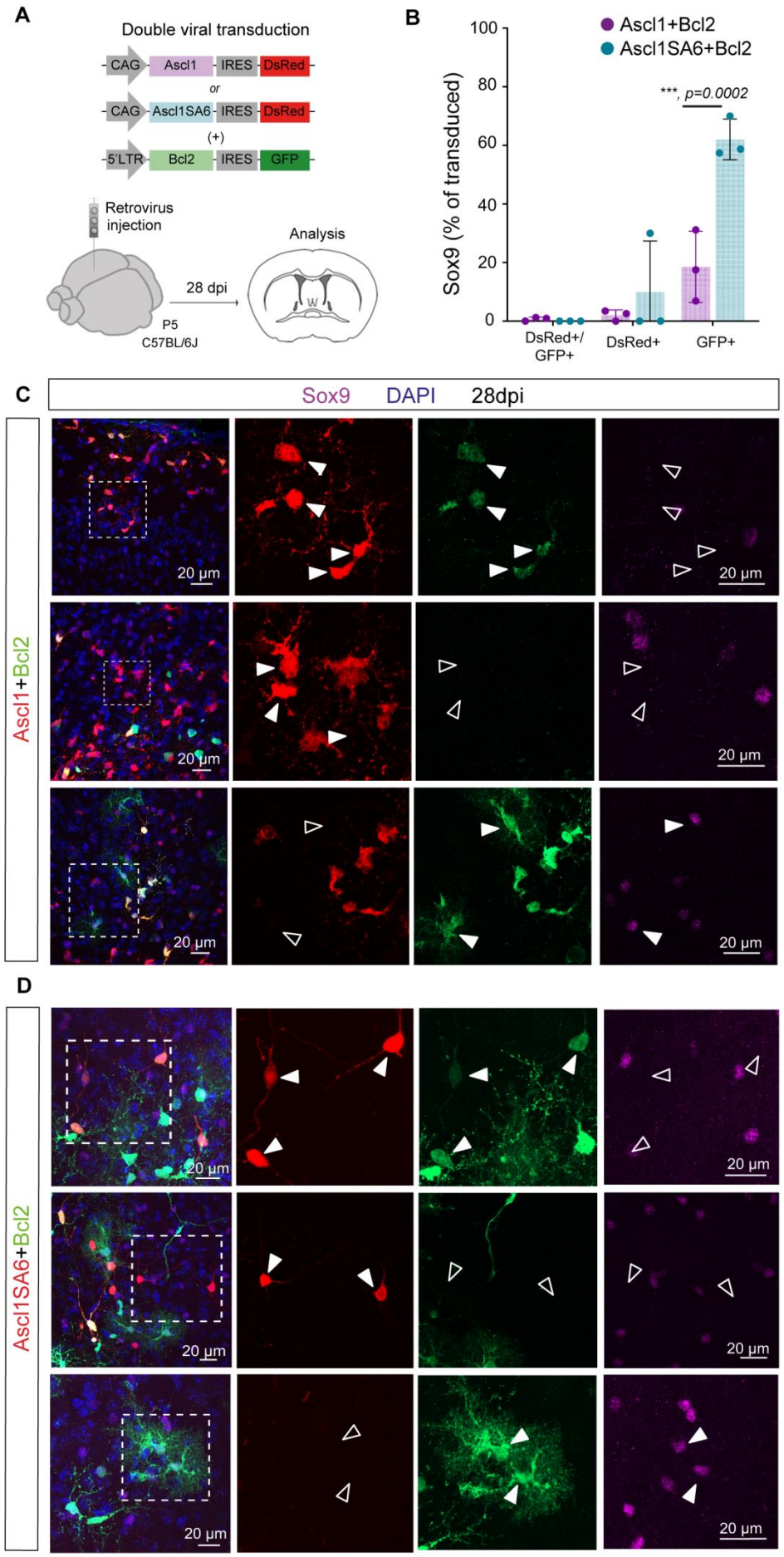
A
Double viral transduction
CAG
Ascl1
IRES
DsRed
or
CAG
Ascl1SA6
IRES
DsRed
(+)
5'LTR
Bcl2
IRES
GFP
Retrovirus injection
28 dpi
P5
C57BL/6J
Analysis
B
Ascl1+Bcl2
Ascl1SA6+Bcl2
***, p=0.0002
Sox9 (% of transduced)
100
80
60
40
20
0
DsRed+/ GFP+
DsRed+
GFP+
C
Sox9
DAPI
28dpi
Ascl1+Bcl2
20 μm
D
Ascl1SA6+Bcl2
20 μm

Figure 3.5. Co-transduced cells with Ascl1 or Ascl1SA6 and Bcl2 do not retain astroglial identity. (A) Schematic representation of experimental design. Retroviral constructs encoding for Ascl1 (pCAG-Ascl1-DsRed) or Ascl1SA6 (pCAG-Ascl1SA6-DsRed) together with Bcl2 (5'LTR-Bcl2-GFP) were injected in the mouse cerebral cortex at P5, and expression of the astroglial marker Sox9 was analysed at 28dpi. (B) Quantification of the percentage of cells co-transduced with Ascl1 and Bcl2 or Ascl1SA6 and Bcl2 or single-transduced with Ascl1SA6, Ascl1 or Bcl2 expressing Sox9 at 28 dpi. Data shown as mean ± SD. Two-way ANOVA followed by Bonferroni's multiple comparisons *post hoc* test, P>0.9999 for co-transduced cells with Ascl1+Bcl2 vs Ascl1SA6+Bcl2, P=0.9158 for single-transduced cells with Ascl1 vs Ascl1SA6, *** P=0.0002 for single-transduced cells with Bcl2, n = 3 (527 cells) for Ascl1 + Bcl2, n = 3 (722 cells) for Ascl1, n = 3 (228 cells) for Bcl2 (in Ascl1+Bcl2 injected brains), n = 3 (342 cells) for Ascl1SA6 + Bcl2, n = 3 (28 cells) for Ascl1SA6, n = 3 (494 cells) for Bcl2 (in Ascl1SA6+Bcl2 injected brains). (C) Confocal images depicting Sox9 expression (in magenta) in transduced cells with Ascl1 and Bcl2 (left insets), Ascl1 (middle insets) or Bcl2 (right insets) only at 28 dpi. (D) Confocal images depicting Sox9 expression (in magenta) in transduced cells with Ascl1SA6 and Bcl2 (left insets), Ascl1SA6 (middle insets) or Bcl2 (right insets) only at 28 dpi.

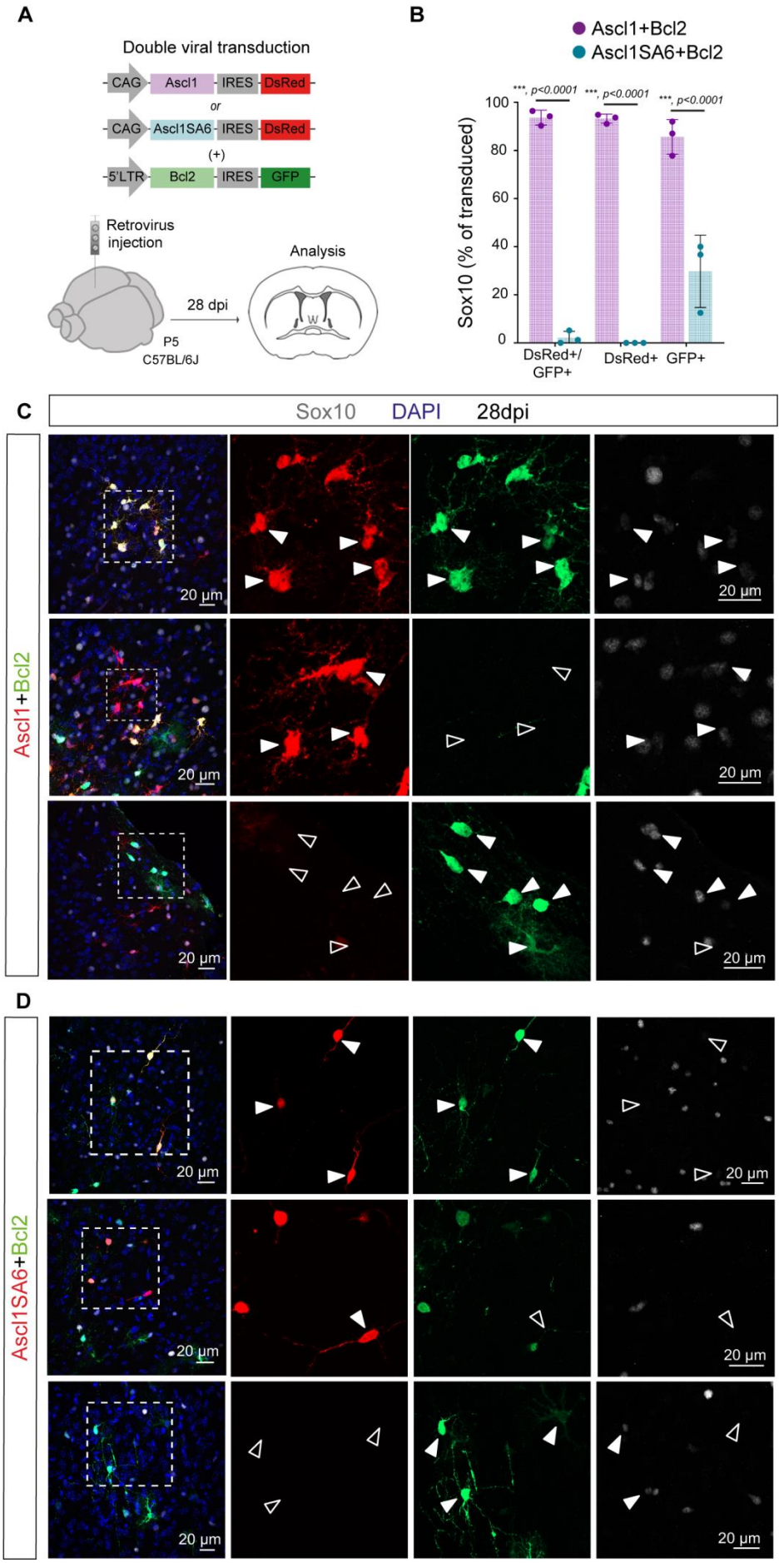
A
Double viral transduction
CAG
Ascl1
IRES
DsRed
or
CAG
Ascl1SA6
IRES
DsRed
(+)
5'LTR
Bcl2
IRES
GFP
Retrovirus injection
28 dpi
Analysis
P5
C57BL/6J
B
Ascl1+Bcl2
Ascl1SA6+Bcl2
***, p<0.0001
***, p<0.0001
***, p<0.0001
Sox10 (% of transduced)
100
80
60
40
20
0
DsRed+/ GFP+
DsRed+
GFP+
C
Sox10
DAPI
28dpi
Ascl1+Bcl2
20 µm
D
Ascl1SA6+Bcl2
20 µm

Figure 3.6. Most of co-transduced cells with Ascl1 and Bcl2 show oligodendroglial identity. (A) Schematic representation of experimental design. Retroviral constructs encoding for Ascl1 (pCAG-Ascl1-DsRed) or Ascl1SA6 (pCAG-Ascl1SA6-DsRed) together with Bcl2 (5'LTR-Bcl2-GFP) were injected in the mouse cerebral cortex at P5, and expression of the astroglial marker Sox10 was analysed at 28dpi. (B) Quantification of the percentage of cells co-transduced with Ascl1 and Bcl2 or Ascl1SA6 and Bcl2 or single-transduced with Ascl1SA6, Ascl1 or Bcl2 expressing Sox10 at 28 dpi. Data shown as mean ± SD. Two-way ANOVA followed by Bonferroni's multiple comparisons *post hoc* test, *** P<0.0001 for co-transduced cells with Ascl1+Bcl2 vs Ascl1SA6+Bcl2, *** P<0.0001 for single-transduced cells with Ascl1 vs Ascl1SA6, *** P<0.0001 for single-transduced cells with Bcl2, n = 3 (374 cells) for Ascl1 + Bcl2, n = 3 (698 cells) for Ascl1, n = 3 (236 cells) for Bcl2 (in Ascl1+Bcl2 injected brains), n = 3 (240 cells) for Ascl1SA6 + Bcl2, n = 3 (27 cells) for Ascl1SA6, n = 3 (332 cells) for Bcl2 (in Ascl1SA6+Bcl2 injected brains). (C) Confocal images depicting Sox10 expression (in grey) in transduced cells with Ascl1 and Bcl2 (left insets), Ascl1 (middle insets) or Bcl2 (right insets) only at 28 dpi. (D) Confocal images depicting Sox10 expression (in grey) in transduced cells with Ascl1SA6 and Bcl2 (left insets), Ascl1SA6 (middle insets) or Bcl2 (right insets) only at 28 dpi.

1.5. Overexpression of Ascl1SA6 and Bcl2 instructs cortical postnatal glia to reprogram into PV interneuron-like iNs.

Ascl1 is known to be a pioneer proneural gene involved in GABAergic neuronal fate specification at early embryonic stages (Casarosa et al., 1999b; Fode et al., 2000; Horton et al., 1999). Thus, I next evaluated whether glia-derived iNs generated upon co-expression of Ascl1 or Ascl1SA6 together with Bcl2 acquired GABAergic neuron identity. To follow specification towards a GABAergic phenotype, I performed immunostaining of cortical sections against reporter genes as well as the marker GABA at 28 dpi. Quantifications showed that the majority of co-transduced cells with Ascl1 and Bcl2 remained committed to the glial lineage and only a minority entered the GABAergic lineage (1.6 ± 0.3% of GABA+/GFP+/DsRed+ cells; Fig. 3.7A-B). In contrast, combining expression of Ascl1SA6 with Bcl2 increased fate conversion of glia into iNs which had acquired a GABAergic identity (23.4 ± 6.1% of GABA+/GFP+/DsRed+ cells; Fig. 3.7A-B). Previous studies have shown that iNs derived from human pericytes *in vitro* bifurcate into two cell populations that acquire either glutamatergic or GABAergic identity (Karow et al., 2018). Thus, it could be hypothesised that the remaining population of iNs may acquire a glutamatergic identity. On the other hand, it would be possible that all iNs are committed to acquire a GABAergic phenotype, but part of this population gets stalled in an immature state that prevents iNs to fully acquire an interneuron-like identity.

To determine whether iNs were endowed with the ability to generate distinct subtypes of interneurons, I next investigated the expression of the two main interneuron subpopulations in the cortex: PV and SST. For this purpose, I performed immunostaining to detect PV expression and RNAscope to detect SST mRNA transcripts, as immunostaining did not work very well for this marker. In agreement with previous observations, almost none of the Ascl1 and Bcl2 co-transduced cells acquired the expression of subtype-specific interneuronal markers (0.4 ± 0.3% of PV+/GFP+/DsRed+ cells; Fig. 3.7C-D). Strikingly, forced expression of Ascl1SA6 and Bcl2 generated a significant fraction of PV-expressing iNs (21.0 ± 2.2% of PV+/GFP+/DsRed+ cells; Fig. 3.7C-D), almost corresponding with the total amount of GABA-expressing iNs generated. Indeed, RNAscope revealed that none of the co-transduced cells with Ascl1 or Ascl1SA6 together with Bcl2 acquired the expression of SST at mRNA level (Fig. 3.7E), suggesting that iNs differentiation is specific towards a PV interneuron-like phenotype. These results corroborate the electrophysiology data demonstrating that a significant fraction of the iNs display fast-spiking activity (Fig. 1.3).

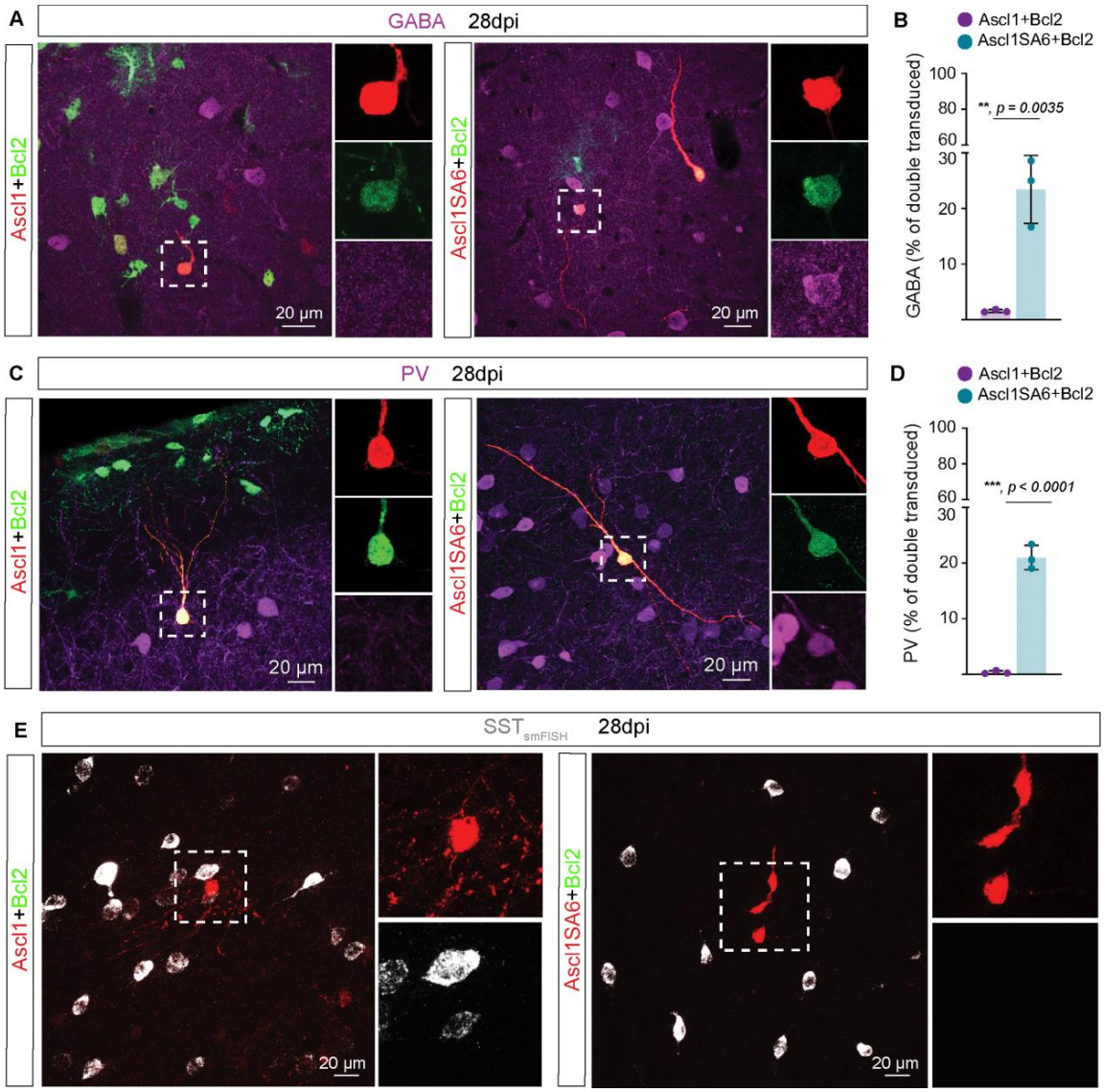

Figure 3.7. Forced co-expression of Ascl1SA6 and Bcl2 converts cortical postnatal glia into GABA and PV-expressing iNs. (A) Confocal images depicting the lack of GABA expression (in magenta) in Ascl1 + Bcl2-transduced cells in contrast to the acquisition of GABA expression (in magenta) in Ascl1SA6 + Bcl2-transduced cells. (B) Quantification of the percentage of double-transduced cells expressing GABA at 28dpi. Data shown as mean ± SD. Two-tailed Student's unpaired t-test, ** P=0.0036, n = 3 mice (634 cells) for Ascl1 + Bcl2, n = 3 mice (78 cells) for Ascl1SA6 + Bcl2. (C) Confocal images depicting the lack of PV (in magenta) expression in Ascl1 + Bcl2-transduced cells in contrast to the acquisition of PV (in magenta) expression in Ascl1SA6 + Bcl2-transduced cells. (D) Quantification of the percentage of double-transduced cells expressing PV at 28dpi. Data shown as mean ± SD. Two-tailed Student's unpaired t-test, *** P<0.0001, n = 3 mice (2995 cells) for Ascl1 + Bcl2, n = 3 mice (208 cells) for Ascl1SA6 + Bcl2. (E) Confocal images depicting the lack of SST mRNA particles (in white) in Ascl1 and Ascl1SA6 + Bcl2-transduced cells.

Next, I investigated to which extent PV-expressing iNs are similar to endogenous cortical PV interneurons. To this end, I compared PV expression levels of both cell populations at 28 dpi. As evidenced by immunohistochemistry, I found a lot of variability in PV expression levels throughout both endogenous PV interneurons and PV iNs populations (Fig. 3.8A). In agreement with these findings, it has been previously reported that PV expression levels are very variable as they are strongly regulated by activity and recent experience (Donato et al., 2013, 2015). Interestingly, when comparing PV expression levels between endogenous neurons and iNs, I found that the majority of glia-derived PV+ iNs expressed low levels of PV and their mean PV intensity was less than half when compared to endogenous PV interneurons (Fig. 3.8A-B).

Despite the results demonstrating high glia-to-neuron conversion efficiency as well as the acquisition of expression of subtype-specific interneuronal markers, I observed that most of the iNs remained morphologically less mature than endogenous ones. To further investigate this aspect, I next examined to which extent iNs co-transduced with Ascl1SA6 and Bcl2 morphologically resemble endogenous neurons by comparing their soma size and circularity index. DsRed signal was used to measure the soma area for iNs and PV signal was used as a proxy for the soma area of endogenous PV interneurons. Importantly, soma size of iNs was significantly smaller when compared to the soma of endogenous PV interneurons, regardless of the expression of PV in the iNs population (Fig. 3.8C-D). In addition, my results showed that iNs have a more irregular soma shape when compared to endogenous PV interneurons (Fig. 3.8C, E).

These data prompted us to further investigate other differences among PV-expressing iNs compared to endogenous ones. In the mouse cerebral cortex, PV interneurons are only found distributed across deep layers, but never in layer I (Fig. 3.8F). Something that drew my attention was the fact that I found ectopic generation of many PV-expressing iNs in layer I (Fig. 3.8G), a cortical layer that is devoid of endogenous PV interneurons. The absolute number of PV-expressing iNs in layer I was high and, therefore, I next asked whether glial cells had a preference for converting towards PV iNs specifically in this layer. The proportion of Ascl1SA6+Bcl2 iNs that expressed PV among the total iNs located in layer I or in deeper layers (layers II-IV) was similar (Fig. 3.8H), suggesting that PV+ iNs can be equally generated in the different layers of the cortex. This finding suggests that overexpression of Ascl1SA6 together with Bcl2 can induce transcriptional programs on glial cells that superimpose the acquisition of a novel neuronal identity beyond cortical layer specification.

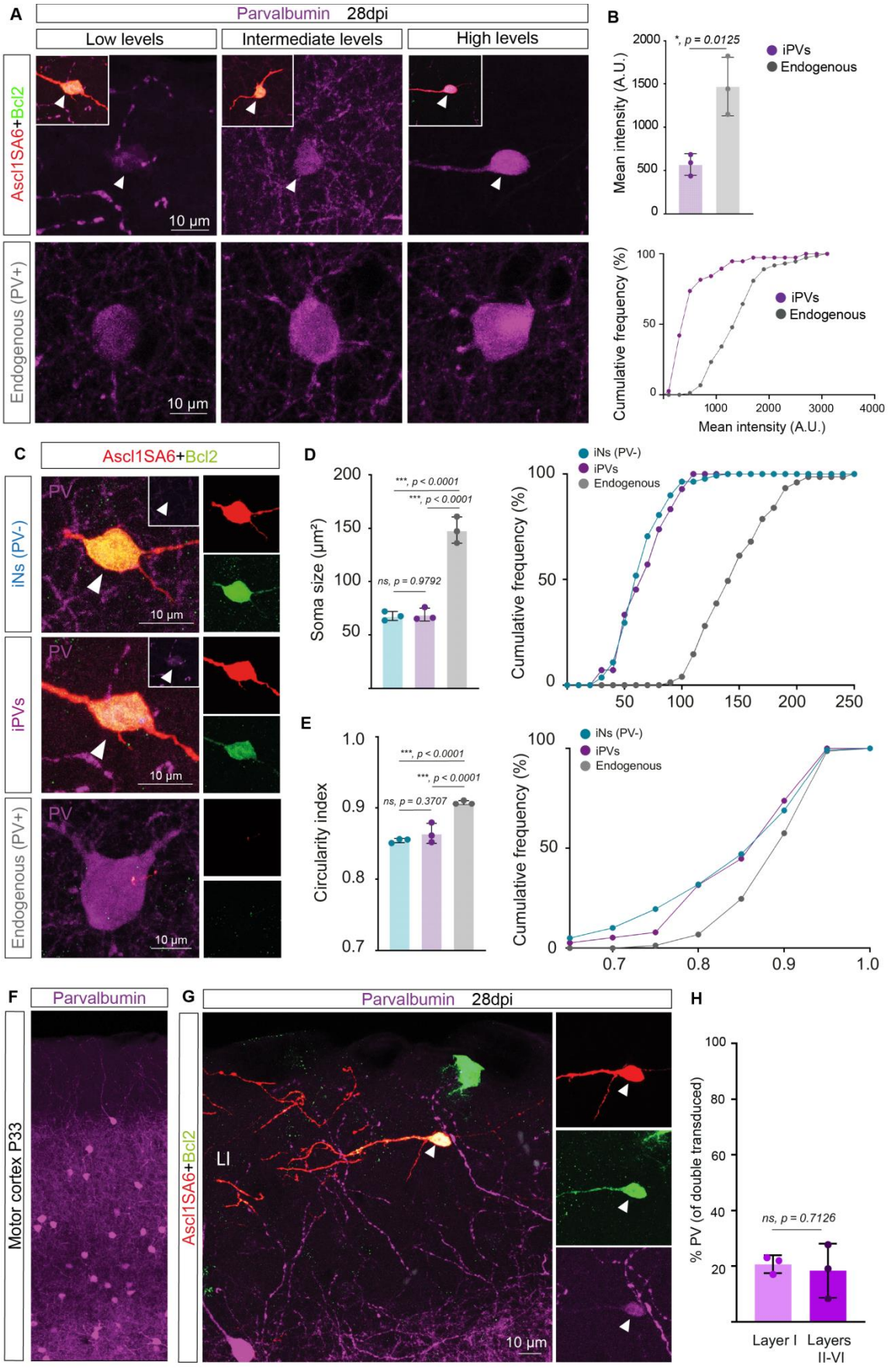
A
Parvalbumin 28dpi
Low levels
Intermediate levels
High levels
Ascl1SA6+Bcl2
Endogenous (PV+)
10 µm
B
*, p = 0.0125
iPVs
Endogenous
Mean intensity (A.U.)
Cumulative frequency (%)
C
Ascl1SA6+Bcl2
iNs (PV-)
iPVs
Endogenous (PV+)
PV
D
***, p < 0.0001
ns, p = 0.9792
Soma size (µm²)
iNs (PV-)
E
ns, p = 0.3707
Circularity index
F
Parvalbumin
Motor cortex P33
G
LI
H
ns, p = 0.7126
% PV (of double transduced)
Layer I
Layers II-VI

Figure 3.8. Ascl1SA6 and Bcl2-iNs display differences in PV expression levels, soma size and layer distribution in the mouse cortex compared to endogenous PV neurons. (A) Confocal images depicting different PV expression levels in AsclSA6 + Bcl2-iNs (upper panels) and endogenous PV neurons (lower panels) in the mouse cerebral cortex at 28dpi. (B) Bar graph representing mean intensity levels of PV expression measured in iNs and endogenous neurons at 28dpi. Data shown as mean ± SD. Two-tailed Student's unpaired t-test, * P=0.0125, n = 3 mice (38 cells) for iNs, n = 3 mice (73 cells) for endogenous neurons. Cumulative frequency distribution of PV intensity levels of iNs and endogenous neurons at 28dpi. Non-parametric Kolgomorov-Smirnof test's, P= 0.0935 (ns), n = 3 mice (38 cells) for iNs, n = 3 mice (73 cells) for endogenous neurons. (C) Confocal images depicting soma size and morphology of PV- iNs, PV+ iNs and endogenous neurons at 28dpi. (D) Bar graph representing mean soma area (μm^2) of PV- iNs, PV+ iNs and endogenous neurons at 28dpi. One-way ANOVA followed by Tukey's multiple comparisons *post hoc* test, *** P<0.0001 for endogenous neurons vs PV- iNs and for endogenous neurons vs PV+ iNs, P=0.09792 for PV- iNs vs PV+ iNs, n = 3 mice (139 cells) for PV- iNs, n = 3 mice (42 cells) for PV+ iNs, n = 3 mice (75 cells) for endogenous neurons. Cumulative frequency distribution of PV intensity levels of PV- iNs, PV+ iNs and endogenous neurons at 28dpi, n = 3 mice (139 cells) for PV- iNs, n = 3 mice (42 cells) for PV+ iNs, n = 3 mice (75 cells) for endogenous neurons. (E) Bar graph representing circularity index of PV- iNs, PV+ iNs and endogenous neurons at 28dpi. One-way ANOVA followed by Tukey's multiple comparisons *post hoc* test, *** P<0.0001 for endogenous neurons vs PV- iNs and for endogenous neurons vs PV+ iNs, P=0.03707 for PV- iNs vs PV+ iNs, n = 3 mice (139 cells) for PV- iNs, n = 3 mice (38 cells) for PV+ iNs, n = 3 mice (73 cells) for endogenous neurons. Cumulative frequency distribution of circularity index of PV- iNs, PV+ iNs and endogenous neurons at 28dpi, n = 3 mice (139 cells) for PV- iNs, n = 3 mice (38 cells) for PV+ iNs, n = 3 mice (73 cells) for endogenous neurons. (F) Low-magnification confocal image depicting distribution of endogenous PV neurons across cortical layers at P33. (G) Confocal image depicting ectopic generation of PV+ iNs in cortical layer I at 28dpi. (H) Quantification of the percentage of PV+ iNs and PV- iNs distributed in layer I compared to deeper layers (II-VI). Two-tailed Student's unpaired t-test, P=0.7126 for layer I vs deeper layers (II-VI) for both PV- and PV+ iNs, n = 3 (161 cells) for PV- iNs, n = 3 (42 cells) for PV+ iNs.

Altogether, these data demonstrate the generation of GABA and PV-expressing iNs in the mouse cerebral cortex by forced expression of Ascl1SA6 and Bcl2. However, I found several differences between glia-derived PV-expressing iNs and endogenous PV interneurons, suggesting that iNs are missing some features from PV interneurons due to the artificial nature of the neuronal reprogramming system.

1.6. Ascl1SA6 and Bcl2-derived iNs acquire expression of hallmark genes from fast-spiking PV interneurons.

Based on our previous findings demonstrating that Ascl1SA6 and Bcl2-derived iNs display functional properties resembling fast-spiking interneurons, I next investigated the expression of voltage-gated channels necessary for the acquisition of high-frequency firing in the reprogrammed iNs (Lien & Jonas, 2003; Rudy & McBain, 2001). Due to the difficulty in detecting channels in the cell membrane through immunostaining, I decided to use RNAscope to test the expression of mRNA transcripts of the Kv3.1voltage-gated channel, which is primarily restricted to fast-spiking interneurons and is critical for fast-spiking physiology by providing rapid membrane repolarization after an action potential (Erisir et al., 1999; Labro et al., 2015). The GFP signal from the reporter gene could not be recovered after RNAscope, thus only DsRed reporter gene was used to identify iNs. In contrast to co-transduced cells with Ascl1 and Bcl2, I found that most of Ascl1SA6 and Bcl2-derived iNs acquired significantly higher mRNA expression of Kv3.1 (Fig. 3.9A, C, D). Importantly, I also observed that the expression levels of Kv3.1 mRNA were remarkably lower in iNs when compared to endogenous neurons (Fig. 3.9A, C, D).

Next, to investigate the possibility that iNs are endowed with the machinery to form synapses, I tested the expression of pre-synaptic markers. As I found difficulties to detect neuronal processes just through the expression of the reporter gene DsRed, I again decided to use RNAscope to check mRNA expression of Synaptotagmin 2 (Syt2), a pre-synaptic marker enriched in PV interneurons (Sommeijer & Levelt, 2012). A low number of cells co-transduced with Ascl1 and Bcl2 expressed very low levels of Syt2 mRNA transcript (Fig. 3.9B, E, F). In contrast, a significant fraction of co-transduced cells with Ascl1SA6 and Bcl2 expressed mRNA transcripts of the pre-synaptic marker Syt2, although the mean Syt2 mRNA expression levels were not significantly higher in this group compared to cells co-transduced with Ascl1 and Bcl2 (Fig. 3.9F). Again, I observed that Syt2 expression levels remained significantly lower when compared to those expressed by endogenous neurons (Fig. 3.9B, E, F).

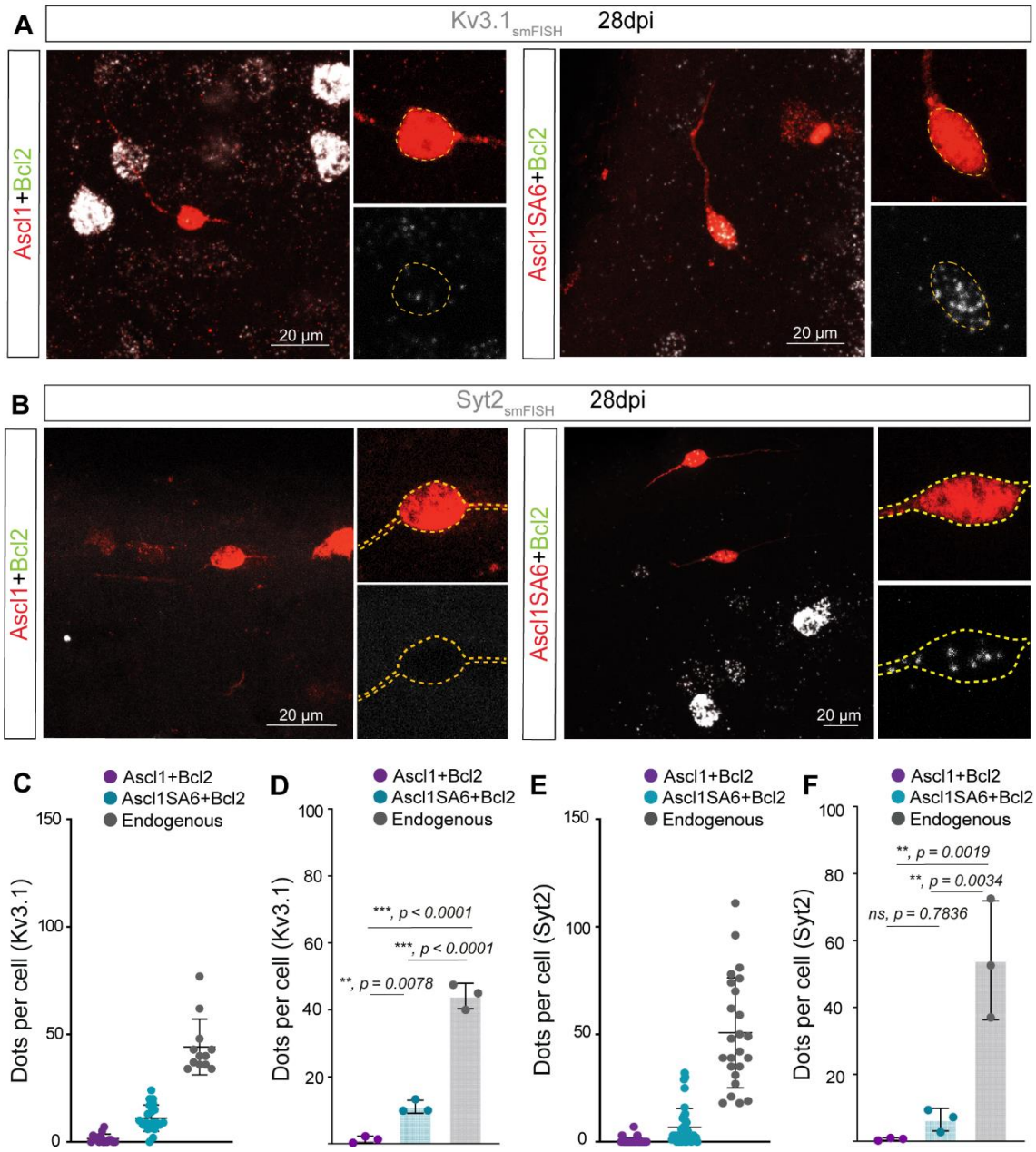
A
Kv3.1smFISH 28dpi
Ascl1+Bcl2
Ascl1SA6+Bcl2
20 µm
B
Syt2smFISH 28dpi
C
D
E
F
Ascl1+Bcl2
Ascl1SA6+Bcl2
Endogenous
Dots per cell (Kv3.1)
Dots per cell (Syt2)
***, p < 0.0001
**, p = 0.0078
**, p = 0.0019
**, p = 0.0034
ns, p = 0.7836

Figure 3.9. Ascl1SA6 and Bcl2-iNs acquire expression of of Kv3.1 and Syt2 at mRNA level. (A) Confocal images depicting expression of Kv3.1 mRNA particles (in white) in cells transduced with Ascl1 or Ascl1SA6 together with Bcl2. (B) Confocal images depicting expression of Syt2 mRNA particles (in white) in cells transduced with Ascl1 or Ascl1SA6 together with Bcl2. (C) Quantification of the number of Kv3.1 mRNA particles in Ascl1/Ascl1SA6 + Bcl2-transduced cells and endogenous neurons. Each dot represents one cell, 15 cells (n = 3) for Ascl1 + Bcl2-transduced cells, 21 cells (n = 3) for Ascl1SA6 + Bcl2-transduced cells, 12 cells (n = 3) for endogenous neurons. (D) Bar graph representing the mean number of Kv3.1 mRNA particles in Ascl1/Ascl1SA6 + Bcl2-transduced cells and endogenous neurons. One-way ANOVA followed by Tukey's multiple comparisons *post hoc* test, *** P<0.0001 for endogenous neurons vs Ascl1+Bcl2-transduced cells and Ascl1SA6+Bcl2-transduced cells, ** P=0.0078 for Ascl1+Bcl2-transduced cells vs Ascl1SA6+Bcl2-transduced cells, 15 cells (n = 3) for Ascl1 + Bcl2-transduced cells, 21 cells (n = 3) for Ascl1SA6 + Bcl2-transduced cells, 12 cells (n = 3) for endogenous neurons. (E) Quantification of the number of Syt2 mRNA particles in Ascl1/Ascl1SA6 + Bcl2-transduced cells and endogenous neurons. Each dot represents one cell, 30 cells (n = 3) for Ascl1 + Bcl2-transduced cells, 39 cells (n = 3) for Ascl1SA6 + Bcl2-transduced cells, 24 cells (n = 3) for endogenous neurons. (F) Bar graph representing the mean number of Syt2 mRNA particles in Ascl1/Ascl1SA6 + Bcl2-transduced cells and endogenous neurons. One-way ANOVA followed by Tukey's multiple comparisons *post hoc* test, ** P=0.0019 for endogenous neurons vs Ascl1SA6+Bcl2-transduced cells, ** P=0.0034 for endogenous neurons vs Ascl1+Bcl2-transduced cells and P=0.7836 for Ascl1+Bcl2-transduced cells vs Ascl1SA6+Bcl2-transduced cells, 30 cells (n = 3) for Ascl1 + Bcl2-transduced cells, 39 cells (n = 3) for Ascl1SA6 + Bcl2-transduced cells, 24 cells (n = 3) for endogenous neurons.

Taken together, these results corroborate that co-expression of Ascl1SA6 and Bcl2 activate a PV-like programme, evidenced by the expression of mRNA transcripts of PV hallmark genes important for the functional properties of this cell population.

1.7. *In vivo* reprogramming of cortical postnatal glia using a tri-cistronic retroviral vector.

One of the limitations of using two different retroviral constructs to induce fate conversion is the low and variable number of co-transduced cells. Thus, to pursue my quest to increase the number of iNs, I generated tri-cistronic retroviral vectors encoding for the reprogramming factors Ascl1 or Ascl1SA6 and Bcl2 as well as the reporter gene DsRed. In this construct, both genes were linked by the "self-cleavage" peptide sequence T2A and their transcription was driven under control of the constitutive and strong CAG promoter (Fig. 3.10A).

The efficiency of glia-to-neuron conversion by the tri-cistronic retroviral vectors was assessed by immunostaining against the neuronal marker NeuN at 28 dpi. Consistent with what I had previously observed with co-transduction of separate vectors, most of the cells that expressed Ascl1-Bcl2 failed to reprogram into NeuN-expressing iNs (7.0 ± 4.4%of NeuN+/DsRed+ cells; Fig. 3.10B-C). In sharp contrast, the majority of cells transduced with Ascl1SA6-Bcl2 acquired the expression of the neuronal marker NeuN (78.3 ± 2.3% of NeuN+/DsRed+ cells; Fig. 3.10B-C).

Overall, these data suggest that transducing cells with a tri-cistronic vector encoding for both reprogramming factors elicits a similar reprogramming efficiency as when using separate single vectors.

1.8. Fate-mapping experiments unveil a predominant astrocytic origin of glia-derived iNs by forced co-expression of Ascl1SA6 and Bcl2.

Over the past years, several studies have raised serious scepticism regarding the glial origin of the putative iNs due to the use of genetic tools employed to induce transgene expression specifically to glial cells, as it seems to be the case for the reports using AAVs or lentivirus for transgene delivery (reviewed in Leaman et al., 2022). Most of the studies employing these strategies rely on the gradual loss of glial markers and the acquisition of neuronal identity to claim glia-to-neuron conversion, but do not provide compelling evidence to unambiguously demonstrate the glial origin of the putative iNs.

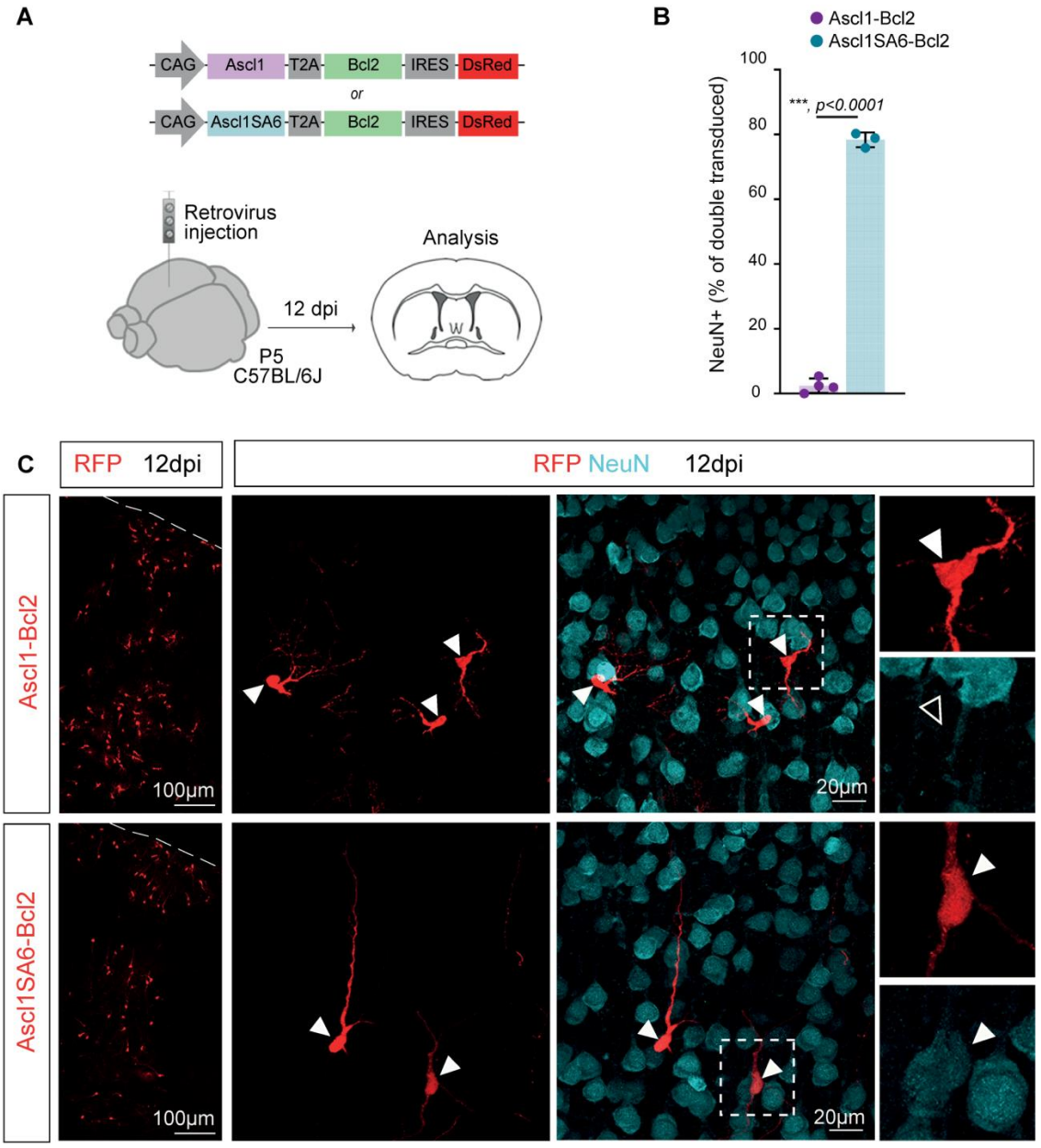

Figure 3.10. Tri-cistronic vector encoding for Ascl1SA6-Bcl2 yields high glia-to-neuron conversion rate in the postnatal mouse cerebral cortex. (A) Schematic representation of experimental design. Retroviral constructs encoding Ascl1-Bcl2 (pCAG-Ascl1-T2A-Bcl2-DsRed) or Ascl1SA6-Bcl2 (pCAG-Ascl1SA6-T2A-Bcl2-DsRed) were injected in the mouse cerebral cortex at P5, and the reprogramming efficiency was analysed at 12dpi. (B) Quantification of the percentage of transduced cells expressing NeuN at 12dpi. Data shown as mean ± SD. Two-tailed Student's unpaired t-test, *** P<0.0001, n = 4 mice (1002 cells) for Ascl1- Bcl2, n = 3 mice (1224 cells) for Ascl1SA6-Bcl2. (C) Low-magnification images showing Ascl1-Bcl2 (upper insets) or Ascl1SA6-Bcl2 (lower insets) transduced cells at cortical site of injection and confocal images depicting NeuN expression (in cyan) in Ascl1-Bcl2 (upper insets) or Ascl1SA6-Bcl2 (lower insets) transduced cells. Empty arrows indicate marker-negative cells.

In the light of this recent controversy concerning the glial origin of iNs, it is of crucial importance to develop robust lineage-tracing strategies that demonstrate the veracity of glia-to-neuron conversion in the brain (L. L. Wang et al., 2021a). Taking advantage of the generation of a tri-cistronic retroviral vector encoding for both reprogramming factors and the reporter gene DsRed, which can induce a high number of iNs, I decided to use two strategies to provide strong evidence for glia-derived neuronal reprogramming.

As previously demonstrated, only glial cells proliferate in the postnatal mouse cerebral cortex at the time of the retroviral injection (Fig. 3.1C-F). Thus, to first demonstrate that iNs originate from proliferative cells, mice received a single intraperitoneal injection of EdU on the same day of the retroviral intracortical injection. The incorporation of EdU in iNs was assessed by immunostaining in reporter-positive transduced cells at 28dpi (Fig. 3.11A). Interestingly, I found that one single dose of EdU was enough to detect EdU incorporation on more than half of transduced cells (58.7 ± 4.4%of EdU+/DsRed+ cells; Fig. 3.11B-C). Importantly, the majority of transduced cells that had incorporated EdU also acquired the expression of the neuronal marker NeuN (48.5 ± 5.1% of NeuN+/EdU+/DsRed+ cells; Fig. 3.11B-C), indicating that these iNs originated from proliferating glia at the time of the injection. Of note, the number of transduced cells that incorporated EdU but lacked NeuN expression was significantly smaller (Fig. 3.11B-C). One possible explanation for this result is that glial cells that did not successfully reprogram might have kept proliferating and diluted the incorporated EdU over rounds of division.

Second, I decided to use transgenic mouse lines known to reliably label astrocytes and OPCs to trace the iNs origins after inducing glia-to-neuron conversion. To this end, the transgenic mouse line Aldh1l1-CreER^{T2} (Srinivasan et al., 2016) was crossed with RCE:loxP mice (Sousa et al., 2009) and tamoxifen was administered subcutaneously from P2-P5 to induce Cre-mediated recombination and achieve astrocyte labelling in the mouse brain. Mice received an intracranial injection in the cerebral cortex at P5 with a retroviral vector encoding for Ascl1SA6, Bcl2 and DsRed. The glial origin of iNs was assessed by performing immunostaining of cortical sections for the GFP reporter gene from the Aldh1l1-CreER^{T2};RCE transgenic mouse line, the retroviral DsRed reporter gene and the neuronal markers Dcx and NeuN at 12 dpi. Remarkably, I found that in the Aldh1l1-CreER^{T2}/RCE transgenic mice the majority of DsRed+ transduced cells also co-expressed the GFP+ reporter gene (~73% of GFP+/DsRed+; Fig. 3.12B-E). Importantly, most of the fate-mapped transduced cells

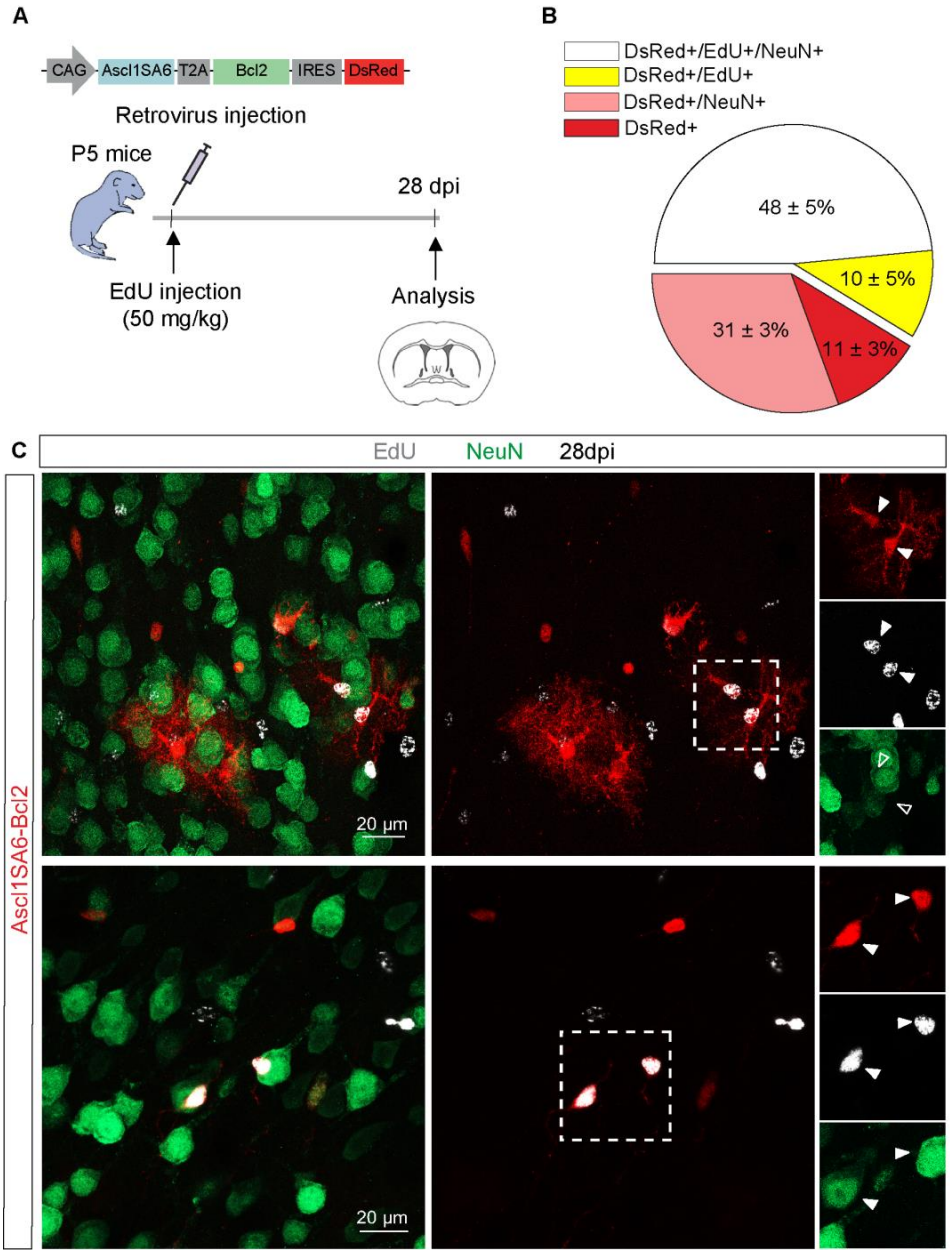

Figure 3.11. EdU incorporation in Ascl1SA6-Bcl2-derived iNs reveals their origin from proliferating glial cells. (A) Schematic representation of experimental design. Retroviral constructs encoding for Ascl1SA6-Bcl2 (pCAG-Ascl1SA6-T2A-Bcl2-DsRed) were injected in the postnatal mouse cerebral cortex at P5 and mice received an intraperitoneal injection of EdU (50mg/kg) at time of the retroviral injection. Mice were sacrificed at 28dpi to investigate incorporation of EdU in transduced cells. (B) Pie chart showing the relative number of transduced cells (DsRed+) expressing NeuN (iNs) or not (most likely glia) and had incorporated EdU. Data shown as mean ± SD, n = 4 mice (464 cells). (C) Confocal images depicting EdU incorporation in transduced cells (DsRed+) lacking NeuN expression (upper insets) and in transduced cells (DsRed+) expressing NeuN (lower insets).

also co-expressed the neuronal markers Dcx (49.1 ± 13.0% of Dcx+/GFP+/DsRed+; Fig. 3.12B, D) or NeuN (60.4 ± 9.8% of NeuN+/GFP+/DsRed+; Fig. Fig. 3.12C, E), providing strong evidence for astrocyte-to-neuron conversion in the mouse cortex by co-expression of Ascl1SA6 and Bcl2. To assess the labelling efficiency of astrocytes in Aldh1l1-CreER^{T2}/RCE mice, I next analysed the number of Sox9+ cells that were co-expressing the reporter gene GFP in the cortex of transgenic mice at 12dpi upon tamoxifen injection from P2 to P5. Remarkably, I found that most of the Sox9+ cells in the cortex also expressed the reporter gene GFP from the mice line (94.1 ± 7.1% of Sox9+/GFP+; Fig. 3.12F-G), showing a very high recombination efficiency after tamoxifen administration. Altogether, these data suggest that most of the transduced cells are fate-mapped astrocytes, in agreement with my results and our previous published studies showing that control retrovirus mostly target astroglia (Fig. 3.2B-C; Galante et al., 2022). It could be possible that some of the iNs that could not be fate-mapped derived from residual astrocytes present in the SVZ, instead of coming from parenchymal astrocytes. However, this possibility is quite unlikely given that retroviral injections are locally restricted to the cortex and, therefore, transduced cells in the SVZ would need to migrate towards the cortex. Some studies have reported that neuroblasts derived from the SVZ can migrate towards the injured site (Jin et al., 2003; Yamashita et al., 2006), but these migrating cells would need to remain in a proliferating state in order to be transduced by the injected retrovirus. In any case, to rule out the possibility that cells derived from SVZ become transduced, it would be required to develop a fate-mapping strategy that specifically labels astrocytes present in the SVZ without labelling astrocytes residing in the parenchyma.

Likewise, NG2-CreER^{TM} BAC transgenic mice (Zhu et al., 2011) was bred with RCE:loxP mice (Sousa et al., 2009) and the offspring received tamoxifen intraperitoneally at P2 and P5 to induce Cre-mediated recombination to label OPCs in the mouse brain (Fig. 3.13A). Mice were injected in the postnatal cerebral cortex with a retroviral construct encoding Ascl1SA6, Bcl2 and DsRed, and the glial origin of iNs was investigated by immunostaining of cortical sections for the GFP reporter gene from the transgenic mouse lines, the retroviral DsRed reporter gene and the neuronal markers Dcx and NeuN at 12 dpi. In contrast, I observed that only very few transduced cells in the NG2-CreER^{TM} /RCE transgenic mice co-expressed both reporter genes GFP and DsRed (~3% of GFP+/DsRed+ cells; Fig. 3.13I-J). Still, I could find some of the fate-mapped transduced cells that also expressed the neuronal markers Dcx (3.3 ± 3.2% of Dcx+/GFP+/DsRed+; Fig. 3.13G, I) or NeuN (2.1 ± 3.6% of NeuN+/GFP+/DsRed+; Fig. 3.13H, J), providing proof-of-principle that OPCs can also be converted into iNs. As

described at the beginning of this chapter and in previous work (Galante et al., 2022), around 35% of proliferating oligodendroglia (Sox10+ cells) are targeted by control retrovirus injected in the P5 cerebral cortex (Fig. 3.2B-C). Thus, the low number of iNs fate-mapped in the NG2-CreER^{TM};RCE transgenic mice indicate that most likely not many OPCs are able to successfully convert into iNs by co-expression of Ascl1SA6 and Bcl2 reprogramming factors. Next, I investigated the labelling efficiency of OPCs in the NG2-CreER^{TM};RCE transgenic mice line. For this purpose, I quantified the number of NG2+ cells that co-expressed the reporter gene GFP in the cortex of transgenic mice at 12dpi upon tamoxifen injection on P2 and P5. Importantly, I found that many NG2+ cells in the cortex also expressed the reporter gene GFP from the mice line (72.4 ± 9.3% of NG2+/GFP+; Fig. 3.13F-G). Although the majority of NG2+ cells were successfully labelled, the recombination efficiency in the NG2-CreER^{TM};RCE mice was much lower compared to Aldh1l1-CreER^{T2}/RCE mice, which might have reduced the number of iNs that were fate-mapped.

To further investigate the identity of cells co-transduced in these transgenic mouse lines, a control retrovirus encoding for DsRed but none reprogramming factors was injected in the postnatal cerebral cortex of Aldh1l1-CreER^{T2}/RCE and the identity of targeted cells was analysed by immunostaining against GFP to label Cre-recombined astroglia and Sox10 to label oligodendroglia at 12 dpi (Fig. 3.14A). Similar to my previous findings (Fig. 3.2), most of the transduced cells with the control retrovirus showed an astroglial identity, revealed by the expression of the reporter gene GFP from the Aldh1l1-CreER^{T2}/RCE transgenic mouse line (69.1 ± 1.4% of GFP+/DsRed+ cells; Fig. 3.14B-C). Almost the remaining population of transduced cells revealed an oligodendroglial phenotype, evidenced by the expression of the marker Sox10 (25.4 ± 2.3% of Sox10+/DsRed+ cells; Fig. 3.14B-C). Next, I decided to inject a control retrovirus in the postnatal cerebral cortex of NG2-CreER^{TM}/RCE transgenic mice and analyse the phenotype of transduced cells by immunoreactivity against GFP to label Cre-recombined OPCs and Sox9 to label astrocytes at 12 dpi (Fig. 3.14D). Consistent with my previous observations (Fig. 3.2), most of the targeted cells with the control retrovirus were Sox9+ astrocytes, (66.6 ± 2.1% of Sox9+/DsRed+ cells; Fig. 3.14E-F), whereas about a quarter of targeted cells were identified as fate-mapped OPCs (22.0 ± 5.7% of GFP+/DsRed+ cells; Fig. 3.14E-F). Thus, a relevant fraction of OPCs can also be traced using this transgenic mouse line.

Altogether, these data demonstrate that iNs originate from glial cells in the postnatal mouse cerebral cortex, with astrocytes being the main cell population from which neuronal reprogramming takes place.

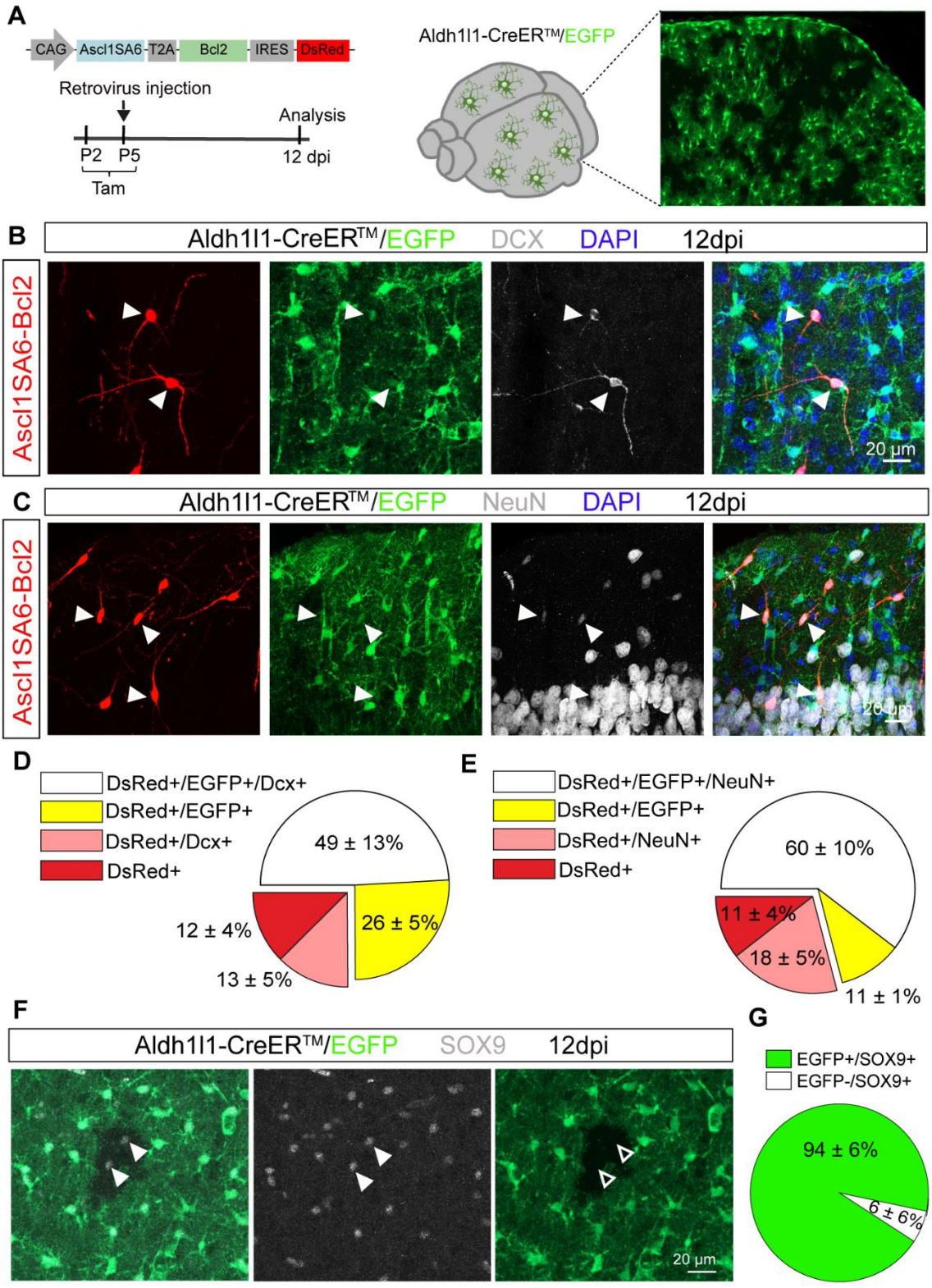
A
CAG
Ascl1SA6
T2A
Bcl2
IRES
DsRed
Retrovirus injection
Analysis
P2
P5
12 dpi
Tam
Aldh1l1-CreER™/EGFP
B
Aldh1l1-CreER™/EGFP DCX DAPI 12dpi
Ascl1SA6-Bcl2
20 μm
C
Aldh1l1-CreER™/EGFP NeuN DAPI 12dpi
Ascl1SA6-Bcl2
20 μm
D
DsRed+/EGFP+/Dcx+
DsRed+/EGFP+
DsRed+/Dcx+
DsRed+
49 ± 13%
26 ± 5%
12 ± 4%
13 ± 5%
E
DsRed+/EGFP+/NeuN+
DsRed+/EGFP+
DsRed+/NeuN+
DsRed+
60 ± 10%
11 ± 4%
18 ± 5%
11 ± 1%
F
Aldh1l1-CreER™/EGFP SOX9 12dpi
20 μm
G
EGFP+/SOX9+
EGFP-/SOX9+
94 ± 6%
6 ± 6%

Figure 3.12. Fate-mapping experiments reveal that most Ascl1SA6-Bcl2-derived iNs have an astroglial origin. (A) Schematic representation of experimental design. Retroviral constructs encoding for Ascl1SA6-Bcl2 (pCAG-Ascl1SA6-T2A-Bcl2-DsRed) were injected in the cortex of Aldh1l1-CreER^{T2}/RCE transgenic mice at P5. Mice received a subcutaneous injection of tamoxifen daily between P2-P5 to induce Cre-mediated recombination and achieve irreversible labelling of astrocytes with GFP in the mouse brain. The proportion of cells with astroglial origin was analysed at 12dpi. (B-C) Confocal images depicting Ascl1SA6-Bcl2-derived iNs co-expressing Dcx (B) or NeuN (C) as well as the reporter genes DsRed and GFP in Aldh1l1-CreER^{T2}/RCE mice at 12dpi. (D-E) Pie charts showing the relative number of transduced cells (DsRed+) co-expressing GFP and/or Dcx (D) or NeuN (E) or none of them in Aldh1l1-CreER^{T2}/RCE mice at 12dpi. Data shown as mean ± SD, n = 3 mice (523 cells) for Dcx analysis, n = 3 mice (473 cells) for NeuN analysis. (F) Confocal images depicting the labelling efficiency of Aldh1l1-CreER^{T2}/RCE transgenic mice at 12dpi after tamoxifen injections from P2 to P5. (G) Pie chart showing the relative number of Sox9+ cells that co-expressed the GFP reporter gene from Aldh1l1-CreER^{T2}/RCE mice in the cortex at 12dpi.

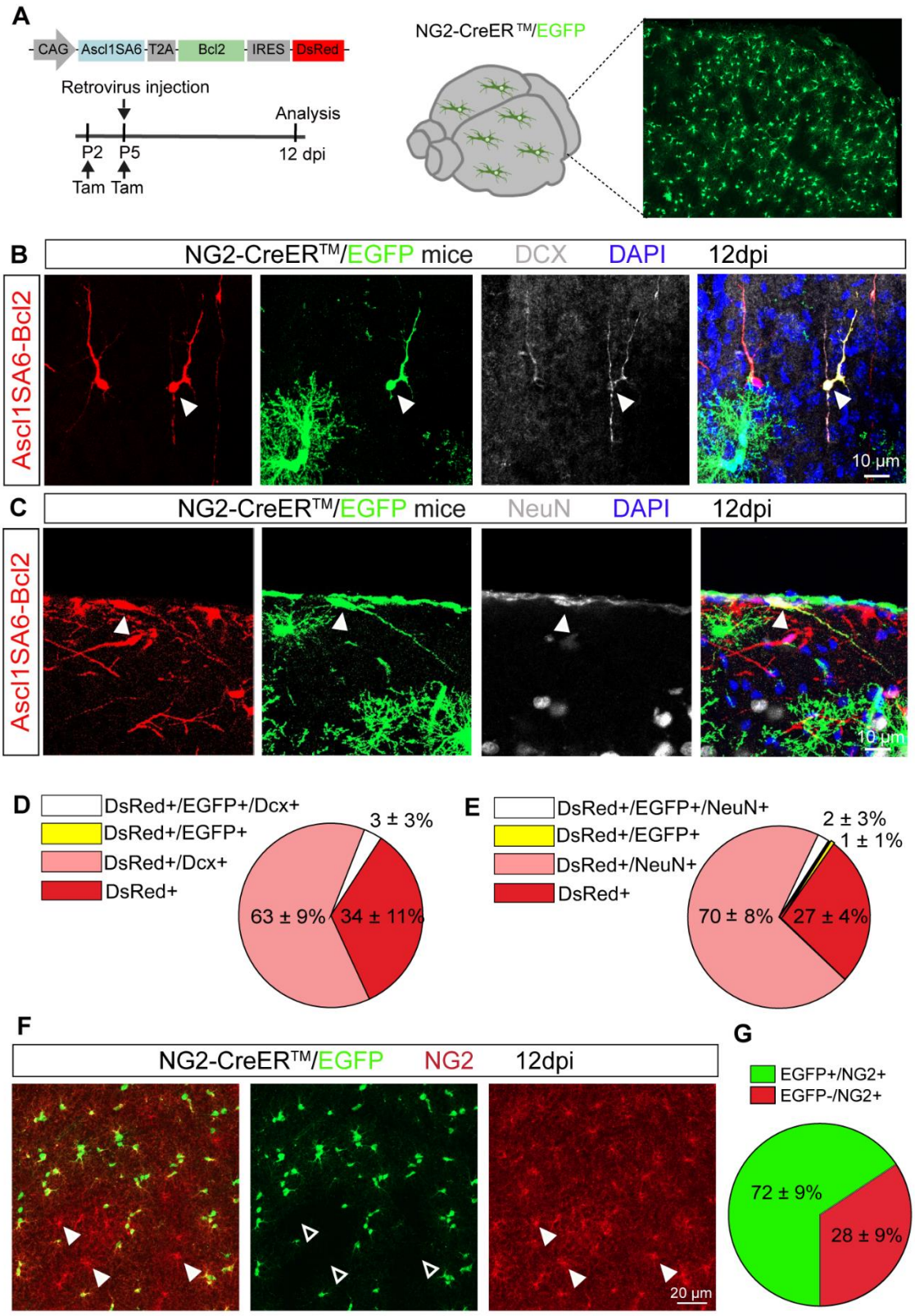
A
CAG
Ascl1SA6
T2A
Bcl2
IRES
DsRed
Retrovirus injection
Analysis
P2
P5
12 dpi
Tam Tam
NG2-CreER™/EGFP
B
NG2-CreER™/EGFP mice
DCX
DAPI
12dpi
Ascl1SA6-Bcl2
10 μm
C
NG2-CreER™/EGFP mice
NeuN
DAPI
12dpi
Ascl1SA6-Bcl2
10 μm
D
DsRed+/EGFP+/Dcx+
DsRed+/EGFP+
DsRed+/Dcx+
DsRed+
3 ± 3%
63 ± 9%
34 ± 11%
E
DsRed+/EGFP+/NeuN+
DsRed+/EGFP+
DsRed+/NeuN+
DsRed+
2 ± 3%
1 ± 1%
70 ± 8%
27 ± 4%
F
NG2-CreER™/EGFP
NG2
12dpi
20 μm
G
EGFP+/NG2+
EGFP-/NG2+
72 ± 9%
28 ± 9%

Figure 3.13. Fate-mapping experiments reveal that few Ascl1SA6-Bcl2-derived iNs originate from OPCs. (A) Schematic representation of experimental design. Retroviral constructs encoding for Ascl1SA6-Bcl2 (pCAG-Ascl1SA6-T2A-Bcl2-DsRed) were injected in the cortex of NG2-CreER^{TM}/RCE transgenic mice at P5. Mice received a subcutaneous injection of tamoxifen on days P2 and P5 to induce Cre-mediated recombination and achieve irreversible labelling of OPCs with GFP in the mouse brain. The proportion of cells with oligodendroglial origin was analysed at 12dpi. (B-C) Confocal images depicting Ascl1SA6-Bcl2-derived iNs co-expressing Dcx (B) or NeuN (C) as well as the reporter genes DsRed and GFP in NG2-CreER^{TM}/RCE mice at 12dpi. (D-E) Pie charts showing the relative number of transduced cells (DsRed+) co-expressing GFP and/or Dcx (D) or NeuN (E) or none of them in NG2-CreER^{TM}/RCE mice at 12dpi. Data shown as mean ± SD, n = 3 mice (416 cells) for Dcx analysis, n = 3 mice (169 cells) for NeuN analysis. (F) Confocal images depicting the labelling efficiency of NG2-CreER^{TM}/RCE transgenic mice at 12dpi after tamoxifen injections at P2 and P5. (G) Pie chart showing the relative number of NG2+ cells that co-expressed the GFP reporter gene from NG2-CreER^{TM}/RCE mice in the cortex at 12dpi.

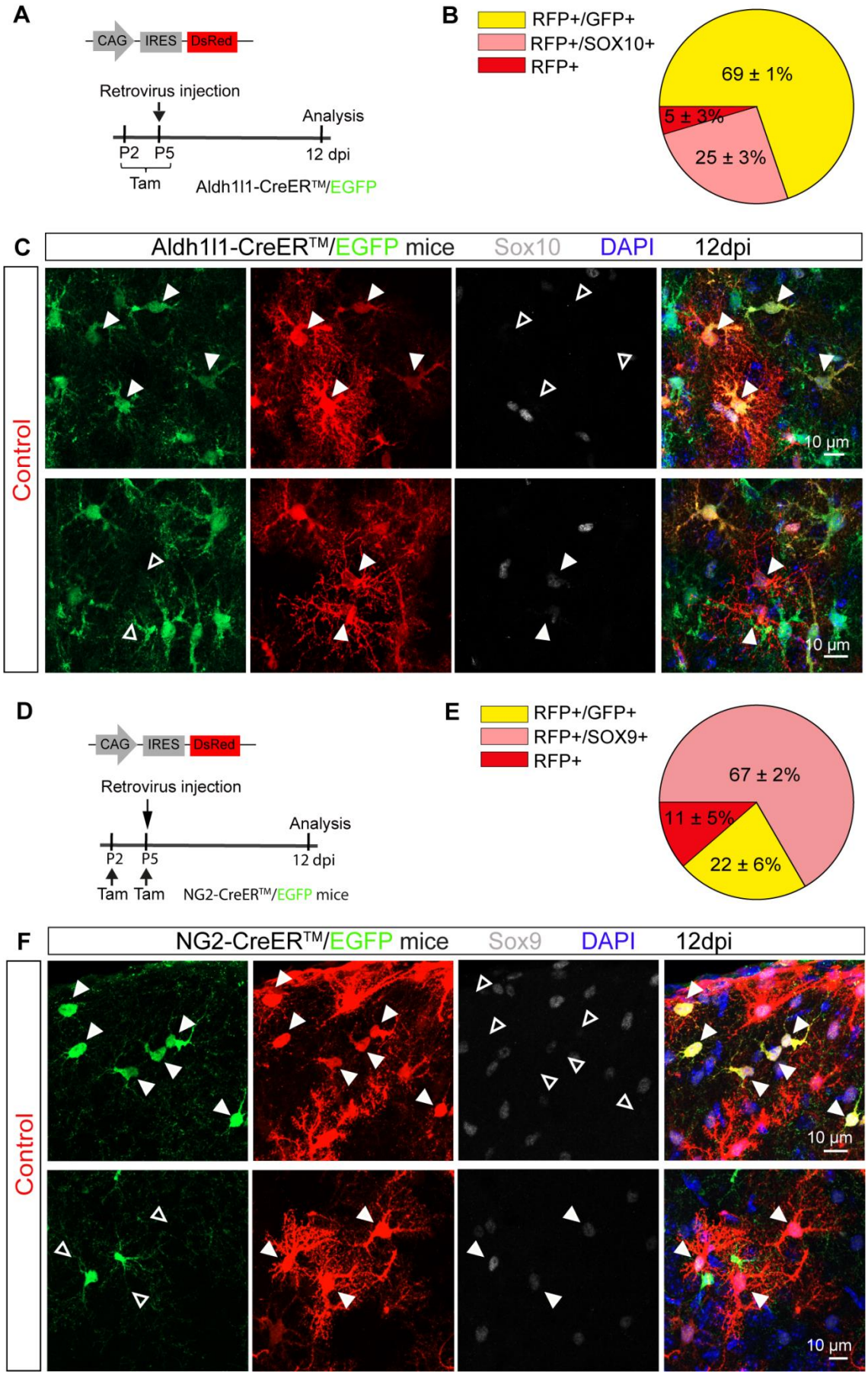
A
CAG
IRES
DsRed
Retrovirus injection
Analysis
P2
P5
12 dpi
Tam
Aldh1l1-CreER™/EGFP
B
RFP+/GFP+
RFP+/SOX10+
RFP+
69 ± 1%
5 ± 3%
25 ± 3%
C
Aldh1l1-CreER™/EGFP mice
Sox10
DAPI
12dpi
Control
10 µm
10 µm
D
CAG
IRES
DsRed
Retrovirus injection
Analysis
P2
P5
12 dpi
Tam
Tam
NG2-CreER™/EGFP mice
E
RFP+/GFP+
RFP+/SOX9+
RFP+
67 ± 2%
11 ± 5%
22 ± 6%
F
NG2-CreER™/EGFP mice
Sox9
DAPI
12dpi
Control
10 µm
10 µm

Figure 3.14. Fate-mapping experiments reveal the glial origin of cells targeted by control retroviruses in the mouse cerebral cortex. (A) Schematic representation of experimental design. Control retroviral constructs encoding for DsRed only (pCAG-DsRed) were injected in the cortex of Aldh1l1CreER^{T2}/RCE transgenic mice at P5. Mice received a subcutaneous injection of tamoxifen from P2-P5 to induce Cre-mediated recombination and achieve irreversible marking of astrocytes with GFP in the mouse brain. The proportion of cells with astroglial origin was analysed at 12dpi. (B) Pie chart showing the relative number of transduced cells (DsRed+) expressing Sox10, GFP or none of them in Aldh1l1CreER^{T2}/RCE mice at 12dpi. Data shown as mean ± SD, n = 2 mice (588 cells). (C) Confocal images depicting transduced cells expressing GFP (upper insets) or Sox10 (in white, lower insets) at 12 dpi. (D) Schematic representation of experimental design. Control retroviral constructs encoding for DsRed only (pCAG-DsRed) were injected in the cortex of NG2CreER^{TM}/RCE transgenic mice at P5. Mice received a subcutaneous injection of tamoxifen on days P2 and P5 to induce Cre-mediated recombination and achieve irreversible marking of OPCs with GFP in the mouse brain. The proportion of cells with oligodendroglial origin was analysed at 12dpi. (E) Pie chart showing the relative number of transduced cells (DsRed+) expressing Sox9, GFP or none of them in NG2CreER^{TM}/RCE mice at 12dpi. Data shown as mean ± SD, n = 3 mice (1374 cells). (F) Confocal images depicting transduced cells expressing GFP (upper insets) or Sox9 (in white, lower insets) at 12 dpi.

1.9. Tri-cistronic vector encoding for Ascl1-Bcl2 generates GABAergic iNs that lack PV specification properties.

I next asked the question whether the tri-cistronic retroviral vector co-expressing Ascl1SA6 and Bcl2 preserves the same specification properties as separate vectors to drive glia-to-interneuron conversion in the mouse cerebral cortex. For this purpose, postnatal glial cells were transduced with the tri-cistronic retroviral vector and immunostaining of cortical sections was performed against DsRed reporter gene and the interneuronal marker GABA at 28 dpi. In agreement with what was observed when co-expressing Ascl1SA6 and Bcl2 in different vectors, a remarkable proportion of transduced cells with the tri-cistronic vector acquired GABA expression (30.6 ± 3.9% of GABA+/DsRed+ cells; Fig. 3.15A, D). To further follow conversion of glia towards the GABAergic lineage, I took advantage of the transgenic mouse line Vgat-Cre (Vong et al., 2011) crossed with RCE:loxP (Sousa et al., 2009), from which glia-derived iNs may turn on GFP expression under the Vgat promoter. Intriguingly, none of the Ascl1SA6-Bcl2 transduced cells were found to co-express GFP and the reporter gene DsRed (0.0 ± 0.0% of GFP+/DsRed+ cells; Fig. 3.15B, D).

Next, to evaluate whether Ascl1SA6-Bcl2 transduced cells were also able to differentiate into PV-expressing iNs, I again injected the tri-cistronic vector in the postnatal mouse cortex and analysed the phenotype acquired by transduced cells 28 days later. Surprisingly, the results showed that almost none of the cells transduced with Ascl1SA6-Bcl2 acquired the expression of PV (0.4 ± 0.7% of PV+/DsRed+ cells; Fig. 3.15B, D). In addition, to determine whether iNs were functional, whole-cell patch-clamp electrophysiological recordings were performed on acute brain slices at 28 dpi by Dr. Nicolas Marichal. Current-clamp recordings revealed that cells transduced with the tri-cistronic vector were able to generate repetitive action potentials, suggesting the acquisition of functional properties. Although the number of recorded cells was low (n=4), we did not find any cells that exhibited high-frequency firing (Fig. 3.15E).

Taken together, these results showed that forced co-expression of Ascl1SA6 and Bcl2 in a polycistronic retroviral vector drives conversion of glial cells into a significant proportion of iNs that acquired GABAergic phenotype but lack specific features of fast-spiking PV interneurons. Unexpectedly, the fate specification properties of Ascl1SA6 and Bcl2 were different in the polycistronic vector compared to single retroviral vectors. Whereas co-expression of Ascl1SA6 and Bcl2 in single retroviral vectors generated around 20% of PV-expressing iNs, transduced cells with the polycistronic vector did not acquire this interneuron subclass identity.

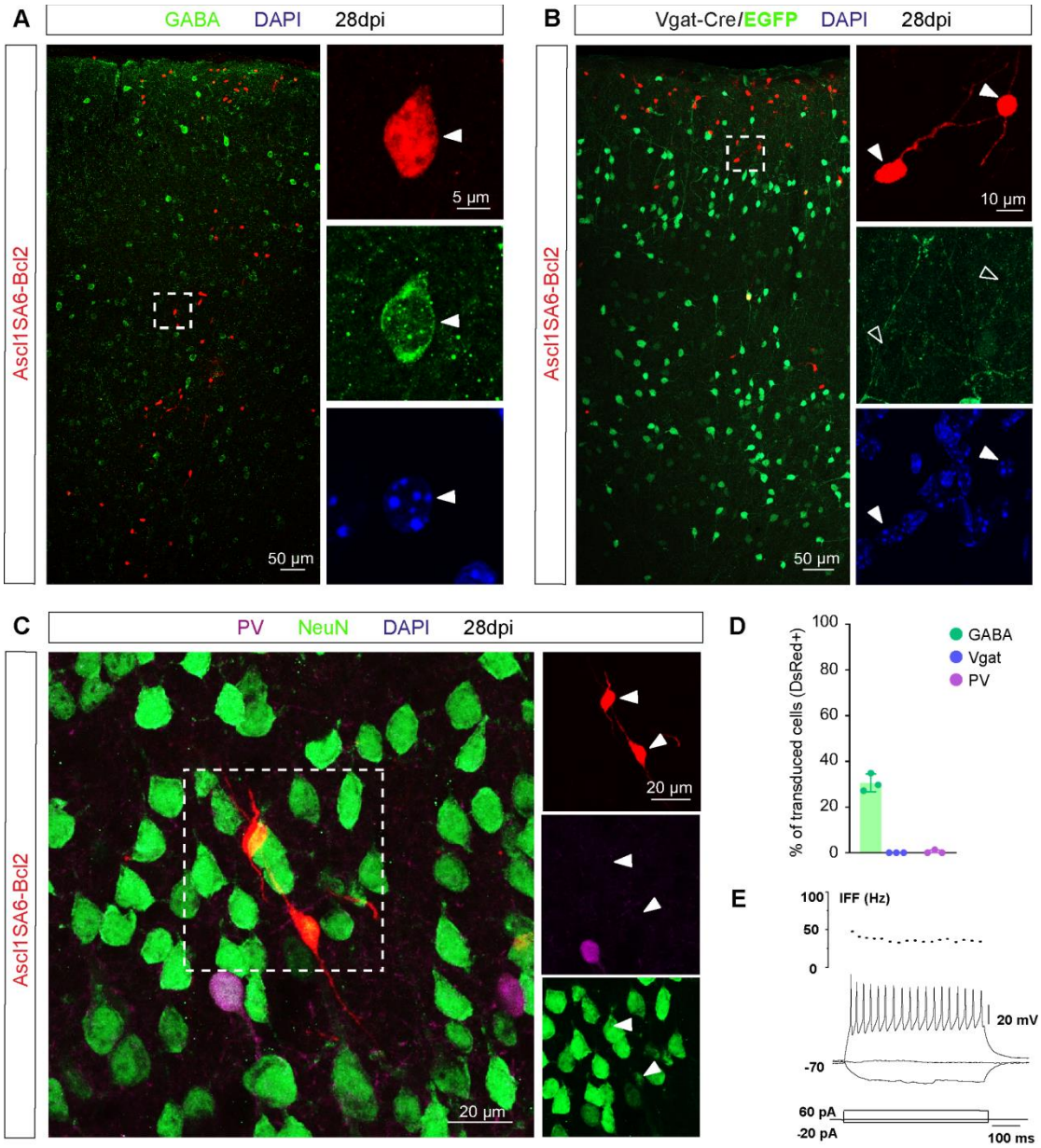

Figure 3.15. Tri-cistronic vector encoding for Ascl1SA6-Bcl2 generates iNs that expressed GABA but lack specific features of fast-spiking PV interneurons. (A) Confocal images depicting acquisition of GABA expression (in green) in Ascl1SA6-Bcl2-derived iNs at 28dpi. (B) Confocal images depicting lack of GFP expression in Ascl1SA6-Bcl2-derived iNs in Vgat-Cre/EGFP mice at 28dpi. (C) Confocal images depicting lack of PV expression (in magenta) in NeuN-expressing Ascl1SA6-Bcl2-derived iNs at 28dpi. (D) Quantification of the percentage of transduced cells expressing GABA, GFP in Vgat-Cre/EGFP mice or PV. Data shown as mean ± SD, n = 3 mice (554 cells) for GABA, n = 3 mice (526 cells) for GFP, n = 3 mice (1224 cells) for PV. (D) Current-clamp recording showing one Ascl1SA6-Bcl2-transduced cell that generates repetitive action potentials but do not exhibit high firing frequency (>100Hz).

In conclusion, in this chapter I demonstrated that MMLV retroviruses injected in the postnatal mouse cerebral cortex specifically transduced proliferating astrocytes and OPCs. Importantly, Ascl1 overexpression in proliferating glial cells induced an increase in the number of Sox10-positive cells, whereas forced expression of Ascl1SA6 instructed glia to convert into iNs in the postnatal mouse cortex. These findings suggest that Ascl1 fate decisions are highly influenced by its phosphorylation state. In addition, combined expression of Ascl1SA6 and Bcl2 significantly enhanced the reprogramming efficiency. Using reliable fate-mapping approaches, I showed that most of converted iNs have an astroglial origin. Remarkably, a notable proportion of Ascl1SA6 and Bcl2-transduced cells exhibited hallmark neurochemical and electrophysiological features of fast-spiking PV interneurons. A fraction of these PV-like iNs were present in cortical layers devoid of endogenous PV interneurons, suggesting that an imposed genetic programme can override extrinsic region-specific cues. Surprisingly, I observed that PV-like iNs exhibited small soma size and low PV expression levels, indicating that their maturation is hindered during glia-to-neuron conversion. Finally, I observed that fate specification properties of reprogramming factors are influenced by the retroviral vector used, suggesting that changes in gene expression levels might affect the reprogramming outcome.

CHAPTER II.

In vivo glia-to-interneuron conversion in the postnatal mouse cerebral cortex by forced expression of Ascl1SA6 and Dlx2

2.1. Ascl1SA6 and Bcl2-derived iNs exhibit ectopic mRNA expression of Ascl1 and lack endogenous Dlx2 mRNA expression.

Dlx2 is a downstream target of Ascl1 in GABAergic specification during embryonic development (Lindtner et al., 2019; Long et al., 2009; Petryniak et al., 2007). Thus, I asked the question whether forced expression of Ascl1SA6 and Bcl2 was sufficient to induce Dlx2 expression during glia-to-neuron conversion in the postnatal mouse cortex.

First, I checked that Ascl1 was indeed being expressed in cells that were co-transduced with Ascl1SA6 and Bcl2. Indeed, RNAscope assays revealed that Ascl1 was overexpressed in reporter-positive cells, which displayed high levels of Ascl1 mRNA transcripts both in the nucleus and soma even at 28 dpi (Fig. 3.16B). Of note, Ascl1 mRNA expression was not detected in any other cells throughout the mouse cerebral cortex at this age. The specificity of Ascl1 mRNA signal was corroborated by finding Ascl1 expression in putative transit amplifying progenitors (TAPs) in the lateral ventricle of the contralateral hemisphere (Fig. 3.16A) (Parras et al., 2004).

Next, I investigated whether co-expression of Ascl1SA6 and Bcl2 was able to activate endogenous expression of Dlx2. Despite the high levels of Ascl1 expression found in cells co-transduced with Ascl1SA6 and Bcl2, none of these cells expressed Dlx2 at the mRNA level at 28 dpi (Fig. 3.16D). Here, I confirmed the specificity of Dlx2 signal by observing its expression in putative endogenous interneurons in the mouse cerebral cortex of the contralateral hemisphere (Fig. 3.16C) (Saino-Saito et al., 2003).

Taken together, these results confirm the ectopic overexpression of Ascl1 mRNA transcripts in iNs by forced expression of retroviral vectors encoding for Ascl1SA6 and Bcl2. However, Ascl1 ectopic expression does not trigger endogenous expression of Dlx2 in these cells.

2.2. Ascl1SA6 and Dlx2 synergise to convert cortical postnatal glia into NeuN-expressing iNs.

Dlx2 expression is found in postmitotic cortical interneurons in the adult mouse cerebral cortex and plays important roles in regulating GABA synthesis and synaptogenesis of these cells (Pla et al., 2018). Additionally, Dlx2 has been successfully used *in vitro* and, more recently, *in vivo* to reprogram astrocytes and hippocampal reactive glia into GABAergic iNs (Heinrich et al., 2010; Lentini et al., 2021).

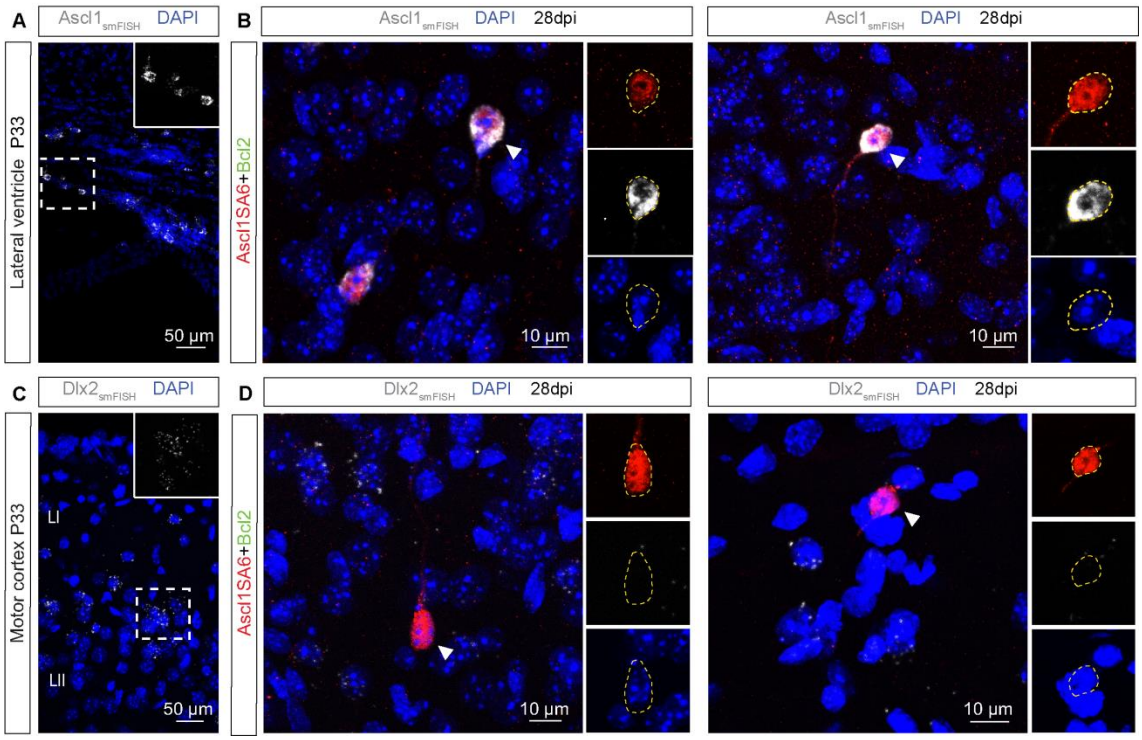

Figure 3.16. Ascl1SA6 and Bcl2-derived iNs exhibit ectopic overexpression of Ascl1 but lack Dlx2 expression at the mRNA level. (A) Low-magnification confocal image depicting endogenous Ascl1 mRNA expression (in white) in putative transient TAPs in the lateral wall of the ventricle in P33 mice. (B) Confocal images depicting Ascl1 mRNA ectopic overexpression (in white) in Ascl1SA6 and Bcl2-derived iNs at 28dpi, 15 cells (n = 2). (C) Low-magnification confocal image depicting endogenous Dlx2 mRNA expression (in white) in putative interneurons in the P33 mouse cortex. (D) Confocal images depicting lack of Dlx2 mRNA expression (in white) in Ascl1SA6 and Bcl2-derived iNs at 28dpi, 25 cells (n = 3).

Based on all these findings, I hypothesised that Dlx2 could be a potential candidate to drive glia-to-interneuron conversion in the context of the postnatal mouse cerebral cortex. To test this hypothesis, I first evaluated the reprogramming efficiency of Dlx2 alone by injecting a retroviral construct encoding for Dlx2 and the reporter gene GFP under the control of CAG promoter in the postnatal mouse cortex (CAG-Dlx2-IRES-GFP) and performing immunohistochemistry against the neuronal markers Dcx and NeuN at 12 dpi. A remarkable proportion of GFP+ transduced cells acquired the expression of the immature marker Dcx (29.6 ± 3.2% of Dcx+/GFP+ cells; Fig. 3.17A, C) and displayed neuronal morphology. Among the population of Dcx-expressing cells, I found a fraction that accumulated in cell clusters (Fig. 3.17A, right insets). In sharp contrast, none of the GFP+ transduced cells acquired the expression of the neuronal marker NeuN (0.0 ± 0.0% of NeuN+/GFP+ cells; Fig. 3.17A, C). To determine whether cells transduced with Dlx2-encoding retroviruses were indeed exogenously expressing the proneural factor *in vivo*, I performed RNAscope assays against Dlx2 mRNA transcript. These results showed that Dlx2 was successfully detected in transduced cells, which displayed Dlx2 mRNA transcript at high levels both in the nucleus and soma (Fig. 3.17B). Of note, the signal from the GFP reporter gene could not be recovered by immunostaining after RNAscope, thus the putative transduced cells were detected based on the high levels of expression of Dlx2 mRNA transcripts.

Based on previous studies showing synergy between Ascl1 and Dlx2 to induce neuronal reprogramming (Heinrich et al., 2010; Lentini et al., 2021), I next co-injected retroviral constructs encoding for Ascl1 together with Dlx2 (Fig. 3.18A). I found that co-expression of Ascl1 and Dlx2 rarely induced the generation of NeuN-expressing iNs (0.8 ± 1.4% of NeuN+/GFP+/DsRed cells; Fig. 3.18 B-C). Since my previous results demonstrated a higher neurogenic ability of Ascl1SA6, I next decided to co-express Ascl1SA6 together with Dlx2. In sharp contrast, combined expression of Ascl1SA6 with Dlx2 generated a significantly higher number of iNs that acquired the expression of the neuronal marker NeuN (86.6 ± 4.8% of NeuN+/GFP+/DsRed+ cells; Fig. 3.18B, D).

Likewise, RNAscope assays revealed that cells co-transduced with Ascl1 or Ascl1SA6 together with Dlx2 also acquired ectopic overexpression of Dlx2 mRNA transcript at high levels (Fig. 3.18E-F). Of note, the majority of cells co-expressing Ascl1 and Dlx2 remained with glial-like morphology and even some of them were able to fully differentiate into oligodendrocytes (Fig. 3.18E), despite overexpression of both proneural factors. In contrast, most of the cells co-expressing Ascl1SA6 and Dlx2 revealed a neuronal-like morphology, with Dlx2 expression detected in both nucleus and neural-like processes (Fig. 3.18F).

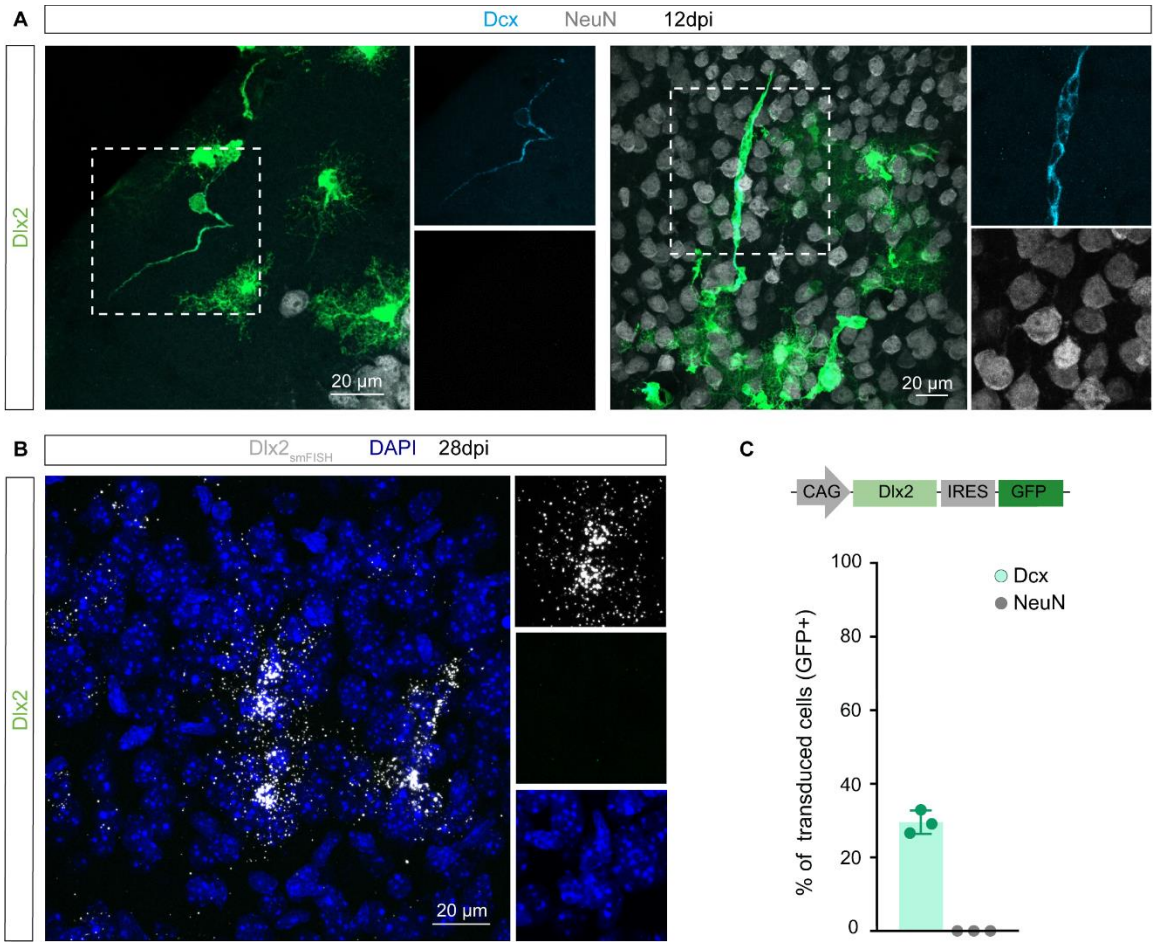

Figure 3.17. Forced expression of Dlx2 generates some Dcx-expressing iNs. (A) Confocal images depicting Dcx expression (in cyan) and lack of NeuN expression (in white) in Dlx2-transduced cells at 12dpi. (B) Confocal images depicting Dlx2 mRNA ectopic overexpression (in white) and lack of Ascl1 mRNA expression (in green) in transduced cells at 28dpi. (C) Schematic representation of retroviral construct encoding for Dlx2 (pCAG-Dlx2-GFP). Quantification of the percentage of transduced cells expressing Dcx or NeuN at 12dpi. Data shown as mean ± SD, n = 3 mice (1119 cells).

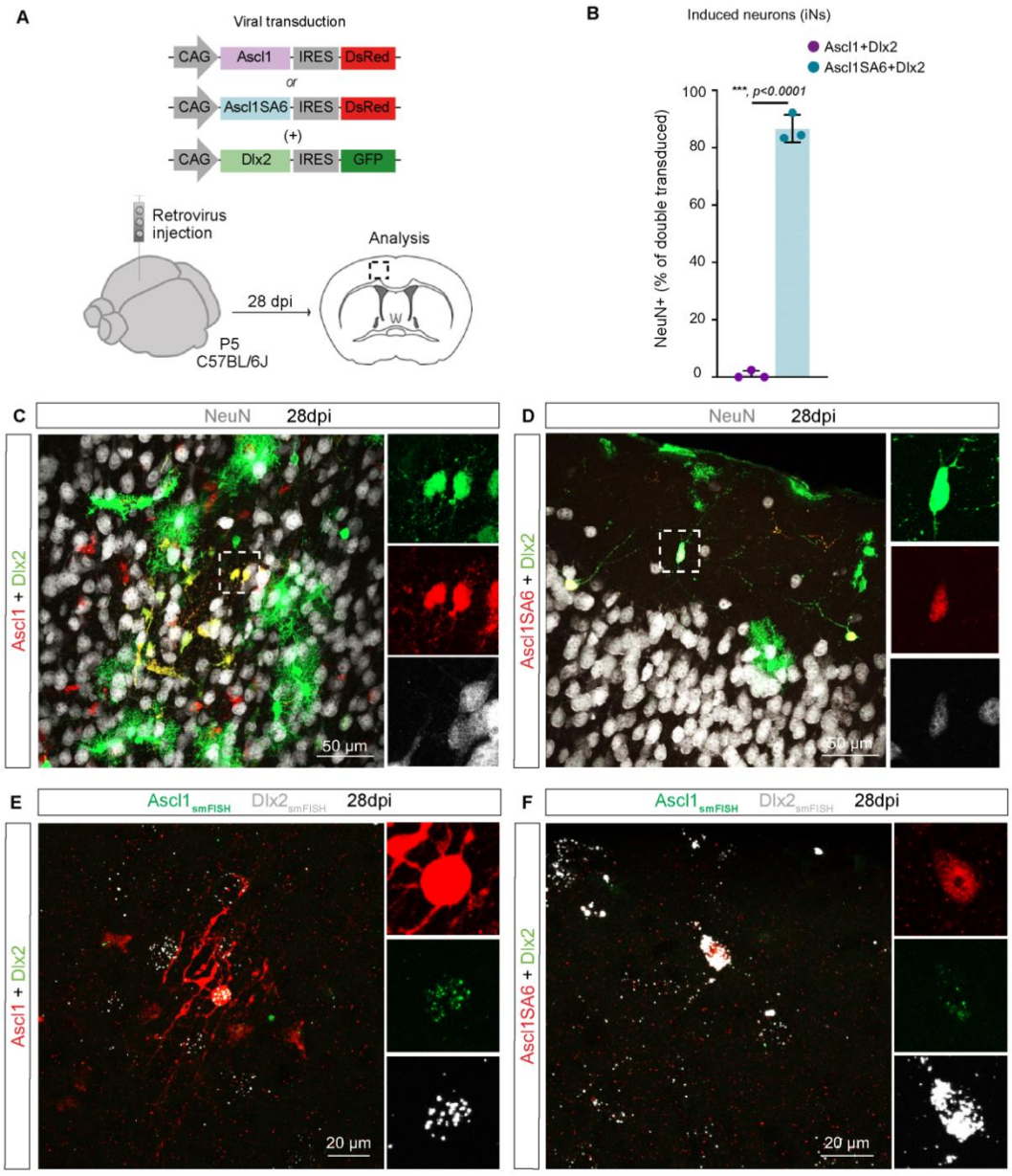

Figure 3.18. Forced co-expression of Ascl1SA6 and Dlx2 drives conversion of postnatal glial cells into NeuN-expressing iNs. (A) Schematic representation of experimental design. Retroviral constructs encoding for Ascl1 (pCAG-Ascl1-DsRed) or Ascl1SA6 (pCAG-Ascl1SA6-DsRed) together with Dlx2 (pCAG-Dlx2-GFP) were injected in the mouse cerebral cortex at P5, and the reprogramming efficiency was analysed at 28dpi. (B) Quantification of the percentage of double-transduced cells expressing NeuN at 28dpi. Data shown as mean ± SD. Two-tailed Student's unpaired t-test, *** P<0.0001, n = 3 mice (304 cells) for Ascl1 + Dlx2, n = 3 mice (157 cells) for Ascl1SA6 + Dlx2. (C-D) Confocal images depicting NeuN expression (in white) in Ascl1 (C) or Ascl1SA6 (D) + Dlx2-transduced cells at 28dpi. (E-F) Confocal images depicting ectopic mRNA expression of Ascl1 (in green) and Dlx2 (in white) in Ascl1 (E) or Ascl1SA6 (F) + Dlx2-transduced cells at 28 dpi.

Altogether, these data indicate that Dlx2 is a potent candidate to induce glia-to-neuron conversion in the postnatal cortex, as forced expression of this transcription factor alone generates Dcx-expressing iNs and, more importantly, it is capable to synergise with Ascl1SA6 to generate a high number of NeuN-expressing iNs. Again, the phosphorylation state of Ascl1 strongly influences the reprogramming efficiency, as combination of wildtype Ascl1 and Dlx2 did not yield a high number of iNs.

2.3. Forced co-expression of Ascl1SA6 and Dlx2 generates GABAergic iNs that do not acquire any subtype-specific identity.

As previously described, Dlx2 plays a major role in the specification of interneurons during cortical development (Alzu'bi & Clowry, 2019; Petryniak et al., 2007). Therefore, I next asked the question whether iNs generated by forced expression of Ascl1SA6 together with Dlx2 specified into GABAergic interneuron-like iNs. The results showed that the majority of co-transduced cells entered the GABAergic lineage, as revealed by acquisition of expression of GABA, (71.2 ± 7.10% of GABA+/GFP+/DsRed+ cells; Fig. 3.19A-B), which was significantly higher than the number of cells co-transduced with Ascl1SA6 and Bcl2 which acquired a GABAergic identity (23.4 ± 6.1% of GABA+/GFP+/DsRed+ cells; Fig. 3.19B).

Given the high proportion of iNs that acquired a GABAergic phenotype, I next investigated whether iNs could further specify into different interneuron subtypes. To my surprise, I found that none of the cells co-transduced with Ascl1SA6 and Dlx2 generated distinct subtypes of interneurons, such as PV, SST or VIP (0.0 ± 0.0% of PV+/GFP+/DsRed+ cells; 0.0 ± 0.0% of SST+/GFP+/DsRed+ cells; 0.0 ± 0.0% of VIP+/GFP+/DsRed+ cells Fig. 3.19C).

Next, I tested for the presence of Kv3.1 voltage-gated channel in Ascl1SA6 and Dlx2-derived iNs and compared its expression with cells co-transduced with Ascl1SA6 and Bcl2. For this purpose, I used RNAscope to detect Kv3.1 mRNA transcripts in this cell population. Surprisingly, I found that iNs co-transduced with Ascl1SA6 and Dlx2 acquired the expression of Kv3.1 channel at similar mRNA levels of iNs generated by co-expression of Ascl1SA6 and Bcl2 (Fig. 3.20A-C). Thus, I next asked whether iNs generated by co-expression of Ascl1SA6 and Dlx2 were physiologically functional and could display a high-frequency firing rate. For this purpose, whole-cell patch-clamp electrophysiological recordings were performed on acute brain slices at 28 dpi by Dr. Nicolas Marichal. Interestingly, current-clamp recordings showed that co-transduced

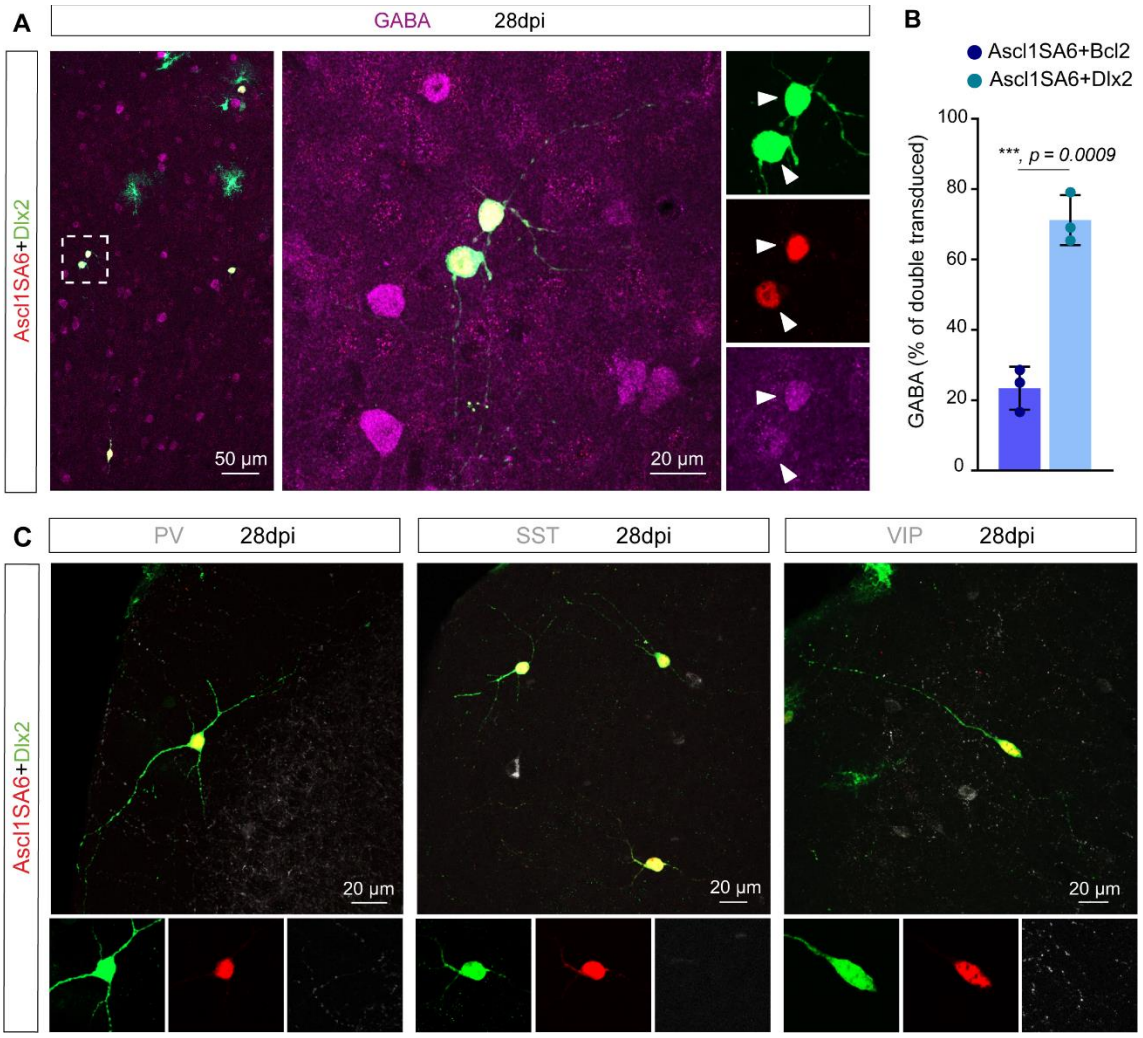

Figure 3.19. Forced co-expression of Ascl1SA6 and Dlx2 generates GABA-expressing iNs that do not differentiate into interneuron-specific subtypes. (A) Low-magnification confocal image illustrating Ascl1SA6 and Dlx2-transduced cells surrounded by endogenous GABAergic neurons at the cortical site of injection at 28dpi (left inset). Confocal images depicting expression of GABA (in magenta) in Ascl1SA6 and Dlx2-transduced cells at 28dpi. (B) Quantification of the percentage of cells expressing GABA in Ascl1SA6 + Bcl2 and Ascl1SA6 + Dlx2-transduced cells at 28dpi. Data shown as mean ± SD. Two-tailed Student's unpaired t-test, *** P=0.0009, n = 3 mice (78 cells) for Ascl1SA6 + Bcl2, n = 3 mice (171 cells) for Ascl1SA6 + Dlx2. Note that data for Ascl1SA6 + Bcl2-transduced cells are the same shown in Figure 3.7. (C) Confocal images depicting lack of expression of PV, SST and VIP (in white) in Ascl1SA6 and Dlx2-transduced cells at 28dpi.

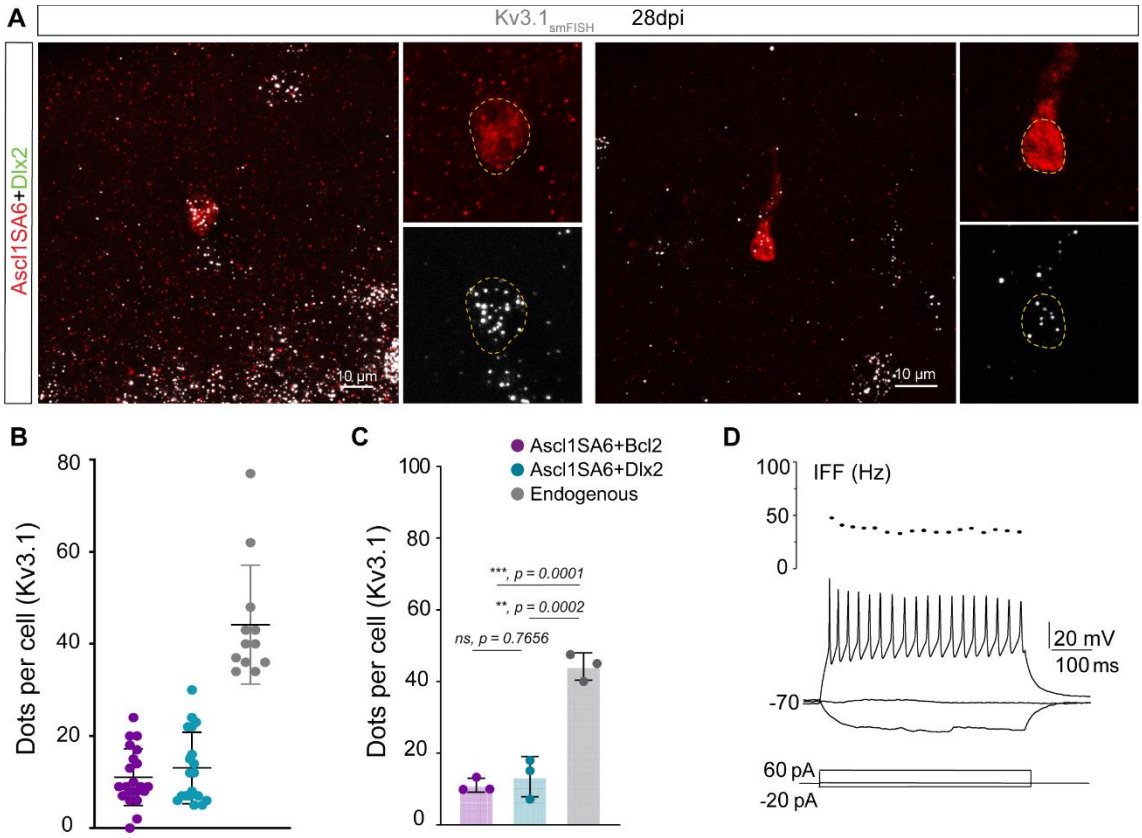

Figure 3.20. Ascl1SA6 and Dlx2-derived iNs express Kv3.1 mRNA but do not display a high-frequency firing pattern. (A) Confocal images depicting expression of Kv3.1 mRNA (in white) in Ascl1SA6 and Dlx2-transduced cells at 28dpi. (B) Quantification of the number of Kv3.1 mRNA particles in Ascl1SA6 + Bcl2-transduced cells, Ascl1SA6 + Dxl2-transduced cells and endogenous neurons. Each dot represents one cell, n = 3 (21 cells) for Ascl1SA6 + Bcl2-transduced cells, n = 3 (19 cells) for Ascl1SA6 + Dlx2-transduced cells, n = 3 (12 cells) for endogenous neurons. Note that data for Ascl1SA6 + Bcl2-transduced cells and endogenous neurons are the same shown in Figure 3.9. (C) Bar graph representing the mean number of Kv3.1 mRNA particles in cells co transduced with Ascl1SA6 + Dxl2 or Ascl1SA6 + Bcl2-transduced cells and endogenous neurons. One-way ANOVA followed by Tukey's multiple comparisons *post hoc* test, *** P=0.0001 for endogenous neurons vs Ascl1+Bcl2-transduced cells, *** P=0.0002 for endogenous neurons vs Ascl1+Dlx2-transduced cells, P=0.7656 for Ascl1+Bcl2-transduced cells vs Ascl1SA6+Bcl2-transduced cells, 15 cells (n = 3) for Ascl1 + Bcl2-transduced cells, 21 cells (n = 3) for Ascl1SA6 + Bcl2-transduced cells, 12 cells (n = 3) for endogenous neurons. (D) Current-clamp recording showing one cell co-transduced with Ascl1SA6 and Dlx2 that generates repetitive action potentials but do not exhibit high firing frequency (>100Hz).

cells were able to generate repetitive action potentials, revealing a remarkable degree of maturation (Fig. 3.20D). Consistent with my findings revealing lack of PV expression, co-transduced cells that were recorded did not display a high-frequency firing pattern. Of note, only 5 cells were recorded and it is necessary to increase the number to confirm the electrophysiological phenotype of co-transduced cells with Ascl1SA6 and Dlx2. It would be interesting to increase the number of recorded co-transduced cells to investigate whether some of these cells may display fast-spiking activity.

Taken together, these data reveal that forced co-expression of Ascl1SA6 and Dlx2 in proliferating cortical glia instructs their conversion into GABAergic iNs within the postnatal mouse cortex. However, these iNs do not acquire subtype-specific interneuron identity.

2.4. Tri-cistronic vector co-expressing Ascl1SA6 and Dlx2 yields a high number of NeuN-expressing iNs.

In order to control the number of cells co-transduced with different reprogramming factors and to regulate their expression levels in an equivalent stoichiometric manner, I cloned a tri-cistronic retroviral vector encoding Ascl1SA6 linked by the "self-cleavage" peptide sequence T2A to Dlx2 and followed by an IRES region that linked the reporter gene DsRed. The transcription of both genes was controlled by the strong and constitutively expressed CAG promoter. A tri-cistronic retroviral vector encoding the wildtype Ascl1 together with Dlx2 was a kind gift from Prof. Christophe Heinrich (Lentini et al., 2021). These tri-cistronic retroviral vectors were injected in the postnatal cerebral cortex at postnatal day 5 and analysed 28 days later by immunohistochemistry assays (Fig. 3.21A).

Consistent with my previous observations when co-transducing with single vectors, I found that very few cells transduced with Ascl1-Dlx2 reprogrammed into NeuN-expressing iNs (2.1 ± 2.4% NeuN+/DsRed+ cells; Fig. 3.21B-C), whereas the vast majority of Ascl1SA6-Dlx2 transduced cells acquired the expression of the neuronal marker NeuN (73.6 ± 3.3% NeuN+/DsRed+ cells; Fig. 3.21B-C).

Overall, expression of Ascl1 or Ascl1SA6 together with Dlx2 within the same retroviral vector elicits similar conversion rates as when co-expressed via separate constructs, evidenced by the generation of a significantly higher proportion of NeuN-expressing iNs when Dlx2 is combined with the phosphor-site mutant Ascl1SA6.

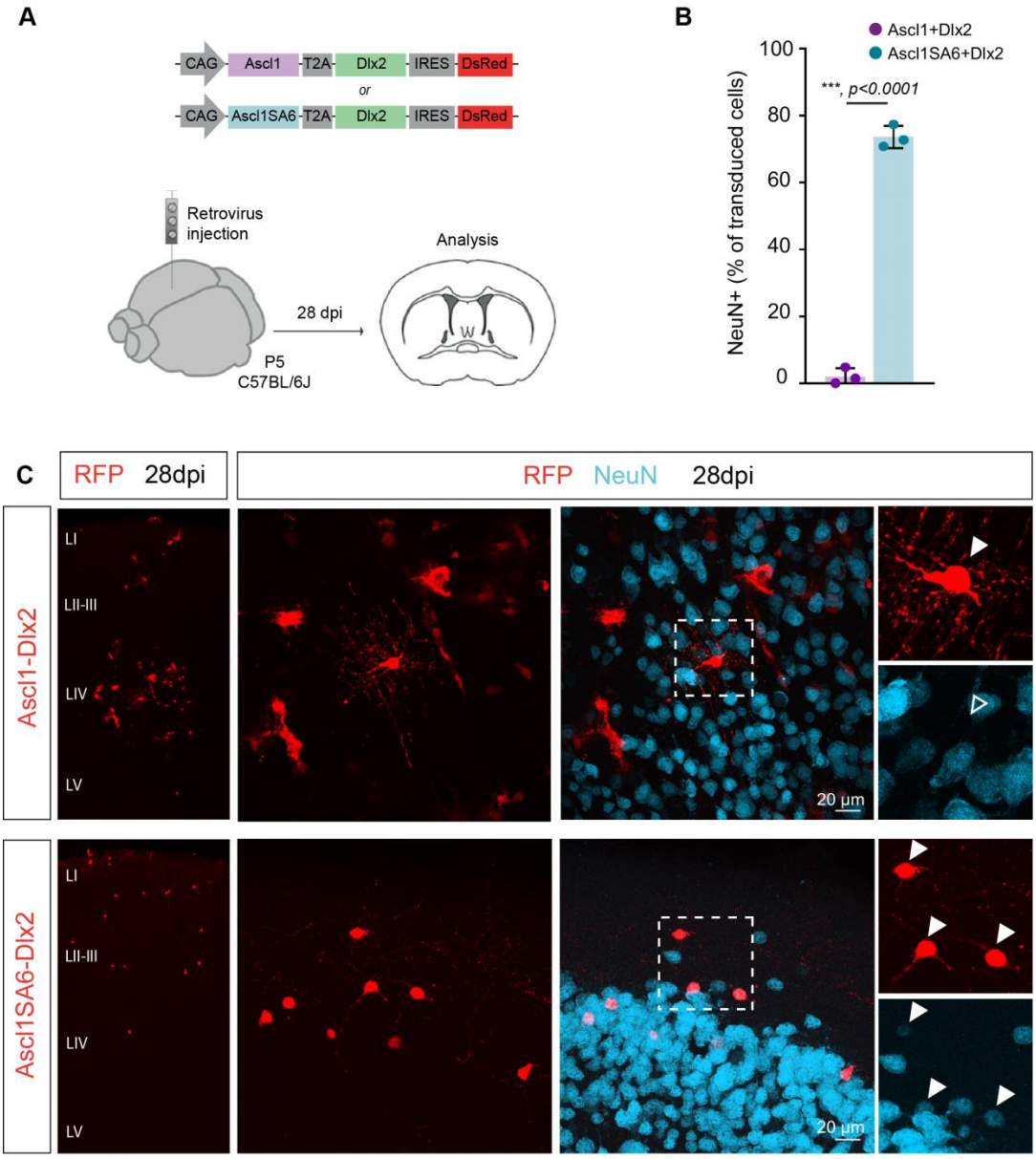

Figure 3.21. Tri-cistronic vector encoding for Ascl1SA6-Bcl2 drives efficient glia-to-neuron conversion in the postnatal mouse cortex. (A) Schematic representation of experimental design. Retroviral constructs encoding Ascl1-Dlx2 (pCAG-Ascl1-T2A-Dlx2-DsRed) or Ascl1SA6-Dlx2 (pCAG-Ascl1SA6-T2A-Dlx2-DsRed) were injected in the mouse cerebral cortex at P5, and the reprogramming efficiency was analysed at 28dpi. (B) Quantification of the percentage of transduced cells expressing NeuN at 28dpi. Data shown as mean ± SD. Two-tailed Student's unpaired t-test, *** P<0.0001, n = 3 mice (155 cells) for Ascl1-Dlx2, n = 3 mice (259 cells) for Ascl1SA6-Dlx2. (C) Low-magnification confocal images showing Ascl1-Dlx2 (upper insets) or Ascl1SA6-Dlx2 (lower insets) transduced cells at the cortical site of injection (left inset). Confocal images depicting NeuN expression (in cyan) in (upper insets) or Ascl1SA6-Dlx2 (lower insets) transduced cells. Empty arrows indicate marker-negative cells.

2.5. Fate-mapping experiments reveal astroglial origin of Ascl1-Dlx2-derived iNs.

Using fate-mapping strategies, I have previously demonstrated that iNs generated by overexpression of the tri-cistronic vector encoding for the reprogramming factors Ascl1SA6 and Bcl2 mostly originate from astroglia. Given that forced expression of Ascl1SA6 together with Dlx2 is able to generate a high number of GABAergic iNs (Fig. 3.22A-B), I decided to explore whether iNs have a different glial origin. In addition, another study suggested that co-expression of Ascl1 and Dlx2 can efficiently convert OPCs into interneuron-like iNs in the epileptic hippocampus (Lentini et al., 2021), which made us wonder whether the same occurs in the context of the postnatal cerebral cortex.

To specifically trace the iNs origins from astrocytes and OPCs, I decided to use the transgenic mouse lines Aldh1l1-CreER^{T2}, mGFAp-Cre and NG2CreER^{TM} and followed the same breeding and recombination strategies previously described in Chapter I (see section 1.8). Mice received a stereotactic injection in the postnatal cerebral cortex with the tri-cistronic retroviral construct encoding for Ascl1SA6, Dlx2 and DsRed, and the glial origin of iNs was assessed by immunostaining of cortical sections for the reporter genes both from the transgenic mouse lines and the retroviral construct as well as the neuronal marker NeuN at 12 dpi (Fig. 3.22A, D). Consistent with my results observed with the Ascl1SA6-Bcl2 tri-cistronic vector, most of Ascl1SA6-Bcl2 transduced cells have an astroglial origin, evidenced by co-labelling with the GFP+ reporter gene in the Aldh1l1-CreER^{T2};RCE:loxP transgenic mice (~70% of GFP+/DsRed+; Fig. 3.22B-C). Again, the majority of fate-mapped cells also acquired the expression of the neuronal marker NeuN (59.8 ± 9.5 %of NeuN+/GFP+/DsRed+; Fig. 3.22B-C), demonstrating that postnatal cortical astrocytes serve as a cell source for neuronal reprogramming. Furthermore, we performed a similar experiment in a second double-transgenic mouse that also labels cortical astrocytes, in which GFP reporter expression can be specifically induced by the mouse GFAP promoter (Gregorian et al., 2009). We also found that a substantial proportion of NeuN+ transduced cells were GFP+ (44.6 ± 4.7% of NeuN+/GFP+/DsRed+ cells; Fig. 3.22E-F). Also, in agreement with my previous observations, I found that DsRed+ transduced cells in the NG2CreER^{TM} BAC transgenic mice were rarely co-labelled with both reporter genes GFP and DsRed (0.7 ± 0.7% of GFP+/DsRed+ cells; Fig. 3.22H, I). Still, I could find a small number of transduced cells expressing GFP that also acquired the expression of NeuN (0.3 ± 0.3% of NeuN+/GFP+/DsRed+ cells; Fig. 3.22H,I), indicating that it is possible to reprogram cortical OPCs to iNs by overexpression of Ascl1SA6-Dlx2.

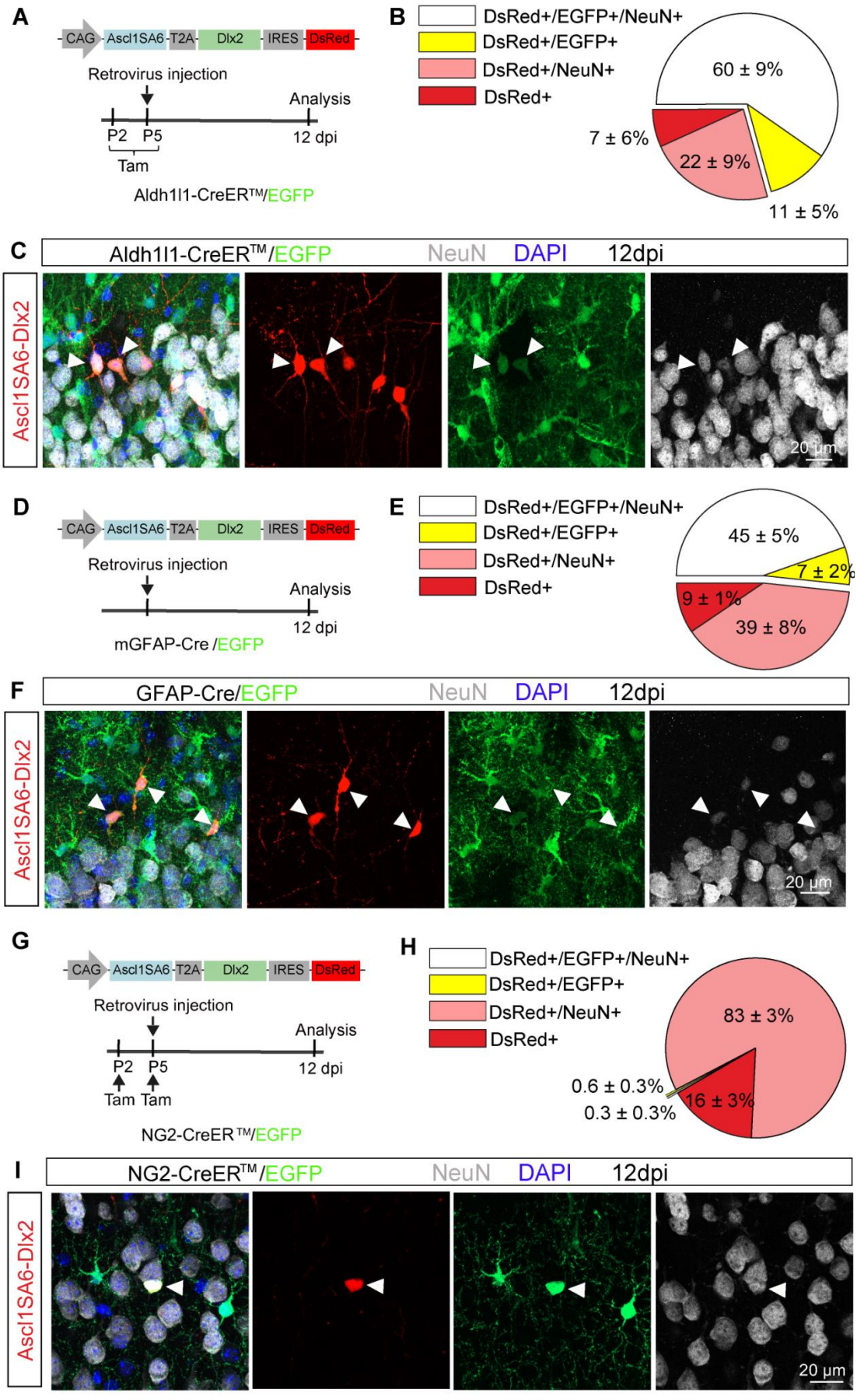
A
CAG
Ascl1SA6
T2A
Dlx2
IRES
DsRed
Retrovirus injection
Analysis
P2
P5
12 dpi
Tam
Aldh1l1-CreER™/EGFP
B
DsRed+/EGFP+/NeuN+
DsRed+/EGFP+
DsRed+/NeuN+
DsRed+
60 ± 9%
7 ± 6%
22 ± 9%
11 ± 5%
C
Aldh1l1-CreER™/EGFP
NeuN
DAPI
12dpi
Ascl1SA6-Dlx2
20 µm
D
mGFAP-Cre /EGFP
E
45 ± 5%
7 ± 2%
9 ± 1%
39 ± 8%
F
GFAP-Cre/EGFP
G
NG2-CreER™/EGFP
H
83 ± 3%
0.6 ± 0.3%
0.3 ± 0.3%
16 ± 3%
I
NG2-CreER™/EGFP

Figure 3.22. Fate-mapping experiments reveal glial origin of Ascl1SA6-Bcl2-derived iNs. (A) Schematic representation of experimental design. Retroviral constructs encoding for Ascl1SA6-Dlx2 (pCAG-Ascl1SA6-T2A-Dlx2-DsRed) were injected in the cortex of Aldh1l1-CreER^{T2};RCE:loxP transgenic mice at P5. Mice received a subcutaneous injection of tamoxifen daily between P2-P5 to induce Cre-mediated recombination and achieve astrocyte labelling with GFP in the mouse brain. The proportion of cells with astroglial origin was analysed at 12dpi. (B) Pie chart showing the relative number of transduced cells (DsRed+) co-expressing GFP and/or NeuN in Aldh1l1-CreER^{T2};RCE:loxP mice at 12dpi. Data shown as mean ± SD, n = 3 mice (577 cells). (C) Confocal images depicting Ascl1SA6-Dlx2-derived iNs co-expressing NeuN as well as the reporter genes DsRed and GFP in Aldh1l1-CreER^{T2};RCE:loxP mice at 12dpi. (D) Schematic representation of experimental design. Retroviral constructs encoding for Ascl1SA6-Dlx2 (pCAG-Ascl1SA6-T2A-Dlx2-DsRed) were injected in the cortex of mGFAP-CreER;RCE:loxP transgenic mice at P5. The proportion of cells with astroglial origin was analysed at 12dpi. (E) Pie chart showing the relative number of transduced cells (DsRed+) co-expressing GFP and/or NeuN in NG2CreER^{TM} BAC mice at 12dpi. Data shown as mean ± SD, n = 3 mice (765 cells). (F) Confocal images depicting Ascl1SA6-Bcl2-derived iNs co-expressing NeuN as well as the reporter genes DsRed and/or GFP in mGFAP-Cre;RCE:loxP mice at 12dpi. (G) Schematic representation of experimental design. Retroviral constructs encoding for Ascl1SA6-Dlx2 (pCAG-Ascl1SA6-T2A-Dlx2-DsRed) were injected in the cortex of NG2CreER^{TM};RCE:loxP transgenic mice at P5. Mice received a subcutaneous injection of tamoxifen on days P2 and P5 to induce Cre-mediated recombination and achieve OPCs labelling with GFP in the mouse brain. The proportion of cells with OPCsl origin was analysed at 12dpi. (H) Pie chart showing the relative number of transduced cells (DsRed+) co-expressing GFP and/or NeuN in NG2CreER^{TM};RCE:loxP mice at 12dpi. Data shown as mean ± SD, n = 3 mice (852 cells). (I) Confocal images depicting Ascl1SA6-Bcl2-derived iNs co-expressing NeuN as well as the reporter genes DsRed and/or GFP in NG2CreER^{TM};RCE:loxP mice at 12dpi.

Altogether, these data demonstrate that Ascl1SA6-Dlx2-derived iNs originate from proliferative glial in the postnatal mouse cortex, with astrocytes being the main cell source for conversion.

2.6. A low number of Ascl1SA6-Dlx2-derived iNs acquire GABAergic identity.

Due to a high commitment of iNs co-transduced with Ascl1SA6 and Dlx2 towards the GABAergic lineage, I next wondered whether the tri-cistronic vector co-expressing both TFs was still able to efficiently drive glia-to-interneuron conversion. As revealed by DsRed reporter co-expression and GABA immunoreactivity, I found a drastic decrease in the proportion of Ascl1SA6-Dlx2 iNs that acquired interneuronal identity (19.9 ± 7.3% of GABA+/DsRed+; Fig. 3.23A, C) compared to iNs co-transduction with separate retroviral vectors. To further corroborate this rare redirection of iNs towards the GABAergic lineage, I took advantage of the transgenic mouse line Vgat-Cre (Vong et al., 2011) crossed with RCE:loxP (Sousa et al., 2009). In agreement with my previous findings, almost none of the Ascl1SA6-Dlx2-derived iNs turned on GFP expression from the transgenic mouse line (0.3 ± 0.5% of GFP+/DsRed+ cells; Fig. 3.23B-C), revealing that Vgat promoter was not active in the iNs.

Although these data suggest that Ascl1SA6-Dlx2 iNs did not show specification into interneuron-like cells, I still wondered whether these cells were endowed with the ability to acquire identity of distinct subtypes of interneurons, such as PV-expressing interneurons. As expected, all Ascl1SA6-Dlx2 transduced cells were found to lack expression of the subtype interneuronal marker PV (0.0 ± 0.0% of PV+/DsRed+ cells; Fig. 3.23D, F). Based on my observations in the previous chapter, I hypothesised that Bcl2 might play a role not only in the survival of iNs during reprogramming (Gascón et al., 2016), but also on specification of iNs towards PV+ interneurons-like cells. To test this hypothesis, I decided to combine expression of Ascl1SA6-Dlx2 in the tri-cistronic vector, which was shown to generate a large number of iNs, together with Bcl2 in a separate construct and analyse iNs identity at 28dpi. Intriguingly, I found that combined expression of these three reprogramming factors did not result in acquisition of a PV interneuron identity, as revealed by immunohistochemistry assays (0.7 ± 1.3% of PV+/GFP+/DsRed+; Fig. 3.23E-F).

Taken together, these data indicate that tri-cistronic vectors encoding for several TFs changes the reprogramming outcome by changing the specification properties of generated iNs.

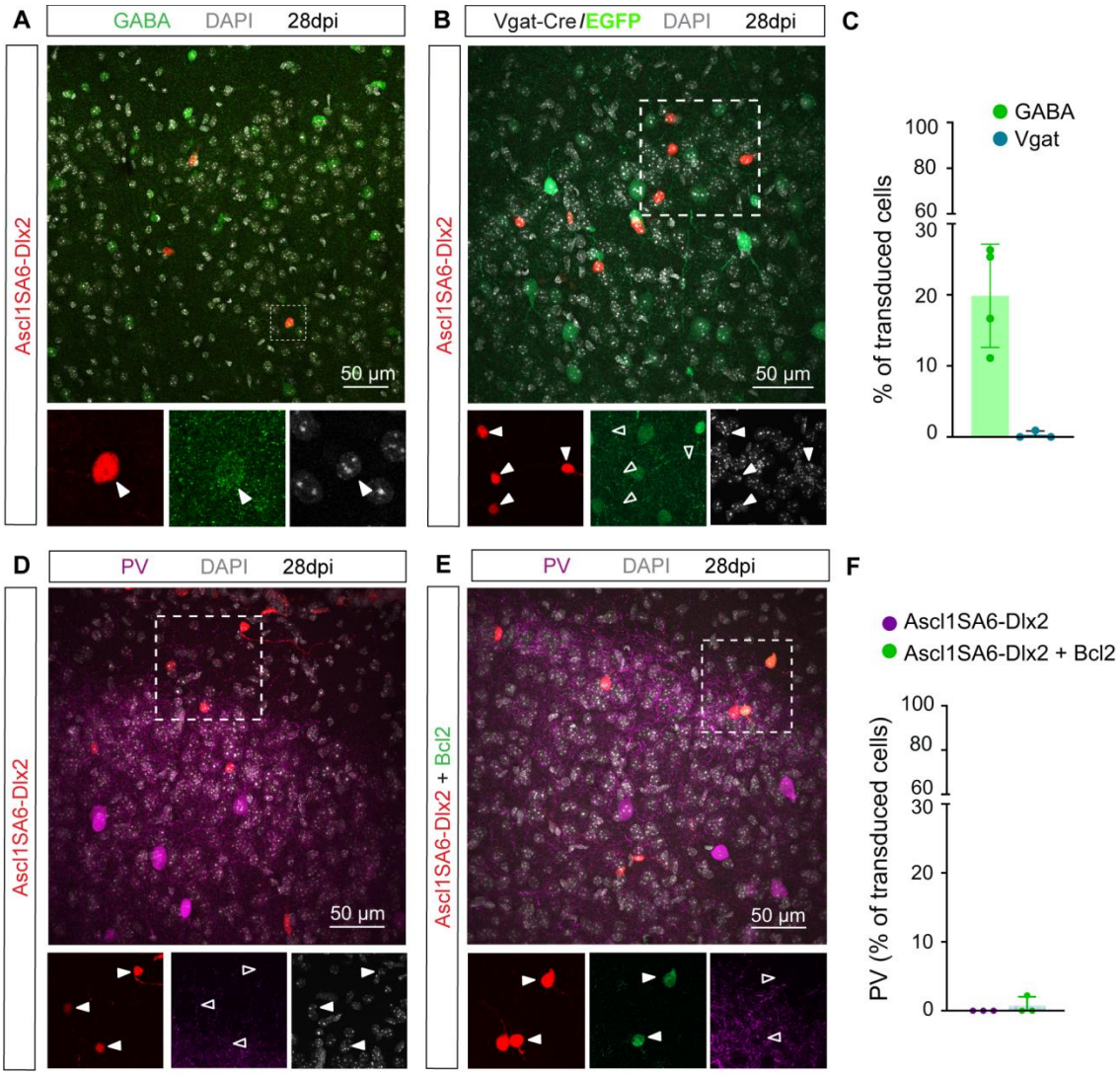

Figure 3.23. Transduced cells with Ascl1SA6-Dlx2 retroviral vector instructs conversion of glia into some GABAergic-like iNs that do not acquire PV identity. (A) Confocal images depicting acquisition of GABA expression (in green) in Ascl1SA6-Dlx2 transduced cells at 28dpi. (B) Confocal images depicting lack of GFP expression in Ascl1SA6-Dlx2 transduced cells in Vgat-Cre/EGFP mice at 28dpi. (C) Quantification of the percentage of transduced cells with Ascl1SA6-Dlx2 expressing GABA or GFP in Vgat-Cre/EGFP transgenic mice. Data shown as mean ± SD, n = 4 mice (272 cells) for GABA, n = 3 mice (257 cells) for GFP. (D) Confocal images depicting lack of PV expression (in magenta) in Ascl1SA6-Dlx2-derived iNs at 28dpi. (E) Confocal images depicting lack of PV expression (in magenta) in cells co-transduced with Ascl1SA6-Dlx2 and Bcl2 at 28dpi. (F) Quantification of the percentage of transduced cells with Ascl1SA6-Dlx2 with or without Bcl2. Data shown as mean ± SD, n = 3 (272 cells) for Ascl1SA6-Dlx2, n = 3 (98 cells) for Ascl1SA6-Dlx2 + Bcl2.

In this chapter, I have demonstrated that ectopic expression of Dlx2 instructed postnatal proliferating glia to generate a fraction of Dcx-expressing cells. Co-expression of Dlx2 and Ascl1 failed to induce efficient glia-to-neuron conversion. In sharp contrast, Dlx2 and Ascl1SA6 synergised to generate a high number of NeuN-expressing cells. Remarkably, a significant proportion of Ascl1SA6 and Dlx2-derived iNs exhibited a GABAergic identity. Intriguingly, iNs did not seem to differentiate into subtype-specific interneurons. In line with my findings in the previous chapter, fate-mapping experiments revealed that astrocytes were the main starting cell population from which iNs were generated.

CHAPTER III.

Modulation of iNs activity by chemogenetic-mediated stimulation.

3.1. Establishing a model for activation of iNs through chemogenetic-mediated stimulation.

Several lines of evidence have previously suggested that activity-dependent mechanisms have a profound effect on maturation, specification and integration of interneurons during different development stages (De Marco García et al., 2011; Wong et al., 2018). For instance, it has been suggested that there is a direct correlation between increased excitatory inputs onto PV interneurons and the maturation of their electrophysiological properties during development (Anastasiades et al., 2016; Miyamae et al., 2017; Okaty et al., 2009). In addition, previous studies have demonstrated that activity-dependent release of Otx2 and BDNF promotes maturation of PV interneurons (Huang et al., 1999; Sugiyama et al., 2008).

Based on these findings, I hypothesised that enhancing the activity of PV-like iNs during the reprogramming process could improve their maturation. For this purpose, I used a chemogenetic strategy to increase their activity based on Designer Receptors Exclusively Activated by Designer Drugs (DREADDs) that induce neuronal activation following administration of clozapine-N-oxide (CNO) (Roth, 2016). First, I injected in the postnatal mouse cerebral cortex the reprogramming factor cocktail which I previously demonstrated to give rise to PV-expressing iNs (Ascl1SA6 + Bcl2) together with a retroviral vector encoding for the activating hM3Dq DREADD. In this case, the reprogramming factor Bcl2 was cloned in a retroviral construct where the reporter gene was replaced by a Cre sequence, which was not used for recombination purposes in this experiment, but as a substitute of the reporter gene instead. Ascl1SA6 and hM3Dq-expressing retroviral vectors were encoding for the reporter genes DsRed and GFP respectively (Fig. 3.24A). Since I have shown that Bcl2 is necessary to drive efficient glia-to-neuron conversion, cells that expressed the reporter gene DsRed and acquired neuronal morphology were considered as putative iNs expressing both reprogramming factors. On the other hand, iNs that acquired the expression of the reporter gene GFP were considered as putative cells that can be activated upon CNO administration, whereas iNs lacking GFP expression were considered as control cells that should not be directly influenced by CNO administration. In addition, cells expressing the reporter gene GFP but did not acquire neuronal morphology, being most likely astrocytes, were also considered as another control to evaluate specificity of hM3Dq-mediated activation in neurons.

Given that co-transduced cells with Ascl1SA6 and Bcl2 can successfully activate a neurogenic programme, but get stalled during their maturation process, I

decided to inject CNO during a time window when iNs have already successfully reprogrammed and should start to become mature. For this purpose, CNO or vehicle was injected once daily between 13 and 24 days after the retroviral injection, with a 2-day break following the first 5 doses (Fig. 3.24A). Mice were sacrificed at 28dpi and injected one last dose of CNO or vehicle one hour before perfusion to test whether CNO was specifically driving iN activation.

3.2. Ascl1SA6 and Bcl2-derived iNs can be specifically activated through DREADD-mediated stimulation.

First, to evaluate whether iNs can be activated following hM3Dq-mediated stimulation, I used c-Fos as a well-known immediate early gene (IEG) that is rapidly and transiently upregulated upon neuronal activation (Morgan et al., 1987; Sagar et al., 1988). Since the last CNO administration was carried out one hour prior to sacrifice, it was possible to evaluate whether iNs were responsive to chemogenetic activation through c-Fos expression by immunohistochemistry.

It is important taking into account that one caveat of these experiments is that intrinsic network activity can highly vary between mice and this difference can influence the activation of iNs connected to the brain circuitry. Therefore, direct comparison of the number of cells expressing c-Fos between different mice might not show the effect of hM3Dq-mediated stimulation. For this reason, I decided to compare iNs that were transduced with the retroviral vector encoding hM3Dq to iNs that were not transduced with this vector within the same brains.

Strikingly, I found that most of the iNs co-expressing both the reprogramming factors and hM3Dq in CNO-treated mice, as revealed by the expression of reporter genes DsRed and GFP, expressed c-Fos (63.3 ± 5.8% cells c-Fos+/GFP+/DsRed+; Fig. 3.24B, D). In sharp contrast, only a small number of iNs that expressed DsRed but not GFP in the same CNO-treated mice exhibited c-Fos expression (16.9 ± 7.6% cells c-Fos+/DsRed+; Fig. 3.24B, D) indicating that iN activation was being specifically mediated by DREADD stimulation. Moreover, very few cells that were transduced only with the retroviral vector encoding for hM3Dq, but not with the vectors encoding for the reprogramming factors and therefore had remained with glial identity, expressed c-Fos (2.3 ± 3.1% cells c-Fos+/GFP+; Fig. 3.24B, D). This result suggests that hM3Dq-mediated activation is mainly specific to neurons and glial cells are not responsive to this stimulation.

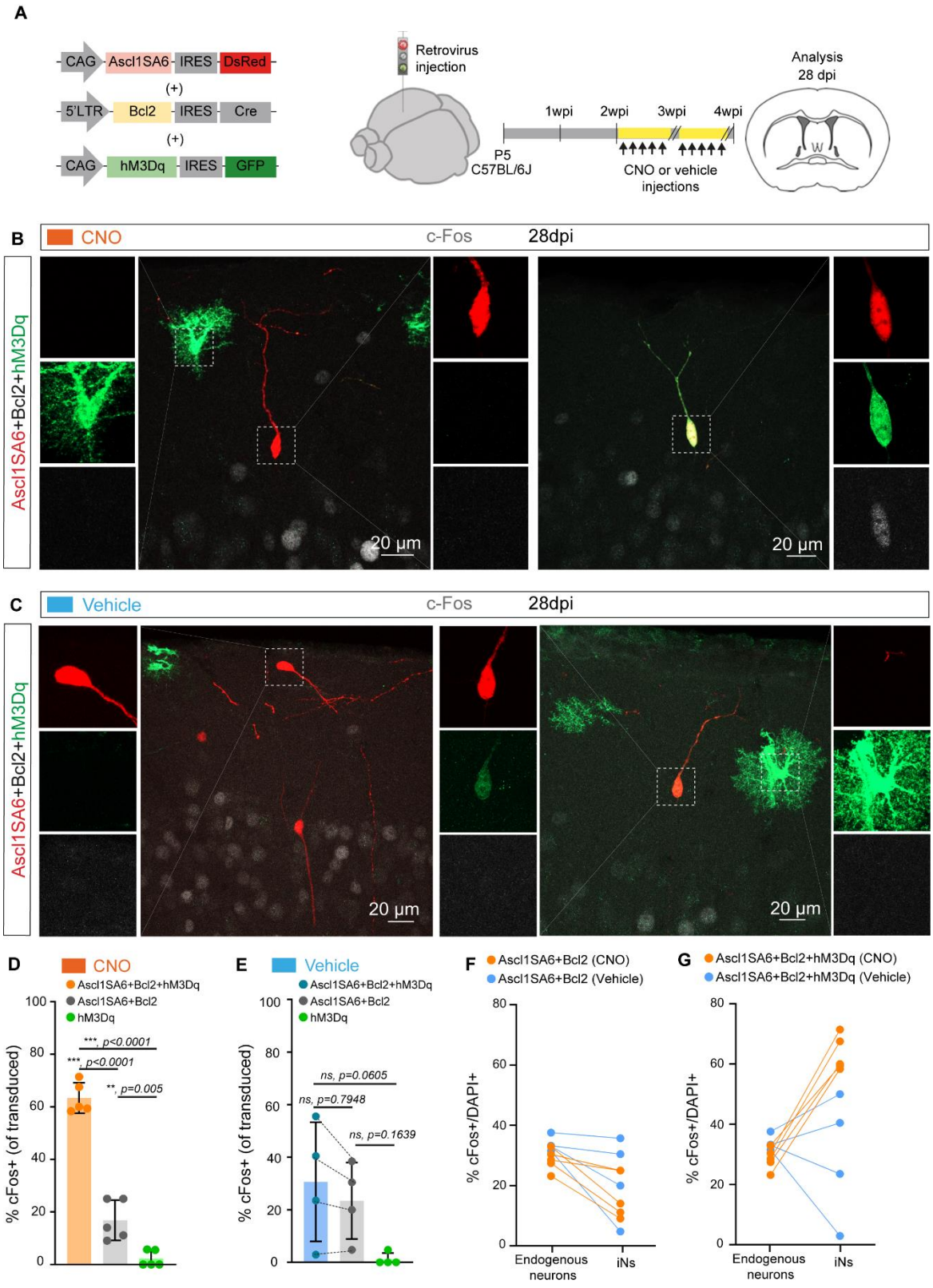
A
CAG
Ascl1SA6
IRES
DsRed
(+)
5'LTR
Bcl2
IRES
Cre
(+)
CAG
hM3Dq
IRES
GFP
Retrovirus injection
P5
C57BL/6J
1wpi
2wpi
3wpi
4wpi
CNO or vehicle injections
Analysis
28 dpi
B
CNO
c-Fos
28dpi
Ascl1SA6+Bcl2+hM3Dq
20 µm
20 µm
C
Vehicle
c-Fos
28dpi
Ascl1SA6+Bcl2+hM3Dq
20 µm
20 µm
D
CNO
Ascl1SA6+Bcl2+hM3Dq
Ascl1SA6+Bcl2
hM3Dq
***, p<0.0001
***, p<0.0001
**, p=0.005
% cFos+ (of transduced)
E
Vehicle
Ascl1SA6+Bcl2+hM3Dq
Ascl1SA6+Bcl2
hM3Dq
ns, p=0.0605
ns, p=0.7948
ns, p=0.1639
% cFos+ (of transduced)
F
Ascl1SA6+Bcl2 (CNO)
Ascl1SA6+Bcl2 (Vehicle)
% cFos+/DAPI+
Endogenous neurons
iNs
G
Ascl1SA6+Bcl2+hM3Dq (CNO)
Ascl1SA6+Bcl2+hM3Dq (Vehicle)
% cFos+/DAPI+
Endogenous neurons
iNs

Figure 3.24. Activation of iNs through chemogenetic-mediated stimulation. (A) Schematic representation of experimental design. Retroviral constructs encoding for Ascl1SA6 (pCAG-Ascl1SA6-DsRed), Bcl2 (5'LTR-Bcl2-GFP) and hM3Dq (pCAG-hM3Dq-GFP) were injected in the mouse cerebral cortex at P5. CNO or vehicle was administered daily after 2wpi for 10 days with a 2-day break after the first 5 doses. The activation of iNs was analysed by immunohistochemistry at 28dpi. (B-C) Confocal images depicting cFos expression (in white) in transduced cells with: hM3Dq only (left insets), Ascl1SA6 and Bcl2 (middle insets) or Ascl1SA6, Bcl2 and hM3Dq (right insets) in CNO-treated mice (B) or vehicle-treated mice (C). (D) Quantification of the percentage of c-Fos+ transduced cells with: hM3Dq or Ascl1SA6 and Bcl2 or Ascl1SA6, Bcl2 and hM3Dq in CNO-treated mice. Data shown as mean ± SD. One-way ANOVA followed by Tukey's multiple comparisons *post hoc* test, *** P<0.0001 for DsRed+/GFP+ iNs vs DsRed+, *** P<0.0001 for DsRed+/GFP+ iNs vs GFP+, ** P=0.005 for DsRed+ vs GFP+, n = 5 mice (212 cells) for DsRed+/GFP+ cells, n = 5 mice (135 cells) for DsRed+ cells, n = 5 mice (184 cells) for GFP+ cells (E). Quantification of the percentage of c-Fos+ transduced cells with: hM3Dq or Ascl1SA6 and Bcl2 or Ascl1SA6, Bcl2 and hM3Dq in vehicle-treated mice. Data shown as mean ± SD. One-way ANOVA followed by Tukey's multiple comparisons *post hoc* test, P=0.9253 (ns) for DsRed+/GFP+ iNs vs DsRed+, * P=0.0464 for DsRed+/GFP+ iNs vs GFP+, P=0.089 (ns) for DsRed+ vs GFP+, n = 5 mice (148 cells) for DsRed+/GFP+ cells, n = 5 mice (162 cells) for DsRed+ cells, n = 5 mice (85 cells) for GFP+ cells. (F) Low-magnification confocal image depicting endogenous neurons expressing c-Fos in the mouse cerebral cortex. (G) Quantification of the proportion of DAPI+ cells expressing c-Fos at the cortical site of injection compared to the proportion of DsRed+ iNs within the same mouse brains. Each dot represents one mouse.

Additionally, I did not find a significant difference in c-Fos expression when comparing iNs co-expressing DsRed and GFP and iNs that only expressed DsRed in vehicle-treated mice (38.4 ± 26.2% cells c-Fos+/GFP+/DsRed+ and 33.4 ± 25.6% cells c-Fos+/DsRed+; Fig. 3.24C, E). These data indicates that hM3Dq-mediated activation is specific to CNO administration. In agreement with previous results, vehicle-treated mice also had a smaller proportion of glial cells transduced only with DREADDs that expressed c-Fos when compared to iNs regardless of whether they were transduced with hM3Dq or not (2.1 ± 2.8% cells c-Fos+/GFP+; Fig. 3.24C, E).

It is important to consider that, even if vehicle-treated mice did not show any difference in the number of iNs that expressed c-Fos between hM3Dq-positive and hM3Dq-negative groups, the proportion of cells that acquired c-Fos expression was very variable between different mice (Fig. 3.24E). Interestingly, I observed that mice showing a high proportion of hM3Dq-positive iNs expressing c-Fos, also had a high number of hM3Dq -negative iNs that expressed c-Fos, suggesting that those mice might have higher levels of activation in the whole cortical network. To rule out the possibility that hM3Dq expression was having a cell-autonomous effect on iN activation, I calculated a correlation between activation levels of the endogenous neuronal network and activation levels of iNs. To this end, the proportion of cells that expressed c-Fos in the cortical regions around iNs (Fig. 3.24F) was measured using a Python script to detect cFos-expressing cells over all DAPI+ nuclei and compared it to the proportion of iNs expressing c-Fos within the same brains. Interestingly, I found that some of the mice showing the highest activation levels of the endogenous neuronal circuitry also had a bigger proportion of iNs that acquired expression of c-Fos, regardless of whether they were administered CNO or vehicle (Fig. 3.24G).

Taken together, these data indicates that iNs can be specifically activated through hM3Dq-mediated chemogenetic stimulation, opening up new avenues to study how activity can influence their conversion and maturation process.

3.3. Chemogenetic activation of Ascl1SA6 and Bcl2-derived iNs does not influence their expression levels of PV.

Previous studies have demonstrated that neuronal activity can regulate the intrinsic properties and plasticity of specific interneuron subtypes in the cortex, such as PV

interneurons (Dehorter et al., 2015; Favuzzi et al., 2017). In addition, PV interneurons have been shown to exhibit a high degree of plasticity upon recent experience, evidenced by changes in their PV expression levels (Donato et al., 2013, 2015). Based on my previous findings suggesting that iNs can get specifically activated by DREADD-mediated stimulation, I reasoned that activation of PV-like iNs could modulate their PV expression levels.

First, I evaluated whether the number of PV-expressing iNs was similar between cells that acquired ectopic expression of hM3Dq and cells that were not transduced with hM3Dq-encoding retroviral constructs in both CNO and vehicle conditions. The results showed that the proportion of PV+ iNs expressing hM3Dq was higher compared to those iNs that did not express hM3Dq in CNO-treated mice (24.2 ± 9.8% cells PV+/GFP+/DsRed+ vs 9.6 ± 6.7% cells PV+/DsRed+; Fig. 3.25A-B). However, I also found similar results when comparing the number of cells expressing PV in vehicle-treated mice (19.7 ± 5.8% cells PV+/GFP+/DsRed+ vs 12.5 ± 2.2% cells PV+/DsRed+; Fig. 3.25D-E).

Next, I investigated whether iNs activation had any effect on modulating PV expression levels. To this end, I measured PV intensity levels in iNs transduced with the hM3Dq-encoding retroviral vectors and compared them with iNs neurons not expressing hM3Dq. Interestingly, I observed that iNs did not show any significant differences in their PV expression levels, regardless of their transduction with hM3Dq or whether they were administered CNO or vehicle (Fig. 3.25C, F). Of note, the number of cells analysed in both conditions might have not been high enough to draw robust conclusions and it would be interesting to increase these numbers to obtain more conclusive results.

Taken together, these data suggest that activation of iNs through chemogenetic stimulation is not sufficient to induce a change on their levels of PV expression.

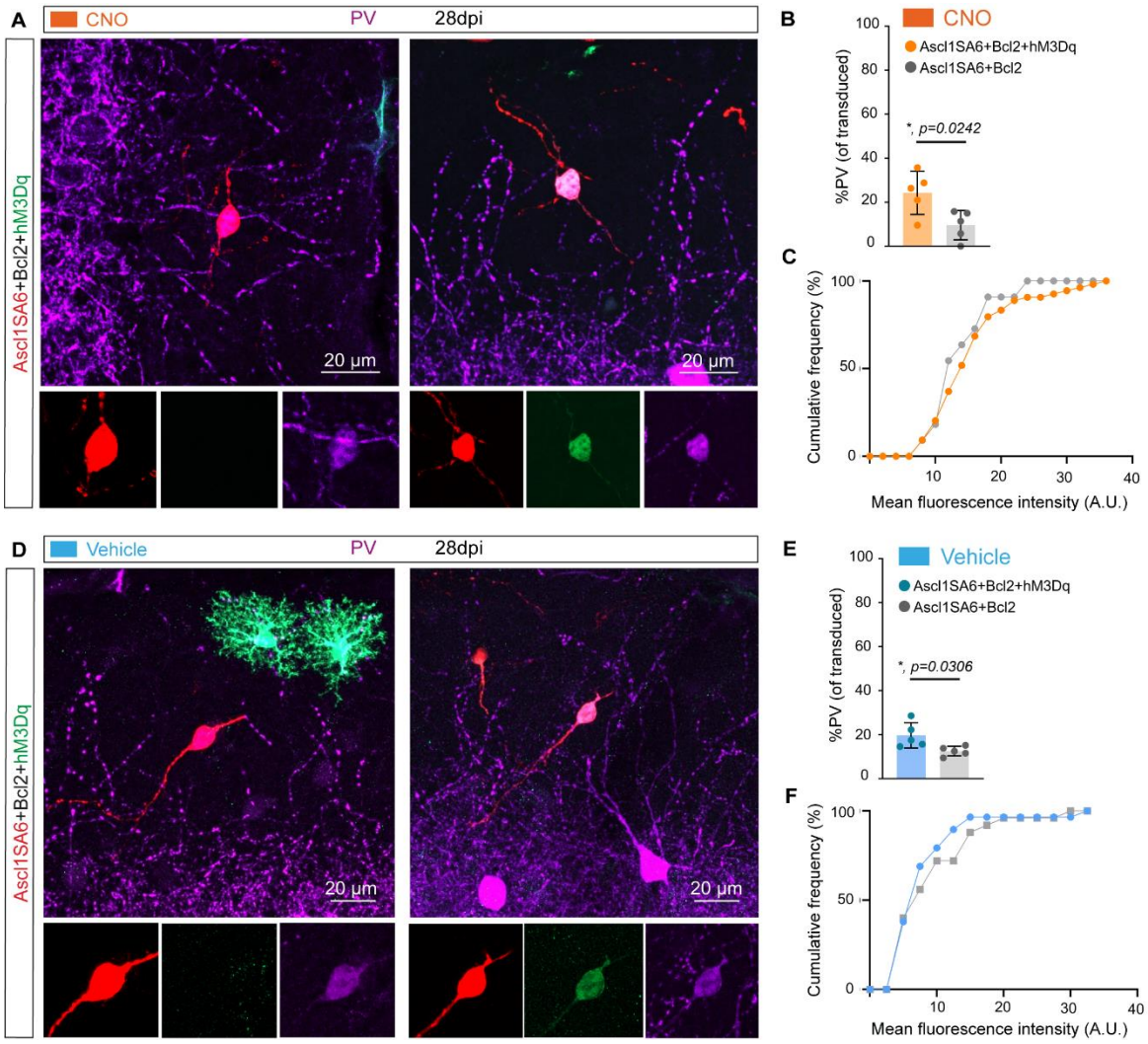
A
CNO
PV
28dpi
Ascl1SA6+Bcl2+hM3Dq
20 µm
20 µm
B
CNO
Ascl1SA6+Bcl2+hM3Dq
Ascl1SA6+Bcl2
%PV (of transduced)
*, p=0.0242
C
Cumulative frequency (%)
Mean fluorescence intensity (A.U.)
D
Vehicle
PV
28dpi
Ascl1SA6+Bcl2+hM3Dq
20 µm
20 µm
E
Vehicle
Ascl1SA6+Bcl2+hM3Dq
Ascl1SA6+Bcl2
%PV (of transduced)
*, p=0.0306
F
Cumulative frequency (%)
Mean fluorescence intensity (A.U.)

Figure 3.25. PV expression levels of iNs do not change upon DREADD-mediated activation. (A) Confocal images depicting PV expression in iNs transduced with Ascl1SA6 and Bcl2 (left insets) and iNs transduced with Ascl1SA6, Bcl2 and hM3Dq (right insets) in CNO-treated mice. (B) Quantification of percentage of PV+ cells transduced with Ascl1SA6 and Bcl2 or with Ascl1SA6, Bcl2 and hM3Dq. Data shown as mean ± SD. Two-tailed Student's unpaired t-test, * P=0.0524, n = 5 mice (231 cells) for DsRed+/GFP+cells, n = 5 mice (139 cells) for DsRed+ cells. (C) Cumulative frequency distribution of PV intensity levels of iNs transduced with Ascl1SA6 and Bcl2 or with Ascl1SA6, Bcl2 and hM3Dq. Non-parametric Kolgomorov-Smirnof test's, P= 0.2997 (ns), n = 5 mice (54 cells) for DsRed+/GFP+cells, n = 5 mice (11 cells) for DsRed+ cells. (D) Confocal images depicting PV expression in iNs transduced with Ascl1SA6 and Bcl2 (left insets) and iNs transduced with Ascl1SA6, Bcl2 and hM3Dq (right insets) in vehicle-treated mice. (E) Quantification of percentage of PV+ cells transduced with Ascl1SA6 and Bcl2 or with Ascl1SA6, Bcl2 and hM3Dq. Data shown as mean ± SD. Two-tailed Student's unpaired t-test, P=0.0533 (ns), n = 5 mice (190 cells) for DsRed+/GFP+cells, n = 5 mice (204 cells) for DsRed+ cells. (F) Cumulative frequency distribution of PV intensity levels of iNs transduced with Ascl1SA6 and Bcl2 or with Ascl1SA6, Bcl2 and hM3Dq. Non-parametric Kolgomorov-Smirnof test's, P= 0.4440 (ns), n = 5 mice (29 cells) for DsRed+/GFP+cells, n = 5 mice (25 cells) for DsRed+ cells.

In conclusion, in this chapter I designed an approach to specifically manipulate the activity of iNs in the postnatal mouse cortex. Importantly, I demonstrated that Ascl1SA6 and Bcl2-derived iNs can selectively be activated upon chemogenetic-mediated stimulation. However, the experimental approach used for iNs activation was not sufficient to induce changes on PV expression levels. Nonetheless, this strategy provides the basis for future work aiming at investigating how activity may influence iNs during lineage conversion.

DISCUSSION

Over the last decade, significant progress has provided proof-of-principle evidence for the conversion of various resident glial cell types into iNs in different brain areas (Vignoles et al., 2019). However, in the quest for iN-mediated brain repair for specific neurological disorders, the actual capability of iNs to acquire distinct neuronal subtype identities and functional integration in the pre-existing brain circuitry remain as fundamental questions. In this PhD thesis, I aimed at generating glia-derived interneuron-like cells via transcription factor-mediated lineage reprogramming. Towards this end, I used the postnatal mouse cerebral cortex as an experimental model to investigate glia-to-interneuron conversion *in vivo*. In addition, I aimed at performing robust strategies to unambiguously demonstrate the glial origin of converted iNs. Finally, I addressed to which extent iNs resemble endogenous neurons and developed an approach aiming at enhancing iNs maturation.

My results provided compelling evidence that proliferating glial cells can be converted into interneuron-like cells in the postnatal mouse cerebral cortex. I demonstrated that expression of wildtype Ascl1 together with other reprogramming factors, such as Bcl2 or Dlx2, can induce moderate glia-to-neuron conversion. However, replacing wildtype Ascl1 by Ascl1SA6, a mutant form in which six serine-proline sites subject to phosphorylation were mutated, generated a significantly higher proportion of NeuN-expressing iNs. Remarkably, a notable proportion of Ascl1SA6 and Bcl2-derived iNs acquired hallmarks of parvalbumin (PV) interneurons, such as expression of PV interneuron-specific markers as well as fast-spiking firing properties. Such PV interneuron-like cells can be induced in cortical layers devoid of this interneuron subtype, supporting the idea that transcriptional mechanisms can override cortical layer specification. Additionally, I reported that Ascl1SA6 and Dlx2 synergise to convert proliferating postnatal glial cells into a higher number of iNs that acquired a GABAergic identity. Using fate-mapping experiments, I presented robust evidence demonstrating that astroglia is the main cell source for retrovirus-mediated neuronal reprogramming in the postnatal mouse cortex. Finally, I demonstrated that iNs can selectively be activated upon chemogenetic-mediated stimulation, opening new avenues to study activity-dependent modulation of iNs during lineage reprogramming.

Altogether, this work provides fundamental understanding of the molecular cues and regulatory mechanisms necessary to induce glial fate switch towards an interneuron identity in the mouse cerebral cortex. These findings shed light on direct lineage reprogramming as a promising therapeutic strategy to replace dysfunctional fast-spiking PV interneurons to treat neuropsychiatric disorders.

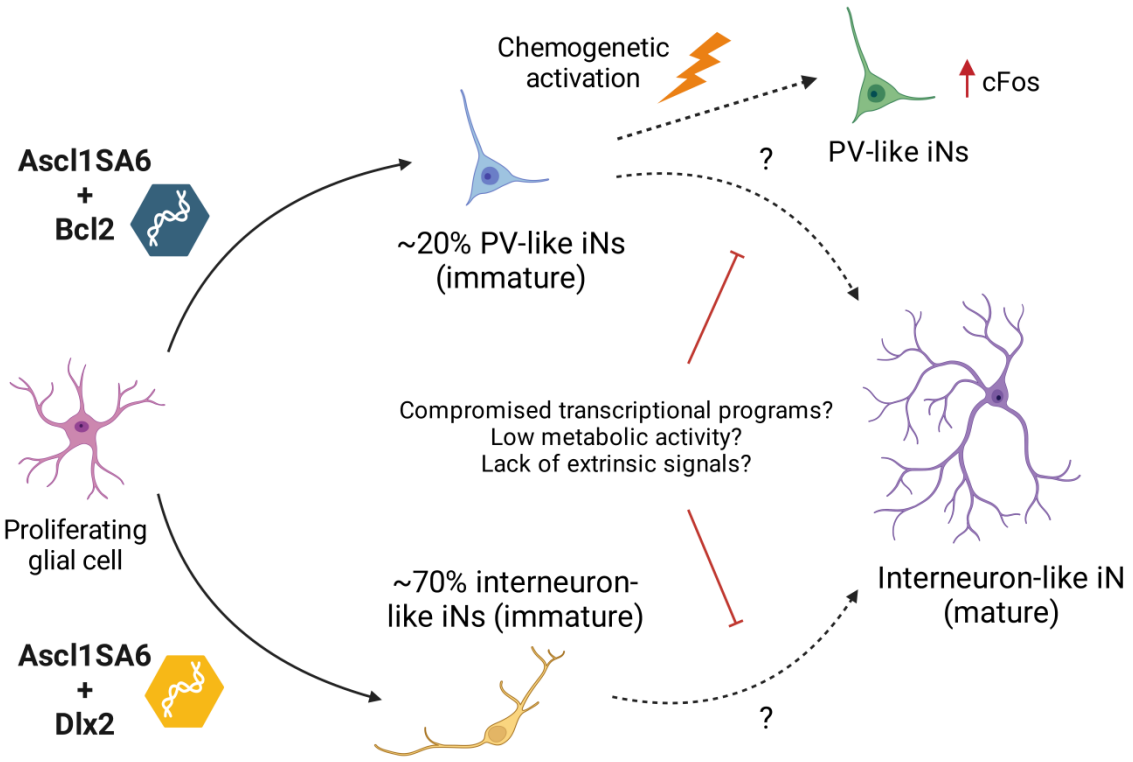

Figure 4.1. Graphical summary of main findings. Overexpression of the phospho-site mutant Ascl1SA6 together with additional reprogramming factors, such as Bcl2 (above) or Dlx2 (below), instructed proliferating cortical postnatal glia to reprogram into interneuron-like iNs. A fraction of Ascl1SA6 and Bcl2-derived iNs acquired hallmark histochemical and electrophysiological properties of PV interneurons. Such PV-like iNs can be selectively activated through chemogenetic stimulation. However, complete maturation of iNs is hindered by multiple intrinsic and extrinsic barriers that need to be overcome.

1. Demonstrating authenticity of glia-to-neuron conversion *in vivo*

Over the past years, there have been an increasing number of publications reporting high-efficiency conversion of multiple cell populations into neurons that differentiate into subtype-specific neuronal subtypes, functionally integrate within the host circuitry and even restored lost function in injury or disease mouse models (Bocchi et al., 2022). Some of these studies have recently reported remarkable reprogramming efficiency and functional repair upon delivery of AAVs encoding the single transcription factor NeuroD1 in multiple neurodegenerative disease mouse models or following cortical ischemic injury (Chen et al., 2020b; Puls et al., 2020; Tang et al., 2021; L. Zhang et al., 2020). Using the same approach, a recent publication claimed efficient neuronal regeneration and recovery of lost functions after stroke in a model of adult non-human primates (L. J. Ge et al., 2020). These exciting findings render the possibility of translating lineage reprogramming into clinical applications for humans more tangible. However, some of the reports have raised serious scepticism concerning the veracity of glia-to-neuron conversion *in vivo*, as it seems to be the case for studies using AAVs or lentivirus for transgene delivery (reviewed in Leaman et al., 2022). Most of the studies employing AAV and lentivirus-based strategies have reported the generation of putative iNs that exhibit suspiciously close similarities to mature endogenous neurons, but they do not provide compelling evidence to unambiguously demonstrate the glial origin of the putative iNs. Instead, they rely on the gradual loss of glial markers and the acquisition of neuronal identity by transduced cells, which does not occur when injecting control AAVs that do not encode for reprogramming factors.

Shortly after the publication of these breakthrough findings in the reprogramming field, other studies started to raise concerns that casted doubt on the authenticity of AAV-based glia-to-neuron conversion (L. L. Wang et al., 2021). As previously described in the introduction (see section 2.3.3), the Zhang lab strongly suggested the artefactual labelling of endogenous neurons, where these cells had acquired a gradual non-specific expression of the reporter gene (L. L. Wang et al., 2021a). Although it is not yet clear how the glial specificity may get lost over time, it has been suggested that leaky expression of astrocyte-specific promoters (Su et al., 2004) could non-specifically label endogenous neurons. Most of these aforementioned studies used astrocyte-specific promoters, such as *mGFAP*, to restrict reprogramming factors expression to this cell type. Alternatively, other studies have used FLEx switch AAV vectors, in which viral constructs encoding reprogramming factors of interest in inverted orientation (“FLEx”) are injected in mouse line expressing Cre recombinase

under control of glial-specific promoters, like mGFAP-Cre o NG2-Cre mouse lines (Mattugini et al., 2019; Pereira et al., 2017; Qian et al., 2020). However, caution is required because some levels of GFAP expression have been observed in neurons as well (Kempf et al., 2021). Additionally, a leaky transgene expression has been reported in neurons when using FLEx switch AAV vectors in the mGFAP-Cre mouse line (Mattugini et al., 2019). Alternative to this hypothesis, another possible explanation is that communication between glia and neurons via exosomes (Frühbeis et al., 2013; Men et al., 2019) could promote the exchange of Cre mRNA particles and induce recombination in endogenous neurons.

In the light of this recent controversy, my PhD thesis work presents several strategies to provide robust evidence for glia-to-neuron conversion in the postnatal mouse cortex. First, my work has demonstrated that Ascl1SA6-Bcl2-derived iNs go through a neuronal intermediate state, evidenced by the expression of the immature neuronal marker Dcx at 12dpi (Fig. 3.12-13B, D). This finding does not provide by itself sufficient evidence for reprogramming, as Dcx-expressing iNs could derive from rejuvenated endogenous neurons (Singh & Zhakupova, 2022). Additionally, Dcx has also been shown to be expressed at lower levels in OPCs (Boulanger & Messier, 2017). However, it hints at the possibility that glial cells undergoing conversion go through an immature neuronal state before giving rise to mature neurons, as occurs during physiological development.

Besides the acquisition of an intermediate immature phenotype, I have also shown that iNs derived from proliferating cells in the postnatal mouse cortex. First, I have confirmed previous work demonstrating that the postnatal cerebral cortex is a “non-neurogenic” structure (Kriegstein & Alvarez-Buylla, 2009), as evidenced by my experiments reporting the lack of endogenous Dcx+/EdU+ neurons in this brain region at P5 (Fig. 3.1B, E). Instead, most of the cells that had incorporated EdU at this time point were astroglia and OPCs (Fig. 3.1B-D). Along these lines, four weeks after injection with a control retrovirus I did not detect any transduced neurons in the cortex, thus confirming that endogenous neurons are not being targeted or gradually mislabelled over time by retrovirus (Fig. 3.2). Then, to demonstrate that iNs originate from proliferative cells in the postnatal cortex, I performed EdU-labelling experiments in which mice received an intraperitoneal injection of EdU on the same day of the retroviral intracortical injection. Therefore, iNs that had incorporated EdU will have originated from proliferating cells in the P5 cerebral cortex. Importantly, I found that a single administration of EdU was enough to detect EdU incorporation on half of NeuN-expressing transduced cells (Fig. 3.11).

In addition, using fate-mapping experiments in Aldh1l1-CreERT2/RCE and GFAP-Cre/RCE transgenic mouse lines to specifically label astroglia, I have provided robust evidence that the majority of iNs derived from this cell population (around 60% of Dcx or NeuN-expressing reporter-positive cells) (Fig. 3.12, 3.22). Despite the remarkable amount of OPCs transduced with control retroviruses, I only found very few examples of iNs that originated from this cell type when performing genetic fate-mapping in the NG2-CreERTM/RCE transgenic mouse line (Fig. 3.13, 3.22). One possible explanation for the low number of NG2-traced iNs could be a partial recombination efficiency of the transgenic mouse line. Indeed, unpublished data from our laboratory has shown that only about 70% of OPCs is labelled with the mouse line reporter gene. It is also worth noting that the tamoxifen administration protocol was changed from the one used for the astroglial fate-mapping, being administered over fewer days in the case of OPCs fate-mapping. Thus, it might be possible that these differences in the protocol used affected the recombination efficiency rate. One cannot discard the possibility that OPCs may also exhibit a molecular context that is more difficult to remodel into a neuronal-like identity. However, previous studies have shown efficient conversion of OPCs in the injured cortex (Heinrich et al., 2014) and in the epileptic hippocampus (Lentini et al., 2021). These findings provide proof-of-principle evidence for the susceptibility of OPCs to neuronal reprogramming, at least under specific contexts. Although further characterisation of the transgenic mouse lines needs to be done to shed light on the origin of the remaining iNs of non-traced origin, I could still demonstrate that the vast majority of iNs generated via retroviral transgene delivery have an astroglial origin.

Finally, my work also showed the ectopic generation of PV-expressing iNs in layer I of the cerebral cortex, a region devoid of endogenous PV interneurons. This surprising fact also provides strong evidence for the generation of iNs through lineage reprogramming rather than mislabelling of resident cortical endogenous neurons.

Taken together, this work reunites multiple lines of evidence that provide compelling support for authentic *in vivo* lineage reprogramming of glial cells into interneuron-like iNs in the postnatal mouse cerebral cortex.

2. Impact of different cell types as source for neuronal reprogramming

In this thesis, I used retroviral vectors to induce the expression of neurogenic transcription factors in endogenous glial cells in the postnatal mouse cerebral cortex aiming at their conversion into iNs. At postnatal day 5, the selected time point for the injection of retroviral constructs in the mouse cortex, I have identified both astroglia and OPCs as the main cell populations that proliferate in this region (Fig. 3.1). Given that retroviruses specifically transduce cells undergoing division, potentially more than one cell type could have been targeted when injecting retroviral constructs in the postnatal mouse cortex. Indeed, my work together with recent studies (Galante et al., 2022) have shown that preferentially astrocytes but also OPCs are transduced by control retrovirus in the postnatal mouse cortex (Fig. 3.2). In this section, I will discuss the relevance of targeting different cell populations for conversion towards a neuronal identity.

2.1. Astroglia as a starting cell population for neuronal reprogramming in the postnatal mouse cerebral cortex

Astroglia have been widely used in multiple studies as cell source for direct *in vivo* reprogramming, as their ubiquitous distribution throughout the CNS makes them a good target for conversion in different brain regions. Using fate-mapping approaches with two transgenic mouse lines that specifically labels astrocytes: Aldh1l1-CreER^{T2};RCE:loxP (Srinivasan et al., 2016) and mGFAP-Cre;RCE:loxP (Gregorian et al., 2009), I have shown that astroglia is the main cell population that contributes to generate iNs in the postnatal mouse cortex (about 60% of Dcx or NeuN-expressing reporter-positive cells) (Fig. 3.12, 3.22). These findings suggest that astrocytes are a powerful cell source for neuronal reprogramming and raise the question of whether this cell type is the most amenable for conversion towards a neuronal identity.

Some studies suggest that cortical layering is essential for the emergence of layer-specific morphological and molecular differences among cortical astrocytes (Lanjakornsiripan et al., 2018). Thus, the existence of layer-specific interactions between astrocytes and neurons might have a significant impact in the reprogramming outcome. A recent study reported the generation of induced pyramidal neurons that acquired layer-specific identity, suggesting that the original position of astrocytes in the cortex influences the fate of the iNs (Mattugini et al., 2019). In contrast to their findings, which were based on an AAV approach, my results demonstrated the ectopic presence

of PV-expressing iNs in layer I of the cortex, a region devoid of endogenous PV interneurons. These data suggest that the layer-specific properties of astrocytes and the extrinsic local environment might not have sufficient power to modulate the reprogramming outcome of iNs driven by the intrinsic effect of the transcription factors.

One important aspect to bear in mind for neuronal reprogramming is the state in which cells are targeted. Whereas several studies have focused on targeting postmitotic astrocytes, my PhD work aimed at targeting proliferating glia at early postnatal stages when local expansion is still taking place in the mouse cerebral cortex. Recent studies have shown that gene expression prolife and chromatin structure hugely differs during astrocyte maturation (Lattke et al., 2021). Indeed, an assay for transposase-accessible chromatin using sequencing (ATACseq) revealed that astrocytes from postnatal and adult mouse brains had significant differences in chromatin accessibility (Lattke et al., 2021). In addition, another study showed that prolonged culture of astrocytes makes them more resistant to lineage reprogramming by a gradual reduction of their chromatin accessibility (Masserdotti et al., 2015). Based on these findings, one could hypothesise that the immature proliferating state of astroglia in the postnatal mouse cortex could make these cells more amenable for neuronal reprogramming. However, studies using AAV-based approaches have claimed to also observe efficient conversion of mature astrocytes into neurons in the adult brain (Chen et al., 2020b; Y. Liu et al., 2015; Mattugini et al., 2019; Niu et al., 2013; Wu et al., 2020). Although these publications remain controversial, it cannot yet be firmly concluded that mature postmitotic astrocytes are less susceptible to lineage reprogramming.

Other studies have aimed at targeting astrocytes that become proliferative upon injury or disease. Following cortical stab-wound injury (Gascón et al., 2016; Heinrich et al., 2014; Mattugini et al., 2019) or injection of neurotoxins (Lentini et al., 2021), several groups have successfully reprogrammed reactive glia into various neuronal subtypes. In this PhD work, I have investigated the susceptibility to conversion of proliferating astrocytes in physiological conditions. As a next step, it would be fascinating to explore whether the different combinations of reprogramming factors used in this thesis would exhibit the same reprogramming efficiency and generate the same iNs phenotypes in an injury context. Even if both postnatal and reactive astrocytes are cell populations undergoing division, it is important considering that reactive astrocytes would receive different external cues and activate a very particular gene expression profile that might influence their susceptibility to reprogramming.

In summary, my results together with previous studies point at astrocytes as excellent candidates for generation of neurons. However, it is still unclear whether astrocytes in different contexts and brain regions exhibit the same susceptibility for reprogramming.

2.2. OPCs as a starting cell population for neuronal reprogramming in the postnatal mouse cerebral cortex

OPCs has also emerged as an interesting candidate for *in vivo* reprogramming and, indeed, many research groups have been able to convert them into neurons in different brain regions and contexts (Guo et al., 2014; Heinrich et al., 2014; Pereira et al., 2017; Torper et al., 2015). My work has shown that OPCs proliferate in the postnatal mouse cerebral cortex and can be successfully targeted with control retroviruses (Fig.3.1, 3.2). Surprisingly, using lineage-tracing experiments with a specific transgenic mouse line to label OPCs (NG2-CreER^{TM}BAC;RCE:loxP; Zhu et al., 2011), I found that very few NeuN-expressing iNs originated from this cell population (≤3% of NeuN-expressing reporter-positive cells) (Fig. 3.13, 3.22). When injecting a control retrovirus in the NG2-CreERTM/RCE transgenic mouse line, I found ~20% of transduced cells labelled with the mouse line reporter gene (Fig. 3.14), whereas injection of a retrovirus encoding reprogramming factors resulted in only ≤3% of transduced cells labelled with the mouse line reporter gene. This difference in the proportion of fate-mapped OPCs may be explained due to the fact that transduced cells with a control retrovirus can keep proliferating over time, whereas transduction with retrovirus encoding for reprogramming factors will most likely cause cell cycle exit as part of the neurogenic differentiation programme. Given the low number of labelled transduced cells, one could argue that the majority of OPCs might die during the process of neuronal reprogramming. Still, I found some examples of fate-mapped cells that expressed neuronal markers, providing proof-of-principle that postnatal OPCs can be converted into iNs. It would be necessary to optimise the protocol for tamoxifen administration or use another mouse transgenic line that ensures a higher labelling efficiency of OPCs to decipher their susceptibility to neuronal reprogramming.

It would be also very interesting to design a viral vector with a promoter that is active in OPCs, such as the platelet-derived growth factor receptor alpha (PDGFRA), NG2 or Sox10 (Xing et al., 2023), in order to specifically study susceptibility of this cell population to reprogramming. Published studies have reported that cell competition

during reprogramming of mouse embryonic fibroblasts (MEFs) gives rise to dominant clones that overtake the reprogramming niche (Shakiba et al., 2019). Thus, one could hypothesise that there might exist an inter-cell-type competition between astrocytes and NG2 during reprogramming that could hinder OPCs conversion into iNs. Finding a reliable experimental approach to target exclusively OPCs could shed light on the susceptibility of reprogramming of this specific cell population.

As previously described in the introduction of this thesis, OPCs and interneurons share a close relationship during brain development. Cortical interneurons and a fraction of OPCs originate in the ventral telencephalon during embryonic development and both cell populations migrate tangentially to populate the cortex (Anderson et al., 1997; Marín & Rubenstein, 2001; Spassky et al., 1998; Sun et al., 1998). OPCs are generated in three successive waves, with two initial waves produced in the ventral forebrain followed by a third wave originated postnatally in the dorsal forebrain (Kessaris et al., 2005). It has been recently reported that first-wave OPCs closely interact with interneurons to guide their migration towards the cortex into defined and separate streams (Lepiemme et al., 2022). However, first-wave OPCs are almost completely replaced by the other two waves in the postnatal cortex (Kessaris et al., 2005). Given that first-wave OPCs and interneurons share regional origins and closely interact during their migration to the cortex, one could hypothesise that this OPCs subpopulation could be more susceptible to interneuron conversion. Indeed, the low number of fate-mapped iNs in the NG2-CreERTM/RCE transgenic mouse line could correlate to the low number of first-wave OPCs that remain in the postnatal cortex (Kessaris et al., 2005). Contrary to this hypothesis, another study using bulk and single-cell transcriptomics has more recently reported that OPCs originated from different waves present similar transcriptomic profiles (S. Marques et al., 2018). Nevertheless, it would be interesting to use transgenic mouse lines to label the different OPCs subpopulation and investigate whether they show different susceptibilities to neuronal conversion.

Taken together, although my results suggest that OPCs do not greatly contribute to the generation of iNs in the postnatal cerebral cortex, their close functional interaction with neurons during development makes them an interesting candidate for neuronal reprogramming.

3. Role of phosphorylation in Ascl1-mediated neuronal reprogramming of postnatal glia in the mouse cortex

In this work, several lines of evidence have demonstrated that the phospho-site mutant form of Ascl1, namely Ascl1SA6, exhibits a higher neurogenic ability as compared to the wildtype Ascl1. First, I showed that Ascl1 alone fails to instruct postnatal cortical glia to convert into NeuN-expressing iNs at 28dpi (Fig. 3.3). Interestingly, a significant proportion of Ascl1-transduced cells expressed the microtubule-associated protein Dcx (~70% of of Dcx+ reporter-positive cells), which is used as a marker for newly generated neurons. These data suggest that Ascl1 might be capable of activating a neuronal transcriptional program that is still not sufficient to fully change the identity of the glial cells. However, a recent publication has shown that Dcx is also expressed in OPCs, although at lower levels than neuronal precursors (Boulanger & Messier, 2017). Given that recent work from our laboratory has demonstrated that OPCs transduced with Ascl1 in the postnatal cortex were still proliferative at 12dpi (Galante et al., 2022), it can be hypothesised that many of the Ascl1-transduced cells expressing Dcx at 28dpi are proliferating OPCs. Indeed, cells overexpressing Ascl1 retained a typical morphology from OPCs and expressed Dcx at much lower levels when compared to new-born neurons in the dentate gyrus of the hippocampus detected in the same brains. In addition, I showed that most of co-transduced cells with Ascl1 and Bcl2 as well as single-transduced cells with Ascl1 within the same brains expressed the oligodendroglial marker Sox10 (Fig. 3.6). Although in this thesis I have not provided direct evidence showing that overexpression of Ascl1 promotes OPCs proliferation, my results clearly indicate that this transcription factor induces a dramatic increase in the number of Sox10-expressing cells, even when combined with Bcl2. It would be interesting to know whether Ascl1-transduced cells keep proliferating at 28dpi, which could be answered by administration of EdU at this time point.

In contrast to the primarily non-neurogenic effect of Ascl1, my results showed that Ascl1SA6 instructs postnatal cortical glia to reprogram into a significant number of NeuN-expressing iNs (~35% of NeuN+ reporter-positive cells) (Fig. 3.3). Even more striking, when Ascl1SA6 expression was combined with other reprogramming factors, such as Bcl2 or Dlx2, the reprogramming efficiency increased up to ~80% of NeuN-expressing co-transduced cells (Fig. 3.4, 3.18). In contrast, co-expression of Ascl1 with these reprogramming factors barely generated NeuN-expressing iNs (<5% of NeuN+ reporter-positive cells) (Fig 3.4, 3.18).

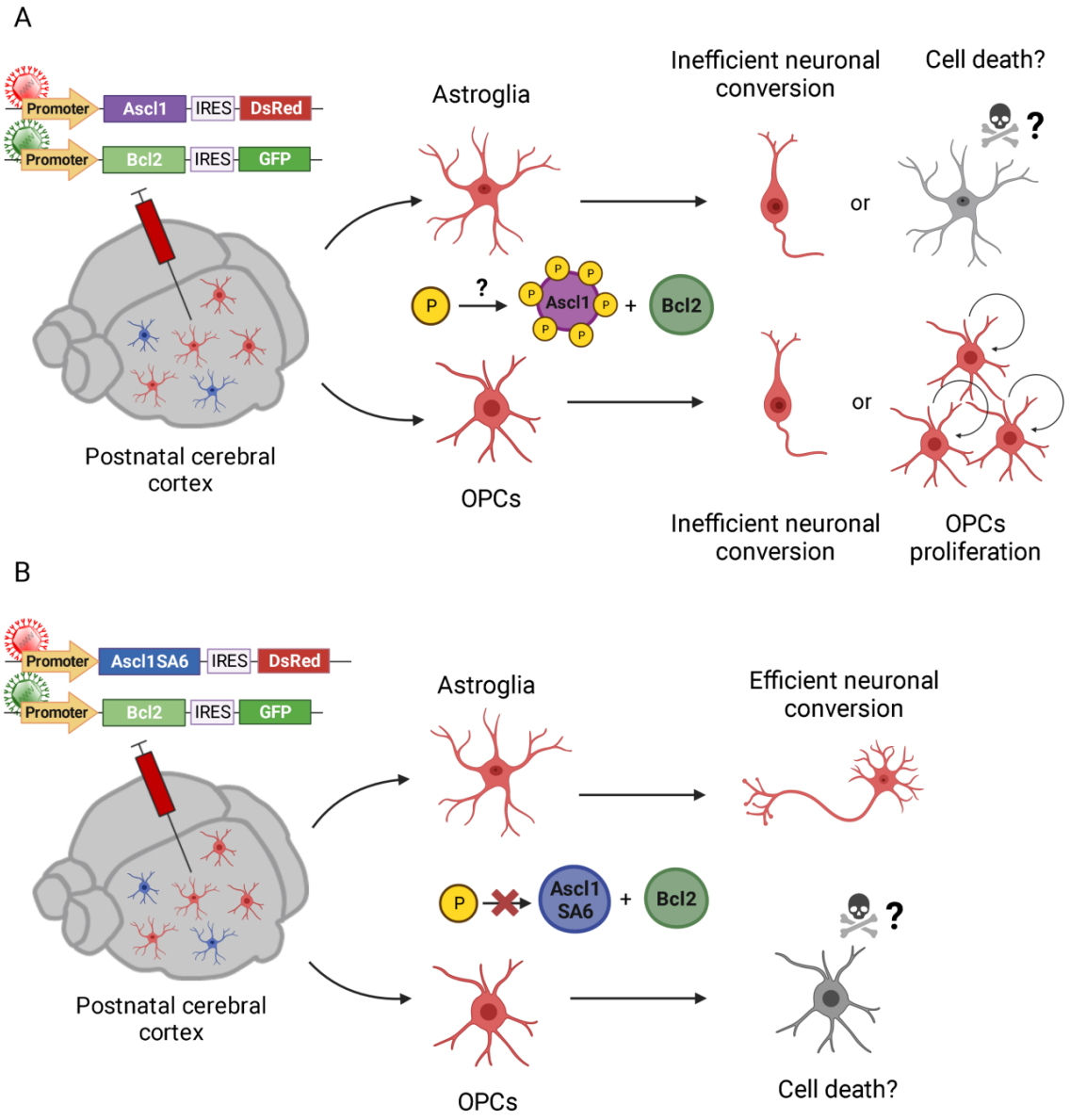

Figure 4.2. Influence of Ascl1 phosphorylation in glia-to-neuron conversion in the postnatal mouse cerebral cortex. (A) Overexpression of Ascl1 together with Bcl2 in proliferating glia in the postnatal mouse cortex resulted in the generation of a small fraction of iNs. Combined expression of Ascl1 and Bcl2 induced a dramatic increase in the number of OPCs, most likely due to enhanced OPCs proliferation. Very few of the Ascl1 and Bcl2 co-transduced cells retained an astroglial identity, as these cells most likely undergo neuronal conversion or cell death. (B) Forced co-expression of the phospho-site mutant form of Ascl1, namely Ascl1SA6, together with Bcl2 generated a high proportion of iNs, with astrocytes being the main starting cell population for conversion. The majority of OPCs co-transduced with Ascl1SA6 and Bcl2 most likely undergo cell death.

These evidences showing higher neurogenic activity of Ascl1SA6 are supported by previous findings describing an enhanced neurogenesis in progenitor cells of *Xenopus* embryos upon ectopic expression of Ascl1SA6 (Ali et al., 2014). Given the role of Ascl1 as pioneer factor that induces chromatin opening and increased accessibility at neuronal genes-associated regions (Raposo et al., 2015), it would be of great interest to explore whether Ascl1SA6 drives the same chromatin-remodelling modifications and binds to the same genomic targets as the wildtype Ascl1. However, it still remains to be elucidated whether enhanced neurogenesis by Ascl1SA6 results from a higher expression of the same genomic targets or whether Ascl1SA6 can bind and activate additional targets with less favourable chromatin configurations. In this work, differences in the promoter occupancy of Ascl1 and Ascl1SA6 target genes has not been investigated; however, it would be of great interest to answer this question by performing assays such as chromatin immunoprecipitation (ChIP).

Another possible explanation for the differences in the neurogenic activity of Ascl1 and Ascl1SA6 could be the protein stability. Of note, phosphorylation can act as a signal for ubiquitination (Hunter, 2007). Recent studies have shown that Ascl1 is modified at the post-translational level by the addition of short ubiquitin chains, whereas cytoplasmic Ascl1 carries long ubiquitin chains that confer a higher susceptibility to proteasomal degradation (Gillotin et al., 2018). Importantly, these differences in ubiquitination result in an increased half-life of Ascl1 (Gillotin et al., 2018). Thus, it might be the case that the phosphorylation state can influence the type of ubiquitination of Ascl1 and affect protein stability. Consequently, the binding efficiency to their target genes could be greatly affected depending on their initial phosphorylation state.

My results showing differences in the neurogenic activity of Ascl1SA6 also suggest that wildtype Ascl1 is, at least, partially phosphorylated in the postnatal mouse cerebral cortex *in vivo*. However, it is not yet clear how Ascl1 is mechanistically regulated at the molecular level. Previous work suggested that Ascl1 is regulated by Cdk-dependent phosphorylation in *Xenopus* embryos (Ali et al., 2014). During cell division, increased levels of cyclins drive higher Cdk kinase activity, which in turn results in phosphorylation of serine-proline sites of Ascl1. Cdks are conserved key regulatory elements of the cell cycle, which have been also found in dividing astroglia (Pedram et al., 1998) and OPCs (Caillava & Baron-Van Evercooren, 2012). Therefore, it could be hypothesised that Ascl1 can be subjected to phosphorylation under similar mechanisms as during brain development in dividing glial cells. However, it is important to keep in mind that the artificial overexpression of Ascl1 and Ascl1SA6 by transduction

with retroviral vectors might influence how these transcription factors are regulated at the molecular level when compared to physiological expression levels of Ascl1 during brain development.

Other studies have demonstrated that Ascl1 phosphorylation and specification properties are also regulated by RAS/ERK signalling pathway in a dosage-dependent manner in the mouse embryonic cortex (S. Li et al., 2014). Upon high levels of RAS activation, Ascl1 is phosphorylated and induces gliogenesis, whereas the exposure to low levels of RAS activity decreases Ascl1 phosphorylation and induces neurogenesis towards a GABAergic lineage (S. Li et al., 2014). Interestingly, this work demonstrated that RAS/ERK signalling promotes proliferation and glial cell fate in cortical progenitors. The fact that there is an increased in ERK activity between P5 and P10 in the mouse brain (Galabova-Kovacs et al., 2008) could explain why Ascl1 is more likely to be phosphorylated and, consequently, induce OPCs proliferation during postnatal development (Galante et al., 2022). Furthermore, Li and colleagues also demonstrated that the number of phospho-sites available regulates the ability of Ascl1 to drive neurogenesis by using a phospho-site mutant form of Ascl1 with only three serine-proline sites mutated, namely Ascl1SA3 (S. Li et al., 2014). Therefore, it would be very interesting to investigate the effect of Ascl1SA3 when overexpressed in cortical postnatal glia, as one could hypothesise that it might show different neurogenic ability and different fate specification properties when compared to Ascl1 and Ascl1SA6.

4. Role of Bcl2 in glia-to-neuron conversion in the mouse postnatal cortex

Cell death during the process of neuronal reprogramming has emerged as one of the most urgent hurdles to overcome (Gascón et al., 2016, 2017). My results demonstrated that co-expression of Ascl1 or Ascl1SA6 together with the pro-survival factor Bcl2, significantly improved reprogramming efficiency of iNs in the postnatal mouse cerebral cortex, based on the acquisition of NeuN expression of co-transduced cells (Fig. 3.4). In this thesis, I have not provided any direct evidence for impaired cell survival during glia-to-neuron conversion and additional experiments, such as terminal deoxynucleotidyl transferase dUTP Nick-End Labelling (TUNEL) assay, would be necessary to confirm cell viability. Although the pro-survival effect of Bcl2 would need to be further validated, my results strongly suggest that the increase in the percentage of NeuN-expressing iNs could be mediated by the facilitating effect of Bcl2.

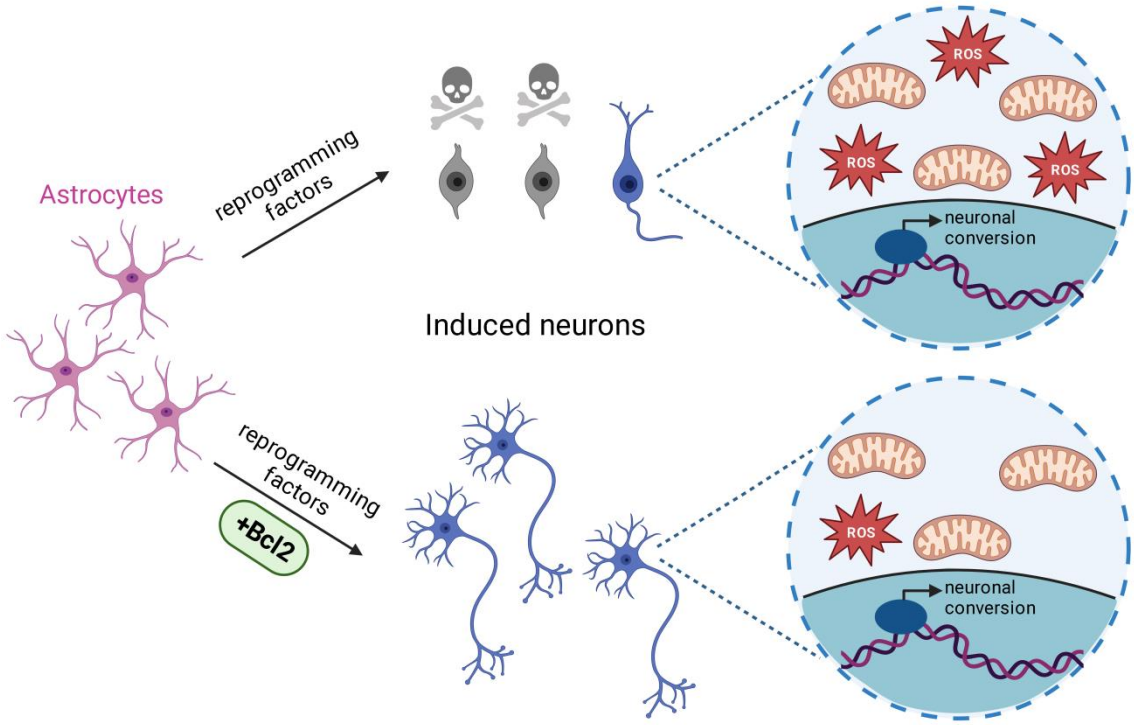

Figure 4.3. Role of Bcl2 in direct lineage reprogramming. Ectopic co-expression of Bcl2 together with other reprogramming factors in glial cells enhances the efficiency of glia-to-neuron conversion by reducing the excess of reactive oxygen species (ROS) generated during cell fate switch. Adapted from Russo, 2019).

Previous work has demonstrated that Bcl2 greatly improves neuronal reprogramming by alleviating the excess of reactive oxygen species (ROS) generated during lineage conversion (Gascón et al., 2016). Using inhibitors of different cell death pathways, this study suggested that the accumulation of ROS in cells during glia-to-neuron conversion was likely caused by ferroptosis, an iron-dependent process of programmed cell death (Dixon et al., 2012; Xie et al., 2016). Indeed, Bcl2 overexpression or administration of different anti-oxidants, such as vitamin E, calcitriol or α-tocopherol, attenuated ROS levels generated during glia-to-neuron conversion using Neurog2 (Gascón et al., 2016). It would be relevant to examine whether these anti-oxidants in combination with Ascl1 or Ascl1SA6 exert the same effects as co-expression with Bcl2. Additionally, detection of peroxiredoxin-2 (Prx2), which is involved in oxidative stress detoxification (Godoy et al., 2011), could be used as a marker to validate the anti-oxidant properties of Bcl2 during neuronal reprogramming.

Another interesting perspective is the role of Bcl2 in the mitochondria. Several studies have previously implicated Bcl2 in the decreasing oxidative stress levels in the

mitochondria (Krishna et al., 2011). Interestingly, during glia-to-neuron conversion cells switch from a glycolytic metabolism used by glial cells towards an oxidative metabolism characteristic from neurons (Gascón et al., 2016; Kim et al., 2018). This metabolic switch results in mitochondrial abnormalities typical of cellular ageing and impaired Adenosin Triphosphate (ATP) production (Kim et al., 2018). Additionally, recent studies have shown that mitochondria metabolism is involved in the timing of cortical neuron maturation (Iwata et al., 2023). Thus, it would be of great interest to investigate whether Bcl2 overexpression induces changes in morphology and functionality of mitochondria in iNs and whether these changes directly influence iNs maturation during conversion.

5. Fate specification of glia-derived iNs into neuronal subtypes

Based on the key role of Ascl1 in differentiation and subtype specification of forebrain interneurons during development (Casarosa et al., 1999b; Horton et al., 1999; Lim et al., 2018), I investigated whether overexpression of Ascl1 or the mutant variant Ascl1SA6 were able to instruct postnatal glia to convert into GABAergic-like iNs in the mouse cerebral cortex. In line with its known fate specification properties, I observed that co-expression of Ascl1SA6 and Bcl2 generated around 20% of iNs that acquired the expression of the neurotransmitter GABA (Fig. 3.7). Remarkably, a similar percentage of iNs also acquired the expression of the subtype-specific interneuronal marker PV and displayed fast-spiking firing properties (Fig. 3.7, 1.3). Of note, none of the co-transduced cells acquired expression of SST, which constitutes the other main MGE-derived interneuron subpopulation in the cortex (Fig. 3.7). It is important to keep in mind that iNs could have also differentiated towards another interneuron subclass that was not tested in this work, such as VIP, CR or NPY. Due to limitations on the amount of fluorophores available, I did not evaluate whether iNs that expressed GABA were the same ones that acquired expression of PV. However, since the percentages of iNs that acquired expression of these markers were very similar and I could not detect other interneuron subpopulations, it is tempting to speculate that all GABAergic iNs specifically differentiated towards a PV-like interneuron identity. Moreover, the specification towards this phenotype was corroborated by finding mRNA expression of other genes expressed in PV interneurons, such as *Kv3.1* and *Syt2* (Fig. 3.9). However, the molecular mechanisms underlying specification towards this very specific phenotype remain unclear and it would be necessary to perform further experiments to answer this question. One interesting aspect to tackle would be to investigate the

identity of the remaining iNs population that does not acquire an interneuron-like phenotype. Previous studies have shown that iNs generated from human pericytes *in vitro* bifurcate into two cell populations that acquire either glutamatergic or GABAergic identity (Karow et al., 2018). One could hypothesise that the remaining population of iNs also acquired a glutamatergic identity. However, electrophysiological recordings from the population of Ascl1SA6 and Bcl2-derived iNs have shown that the cells that do not display fast-spiking activity exhibited a higher input resistance, reminiscent of less differentiated neurons. Thus, it is also possible that all iNs are committed to acquire a PV phenotype, however, some of these cells get stalled in an immature neuronal state that does not allow them to acquire any specific identity.

Another interesting perspective would be to understand the role of Bcl2 in fate specification during lineage reprogramming. As previously described, Bcl2 has been proposed to maintain healthy mitochondrial function via an anti-ferroptotic mechanism (Dixon et al., 2012; Gascón et al., 2016; Krishna et al., 2011). In addition, fast-spiking PV interneurons have a large mitochondrial content necessary for their high energy demand to sustain high-frequency firing during neuronal transmission (Kann et al., 2014; Kann & Kovács, 2007; Kontou et al., 2021). Therefore, one could hypothesise that the role that Blc2 exerts in keeping the correct functioning of mitochondria is involved in the acquisition of a PV-like interneuron identity.

Dlx2 plays important roles in interneuron migration and specification during embryonic development (Lindtner et al., 2019; Long et al., 2009; Petryniak et al., 2007). Given that Dlx2 is a downstream target of Ascl1, it was surprising to find that overexpression of Ascl1SA6 together with Bcl2 did not activate endogenous expression of Dlx2 (Fig. 3.16). Interestingly, using transcriptional reporter assays in embryonic carcinoma cells, one study reported that the phospho-site mutant Ascl1SA6, in contrast to wildtype Ascl1, could not transactivate the Dlx1/2 reporter (S. Li et al., 2014). These findings together with my results suggest that serine-proline sites might be necessary for Ascl1 to activate Dlx1/2. Because Dlx2 expression was not activated in the converted iNs, I decided to investigate whether overexpression of Dlx2 alone or together with Ascl1 or Ascl1SA6 improved glia-to-interneuron conversion in the mouse cerebral cortex. Forced expression of Dlx2 alone led to the generation of some Dcx-expressing immature iNs (Fig. 3.17). Interestingly, some of the generated Dcx+ iNs accumulated in cell clusters. One study suggested that overexpression of Dlx2 in striatal astrocytes generated Dcx-expressing cell clusters with properties of dividing neuronal progenitors (Y. Zhang et al., 2022). Thus, it would be interesting to investigate whether Dlx2-transduced iNs are proliferative cells, which could be answered by

performing EdU labelling assays. Although this aspect has not been tackled in this thesis, an alternative hypothesis could be that these cell clusters behave as migrating interneurons-like cells, given the important role of Dlx2 in migration of interneurons during development (Colasante et al., 2008; Marín & Rubenstein, 2001). In addition, my results showed that co-expression of Ascl1SA6 and Dlx2 instructed postnatal glia to convert into a remarkably higher percentage of GABAergic iNs compared to Ascl1SA6 and Bcl2 co-transduced cells (Fig. 3.19). These data corroborate the important functions of both Ascl1 and Dlx2 in interneuron fate specification (Long et al., 2009) and supports previous findings that demonstrate successful generation of GABAergic iNs by overexpression of these reprogramming factors (Lentini et al., 2021).

Surprisingly, my results indicated that none of the Ascl1SA6 and Dlx2-derived iNs acquired PV, SST or VIP interneuron identities (Fig 3.19). It might be the case that co-expression of Ascl1SA6 and Dlx2-derived iNs that specified towards a very particular interneuron subtype that was not tested in this work, such as CR or NPY. In fact, a recent study has shown that almost half of iNs generated by co-expression of Ascl1 and Dlx2 in the epileptic hippocampus acquired expression of the interneuron subtype marker NPY (Lentini et al., 2021). However, it can also be interpreted as some of these iNs might be committed to certain phenotypes but get stalled in their differentiation process and cannot further specified into any interneuron subclass. A surprising finding is that some of the iNs also acquired mRNA expression of the Kv3.1 channel (Fig. 3.20), which is necessary for acquisition of fast-spiking activity in PV interneurons (Rudy & McBain, 2001). However, preliminary data from patch-clamp recordings of Ascl1SA6 and Dlx2 co-transduced cells (n = 5) suggest that these iNs did not display a high-frequency firing pattern. Of note, half of the iNs generated by co-expression of Ascl1SA6 and Bcl2 did not exhibit fast-spiking activity (Fig. 1.3). Thus, it might be the case that we missed some Ascl1SA6 and Dlx2-derived iNs that also acquired a high-frequency firing pattern. However, one cannot exclude the possibility that Kv3.1 channel mRNA might not be translated into protein and thus, iNs will not acquire fast-spiking properties at the electrophysiological level.

Finally, given the hypothesis that Bcl2 can also play a role in the specification of iNs towards a fast-spiking PV phenotype, I decided to investigate the identity of iNs that were co-transduced with of Ascl1SA6 and Dlx2 in addition to Bcl2. Similar to my previous findings, iNs did not acquire expression of the subtype-specific interneuron marker PV (Fig. 3.23). To explain these results, one could hypothesise that Dlx2 activates a strong and specific molecular programme that does not allow Bcl2 to influence the acquisition of a different cellular identity. Importantly, our laboratory is

currently aiming at investigating the transcriptomic profile of iNs using single-cell RNA sequencing technologies, which will shed light on the specific molecular programmes that are induced in these cell populations. To perform single-cell RNA sequencing analysis, it is necessary to collect around 2000-3000 of transduced cells per reprogramming factor combination. To achieve the collection of these cell numbers, around 8 mice received a retroviral injection in both cortical hemispheres per condition and sorted cells were pulled together for sequencing analysis. Although this approach may not provide a complete answer on the cellular identity of iNs, it will unveil differences in the transcriptomic profiles activated by combination of specific transcription factors.

6. Differences in reprogramming outcome using single retroviral vectors or a tri-cistronic retroviral vector

This work showed that forced expression of single reprogramming factors, such as Ascl1 or Dlx2, is not sufficient to efficiently instruct postnatal glia to convert into iNs in the mouse cerebral cortex. For this reason, I used several viral vectors to overexpress more than one reprogramming factor in the transduced cells. However, using several retroviral constructs encoding for a single reprogramming factor carries certain constrains, such as the low and variable number of co-transduced cells. In addition, some experiments that require the use of transgenic mouse lines that express a reporter gene in a specific cell population (such as Aldh1l1-CreERT2;RCE:loxP, NG2CreERTM BAC;RCE:loxP or Vgat-Cre;RCE:loxP) cannot be easily performed with more than one retroviral construct due to the lack of different reporter genes. For these reasons, I decided to clone tri-cistronic retroviral vectors encoding for two reprogramming factors (either Ascl1 or Ascl1SA6 together Bcl2 or Dlx2) in addition to the reporter gene DsRed. In these retroviral vectors, both reprogramming factors were linked by the “self-cleavage” peptide sequence T2A, followed by an IRES sequence that linked the reporter gene. The transcription of both reprogramming factor and the reporter gene was controlled by the strong and constitutive CAG promoter (Fig. 2.1).

My results showed that using tri-cistronic vectors encoding for the reprogramming factors I could achieve similar reprogramming efficiency as when using single vectors (Fig. 3.10, 3.21). Unexpectedly, the fate specification properties of the tri-cistronic vector towards an interneuron identity were severely hampered. Whereas overexpression of Ascl1SA6 and Bcl2 in single vectors generated PV-expressing iNs, I

could not find any iNs that acquired this phenotype when using the tri-cistronic vector (Fig. 3.15). Along these lines, the percentage of GABAergic iNs generated by overexpressing Ascl1SA6 and Dlx2 was dramatically reduced when using the tri-cistronic vector (Fig. 3.23). It is worth noting that in the first reprogramming strategy, Ascl1 and Ascl1SA6 are expressed under the control of the CAG promoter, whereas Bcl2 expression is controlled under the 5' LTR promoter from the retroviral vector pMIG (a kind gift from Dr. Sergio Gascón). However, when both genes were cloned within the same tri-cistronic vector, their expression was controlled by CAG promoter. Thus, it could be possible that Bcl2 expression levels significantly differ when driven either by 5'LTR promoter in the single vector or the CAG promoter, which has been shown to drive strong expression of downstream genes (Dou et al., 2021), in the tri-cistronic vector. Although this aspect has not been studied in this work, it would be very interesting to investigate whether expression levels differ between single and polycistronic vectors using, for instance, using smFISH technology. Even more important, it would be very fascinating to understand whether specific expression levels of reprogramming factors are required to achieve successful reprogramming and desired identity of iNs.

Another relevant aspect of using tri-cistronic vectors in which both reprogramming factors are linked by a T2A sequence is that both proteins are expected to be expressed at equivalent stoichiometric levels. This has been previously described in some studies that used "self-cleavage" 2A sequences for simultaneous expression of genes (Szymczak & Vignali, 2005). However, other studies have reported differences in expression levels when changing the gene position in the polycistronic vector or when using different types of 2A sequences (Z. Liu et al., 2017). In the context of cardiac reprogramming, Liu and colleagues showed that protein expression dramatically decreased at the second position and the highest efficiency of expression is achieved by using T2A or tandem P2A-T2A sequences (Z. Liu et al., 2017). These findings are of great importance, since many studies related to lineage reprogramming have demonstrated that the way reprogramming factors are expressed strongly influences the conversion outcome. For instance, a recent study has shown that expression of a polycistronic retroviral vectors encoding for Brn4, Klf4, Sox2, and cMyc in fibroblasts induced a transient pluripotent state, whereas expression of the same genes in single retroviral vectors failed to induced pluripotency (Velychko et al., 2019). This difference occurred due to an incomplete cleavage of a F2A sequence that resulted in generation of a fusion Brn4-Klf4 protein, altering the reprogramming process. In addition, it is also important to consider that both upstream and

downstream proteins will carry extra peptides as a result of the 2A sequence cleavage, which could negatively influence the correct functioning of the reprogramming factors. Therefore, further research is needed to investigate the impact of resulting proteins after cleavage by 2A peptides when using polycistronic reprogramming cassettes.

7. Impact of environment and extrinsic inputs on neuronal reprogramming

I have previously discussed the impact of cell intrinsic aspects, such as the cell source heterogeneity or the effect of post-translational modifications of transcription factors, in the outcome of neuronal conversion. Reprogramming mechanisms appear to be directly influenced by cell type-dependent molecular contexts and how the transcription factors interplay within different chromatin landscapes. However, the local microenvironment where reprogramming takes place *in vivo* (Grande et al., 2013) seem also to have a strong impact on conversion efficiency and subtype specification.

Several studies have revealed significant differences in reprogramming outcomes, in terms of efficiency and fate specification, obtained using the same transcription factors *in vitro* and *in vivo*. An illustrative example is the successful neuronal conversion of postnatal cortical astrocytes *in vitro* by forced expression of Ascl1 alone (Berninger et al., 2007; Heinrich et al., 2010), but failing to induce neuronal conversion of proliferating glia in the postnatal cortex, as demonstrated in this PhD thesis (Fig. 3.3) and in agreement with recent findings from our laboratory (Galante et al., 2022). These contradictory results raise the crucial question of to which extent the extrinsic environmental signals influence neuronal identity and subtype specification during lineage conversion.

7.1. Impact of distinct brain areas on neuronal reprogramming

In the recent years, numerous publications have reported successful glia-to-neuron conversion in multiple brain areas. However, the identity of iNs engineered by similar strategies resulted to be different depending on the brain region where they were generated. Interestingly, ectopic expression of Neurog2 generated iNs that displayed features reminiscent of glutamatergic neurons in the adult injured cortex, whereas they acquired identity of striatal projection neurons in the striatum (Gascón et al., 2016; Grande et al., 2013). Moreover, additional studies revealed that both OPCs and astrocytes are specifically converted into inhibitory neurons regardless the transcription

factors employed in the adult striatum (Niu et al., 2015; Pereira et al., 2017), suggesting a preferential conversion towards a GABAergic-like phenotype in this brain region. Thus, one could argue that extrinsic signals from the local environment may superimpose a region-specific neuronal subclass identity onto cells undergoing reprogramming beyond the mere control of reprogramming factors.

In contrast to the striatum, the adult injured cerebral cortex appears to be a more permissive structure supporting the generation of various neuronal subtypes, as revealed by acquisition of neurochemical markers from distinct neuronal populations (Gascón et al., 2016; Grande et al., 2013; Heinrich et al., 2014; Mattugini et al., 2019). My PhD work shows for the first time that proliferating glia can be instructed to generate interneuron-like iNs in the postnatal mouse cortex *in vivo*. Remarkably, Ascl1SA6 and Bcl2-derived iNs could differentiate towards a PV phenotype and exhibited fast-spiking firing activity. In addition, it has been recently reported that forced expression of Neurog2 and Bcl2 in the postnatal cerebral cortex generates iNs that acquire expression of cortical glutamatergic markers, such as Trb1 or Ctip2 (Herrero-Navarro et al., 2021). Thus, the cerebral cortex seems to be a brain region that allows for iN conversion and differentiation towards various neuronal subclasses. To which extent iNs differentiation depends on the neighbouring environment or the imposed expression of transcription factors remains to be determined.

7.2. Impact of injury-mediated signalling on neuronal reprogramming

Besides the influence of the local environment, direct lineage reprogramming *in vivo* also exploits the enhanced cellular plasticity occurring in the brain upon injury (Gascón et al., 2016; Grande et al., 2013; Heinrich et al., 2014; Lentini et al., 2021). Interestingly, whilst Sox2 failed inducing neurogenesis in cortical astrocytes and OPCs in the absence of prior lesion, the same transcription factor elicits the generation of Dcx-expressing iNs upon stab-wound injury in the cortex (Heinrich et al., 2014). Even more strikingly, stroke-derived lesion in the striatum (Magnusson et al., 2014) or excitotoxic induction in a model of Huntington's disease (Nato et al., 2015) showed that striatal astrocytes activated a latent neurogenic programme in the absence of reprogramming factors. Thus, one can speculate that an injury environment can facilitate lineage conversion, although it remains to be elucidated whether this effect is through stimulating cell proliferation or activation of independent molecular programmes that enhance cellular stemness.

More recent work has demonstrated that reactive glia can be instructed to reprogram into GABAergic-like iNs in the epileptic hippocampus by forced expression of Ascl1 and Dlx2 (Lentini et al., 2021). Using the same retroviral construct (a kind gift from Prof. Heinrich's lab), this work showed that postnatal cortical glia failed to induce neuronal conversion (Fig. 3.21). One cannot firmly conclude that the lesioned environment was the only factor influencing glia-to-neuron conversion, since the brain region (hippocampus vs cortex) and the main cell population targeted (OPCs vs astrocytes) were also different in both scenarios. However, one can hypothesise that an injured environment would be more favourable for generation of iNs. The kainate acid-induced epilepsy model used in the aforementioned study generated a drastic decrease in endogenous hippocampal interneurons. Thus, it can be speculated that a reduction of the pool of endogenous interneurons might have favoured the survival of interneuron-like iNs due intrinsic homeostatic mechanisms or less cell competition after the lesion. In addition, Lentini and colleagues showed that most of the iNs differentiated into the specific interneuron subclasses NPY and VIP. It would therefore be interesting to investigate whether forced expression of Ascl1SA6 and Bcl2, which I previously showed to generate PV-expressing iNs in the postnatal cerebral cortex, can also induce this phenotype in the epileptic hippocampus. This experiment would be of great relevance as PV interneurons are preferentially lost in the human epileptic hippocampus (Andrioli et al., 2007; Drexel et al., 2017).

7.3. Impact of activity during neuronal reprogramming

Several studies have previously indicated that activity-dependent mechanisms play an essential role on interneuron maturation, specification and integration into brain circuits during embryonic and postnatal development (de Marco García et al., 2011; Lim et al., 2018; Wong et al., 2018). For instance, maturation of PV interneurons and their electrophysiological properties has been tightly linked to excitatory inputs received from glutamatergic neurons during development (Anastasiades et al., 2016; Miyamae et al., 2017; Okaty et al., 2009).

My PhD work showed that forced expression of Ascl1SA6 and Bcl2 generated fast-spiking PV-like iNs; however, these cells exhibited lower PV expression levels and smaller soma size compared to the endogenous cortical PV interneurons, reminiscent of their stalled maturation (Fig. 3.8). To promote maturation of PV-expressing iNs, I used a chemogenetic strategy based on excitatory hM3Dq DREADDs to artificially

induce iNs activation. This manipulation allowed me to demonstrate that iNs can be specifically activated through chemogenetic-mediated stimulation, as revealed by the expression of the immediate early gene c-Fos (Fig. 3.24). This interesting finding opens new roads to study how activity can influence the process of lineage reprogramming. My results also showed that a small fraction of iNs lacking hM3Dq expression also expressed c-Fos, suggesting that iNs either displayed spontaneous activity or received synaptic inputs from neighbouring neurons. Interestingly, voltage-clamp recordings performed by Dr. Nicolas Marichal in Ascl1SA6 and Bcl2-derived iNs revealed that these cells received sEPSC, suggesting that they can be integrated in the host circuitry (Fig. 1.3). During postnatal cortical development, pyramidal neurons modulate cell death of interneurons through activity-dependent mechanisms (Wong et al., 2018). Then, it would be of great interest to investigate whether activity from excitatory neurons in the cortex exerts the same regulatory mechanisms on GABAergic-like iNs. If this were the case, it would be intriguing to study whether enhancing the activity of neighbouring cortical excitatory neurons would improve survival of GABAergic-like iNs.

PV is a calcium-binding protein whose expression levels have been shown to be tightly modulated by activation of PV interneurons (Donato et al., 2013, 2015). Thus, I reasoned that inducing depolarisation of PV-expressing iNs through chemogenetic stimulation might promote an increase on their PV expression levels. However, I did not observe any significant changes on PV expression levels in the group of PV-like iNs transduced with DREADDs in comparison to cells lacking DREADDs expression upon CNO administration (Fig. 3.25). Although the concentration of CNO administered (5mg/kg) was higher than the one normally used for activation of endogenous neurons (Wong et al., 2018), it is possible that it was not enough to trigger changes on the molecular machinery controlling PV expression levels. On the other hand, it could also be the case that such a prolonged activation over ten days might have desensitised iNs response to changes on activity. Additionally, an alternative explanation is that iNs might have not reached a sufficient maturation degree to cope with increasing amount of PV protein synthesis. In any case, it would be very interesting to further investigate whether iNs experienced changes in other activity-dependent genes, such as Er81, which has been shown to be an essential transcriptional regulator for driving Kv1.1 expression and the acquisition of fast-spiking firing properties of PV interneurons (Dehorter et al., 2015).

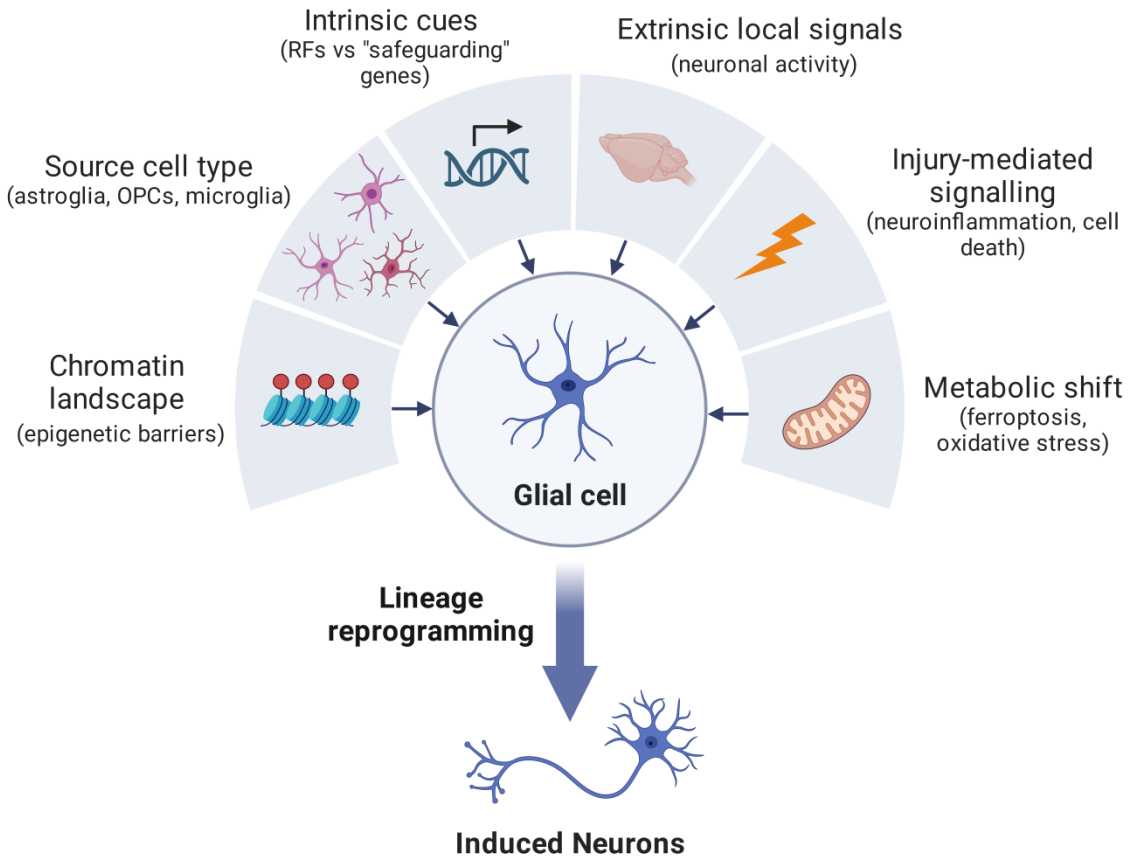

Figure 4.4. Factors influencing direct lineage reprogramming. Transcription factor-based lineage reprogramming is affected by multiple extrinsic and intrinsic factors (represented above within blue squares) that can either boost or hinder the neuronal conversion process. The interplay between all these factors will directly influence the reprogramming outcome.

Additional to the influence of changes in the whole excitatory network, an important question to tackle would be to understand if differences in external inputs received at specific cortical layers would also have an impact on the reprogramming outcome. One could argue that iNs would encounter great difficulties to acquire a particular phenotype if they do not receive the adequate inputs from its endogenous brain region. On the contrary, it can also be hypothesised that overproduction of neurons in physiological conditions could result in a competing mechanism between induced and endogenous neurons to eliminate the excess of cells. Although my results do not show any preference for the generation of PV- iNs in layer I and deeper layers, the absolute numbers of iNs generated regardless of PV expression are much higher in layer I (Fig. 3.8). Thus, one could hypothesise that PV-iNs do not need to receive the

adequate inputs from its endogenous specific cortical layer to achieve successful reprogramming. Interestingly, one study showed that reprogramming L2/3 callosal projection neurons into induced corticofugal projection neurons, normally located in L5, increased the number of inhibitory synapses onto the reprogrammed neurons to similar levels of their endogenous counterparts (Ye et al., 2015). These interesting findings open the question of whether generating subtype-specific iNs in ectopic cortical layers can lead to circuit remodelling.

8. Limitations and challenges on glia-to-neuron conversion in the postnatal mouse cortex

Despite the high reprogramming efficiency exhibited by co-expression of Ascl1SA6 and Bcl2, most of the iNs remained with features typical from immature neurons. Regardless of their PV expression, iNs exhibited a soma half of the size of the ones of endogenous PV interneurons in the cortex (Fig. 3.8). This result is quite striking taking into account that neurons displaying fast-spiking activity demand high energy consumption and cells that are metabolically very active usually exhibit a big soma (Ransdell et al., 2010). In addition, although the arborisation complexity of iNs has not been measured in this thesis, I observed that most of the iNs remained bipolar or with few processes that did not exhibit complex ramification. In the cortex, some types of PV-expressing interneurons, such as basket or chandelier cells, exhibit an outstanding axonal and dendritic arborisation that allows them to innervate cell bodies or axons of large populations of pyramidal cells respectively (Favuzzi et al., 2017; Tremblay et al., 2016). Thus, the lack of morphological maturation of iNs might be directly related with a lack of complete maturation of their functionality.

Besides morphological differences, iNs also exhibited lower expression levels of genes expressed in PV interneurons, such as *PV*, *Kv3.1* or *Syt2* (Fig. 3.8, 3.9). One could hypothesise that terminal specification of glia towards a neuronal phenotype is partially arrested during conversion. One possibility is that iNs are fully committed towards a neuronal identity, but they undergo through certain metabolic deficiencies that prevent them to develop into mature interneurons. As previously discussed, glial cells undergoing reprogramming are forced to switch from a glycolytic metabolism towards an oxidative metabolism typical of neurons. Barriers encountered during this metabolic shift might cause an incomplete maturation of iNs or eventually cause cell

death (Gascón et al., 2016). Future research focused on investigating ways to facilitate this metabolic switch, as I performed by overexpression of Bcl2, might bring novel advances in the reprogramming field. For instance, Peroxisome proliferator-activated receptor gamma coactivator 1-alpha (Ppargc1α) is a transcription factor that regulates the expression of PV-specific genes (Lucas et al., 2014) and, additionally, it is also known to be a master-regulator of mitochondrial biogenesis (Miller et al., 2019; Zehnder et al., 2021). More interestingly, depletion of *Ppargc1*α from cortical interneurons increases oxidative stress (J. Wang et al., 2020). Given that mitochondria metabolism is implicated in the timing of cortical neuron maturation (Iwata et al., 2023), it would be extremely interesting to investigate the role of *Ppargc1*α during glia-to-interneuron conversion in the cortex.

One of the limitations of our reprogramming strategy that might be hindering iNs maturation is the constitutive expression of the reprogramming factors. Ascl1 is a proneural gene activated early during GABAergic fate specification at embryonic stages; however, its expression is downregulated in post-mitotic neurons (Casarosa et al., 1999; Fode et al., 2000). Our retroviral strategy allows the integration of the viral genes in the host genome, consequently driving a constitutive expression of the reprogramming factors over time. Indeed, this work showed that Ascl1 is still expressed at high levels in iNs at four weeks after the retroviral injection. Although this strategy can bring advantages to guarantee a strong and prolonged expression of the reprogramming factors, it can also carry along some problems in regards of iNs maturation. One could hypothesise that long-term expression of Ascl1 in iNs might be keeping them in an immature state typical of newly generated neurons and hampering its development towards a more mature neuronal identity. To overcome this problem, it would be interesting to generate an inducible retroviral vector that allows controlling the expression of desired reprogramming factors during a specific period, this way mimicking what occurs during normal development.

Another caveat encountered during lineage reprogramming is the long-term survival of iNs. Although a quantitative analysis has not been performed, I could observe a sharp decrease in the number of iNs between 12dpi and 28dpi. Even if I did not show direct evidence for cell death taking place, preliminary data from our laboratory using two-photon imaging revealed a dramatic decrease in the number of iNs around the third week after retroviral injection. Furthermore, other set of preliminary experiments from our research group revealed that the number of remaining iNs at 8wpi was very limited. It is necessary to keep in mind that the number of transduced

cells can highly vary between intracranial injections and further experiments would be required to prove cell death. Another alternative explanation is that iNs can silence the expression of integrated viral genes in their genome upon time, including the reporter gene, making impossible to detect transduced cells at long time points.

9. Future directions and clinical translation of neuronal reprogramming

Although the reprogramming approach reported in this thesis is unlikely to generate complete bona fide fast-spiking PV interneurons, our data showing that a fraction of Ascl1SA6 and Bcl2-derived iNs acquired hallmark features of endogenous PV interneurons is of great importance for several reasons. First, differentiation protocols to obtain PV interneurons from embryonic stem cells in vitro has only achieved low efficiency of conversion (Maroof et al., 2013; Nicholas et al., 2013; Yang et al., 2017). Moreover, these protocols often require long timelines and the addition of external cues. Second, growing evidence implicates dysfunction of PV interneurons in neuropsychiatric disorders, such as schizophrenia or ASD, producing devastating impairment in cognitive functions (Chao et al., 2010; T. Hashimoto et al., 2003). Hence, this thesis provides a solid basis for future work aiming, for instance, to replace dysfunctional PV interneurons with glia-derived PV-like iNs counterparts to re-establish an appropriate excitation/inhibition balance as an innovative therapeutic strategy to treat neuropsychiatric disorders.

Towards the use of direct neuronal reprogramming as a therapeutic strategy for restoring damaged or imbalanced neuronal networks, an important pre-requirement is to achieve integration of iNs within the endogenous pathological circuitry. To exert a relevant clinical potential, iNs must not only receive synaptic inputs from endogenous neurons, but also send axonal projections innervating surrounding neurons. In most of the present studies, it remains unclear whether iNs constitute a functional presynaptic partner and, even more critical, specifically target the correct neurons. In the particular case of cortical interneurons, it has been shown that different interneuron subclasses target specific subcellular compartments of pyramidal neurons, which is essential for their ability to shape pyramidal neurons activity (Favuzzi et al., 2017). Importantly, one recent study showed that conversion of reactive glia in the epileptic hippocampus can alleviate chronic seizure activity (Lentini et al., 2021), suggesting a functional integration within the endogenous circuitry. As a long-term goal, it would be interesting

to investigate whether PV-like iNs generated using my reprogramming scenario could also exert an anti-epileptic activity within diseased networks. Related to this issue, long-term stability of iNs also appears to be crucial for ultimately restoring functionality and correct neurological deficits. Whereas various studies claimed the maintenance of iNs integrity over time, their stability needs to be confirmed under pathological conditions *in vivo*.

An additional layer of complexity is whether the human brain also contains cells susceptible to lineage conversion. Previous work demonstrated that human pericytes derived from the cortex of human patients could be converted into iNs *in vitro* by co-expression of Ascl1 and Sox2 (Karow et al., 2012, 2018). This interesting finding indicating that human pericytes can be potential candidates for reprogramming shed light on new directions towards the use of human brain cells for generation of iNs. Later studies demonstrated that isolated human astrocytes derived from foetal cortex could be instructed to generate iNs after grafting in rat brains, providing proof-of-concept evidence for *in vivo* reprogramming of human astrocytes into iNs (Torper et al., 2013). However, whether the human brain also constitutes a permissible environment for neuronal conversion remains an unanswered question.

In respect of future clinical translation, it is also necessary to find safe and reliable strategies to deliver reprogramming factors in the CNS. Viral delivery of desired reprogramming factors in specific cell populations will prove difficult without local surgical interventions in the brain, which brings along additional risks. Specific AAV serotypes have been proposed as attractive candidates for gene delivery due to their low immunogenicity and lack of toxicity (Daya & Berns, 2008; Peel & Klein, 2000). Importantly, they have also been shown to cross the blood brain barrier (BBB), which would bypass the need of surgical interventions, and transduce specific cell types, such as astrocytes (Z. Liu et al., 2017; Merkel et al., 2017). However, the transduction efficiency still remains low for therapeutic impact and further research would be needed to fully confirm that the strategy is safe for use in humans. With respect to its application for neuronal reprogramming, AAVs would also need to be proved to be a reliable delivery system for reprogramming factors that specifically targets the desired cell type and does not mislabel endogenous neurons instead, as recently reported (Rao et al., 2021; L. L. Wang et al., 2021b). Alternatively approaches such as the systemic delivery of modified RNAs (Y. Wang et al., 2013), extracellular microvesicles (Ridder et al., 2014) or electromagnetic gold nanoparticles (T. J. Lee et al., 2017) can be considered as promising non-invasive therapeutic strategies.

Although there is still a long way to go before moving from bench to bedside in the field of *in vivo* glia-to-neuron conversion, this work together with many other studies have achieved many advances in the field, opening new avenues for using this strategy as a promising cell-based therapy.

Conclusions

1. MMLV retroviruses specifically transduce proliferating glial cells in the postnatal mouse cerebral cortex.

2. Ectopic expression of Ascl1 in proliferating glial cells induces an increase in the number of Sox10-expressing cells in the postnatal mouse cortex.

3. A phospho-site mutant form of Ascl1, namely Ascl1SA6, exhibits enhanced reprogramming activity *in vivo*, suggesting that the phosphorylation state influences Ascl1 fate decisions.

4. Ectopic co-expression of Ascl1SA6 together with other reprogramming factors, such as Bcl2 or Dlx2, significantly boosts the efficiency of glia-to-neuron conversion.

5. A fraction of Ascl1SA6 and Bcl2-derived iNs acquire subtype-specific histochemical and electrophysiological features of fast-spiking PV interneurons.

6. PV interneuron-like cells display lower PV expression levels as well as smaller soma size compared to endogenous PV interneurons, suggesting that their specification towards a mature PV interneuron identity is stalled.

7. PV interneuron-like cells can be induced in cortical layers devoid of this interneuron subtype, supporting the idea that transcriptional mechanisms can override cortical layer specification.

8. Unlike wildtype Ascl1, the phospho-site mutant Ascl1SA6 synergise with Dlx2 to efficiently generate a high number of GABAergic-like iNs.

9. Fate-mapping experiments revealed that the vast majority of iNs generated in the postnatal mouse cortex have an astroglial origin.

10. Polycistronic vectors encoding multiple reprogramming factors retain their neurogenic ability but change their fate specification properties.

11. Glia-derived iNs can be selectively activated through chemogenetic-mediated stimulation.

Disclosure statement

All the experimental work, imaging and data analysis presented in this doctoral thesis were carried out by myself. In addition, I have prepared all illustrations and graphics presented in the figures of this thesis. Nonetheless, I have received some additional experimental support during my PhD by other lab members and students under my supervision to complete the work presented here. In this section, I clearly state the experiments in which other lab members have participated.

- All electrophysiological recordings were performed by the lab member Dr. Nicolas Marichal. Corresponding to Figures 1.3, 3.15 and 3.20.

- The Python script to systematically count the number of cells expressing c-Fos over all DAPI+ nuclei in the cortical regions around iNs was written by the PhD student Gabriel Emilio Herrera Oropeza.

- Immunostainings and data analysis of fate-mapping experiments in the NG2-CreERTM/RCE transgenic mice injected with the retroviral construct Ascl1SA6-Bcl2 were performed by the PhD rotation student Franciele Scarante. Corresponding to Figure 3.13.

- Recombination efficiency of the Aldh1l1-CreERT2;RCE and NG2-CreERTM;RCE transgenic mouse lines included in figures 3.12 and 3.13 were quantified by Dr. Nicolas Marichal and Franciele Scarante respectively.

- RNAscope of Ascl1 and Dlx2 mRNA expression in brain slices was carried out by the PhD rotation student Ana Cristina Ojalvo Sanz. Corresponding to Figures 3.18 and 3.19.

REFERENCES

Addis, R. C., Hsu, F. C., Wright, R. L., Dichter, M. A., Coulter, D. A., & Gearhart, J. D. (2011). Efficient Conversion of Astrocytes to Functional Midbrain Dopaminergic Neurons Using a Single Polycistronic Vector. *PLOS ONE*, *6*(12), e28719. https://doi.org/10.1371/JOURNAL.PONE.0028719

Aimone, J. B., Deng, W., & Gage, F. H. (2010). Adult neurogenesis: integrating theories and separating functions. *Trends in Cognitive Sciences*, *14*(7), 325–337. https://doi.org/10.1016/J.TICS.2010.04.003

Akbarian, S., Kim, J. J., Potkin, S. G., Hagman, J. O., Tafazzoli, A., Bunney, W. E., & Jones, E. G. (1995). Gene expression for glutamic acid decarboxylase is reduced without loss of neurons in prefrontal cortex of schizophrenics. *Archives of General Psychiatry*, *52*(4), 258–266. https://doi.org/10.1001/ARCHPSYC.1995.03950160008002

Akimoto, J., Itoh, H., Miwa, T., & Ikeda, K. (1993). Immunohistochemical study of glutamine synthetase expression in early glial development. *Developmental Brain Research*, *72*(1). https://doi.org/10.1016/0165-3806(93)90154-3

Ali, F. R., Cheng, K., Kirwan, P., Metcalfe, S., Livesey, F. J., Barker, R. A., & Philpott, A. (2014). The phosphorylation status of Ascl1 is a key determinant of neuronal differentiation and maturation in vivo and in vitro. *Development*, *141*(11), 2216–2224. https://doi.org/10.1242/DEV.106377

Altman, J. (1962). Are New Neurons Formed in the Brains of Adult Mammals? *Science*, *135*(3509), 1127–1128. https://doi.org/10.1126/SCIENCE.135.3509.1127

Alzu'bi, A., & Clowry, G. J. (2019). Expression of ventral telencephalon transcription factors ASCL1 and DLX2 in the early fetal human cerebral cortex. *Journal of Anatomy*, *235*(3), 555–568. https://doi.org/10.1111/JOA.12971

Amamoto, R., & Arlotta, P. (2014). Development-inspired reprogramming of the mammalian central nervous system. *Science (New York, N.Y.)*, *343*(6170). https://doi.org/10.1126/SCIENCE.1239882

Amir, R. E., Van Den Veyver, I. B., Wan, M., Tran, C. Q., Francke, U., & Zoghbi, H. Y. (1999). Rett syndrome is caused by mutations in X-linked MECP2, encoding methyl-CpG-binding protein 2. *Nature Genetics*, *23*(2), 185–188. https://doi.org/10.1038/13810

Anastasiades, P. G., Marques-Smith, A., Lyngholm, D., Lickiss, T., Raffiq, S., Katzel, D., Miesenbock, G., & Butt, S. J. B. (2016). GABAergic interneurons form transient layer-specific circuits in early postnatal neocortex. *Nature Communications*, *7*. https://doi.org/10.1038/ncomms10584

Anderson, S. A., Eisenstat, D. D., Shi, L., & Rubenstein, J. L. R. (1997). Interneuron migration from basal forebrain to neocortex: Dependence on Dlx genes. *Science*, *278*(5337), 474–476. https://doi.org/10.1126/SCIENCE.278.5337.474/ASSET/7372E40D-0F9F-4ED4-9A0D-67743214189B/ASSETS/GRAPHIC/SE4075793004.JPEG

Andrioli, A., Alonso-Nanclares, L., Arellano, J. I., & DeFelipe, J. (2007). Quantitative analysis of parvalbumin-immunoreactive cells in the human epileptic hippocampus. *Neuroscience*, *149*(1), 131–143. https://doi.org/10.1016/J.NEUROSCIENCE.2007.07.029

Angevine, J. B., & Sidman, R. L. (1961). Autoradiographic Study of Cell Migration during Histogenesis of Cerebral Cortex in the Mouse. *Nature 1961 192:4804*, *192*(4804), 766–768. https://doi.org/10.1038/192766b0

Babij, R., & De Marco Garcia, N. (2016). Neuronal activity controls the development of interneurons in the somatosensory cortex. In *Frontiers in Biology* (Vol. 11, Issue 6). https://doi.org/10.1007/s11515-016-1427-x

Bakken, T. E., Jorstad, N. L., Hu, Q., Lake, B. B., Tian, W., Kalmbach, B. E., Crow, M., Hodge, R. D., Krienen, F. M., Sorensen, S. A., Eggermont, J., Yao, Z., Aevermann, B. D., Aldridge, A. I., Bartlett, A., Bertagnolli, D., Casper, T., Castanon, R. G., Crichton, K., … Lein, E. S. (2021). Comparative cellular analysis of motor cortex in human, marmoset and mouse. *Nature*, *598*(7879). https://doi.org/10.1038/s41586-021-03465-8

Barker, R. A., Götz, M., & Parmar, M. (2018). New approaches for brain repair - from rescue to reprogramming. In *Nature* (Vol. 557, Issue 7705). https://doi.org/10.1038/s41586-018-0087-1

Bartolini, G., Ciceri, G., & Marín, O. (2013). Integration of GABAergic interneurons into cortical cell assemblies: lessons from embryos and adults. *Neuron*, *79*(5), 849–864. https://doi.org/10.1016/J.NEURON.2013.08.014

Bartolini, G., Sánchez-Alcañiz, J. A., Osório, C., Valiente, M., García-Frigola, C., & Marín, O. (2017). Neuregulin 3 Mediates Cortical Plate Invasion and Laminar Allocation of GABAergic Interneurons. *Cell Reports*, *18*(5), 1157. https://doi.org/10.1016/J.CELREP.2016.12.089

Batista-Brito, R., & Fishell, G. (2009). The developmental integration of cortical interneurons into a functional network. *Current Topics in Developmental Biology*, *87*, 81–118. https://doi.org/10.1016/S0070-2153(09)01203-4

Batiuk, M. Y., Martirosyan, A., Wahis, J., de Vin, F., Marneffe, C., Kusserow, C., Koeppen, J., Viana, J. F., Oliveira, J. F., Voet, T., Ponting, C. P., Belgard, T. G., & Holt, M. G. (2020). Identification of region-specific astrocyte subtypes at single cell resolution. *Nature Communications 2020 11:1*, *11*(1), 1–15. https://doi.org/10.1038/s41467-019-14198-8

Baudoin, J. P., Viou, L., Launay, P. S., Luccardini, C., Espeso Gil, S., Kiyasova, V., Irinopoulou, T., Alvarez, C., Rio, J. P., Boudier, T., Lechaire, J. P., Kessaris, N., Spassky, N., & Métin, C. (2012). Tangentially Migrating Neurons Assemble a Primary Cilium that Promotes Their Reorientation to the Cortical Plate. *Neuron*, *76*(6). https://doi.org/10.1016/j.neuron.2012.10.027

Bayraktar, O. A., Fuentealba, L. C., Alvarez-Buylla, A., & Rowitch, D. H. (2015). Astrocyte development and heterogeneity. *Cold Spring Harbor Perspectives in Biology*, *7*(1). https://doi.org/10.1101/cshperspect.a020362

Belforte, J. E., Zsiros, V., Sklar, E. R., Jiang, Z., Yu, G., Li, Y., Quinlan, E. M., & Nakazawa, K. (2010). Postnatal NMDA receptor ablation in corticolimbic interneurons confers schizophrenia-like phenotypes. *Nature Neuroscience*, *13*(1), 76–83. https://doi.org/10.1038/NN.2447

Belichenko, P. V., Kleschevnikov, A. M., Masliah, E., Wu, C., Takimoto-Kimura, R., Salehi, A., & Mobley, W. C. (2009). Excitatory-inhibitory relationship in the fascia dentata in the Ts65Dn mouse model of Down syndrome. *The Journal of Comparative Neurology*, *512*(4), 453–466. https://doi.org/10.1002/CNE.21895

Ben-Ari, Y. (2002). Excitatory actions of gaba during development: the nature of the nurture. *Nature Reviews Neuroscience 2002 3:9*, *3*(9), 728–739. https://doi.org/10.1038/nrn920

Bergles, D. E., Roberts, J. D. B., Somogyl, P., & Jahr, C. E. (2000). Glutamatergic synapses on oligodendrocyte precursor cells in the hippocampus. *Nature*, *405*(6783), 187–191. https://doi.org/10.1038/35012083

Bernier, P. J., Bédard, A., Vinet, J., Lévesque, M., & Parent, A. (2002). Newly generated neurons in the amygdala and adjoining cortex of adult primates. *Proceedings of the National Academy of Sciences of the United States of America*, *99*(17), 11464–11469. https://doi.org/10.1073/PNAS.172403999

Berninger, B., Costa, M. R., Koch, U., Schroeder, T., Sutor, B., Grothe, B., & Götz, M. (2007). Functional properties of neurons derived from in vitro reprogrammed postnatal astroglia. *Journal of Neuroscience*, *27*(32). https://doi.org/10.1523/JNEUROSCI.1615-07.2007

Bertrand, N., Castro, D. S., & Guillemot, F. (2002). Proneural genes and the specification of neural cell types. *Nature Reviews Neuroscience 2002 3:7*, *3*(7), 517–530. https://doi.org/10.1038/nrn874

Bocchi, R., Masserdotti, G., & Götz, M. (2022). Direct neuronal reprogramming: Fast forward from new concepts toward therapeutic approaches. *Neuron*, *110*(3), 366–393. https://doi.org/10.1016/J.NEURON.2021.11.023

Borrell, V., & Reillo, I. (2012). Emerging roles of neural stem cells in cerebral cortex development and evolution. *Developmental Neurobiology*, *72*(7), 955–971. https://doi.org/10.1002/DNEU.22013

Bortone, D. S., Olsen, S. R., & Scanziani, M. (2014). Translaminar inhibitory cells recruited by layer 6 corticothalamic neurons suppress visual cortex. *Neuron*, *82*(2), 474–485. https://doi.org/10.1016/J.NEURON.2014.02.021

Boulanger, J. J., & Messier, C. (2017). Doublecortin in oligodendrocyte precursor cells in the adult mouse brain. *Frontiers in Neuroscience*, *11*(MAR). https://doi.org/10.3389/fnins.2017.00143

Breton-Provencher, V., Lemasson, M., Peralta, M. R., & Saghatelyan, A. (2009). Interneurons Produced in Adulthood Are Required for the Normal Functioning of the Olfactory Bulb Network and for the Execution of Selected Olfactory Behaviors. *Journal of Neuroscience*, *29*(48), 15245–15257. https://doi.org/10.1523/JNEUROSCI.3606-09.2009

Brot, S., Thamrin, N. P., Bonnet, M. L., Francheteau, M., Patrigeon, M., Belnoue, L., & Gaillard, A. (2022). Long-Term Evaluation of Intranigral Transplantation of Human iPSC-Derived Dopamine Neurons in a Parkinson's Disease Mouse Model. *Cells*, *11*(10). https://doi.org/10.3390/cells11101596

Buck, S. B., Bradford, J., Gee, K. R., Agnew, B. J., Clarke, S. T., & Salic, A. (2008). Detection of S-phase cell cycle progression using 5-ethynyl-2'-deoxyuridine incorporation with click chemistry, an alternative to using 5-bromo-2'-deoxyuridine antibodies. *BioTechniques*, *44*(7), 927–929. https://doi.org/10.2144/000112812

Buffo, A., Vosko, M. R., Ertürk, D., Hamann, G. F., Jucker, M., Rowitch, D., & Götz, M. (2005). Expression pattern of the transcription factor Olig2 in response to brain injuries: implications for neuronal repair. *Proceedings of the National Academy of Sciences of the United States of America*, *102*(50), 18183–18188. https://doi.org/10.1073/PNAS.0506535102

Buhl, E. H., Cobb, S. R., Halasy, K., & Somogyi, P. (1995). Properties of unitary IPSPs evoked by anatomically identified basket cells in the rat hippocampus. *European Journal of Neuroscience*, *7*(9), 1989–2004. https://doi.org/10.1111/J.1460-9568.1995.TB00721.X

Burns, K. A., Murphy, B., Danzer, S. C., & Kuan, C. Y. (2009). Developmental and post-injury cortical gliogenesis: A Genetic fate-mapping study with Nestin-CreER mice. *Glia*, *57*(10), 1115–1129. https://doi.org/10.1002/GLIA.20835

Butt, S. J. B., Fuccillo, M., Nery, S., Noctor, S., Kriegstein, A., Corbin, J. G., & Fishell, G. (2005). The temporal and spatial origins of cortical interneurons predict their physiological subtype. *Neuron*, *48*(4), 591–604. https://doi.org/10.1016/J.NEURON.2005.09.034

Butt, S. J. B., Sousa, V. H., Fuccillo, M. V., Hjerling-Leffler, J., Miyoshi, G., Kimura, S., & Fishell, G. (2008). The requirement of Nkx2-1 in the temporal specification of cortical interneuron subtypes. *Neuron*, *59*(5), 722–732. https://doi.org/10.1016/J.NEURON.2008.07.031

Caillard, O., Moreno, H., Schwaller, B., Llano, I., Celio, M. R., & Marty, A. (2000). Role of the calcium-binding protein parvalbumin in short-term synaptic plasticity. *Proceedings of the National Academy of Sciences of the United States of America*, *97*(24), 13372–13377. https://doi.org/10.1073/PNAS.230362997

Caillava, C., & Baron-Van Evercooren, A. (2012). Differential requirement of cyclin-dependent kinase 2 for oligodendrocyte progenitor cell proliferation and differentiation. In *Cell Division* (Vol. 7). https://doi.org/10.1186/1747-1028-7-14

Cajal, S. R. y, & Ramón y Cajal, S. (1909). Histologie du système nerveux de l'homme & des vertébrés. In *Histologie du système nerveux de l'homme & des vertébrés*. Maloine. https://doi.org/10.5962/bhl.title.48637

Cardin, J. A., Carlén, M., Meletis, K., Knoblich, U., Zhang, F., Deisseroth, K., Tsai, L. H., & Moore, C. I. (2009). Driving fast-spiking cells induces gamma rhythm and controls sensory responses. *Nature 2009 459:7247*, *459*(7247), 663–667. https://doi.org/10.1038/nature08002

Casarosa, S., Fode, C., & Guillemot, F. (1999a). Mash1 regulates neurogenesis in the ventral telencephalon. *Development*, *126*(3). https://doi.org/10.1242/dev.126.3.525

Casarosa, S., Fode, C., & Guillemot, F. (1999b). Mash1 regulates neurogenesis in the ventral telencephalon. *Development (Cambridge, England)*, *126*(3), 525–534. https://doi.org/10.1242/DEV.126.3.525

Castro, D. S., Martynoga, B., Parras, C., Ramesh, V., Pacary, E., Johnston, C., Drechsel, D., Lebel-Potter, M., Garcia, L. G., Hunt, C., Dolle, D., Bithell, A., Ettwiller, L., Buckley, N., & Guillemot, F. (2011). A novel function of the proneural factor Ascl1 in progenitor proliferation identified by genome-wide characterization of its targets. *Genes & Development*, *25*(9), 930–945. https://doi.org/10.1101/GAD.627811

Castro, D. S., Skowronska-Krawczyk, D., Armant, O., Donaldson, I. J., Parras, C., Hunt, C., Critchley, J. A., Nguyen, L., Gossler, A., Göttgens, B., Matter, J. M., & Guillemot, F. (2006). Proneural bHLH and Brn proteins coregulate a neurogenic program through cooperative binding to a conserved DNA motif. *Developmental Cell*, *11*(6), 831–844. https://doi.org/10.1016/J.DEVCEL.2006.10.006

Cebrian-Silla, A., Nascimento, M. A., Redmond, S. A., Mansky, B., Wu, D., Obernier, K., Rodriguez, R. R., Gonzalez-Granero, S., Garcia-Verdugo, J. M., Lim, D. A., & Alvarez-Buylla, A. (2021). Single-cell analysis of the ventricular-subventricular zone reveals signatures of dorsal and ventral adult neurogenesis. *ELife*, *10*. https://doi.org/10.7554/ELIFE.67436

Chao, H. T., Chen, H., Samaco, R. C., Xue, M., Chahrour, M., Yoo, J., Neul, J. L., Gong, S., Lu, H. C., Heintz, N., Ekker, M., Rubenstein, J. L. R., Noebels, J. L., Rosenmund, C., & Zoghbi, H. Y. (2010). Dysfunction in GABA signalling mediates autism-like stereotypies and Rett syndrome phenotypes. *Nature*, *468*(7321), 263–269. https://doi.org/10.1038/NATURE09582

Cheah, C. S., Yu, F. H., Westenbroek, R. E., Kalume, F. K., Oakley, J. C., Potter, G. B., Rubenstein, J. L., & Catterall, W. A. (2012). Specific deletion of NaV1.1 sodium channels in inhibitory interneurons causes seizures and premature death in a mouse model of Dravet syndrome. *Proceedings of the National Academy of Sciences of the United States of America*, *109*(36), 14646–14651. https://doi.org/10.1073/PNAS.1211591109/SUPPL_FILE/PNAS.201211591SI.PDF

Chen, Y. C., Ma, N. X., Pei, Z. F., Wu, Z., Do-Monte, F. H., Keefe, S., Yellin, E., Chen, M. S., Yin, J. C., Lee, G., Minier-Toribio, A., Hu, Y., Bai, Y. T., Lee, K., Quirk, G. J., & Chen, G. (2020a). A NeuroD1 AAV-Based Gene Therapy for Functional Brain Repair after Ischemic Injury through In Vivo Astrocyte-to-Neuron Conversion. *Molecular Therapy*, *28*(1). https://doi.org/10.1016/j.ymthe.2019.09.003

Chen, Y. C., Ma, N. X., Pei, Z. F., Wu, Z., Do-Monte, F. H., Keefe, S., Yellin, E., Chen, M. S., Yin, J. C., Lee, G., Minier-Toribio, A., Hu, Y., Bai, Y. T., Lee, K., Quirk, G. J., & Chen, G. (2020b). A NeuroD1 AAV-Based Gene Therapy for Functional Brain Repair after Ischemic Injury through In Vivo Astrocyte-to-Neuron Conversion. *Molecular Therapy*, *28*(1), 217. https://doi.org/10.1016/J.YMTHE.2019.09.003

Clavreul, S., Abdeladim, L., Hernández-Garzón, E., Niculescu, D., Durand, J., Ieng, S. H., Barry, R., Bonvento, G., Beaurepaire, E., Livet, J., & Loulier, K. (2019). Cortical astrocytes develop in a plastic manner at both clonal and cellular levels. *Nature Communications 2019 10:1*, *10*(1), 1–14. https://doi.org/10.1038/s41467-019-12791-5

Cobos, I., Borello, U., & Rubenstein, J. L. R. (2007). Dlx Transcription Factors Promote Migration through Repression of Axon and Dendrite Growth. *Neuron*, *54*(6), 873–888. https://doi.org/10.1016/J.NEURON.2007.05.024

Cobos, I., Calcagnotto, M. E., Vilaythong, A. J., Thwin, M. T., Noebels, J. L., Baraban, S. C., & Rubenstein, J. L. R. (2005). Mice lacking Dlx1 show subtype-specific loss of interneurons, reduced inhibition and epilepsy. *Nature Neuroscience*, *8*(8), 1059–1068. https://doi.org/10.1038/NN1499

Colasante, G., Collombat, P., Raimondi, V., Bonanomi, D., Ferrai, C., Maira, M., Yoshikawa, K., Mansouri, A., Valtorta, F., Rubenstein, J. L. R., & Broccoli, V. (2008). Arx is a direct target of Dlx2 and thereby contributes to the tangential migration of GABAergic interneurons. *The Journal of Neuroscience : The Official Journal of the Society for Neuroscience*, *28*(42), 10674–10686. https://doi.org/10.1523/JNEUROSCI.1283-08.2008

Dani, N., Herbst, R. H., McCabe, C., Green, G. S., Kaiser, K., Head, J. P., Cui, J., Shipley, F. B., Jang, A., Dionne, D., Nguyen, L., Rodman, C., Riesenfeld, S. J., Prochazka, J., Prochazkova, M., Sedlacek, R., Zhang, F., Bryja, V., Rozenblatt-Rosen, O., … Lehtinen, M. K. (2021). A cellular and spatial map of the choroid plexus across brain ventricles and ages. *Cell*, *184*(11), 3056-3074.e21. https://doi.org/10.1016/J.CELL.2021.04.003

Dávid, C., Schleicher, A., Zuschratter, W., & Staiger, J. F. (2007). The innervation of parvalbumin-containing interneurons by VIP-immunopositive interneurons in the primary somatosensory cortex of the adult rat. *European Journal of Neuroscience*, *25*(8), 2329–2340. https://doi.org/10.1111/J.1460-9568.2007.05496.X

Daya, S., & Berns, K. I. (2008). Gene therapy using adeno-associated virus vectors. *Clinical Microbiology Reviews*, *21*(4), 583–593.

https://doi.org/10.1128/CMR.00008-08/ASSET/9446DE05-78BD-413F-8BA4-57A86B8C244A/ASSETS/GRAPHIC/ZCM0040822520003.JPEG

De Lima, A. D., & Morrison, J. H. (1989). Ultrastructural analysis of somatostatin-immunoreactive neurons and synapses in the temporal and occipital cortex of the macaque monkey. *The Journal of Comparative Neurology*, *283*(2), 212–227. https://doi.org/10.1002/CNE.902830205

De Marco García, N. V., Karayannis, T., & Fishell, G. (2011). Neuronal activity is required for the development of specific cortical interneuron subtypes. *Nature*, *472*(7343). https://doi.org/10.1038/nature09865

De Marco García, N. V., Priya, R., Tuncdemir, S. N., Fishell, G., & Karayannis, T. (2015). Sensory inputs control the integration of neurogliaform interneurons into cortical circuits. *Nature Neuroscience*, *18*(3). https://doi.org/10.1038/nn.3946

Deacon, T. W., Pakzaban, P., & Isacson, O. (1994). The lateral ganglionic eminence is the origin of cells committed to striatal phenotypes: neural transplantation and developmental evidence. *Brain Research*, *668*(1–2), 211–219. https://doi.org/10.1016/0006-8993(94)90526-6

Dehorter, N., Ciceri, G., Bartolini, G., Lim, L., Del Pino, I., & Marín, O. (2015). Tuning of fast-spiking interneuron properties by an activity-dependent transcriptional switch. *Science*, *349*(6253), 1216–1220. https://doi.org/10.1126/SCIENCE.AAB3415/SUPPL_FILE/AAB3415_DEHORTER-SM.PDF

Denaxa, M., Neves, G., Rabinowitz, A., Kemlo, S., Liodis, P., Burrone, J., & Pachnis, V. (2018). Modulation of Apoptosis Controls Inhibitory Interneuron Number in the Cortex. *Cell Reports*, *22*(7), 1710. https://doi.org/10.1016/J.CELREP.2018.01.064

Dennison-Cavanagh, M. E., Papadopoulos, G., & Parnavelas, J. G. (1993). The emergence of the cortical GABAergic neuron: with particular reference to some peptidergic subpopulations. *Journal of Neurocytology*, *22*(9), 805–814. https://doi.org/10.1007/BF01181325

Dimou, L., & Götz, M. (2014). Glial cells as progenitors and stem cells: New roles in the healthy and diseased brain. In *Physiological Reviews* (Vol. 94, Issue 3). https://doi.org/10.1152/physrev.00036.2013

Dimou, L., Simon, C., Kirchhoff, F., Takebayashi, H., & Götz, M. (2008). Progeny of Olig2-Expressing Progenitors in the Gray and White Matter of the Adult Mouse Cerebral Cortex. *Journal of Neuroscience*, *28*(41), 10434–10442. https://doi.org/10.1523/JNEUROSCI.2831-08.2008

Dixon, S. J., Lemberg, K. M., Lamprecht, M. R., Skouta, R., Zaitsev, E. M., Gleason, C. E., Patel, D. N., Bauer, A. J., Cantley, A. M., Yang, W. S., Morrison, B., & Stockwell, B. R. (2012). Ferroptosis: An iron-dependent form of nonapoptotic cell death. *Cell*, *149*(5), 1060–1072. https://doi.org/10.1016/j.cell.2012.03.042

Donato, F., Chowdhury, A., Lahr, M., & Caroni, P. (2015). Early- and Late-Born Parvalbumin Basket Cell Subpopulations Exhibiting Distinct Regulation and Roles in Learning. *Neuron*, *85*(4). https://doi.org/10.1016/j.neuron.2015.01.011

Donato, F., Rompani, S. B., & Caroni, P. (2013). Parvalbumin-expressing basket-cell network plasticity induced by experience regulates adult learning. *Nature*, *504*(7479). https://doi.org/10.1038/nature12866

Dou, Y., Lin, Y., Wang, T. yun, Wang, X. Y., Jia, Y. long, & Zhao, C. peng. (2021). The CAG promoter maintains high-level transgene expression in HEK293 cells. *FEBS Open Bio*, *11*(1), 95–104. https://doi.org/10.1002/2211-5463.13029

Drexel, X. M., Romanov, R. A., Wood, J., Weger, S., Heilbronn, R., Wulff, P., Ramon, X., Tasan, O., Harkany, X. T., & Sperk, X. G. (2017). *Neurobiology of Disease Selective Silencing of Hippocampal Parvalbumin Interneurons Induces Development of Recurrent Spontaneous Limbic Seizures in Mice*. https://doi.org/10.1523/JNEUROSCI.3456-16.2017

Durand, C. M., Betancur, C., Boeckers, T. M., Bockmann, J., Chaste, P., Fauchereau, F., Nygren, G., Rastam, M., Gillberg, I. C., Anckarsäter, H., Sponheim, E., Goubran-Botros, H., Delorme, R., Chabane, N., Mouren-Simeoni, M. C., De Mas, P., Bieth, E., Rogé, B., Héron, D., … Bourgeron, T. (2007). Mutations in the gene encoding the synaptic scaffolding protein SHANK3 are associated with autism spectrum disorders. *Nature Genetics*, *39*(1), 25–27. https://doi.org/10.1038/NG1933

Erisir, A., Lau, D., Rudy, B., & Leonard, C. S. (1999). Function of specific K+ channels in sustained high-frequency firing of fast-spiking neocortical interneurons. *Journal of Neurophysiology*, *82*(5), 2476–2489. https://doi.org/10.1152/JN.1999.82.5.2476/ASSET/IMAGES/LARGE/9K1290671009.JPEG

Favuzzi, E., Huang, S., Saldi, G. A., Binan, L., Ibrahim, L. A., Fernández-Otero, M., Cao, Y., Zeine, A., Sefah, A., Zheng, K., Xu, Q., Khlestova, E., Farhi, S. L., Bonneau, R., Datta, S. R., Stevens, B., & Fishell, G. (2021). GABA-receptive microglia selectively sculpt developing inhibitory circuits. *Cell*, *184*(15). https://doi.org/10.1016/j.cell.2021.06.018

Favuzzi, E., Marques-Smith, A., Deogracias, R., Winterflood, C. M., Sánchez-Aguilera, A., Mantoan, L., Maeso, P., Fernandes, C., Ewers, H., & Rico, B. (2017). Activity-Dependent Gating of Parvalbumin Interneuron Function by the Perineuronal Net Protein Brevican. *Neuron*, *95*(3), 639-655.e10. https://doi.org/10.1016/j.neuron.2017.06.028

Finlay, B. L., & Darlington, R. B. (1995). Linked regularities in the development and evolution of mammalian brains. *Science*, *268*(5217). https://doi.org/10.1126/science.7777856

Flames, N., Long, J. E., Garratt, A. N., Fischer, T. M., Gassmann, M., Birchmeier, C., Lai, C., Rubenstein, J. L. R., & Marín, O. (2004). Short- and long-range attraction

of cortical GABAergic interneurons by neuregulin-1. *Neuron*, *44*(2), 251–261. https://doi.org/10.1016/j.neuron.2004.09.028

Fode, C., Ma, Q., Casarosa, S., Ang, S. L., Anderson, D. J., & Guillemot, F. (2000). A role for neural determination genes in specifying the dorsoventral identity of telencephalic neurons. *Genes & Development*, *14*(1), 67. https://doi.org/10.1101/gad.14.1.67

Fogarty, M., Grist, M., Gelman, D., Marín, O., Pachnis, V., & Kessaris, N. (2007). Spatial Genetic Patterning of the Embryonic Neuroepithelium Generates GABAergic Interneuron Diversity in the Adult Cortex. *The Journal of Neuroscience*, *27*(41), 10935. https://doi.org/10.1523/JNEUROSCI.1629-07.2007

Friocourt, G., Kanatani, S., Tabata, H., Yozu, M., Takahashi, T., Antypa, M., Raguénès, O., Chelly, J., Férec, C., Nakajima, K., & Parnavelas, J. G. (2008). Cell-Autonomous Roles of ARX in Cell Proliferation and Neuronal Migration during Corticogenesis. *The Journal of Neuroscience*, *28*(22), 5794. https://doi.org/10.1523/JNEUROSCI.1067-08.2008

Frühbeis, C., Fröhlich, D., Kuo, W. P., & Krämer-Albers, E. M. (2013). Extracellular vesicles as mediators of neuron-glia communication. In *Frontiers in Cellular Neuroscience* (Issue OCT). https://doi.org/10.3389/fncel.2013.00182

Gage, F. H., Coates, P. W., Palmer, T. D., Kuhn, H. G., Fisher, L. J., Suhonen, J. O., Peterson, D. A., Suhr, S. T., & Ray, J. (1995). Survival and differentiation of adult neuronal progenitor cells transplanted to the adult brain. *Proceedings of the National Academy of Sciences of the United States of America*, *92*(25), 11879–11883. https://doi.org/10.1073/PNAS.92.25.11879

Galabova-Kovacs, G., Catalanotti, F., Matzen, D., Reyes, G. X., Zezula, J., Herbst, R., Silva, A., Walter, I., & Baccarini, M. (2008). Essential role of B-Raf in oligodendrocyte maturation and myelination during postnatal central nervous system development. *Journal of Cell Biology*, *180*(5), 947–955. https://doi.org/10.1083/JCB.200709069/VIDEO-3

Galante, C., Marichal, N., Scarante, F. F., Ghayad, L. M., Shi, Y., Schuurmans, C., Berninger, B., & Péron, S. (2022). Enhanced proliferation of oligodendrocyte progenitor cells following retrovirus mediated Achaete-scute complex-like 1 overexpression in the postnatal cerebral cortex in vivo. *Frontiers in Neuroscience*, *16*, 2048. https://doi.org/10.3389/FNINS.2022.919462/BIBTEX

Gallo, N. B., Berisha, A., & Van Aelst, L. (2022). Microglia regulate chandelier cell axo-axonic synaptogenesis. *Proceedings of the National Academy of Sciences of the United States of America*, *119*(11). https://doi.org/10.1073/pnas.2114476119

Gascón, S., Murenu, E., Masserdotti, G., Ortega, F., Russo, G. L., Petrik, D., Deshpande, A., Heinrich, C., Karow, M., Robertson, S. P., Schroeder, T., Beckers, J., Irmler, M., Berndt, C., Angeli, J. P. F., Conrad, M., Berninger, B., & Götz, M. (2016). Identification and Successful Negotiation of a Metabolic Checkpoint in Direct Neuronal Reprogramming. *Cell Stem Cell*, *18*(3), 396–409. https://doi.org/10.1016/j.stem.2015.12.003

Ge, L. J., Yang, F. H., Li, W., Wang, T., Lin, Y., Feng, J., Chen, N. H., Jiang, M., Wang, J. H., Hu, X. T., & Chen, G. (2020). In vivo Neuroregeneration to Treat Ischemic Stroke Through NeuroD1 AAV-Based Gene Therapy in Adult Non-human Primates. *Frontiers in Cell and Developmental Biology*, *8*. https://doi.org/10.3389/FCELL.2020.590008

Ge, W. P., Miyawaki, A., Gage, F. H., Jan, Y. N., & Jan, L. Y. (2012). Local generation of glia is a major astrocyte source in postnatal cortex. *Nature 2012 484:7394*, *484*(7394), 376–380. https://doi.org/10.1038/nature10959

Gelman, D., Griveau, A., Dehorter, N., Teissier, A., Varela, C., Pla, R., Pierani, A., & Marín, O. (2011). A Wide Diversity of Cortical GABAergic Interneurons Derives from the Embryonic Preoptic Area. *The Journal of Neuroscience*, *31*(46), 16570. https://doi.org/10.1523/JNEUROSCI.4068-11.2011

Gelman, D. M., Martini, F. J., Nóbrega-Pereira, S., Pierani, A., Kessaris, N., & Marín, O. (2009). The Embryonic Preoptic Area Is a Novel Source of Cortical GABAergic Interneurons. *Journal of Neuroscience*, *29*(29), 9380–9389. https://doi.org/10.1523/JNEUROSCI.0604-09.2009

Gillotin, S., Davies, J. D., & Philpott, A. (2018). Subcellular localisation modulates ubiquitylation and degradation of Ascl1. *Scientific Reports*, *8*(1). https://doi.org/10.1038/s41598-018-23056-4

Ginhoux, F., Greter, M., Leboeuf, M., Nandi, S., See, P., Gokhan, S., Mehler, M. F., Conway, S. J., Ng, L. G., Stanley, E. R., Samokhvalov, I. M., & Merad, M. (2010). Fate mapping analysis reveals that adult microglia derive from primitive macrophages. *Science (New York, N.Y.)*, *330*(6005), 841–845. https://doi.org/10.1126/SCIENCE.1194637

Godoy, J. R., Oesteritz, S., Hanschmann, E. M., Ockenga, W., Ackermann, W., & Lillig, C. H. (2011). Segment-specific overexpression of redoxins after renal ischemia and reperfusion: protective roles of glutaredoxin 2, peroxiredoxin 3, and peroxiredoxin 6. *Free Radical Biology and Medicine*, *51*(2), 552–561. https://doi.org/10.1016/J.FREERADBIOMED.2011.04.036

Goldberg, E. M., Clark, B. D., Zagha, E., Nahmani, M., Erisir, A., & Rudy, B. (2008). K+ Channels at the Axon Initial Segment Dampen Near-Threshold Excitability of Neocortical Fast-Spiking GABAergic Interneurons. *Neuron*, *58*(3), 387–400. https://doi.org/10.1016/J.NEURON.2008.03.003

Gorski, J. A., Talley, T., Qiu, M., Puelles, L., Rubenstein, J. L. R., & Jones, K. R. (2002). Cortical Excitatory Neurons and Glia, But Not GABAergic Neurons, Are Produced in the Emx1-Expressing Lineage. *Journal of Neuroscience*, *22*(15), 6309–6314. https://doi.org/10.1523/JNEUROSCI.22-15-06309.2002

Götz, M., & Barde, Y. A. (2005). Radial glial cells: Defined and major intermediates between embryonicstem cells and CNS neurons. In *Neuron* (Vol. 46, Issue 3). https://doi.org/10.1016/j.neuron.2005.04.012

Gould, E., Reeves, A. J., Graziano, M. S. A., & Gross, C. G. (1999). Neurogenesis in the neocortex of adult primates. *Science (New York, N.Y.)*, *286*(5439), 548–552. https://doi.org/10.1126/SCIENCE.286.5439.548

Gouwens, N. W., Sorensen, S. A., Baftizadeh, F., Budzillo, A., Lee, B. R., Jarsky, T., Alfiler, L., Baker, K., Barkan, E., Berry, K., Bertagnolli, D., Bickley, K., Bomben, J., Braun, T., Brouner, K., Casper, T., Crichton, K., Daigle, T. L., Dalley, R., … Zeng, H. (2020). Integrated Morphoelectric and Transcriptomic Classification of Cortical GABAergic Cells. *Cell*, *183*(4), 935-953.e19. https://doi.org/10.1016/j.cell.2020.09.057

Grande, A., Sumiyoshi, K., López-Juárez, A., Howard, J., Sakthivel, B., Aronow, B., Campbell, K., & Nakafuku, M. (2013). Environmental impact on direct neuronal reprogramming in vivo in the adult brain. *Nature Communications 2013 4:1*, *4*(1), 1–12. https://doi.org/10.1038/ncomms3373

Gregorian, C., Nakashima, J., Belle, J. Le, Ohab, J., Kim, R., Liu, A., Smith, K. B., Groszer, M., Garcia, A. D., Sofroniew, M. V., Carmichael, S. T., Kornblum, H. I., Liu, X., & Wu, H. (2009). Pten Deletion in Adult Neural Stem/Progenitor Cells Enhances Constitutive Neurogenesis. *Journal of Neuroscience*, *29*(6), 1874–1886. https://doi.org/10.1523/JNEUROSCI.3095-08.2009

Guillemot, F., & Joyner, A. L. (1993). Dynamic expression of the murine Achaete-Scute homologue Mash-1 in the developing nervous system. *Mechanisms of Development*, *42*(3), 171–185. https://doi.org/10.1016/0925-4773(93)90006-J

Gulyás, A. I., Buzsáki, G., Freund, T. F., & Hirase, H. (2006). Populations of hippocampal inhibitory neurons express different levels of cytochrome c. *The European Journal of Neuroscience*, *23*(10), 2581–2594. https://doi.org/10.1111/J.1460-9568.2006.04814.X

Guo, Z., Zhang, L., Wu, Z., Chen, Y., Wang, F., & Chen, G. (2014). In vivo direct reprogramming of reactive glial cells into functional neurons after brain injury and in an Alzheimer's disease model. *Cell Stem Cell*, *14*(2), 188–202. https://doi.org/10.1016/J.STEM.2013.12.001

GURDON, J. B. (1962). The developmental capacity of nuclei taken from intestinal epithelium cells of feeding tadpoles. *Journal of Embryology and Experimental Morphology*, *10*. https://doi.org/10.1242/dev.10.4.622

Hallett, P. J., Deleidi, M., Astradsson, A., Smith, G. A., Cooper, O., Osborn, T. M., Sundberg, M., Moore, M. A., Perez-Torres, E., Brownell, A. L., Schumacher, J. M., Spealman, R. D., & Isacson, O. (2015). Successful function of autologous iPSC-derived dopamine neurons following transplantation in a non-human primate model of Parkinson's disease. *Cell Stem Cell*, *16*(3). https://doi.org/10.1016/j.stem.2015.01.018

Hand, R., Bortone, D., Mattar, P., Nguyen, L., Heng, J. I. T., Guerrier, S., Boutt, E., Peters, E., Barnes, A. P., Parras, C., Schuurmans, C., Guillemot, F., & Polleux, F. (2005). Phosphorylation of Neurogenin2 specifies the migration properties and the

dendritic morphology of pyramidal neurons in the neocortex. *Neuron*, *48*(1), 45–62. https://doi.org/10.1016/J.NEURON.2005.08.032

Hansen, D. V., Lui, J. H., Parker, P. R. L., & Kriegstein, A. R. (2010a). Neurogenic radial glia in the outer subventricular zone of human neocortex. *Nature*, *464*(7288), 554–561. https://doi.org/10.1038/NATURE08845

Hansen, D. V., Lui, J. H., Parker, P. R. L., & Kriegstein, A. R. (2010b). Neurogenic radial glia in the outer subventricular zone of human neocortex. *Nature 2010 464:7288*, *464*(7288), 554–561. https://doi.org/10.1038/nature08845

Harris, K. D., & Mrsic-Flogel, T. D. (2013). Cortical connectivity and sensory coding. In *Nature* (Vol. 503, Issue 7474). https://doi.org/10.1038/nature12654

Harrison, P. J., & Law, A. J. (2006). Neuregulin 1 and schizophrenia: genetics, gene expression, and neurobiology. *Biological Psychiatry*, *60*(2), 132–140. https://doi.org/10.1016/J.BIOPSYCH.2005.11.002

Hartfuss, E., Galli, R., Heins, N., & Götz, M. (2001). Characterization of CNS Precursor Subtypes and Radial Glia. *Developmental Biology*, *229*(1), 15–30. https://doi.org/10.1006/DBIO.2000.9962

Hashimoto, D., Chow, A., Noizat, C., Teo, P., Beasley, M. B., Leboeuf, M., Becker, C. D., See, P., Price, J., Lucas, D., Greter, M., Mortha, A., Boyer, S. W., Forsberg, E. C., Tanaka, M., van Rooijen, N., García-Sastre, A., Stanley, E. R., Ginhoux, F., … Merad, M. (2013). Tissue-resident macrophages self-maintain locally throughout adult life with minimal contribution from circulating monocytes. *Immunity*, *38*(4), 792–804. https://doi.org/10.1016/J.IMMUNI.2013.04.004

Hashimoto, T., Volk, D. W., Eggan, S. M., Mirnics, K., Pierri, J. N., Sun, Z., Sampson, A. R., & Lewis, D. A. (2003). Gene expression deficits in a subclass of GABA neurons in the prefrontal cortex of subjects with schizophrenia. *The Journal of Neuroscience : The Official Journal of the Society for Neuroscience*, *23*(15), 6315–6326. https://doi.org/10.1523/JNEUROSCI.23-15-06315.2003

Haubensak, W., Attardo, A., Denk, W., & Huttner, W. B. (2004). Neurons arise in the basal neuroepithelium of the early mammalian telencephalon: a major site of neurogenesis. *Proceedings of the National Academy of Sciences of the United States of America*, *101*(9), 3196–3201. https://doi.org/10.1073/PNAS.0308600100

He, F., Ge, W., Martinowich, K., Becker-Catania, S., Coskun, V., Zhu, W., Wu, H., Castro, D., Guillemot, F., Fan, G., De Vellis, J., & Sun, Y. E. (2005). A positive autoregulatory loop of Jak-STAT signaling controls the onset of astrogliogenesis. *Nature Neuroscience*, *8*(5). https://doi.org/10.1038/nn1440

He, M., Tucciarone, J., Lee, S. H., Nigro, M. J., Kim, Y., Levine, J. M., Kelly, S. M., Krugikov, I., Wu, P., Chen, Y., Gong, L., Hou, Y., Osten, P., Rudy, B., & Huang, Z. J. (2016). Strategies and Tools for Combinatorial Targeting of GABAergic Neurons in Mouse Cerebral Cortex. *Neuron*, *92*(2), 555. https://doi.org/10.1016/J.NEURON.2016.10.009

He, W., Ingraham, C., Rising, L., Goderie, S., & Temple, S. (2001). Multipotent stem cells from the mouse basal forebrain contribute GABAergic neurons and oligodendrocytes to the cerebral cortex during embryogenesis. *The Journal of Neuroscience : The Official Journal of the Society for Neuroscience*, *21*(22), 8854–8862. https://doi.org/10.1523/JNEUROSCI.21-22-08854.2001

Hébert, J. M., & Fishell, G. (2008). The genetics of early telencephalon patterning: some assembly required. *Nature Reviews. Neuroscience*, *9*(9), 678. https://doi.org/10.1038/NRN2463

Heinrich, C., Bergami, M., Gascón, S., Lepier, A., Viganò, F., Dimou, L., Sutor, B., Berninger, B., & Götz, M. (2014). Sox2-mediated conversion of NG2 glia into induced neurons in the injured adult cerebral cortex. *Stem Cell Reports*, *3*(6), 1000–1014. https://doi.org/10.1016/J.STEMCR.2014.10.007

Heinrich, C., Blum, R., Gascón, S., Masserdotti, G., Tripathi, P., Sánchez, R., Tiedt, S., Schroeder, T., Götz, M., & Berninger, B. (2010). Directing astroglia from the cerebral cortex into subtype specific functional neurons. *PLoS Biology*, *8*(5). https://doi.org/10.1371/journal.pbio.1000373

Heinrich, C., Gascón, S., Masserdotti, G., Lepier, A., Sanchez, R., Simon-Ebert, T., Schroeder, T., Ġtz, M., & Berninger, B. (2011). Generation of subtype-specific neurons from postnatal astroglia of the mouse cerebral cortex. *Nature Protocols*, *6*(2). https://doi.org/10.1038/nprot.2010.188

Heinrich, C., Spagnoli, F. M., & Berninger, B. (2015). In vivo reprogramming for tissue repair. *Nature Cell Biology 2015 17:3*, *17*(3), 204–211. https://doi.org/10.1038/ncb3108

Heins, N., Malatesta, P., Cecconi, F., Nakafuku, M., Tucker, K. L., Hack, M. A., Chapouton, P., Barde, Y. A., & Goötz, M. (2002). Glial cells generate neurons: the role of the transcription factor Pax6. *Nature Neuroscience 2002 5:4*, *5*(4), 308–315. https://doi.org/10.1038/nn828

Herrero-Navarro, Á., Puche-Aroca, L., Moreno-Juan, V., Sempere-Ferràndez, A., Espinosa, A., Susín, R., Torres-Masjoan, L., Leyva-Díaz, E., Karow, M., Figueres-Oñate, M., López-Mascaraque, L., López-Atalaya, J. P., Berninger, B., & López-Bendito, G. (2021). Astrocytes and neurons share region-specific transcriptional signatures that confer regional identity to neuronal reprogramming. *Science Advances*, *7*(15). https://doi.org/10.1126/SCIADV.ABE8978

Higginbotham, H., Eom, T. Y., Mariani, L. E., Bachleda, A., Hirt, J., Gukassyan, V., Cusack, C. L., Lai, C., Caspary, T., & Anton, E. S. (2012). Arl13b in Primary Cilia Regulates the Migration and Placement of Interneurons in the Developing Cerebral Cortex. *Developmental Cell*, *23*(5). https://doi.org/10.1016/j.devcel.2012.09.019

Hilscher, M. M., Langseth, C. M., Kukanja, P., Yokota, C., Nilsson, M., & Castelo-Branco, G. (2022). Spatial and temporal heterogeneity in the lineage progression of fine oligodendrocyte subtypes. *BMC Biology*, *20*(1), 1–18. https://doi.org/10.1186/S12915-022-01325-Z/FIGURES/7

Hindley, C., Ali, F., McDowell, G., Cheng, K., Jones, A., Guillemot, F., & Philpott, A. (2012). Post-translational modification of Ngn2 differentially affects transcription of distinct targets to regulate the balance between progenitor maintenance and differentiation. *Development*, *139*(10), 1718–1723. https://doi.org/10.1242/DEV.077552

Horton, S., Meredith, A., Richardson, J. A., & Johnson, J. E. (1999). Correct coordination of neuronal differentiation events in ventral forebrain requires the bHLH factor MASH1. *Molecular and Cellular Neurosciences*, *14*(4–5). https://doi.org/10.1006/mcne.1999.0791

Hu, H., Gan, J., & Jonas, P. (2014). Fast-spiking, parvalbumin+ GABAergic interneurons: From cellular design to microcircuit function. In *Science* (Vol. 345, Issue 6196). https://doi.org/10.1126/science.1255263

Huang, Z. J., Kirkwood, A., Pizzorusso, T., Porciatti, V., Morales, B., Bear, M. F., Maffei, L., & Tonegawa, S. (1999). BDNF regulates the maturation of inhibition and the critical period of plasticity in mouse visual cortex. *Cell*, *98*(6). https://doi.org/10.1016/S0092-8674(00)81509-3

Hughes, E. G., Kang, S. H., Fukaya, M., & Bergles, D. E. (2013). Oligodendrocyte progenitors balance growth with self-repulsion to achieve homeostasis in the adult brain. *Nature Neuroscience 2013 16:6*, *16*(6), 668–676. https://doi.org/10.1038/nn.3390

Hunter, T. (2007). The Age of Crosstalk: Phosphorylation, Ubiquitination, and Beyond. In *Molecular Cell* (Vol. 28, Issue 5). https://doi.org/10.1016/j.molcel.2007.11.019

Ibrahim, L. A., Huang, S., Fernandez-Otero, M., Sherer, M., Qiu, Y., Vemuri, S., Xu, Q., Machold, R., Pouchelon, G., Rudy, B., & Fishell, G. (2021). Bottom-up inputs are required for establishment of top-down connectivity onto cortical layer 1 neurogliaform cells. *Neuron*, *109*(21), 3473-3485.e5. https://doi.org/10.1016/J.NEURON.2021.08.004

Imayoshi, I., Isomura, A., Harima, Y., Kawaguchi, K., Kori, H., Miyachi, H., Fujiwara, T., Ishidate, F., & Kageyama, R. (2013). Oscillatory control of factors determining multipotency and fate in mouse neural progenitors. *Science (New York, N.Y.)*, *342*(6163), 1203–1208. https://doi.org/10.1126/SCIENCE.1242366

Iwata, R., Casimir, P., Erkol, E., Boubakar, L., Planque, M., López, I. M. G., Ditkowska, M., Gaspariunaite, V., Beckers, S., Remans, D., Vints, K., Vandekeere, A., Poovathingal, S., Bird, M., Vlaeminck, I., Creemers, E., Wierda, K., Corthout, N., Vermeersch, P., … Vanderhaeghen, P. (2023). Mitochondria metabolism sets the species-specific tempo of neuronal development. *Science*. https://doi.org/10.1126/SCIENCE.ABN4705

Jiang, X., Shen, S., Cadwell, C. R., Berens, P., Sinz, F., Ecker, A. S., Patel, S., & Tolias, A. S. (2015). Principles of connectivity among morphologically defined cell types in adult neocortex. *Science (New York, N.Y.)*, *350*(6264). https://doi.org/10.1126/SCIENCE.AAC9462

Jin, K., Sun, Y., Xie, L., Peel, A., Mao, X. O., Batteur, S., & Greenberg, D. A. (2003). Directed migration of neuronal precursors into the ischemic cerebral cortex and striatum. *Molecular and Cellular Neuroscience*, *24*(1), 171–189. https://doi.org/10.1016/S1044-7431(03)00159-3

Johnson, M. B., Wang, P. P., Atabay, K. D., Murphy, E. A., Doan, R. N., Hecht, J. L., & Walsh, C. A. (2015). Single-cell analysis reveals transcriptional heterogeneity of neural progenitors in human cortex. *Nature Neuroscience*, *18*(5). https://doi.org/10.1038/nn.3980

Kann, O., & Kovács, R. (2007). Mitochondria and neuronal activity. *American Journal of Physiology. Cell Physiology*, *292*(2). https://doi.org/10.1152/AJPCELL.00222.2006

Kann, O., Papageorgiou, I. E., & Draguhn, A. (2014). Highly energized inhibitory interneurons are a central element for information processing in cortical networks. *Journal of Cerebral Blood Flow and Metabolism*, *34*(8), 1270–1282. https://doi.org/10.1038/JCBFM.2014.104

Karow, M., Gray Camp, J., Falk, S., Gerber, T., Pataskar, A., Gac-Santel, M., Kageyama, J., Brazovskaja, A., Garding, A., Fan, W., Riedemann, T., Casamassa, A., Smiyakin, A., Schichor, C., Götz, M., Tiwari, V. K., Treutlein, B., & Berninger, B. (2018). Direct pericyte-to-neuron reprogramming via unfolding of a neural stem cell-like program. *Nature Neuroscience*, *21*(7). https://doi.org/10.1038/s41593-018-0168-3

Karow, M., Sánchez, R., Schichor, C., Masserdotti, G., Ortega, F., Heinrich, C., Gascón, S., Khan, M. A., Lie, D. C., Dellavalle, A., Cossu, G., Goldbrunner, R., Götz, M., & Berninger, B. (2012). Reprogramming of pericyte-derived cells of the adult human brain into induced neuronal cells. *Cell Stem Cell*, *11*(4). https://doi.org/10.1016/j.stem.2012.07.007

Kawaguchi, Y., & Kubota, Y. (1996). Physiological and morphological identification of somatostatin- or vasoactive intestinal polypeptide-containing cells among GABAergic cell subtypes in rat frontal cortex. *The Journal of Neuroscience : The Official Journal of the Society for Neuroscience*, *16*(8), 2701–2715. https://doi.org/10.1523/JNEUROSCI.16-08-02701.1996

Kawaguchi, Y., & Kubota, Y. (1997). GABAergic cell subtypes and their synaptic connections in rat frontal cortex. *Cerebral Cortex (New York, N.Y. : 1991)*, *7*(6), 476–486. https://doi.org/10.1093/CERCOR/7.6.476

Kempermann, G., Gage, F. H., Aigner, L., Song, H., Curtis, M. A., Thuret, S., Kuhn, H. G., Jessberger, S., Frankland, P. W., Cameron, H. A., Gould, E., Hen, R., Abrous, D. N., Toni, N., Schinder, A. F., Zhao, X., Lucassen, P. J., & Frisén, J. (2018). Human Adult Neurogenesis: Evidence and Remaining Questions. *Cell Stem Cell*, *23*(1), 25–30. https://doi.org/10.1016/J.STEM.2018.04.004

Kempf, J., Knelles, K., Hersbach, B. A., Petrik, D., Riedemann, T., Bednarova, V., Janjic, A., Simon-Ebert, T., Enard, W., Smialowski, P., Götz, M., & Masserdotti, G. (2021). Heterogeneity of neurons reprogrammed from spinal cord astrocytes by

the proneural factors Ascl1 and Neurogenin2. *Cell Reports*, *36*(3). https://doi.org/10.1016/j.celrep.2021.109409

Kepecs, A., & Fishell, G. (2014). Interneuron cell types are fit to function. *Nature 2014 505:7483*, *505*(7483), 318–326. https://doi.org/10.1038/nature12983

Kessaris, N., Fogarty, M., Iannarelli, P., Grist, M., Wegner, M., & Richardson, W. D. (2005). Competing waves of oligodendrocytes in the forebrain and postnatal elimination of an embryonic lineage. *Nature Neuroscience 2005 9:2*, *9*(2), 173–179. https://doi.org/10.1038/nn1620

Kierdorf, K., Erny, D., Goldmann, T., Sander, V., Schulz, C., Perdiguero, E. G., Wieghofer, P., Heinrich, A., Riemke, P., Hölscher, C., Müller, D. N., Luckow, B., Brocker, T., Debowski, K., Fritz, G., Opdenakker, G., Diefenbach, A., Biber, K., Heikenwalder, M., … Prinz, M. (2013). Microglia emerge from erythromyeloid precursors via Pu.1- and Irf8-dependent pathways. *Nature Neuroscience 2013 16:3*, *16*(3), 273–280. https://doi.org/10.1038/nn.3318

Kim, Y., Zheng, X., Ansari, Z., Bunnell, M. C., Herdy, J. R., Traxler, L., Lee, H., Paquola, A. C. M., Blithikioti, C., Ku, M., Schlachetzki, J. C. M., Winkler, J., Edenhofer, F., Glass, C. K., Paucar, A. A., Jaeger, B. N., Pham, S., Boyer, L., Campbell, B. C., … Gage, F. H. (2018). Mitochondrial Aging Defects Emerge in Directly Reprogrammed Human Neurons due to Their Metabolic Profile. *Cell Reports*, *23*(9), 2550–2558. https://doi.org/10.1016/J.CELREP.2018.04.105

Kleschevnicov, A. M., Belichenko, P. V., Villar, A. J., Epstein, C. J., Malenka, R. C., & Mobley, W. C. (2004). Hippocampal long-term potentiation suppressed by increased inhibition in the Ts65Dn mouse, a genetic model of Down syndrome. *The Journal of Neuroscience : The Official Journal of the Society for Neuroscience*, *24*(37), 8153–8160. https://doi.org/10.1523/JNEUROSCI.1766-04.2004

Klum, S., Zaouter, C., Alekseenko, Z., Björklund, Å. K., Hagey, D. W., Ericson, J., Muhr, J., & Bergsland, M. (2018). Sequentially acting SOX proteins orchestrate astrocyte- and oligodendrocyte-specific gene expression. *EMBO Reports*, *19*(11). https://doi.org/10.15252/embr.201846635

Kokoeva, M. V., Yin, H., & Flier, J. S. (2005). Neurogenesis in the hypothalamus of adult mice: potential role in energy balance. *Science (New York, N.Y.)*, *310*(5748), 679–683. https://doi.org/10.1126/SCIENCE.1115360

Kontou, G., Antonoudiou, P., Podpolny, M., Szulc, B. R., Arancibia-Carcamo, I. L., Higgs, N. F., Lopez-Domenech, G., Salinas, P. C., Mann, E. O., & Kittler, J. T. (2021). Miro1-dependent mitochondrial dynamics in parvalbumin interneurons. *ELife*, *10*. https://doi.org/10.7554/ELIFE.65215

Korotkova, T., Fuchs, E. C., Ponomarenko, A., von Engelhardt, J., & Monyer, H. (2010). NMDA receptor ablation on parvalbumin-positive interneurons impairs hippocampal synchrony, spatial representations, and working memory. *Neuron*, *68*(3), 557–569. https://doi.org/10.1016/J.NEURON.2010.09.017

Kriegstein, A., & Alvarez-Buylla, A. (2009). The glial nature of embryonic and adult neural stem cells. *Annual Review of Neuroscience*, *32*, 149–184. https://doi.org/10.1146/ANNUREV.NEURO.051508.135600

Krishna, S., Low, I. C. C., & Pervaiz, S. (2011). Regulation of mitochondrial metabolism: yet another facet in the biology of the oncoprotein Bcl-2. *Biochemical Journal*, *435*(3), 545–551. https://doi.org/10.1042/BJ20101996

Kuhlbrodt, K., Herbarth, B., Sock, E., Hermans-Borgmeyer, I., & Wegner, M. (1998). Sox10, a novel transcriptional modulator in glial cells. *Journal of Neuroscience*, *18*(1). https://doi.org/10.1523/jneurosci.18-01-00237.1998

Labro, A. J., Priest, M. F., Lacroix, J. J., Snyders, D. J., & Bezanilla, F. (2015). Kv3.1 uses a timely resurgent K+ current to secure action potential repolarization. *Nature Communications 2015 6:1*, *6*(1), 1–12. https://doi.org/10.1038/ncomms10173

Lanjakornsiripan, D., Pior, B. J., Kawaguchi, D., Furutachi, S., Tahara, T., Katsuyama, Y., Suzuki, Y., Fukazawa, Y., & Gotoh, Y. (2018). Layer-specific morphological and molecular differences in neocortical astrocytes and their dependence on neuronal layers. *Nature Communications*, *9*(1). https://doi.org/10.1038/s41467-018-03940-3

Lattke, M., Goldstone, R., Ellis, J. K., Boeing, S., Jurado-Arjona, J., Marichal, N., MacRae, J. I., Berninger, B., & Guillemot, F. (2021). Extensive transcriptional and chromatin changes underlie astrocyte maturation in vivo and in culture. *Nature Communications 2021 12:1*, *12*(1), 1–18. https://doi.org/10.1038/s41467-021-24624-5

Le, T. N., Du, G., Fonseca, M., Zhou, Q. P., Wigle, J. T., & Eisenstat, D. D. (2007). Dlx homeobox genes promote cortical interneuron migration from the basal forebrain by direct repression of the semaphorin receptor neuropilin-2. *The Journal of Biological Chemistry*, *282*(26), 19071–19081. https://doi.org/10.1074/JBC.M607486200

Leaman, S., Marichal, N., & Berninger, B. (2022). Reprogramming cellular identity in vivo. *Development (Cambridge, England)*, *149*(4). https://doi.org/10.1242/dev.200433

Lee, S. H., Hjerling-Leffler, J., Zagha, E., Fishell, G., & Rudy, B. (2010). The Largest Group of Superficial Neocortical GABAergic Interneurons Expresses Ionotropic Serotonin Receptors. *Journal of Neuroscience*, *30*(50), 16796–16808. https://doi.org/10.1523/JNEUROSCI.1869-10.2010

Lee, T. J., Yoo, J. Y., Shu, D., Li, H., Zhang, J., Yu, J. G., Jaime-Ramirez, A. C., Acunzo, M., Romano, G., Cui, R., Sun, H. L., Luo, Z., Old, M., Kaur, B., Guo, P., & Croce, C. M. (2017). RNA Nanoparticle-Based Targeted Therapy for Glioblastoma through Inhibition of Oncogenic miR-21. *Molecular Therapy*, *25*(7). https://doi.org/10.1016/j.ymthe.2016.11.016

Lentini, C., d'Orange, M., Marichal, N., Trottmann, M. M., Vignoles, R., Foucault, L., Verrier, C., Massera, C., Raineteau, O., Conzelmann, K. K., Rival-Gervier, S., Depaulis, A., Berninger, B., & Heinrich, C. (2021). Reprogramming reactive glia into interneurons reduces chronic seizure activity in a mouse model of mesial temporal lobe epilepsy. *Cell Stem Cell*, *28*(12). https://doi.org/10.1016/j.stem.2021.09.002

Lepiemme, F., Stoufflet, J., Javier-Torrent, M., Mazzucchelli, G., Silva, C. G., & Nguyen, L. (2022). Oligodendrocyte precursors guide interneuron migration by unidirectional contact repulsion. *Science (New York, N.Y.)*, *376*(6595). https://doi.org/10.1126/SCIENCE.ABN6204

Li, H., Paes de Faria, J., Andrew, P., Nitarska, J., & Richardson, W. D. (2011). Phosphorylation Regulates OLIG2 Cofactor Choice and the Motor Neuron-Oligodendrocyte Fate Switch. *Neuron*, *69*(5), 918. https://doi.org/10.1016/J.NEURON.2011.01.030

Li, S., Mattar, P., Dixit, R., Lawn, S. O., Wilkinson, G., Kinch, C., Eisenstat, D., Kurrasch, D. M., Chan, J. A., & Schuurmans, C. (2014). RAS/ERK signaling controls proneural genetic programs in cortical development and gliomagenesis. *Journal of Neuroscience*, *34*(6). https://doi.org/10.1523/JNEUROSCI.4077-13.2014

Lien, C. C., & Jonas, P. (2003). Kv3 potassium conductance is necessary and kinetically optimized for high-frequency action potential generation in hippocampal interneurons. *Journal of Neuroscience*, *23*(6). https://doi.org/10.1523/jneurosci.23-06-02058.2003

Lim, L., Mi, D., Llorca, A., & Marín, O. (2018). Development and Functional Diversification of Cortical Interneurons. In *Neuron* (Vol. 100, Issue 2). https://doi.org/10.1016/j.neuron.2018.10.009

Lin, S. C., & Bergles, D. E. (2004). Synaptic signaling between GABAergic interneurons and oligodendrocyte precursor cells in the hippocampus. *Nature Neuroscience*, *7*(1). https://doi.org/10.1038/nn1162

Lindtner, S., Catta-Preta, R., Tian, H., Su-Feher, L., Price, J. D., Dickel, D. E., Greiner, V., Silberberg, S. N., McKinsey, G. L., McManus, M. T., Pennacchio, L. A., Visel, A., Nord, A. S., & Rubenstein, J. L. R. (2019). Genomic Resolution of DLX-Orchestrated Transcriptional Circuits Driving Development of Forebrain GABAergic Neurons. *Cell Reports*, *28*(8). https://doi.org/10.1016/j.celrep.2019.07.022

Lindvall, O. (2012). Why is it taking so long to develop clinically competitive stem cell therapies for CNS disorders? *Cell Stem Cell*, *10*(6), 660–662. https://doi.org/10.1016/J.STEM.2012.04.004

Lindvall, O., & Kokaia, Z. (2010). Stem cells in human neurodegenerative disorders — time for clinical translation? *The Journal of Clinical Investigation*, *120*(1), 29. https://doi.org/10.1172/JCI40543

Liu, Y., Miao, Q., Yuan, J., Han, S., Zhang, P., Li, S., Rao, Z., Zhao, W., Ye, Q., Geng, J., Zhang, X., & Cheng, L. (2015). Ascl1 converts dorsal midbrain astrocytes into functional neurons In Vivo. *Journal of Neuroscience*, *35*(25). https://doi.org/10.1523/JNEUROSCI.3975-14.2015

Liu, Z., Chen, O., Wall, J. B. J., Zheng, M., Zhou, Y., Wang, L., Ruth Vaseghi, H., Qian, L., & Liu, J. (2017). Systematic comparison of 2A peptides for cloning multi-genes in a polycistronic vector. *Scientific Reports 2017 7:1*, *7*(1), 1–9. https://doi.org/10.1038/s41598-017-02460-2

Llorens-Bobadilla, E., Zhao, S., Baser, A., Saiz-Castro, G., Zwadlo, K., & Martin-Villalba, A. (2015). Single-Cell Transcriptomics Reveals a Population of Dormant Neural Stem Cells that Become Activated upon Brain Injury. *Cell Stem Cell*, *17*(3), 329–340. https://doi.org/10.1016/j.stem.2015.07.002

Lois, C., & Alvarez-Buylla, A. (1994). Long-distance neuronal migration in the adult mammalian brain. *Science (New York, N.Y.)*, *264*(5162), 1145–1148. https://doi.org/10.1126/SCIENCE.8178174

Long, J. E., Cobos, I., Potter, G. B., & Rubenstein, J. L. R. (2009). Dlx1&2 and Mash1 transcription factors control MGE and CGE patterning and differentiation through parallel and overlapping pathways. *Cerebral Cortex (New York, N.Y. : 1991)*, *19 Suppl 1*(Suppl 1). https://doi.org/10.1093/CERCOR/BHP045

Loomba, S., Straehle, J., Gangadharan, V., Heike, N., Khalifa, A., Motta, A., Ju, N., Sievers, M., Gempt, J., Meyer, H. S., & Helmstaedter, M. (2022). Connectomic comparison of mouse and human cortex. *Science*, *377*(6602). https://doi.org/10.1126/science.abo0924

López-Bendito, G., Antonio Sánchez-Alcañiz, J., Pla, R., Borrell, V., Picó, E., Valdeolmillos, M., & Marín, O. (2008). *Chemokine Signaling Controls Intracortical Migration and Final Distribution of GABAergic Interneurons*. https://doi.org/10.1523/JNEUROSCI.4651-07.2008

López-Bendito, G., Sturgess, K., Erdélyi, F., Szabó, G., Molnár, Z., & Paulsen, O. (2004). Preferential Origin and Layer Destination of GAD65-GFP Cortical Interneurons. *Cerebral Cortex*, *14*(10), 1122–1133. https://doi.org/10.1093/CERCOR/BHH072

Lucas, E. K., Dougherty, S. E., McMeekin, L. J., Reid, C. S., Dobrunz, L. E., West, A. B., Hablitz, J. J., & Cowell, R. M. (2014). PGC-1α provides a transcriptional framework for synchronous neurotransmitter release from parvalbumin-positive interneurons. *Journal of Neuroscience*, *34*(43). https://doi.org/10.1523/JNEUROSCI.1222-14.2014

Lysko, D. E., Putt, M., & Golden, J. A. (2011). SDF1 regulates leading process branching and speed of migrating interneurons. *Journal of Neuroscience*, *31*(5). https://doi.org/10.1523/JNEUROSCI.3118-10.2011

Ma, N. X., Puls, B., & Chen, G. (2022). Transcriptomic analyses of NeuroD1-mediated astrocyte-to-neuron conversion. *Developmental Neurobiology*, *82*(5), 375–391. https://doi.org/10.1002/DNEU.22882

Ma, T., Zhang, Q., Cai, Y., You, Y., Rubenstein, J. L. R., & Yang, Z. (2012). A Subpopulation of Dorsal Lateral/Caudal Ganglionic Eminence-Derived Neocortical Interneurons Expresses the Transcription Factor Sp8. *Cerebral Cortex*, *22*(9), 2120–2130. https://doi.org/10.1093/CERCOR/BHR296

Ma, Y., Hu, H., Berrebi, A. S., Mathers, P. H., & Agmon, A. (2006). Distinct subtypes of somatostatin-containing neocortical interneurons revealed in transgenic mice. *The Journal of Neuroscience : The Official Journal of the Society for Neuroscience*, *26*(19), 5069–5082. https://doi.org/10.1523/JNEUROSCI.0661-06.2006

Magnusson, J. P., Göritz, C., Tatarishvili, J., Dias, D. O., Smith, E. M. K., Lindvall, O., Kokaia, Z., & Frisén, J. (2014). A latent neurogenic program in astrocytes regulated by Notch signaling in the mouse. *Science*, *346*(6206). https://doi.org/10.1126/science.346.6206.237

Magnusson, J. P., Zamboni, M., Santopolo, G., Mold, J. E., Barrientos-Somarribas, M., Talavera-Lopez, C., Andersson, B., & Frisén, J. (2020). Activation of a neural stem cell transcriptional program in parenchymal astrocytes. *ELife*, *9*, 1–25. https://doi.org/10.7554/ELIFE.59733

Mardinly, A. R., Spiegel, I., Patrizi, A., Centofante, E., Bazinet, J. E., Tzeng, C. P., Mandel-Brehm, C., Harmin, D. A., Adesnik, H., Fagiolini, M., & Greenberg, M. E. (2016). Sensory experience regulates cortical inhibition by inducing IGF1 in VIP neurons. *Nature 2016 531:7594*, *531*(7594), 371–375. https://doi.org/10.1038/nature17187

Marín, O. (2012). Interneuron dysfunction in psychiatric disorders. *Nature Reviews Neuroscience 2012 13:2*, *13*(2), 107–120. https://doi.org/10.1038/nrn3155

Marín, O., Hern andez, M., & Joan, S. (2013). Cellular and molecular mechanisms controlling the migration of neocortical interneurons. *European Journal of Neuroscience*, *38*(1), 2019–2029. https://doi.org/10.1111/EJN.12225

Marín, O., & Rubenstein, J. L. R. (2001). A long, remarkable journey: Tangential migration in the telencephalon. *Nature Reviews Neuroscience 2001 2:11*, *2*(11), 780–790. https://doi.org/10.1038/35097509

Markakis, E. A., & Gage, F. H. (1999). Adult-Generated Neurons in the Dentate Gyrus Send Axonal Projections to Field CA 3 and Are Surrounded by Synaptic Vesicles. *J. Comp. Neurol*, *406*, 449–460. https://doi.org/10.1002/(SICI)1096-9861(19990419)406:4

Marques, B. L., Carvalho, G. A., Freitas, E. M. M., Chiareli, R. A., Barbosa, T. G., Di Araújo, A. G. P., Nogueira, Y. L., Ribeiro, R. I., Parreira, R. C., Vieira, M. S., Resende, R. R., Gomez, R. S., Oliveira-Lima, O. C., & Pinto, M. C. X. (2019). The role of neurogenesis in neurorepair after ischemic stroke. *Seminars in Cell &*

Developmental Biology, *95*, 98–110. https://doi.org/10.1016/J.SEMCDB.2018.12.003

Marques, S., van Bruggen, D., Vanichkina, D. P., Floriddia, E. M., Munguba, H., Väremo, L., Giacomello, S., Falcão, A. M., Meijer, M., Björklund, Å. K., Hjerling-Leffler, J., Taft, R. J., & Castelo-Branco, G. (2018). Transcriptional Convergence of Oligodendrocyte Lineage Progenitors during Development. *Developmental Cell*, *46*(4), 504-517.e7. https://doi.org/10.1016/j.devcel.2018.07.005

Marques, S., Zeisel, A., Codeluppi, S., Van Bruggen, D., Falcão, A. M., Xiao, L., Li, H., Häring, M., Hochgerner, H., Romanov, R. A., Gyllborg, D., Muñoz-Manchado, A. B., La Manno, G., Lönnerberg, P., Floriddia, E. M., Rezayee, F., Ernfors, P., Arenas, E., Hjerling-Leffler, J., … Castelo-Branco, G. (2016). Oligodendrocyte heterogeneity in the mouse juvenile and adult central nervous system. *Science*, *352*(6291), 1326–1329. https://doi.org/10.1126/SCIENCE.AAF6463

Martini, S., Bernoth, K., Main, H., Ortega, G. D. C., Lendahl, U., Just, U., & Schwanbeck, R. (2013). A critical role for Sox9 in Notch-induced astrogliogenesis and stem cell maintenance. *Stem Cells*, *31*(4). https://doi.org/10.1002/stem.1320

Masserdotti, G., Gillotin, S., Sutor, B., Drechsel, D., Irmler, M., Jørgensen, H. F., Sass, S., Theis, F. J., Beckers, J., Berninger, B., Guillemot, F., & Götz, M. (2015). Transcriptional Mechanisms of Proneural Factors and REST in Regulating Neuronal Reprogramming of Astrocytes. *Cell Stem Cell*, *17*(1), 74. https://doi.org/10.1016/J.STEM.2015.05.014

Matsuda, T., Irie, T., Katsurabayashi, S., Hayashi, Y., Nagai, T., Hamazaki, N., Adefuin, A. M. D., Miura, F., Ito, T., Kimura, H., Shirahige, K., Takeda, T., Iwasaki, K., Imamura, T., & Nakashima, K. (2019). Pioneer Factor NeuroD1 Rearranges Transcriptional and Epigenetic Profiles to Execute Microglia-Neuron Conversion. *Neuron*, *101*(3). https://doi.org/10.1016/j.neuron.2018.12.010

Mattugini, N., Bocchi, R., Scheuss, V., Russo, G. L., Torper, O., Lao, C. L., & Götz, M. (2019). Inducing Different Neuronal Subtypes from Astrocytes in the Injured Mouse Cerebral Cortex. *Neuron*, *103*(6), 1086-1095.e5. https://doi.org/10.1016/J.NEURON.2019.08.009

Mayer, C., Hafemeister, C., Bandler, R. C., Machold, R., Batista Brito, R., Jaglin, X., Allaway, K., Butler, A., Fishell, G., & Satija, R. (2018). Developmental diversification of cortical inhibitory interneurons. *Nature*, *555*(7697), 457–462. https://doi.org/10.1038/NATURE25999

McGarry, L. M., Packer, A. M., Fino, E., Nikolenko, V., Sippy, T., & Yuste, R. (2010). Quantitative classifi cation of somatostatin-positive neocortical interneurons identifi es three interneuron subtypes. *Frontiers in Neural Circuits*, *4*, 12. https://doi.org/10.3389/FNCIR.2010.00012/

Mei, L., & Xiong, W. C. (2008). Neuregulin 1 in neural development, synaptic plasticity and schizophrenia. *Nature Reviews. Neuroscience*, *9*(6), 437. https://doi.org/10.1038/NRN2392

Men, Y., Yelick, J., Jin, S., Tian, Y., Chiang, M. S. R., Higashimori, H., Brown, E., Jarvis, R., & Yang, Y. (2019). Exosome reporter mice reveal the involvement of exosomes in mediating neuron to astroglia communication in the CNS. *Nature Communications*, *10*(1). https://doi.org/10.1038/s41467-019-11534-w

Merkel, S. F., Andrews, A. M., Lutton, E. M., Mu, D., Hudry, E., Hyman, B. T., Maguire, C. A., & Ramirez, S. H. (2017). Trafficking of adeno-associated virus vectors across a model of the blood–brain barrier; a comparative study of transcytosis and transduction using primary human brain endothelial cells. *Journal of Neurochemistry*, *140*(2), 216–230. https://doi.org/10.1111/JNC.13861

Mertens, J., Paquola, A. C. M., Ku, M., Hatch, E., Böhnke, L., Ladjevardi, S., McGrath, S., Campbell, B., Lee, H., Herdy, J. R., Gonçalves, J. T., Toda, T., Kim, Y., Winkler, J., Yao, J., Hetzer, M. W., & Gage, F. H. (2015). Directly Reprogrammed Human Neurons Retain Aging-Associated Transcriptomic Signatures and Reveal Age-Related Nucleocytoplasmic Defects. *Cell Stem Cell*, *17*(6). https://doi.org/10.1016/j.stem.2015.09.001

Mi, D., Li, Z., Lim, L., Li, M., Moissidis, M., Yang, Y., Gao, T., Hu, T. X., Pratt, T., Price, D. J., Sestan, N., & Marín, O. (2018). Early emergence of cortical interneuron diversity in the mouse embryo. *Science (New York, N.Y.)*, *360*(6384), 81–85. https://doi.org/10.1126/SCIENCE.AAR6821

Miller, K. N., Clark, J. P., & Anderson, R. M. (2019). Mitochondrial regulator PGC-1a—Modulating the modulator. In *Current Opinion in Endocrine and Metabolic Research* (Vol. 5). https://doi.org/10.1016/j.coemr.2019.02.002

Miyamae, T., Chen, K., Lewis, D. A., & Gonzalez-Burgos, G. (2017). Distinct physiological maturation of parvalbumin-positive neuron subtypes in mouse prefrontal cortex. *Journal of Neuroscience*, *37*(19). https://doi.org/10.1523/JNEUROSCI.3325-16.2017

Miyoshi, G., Hjerling-Leffler, J., Karayannis, T., Sousa, V. H., Butt, S. J. B., Battiste, J., Johnson, J. E., Machold, R. P., & Fishell, G. (2010). Genetic fate mapping reveals that the caudal ganglionic eminence produces a large and diverse population of superficial cortical interneurons. *The Journal of Neuroscience : The Official Journal of the Society for Neuroscience*, *30*(5), 1582–1594. https://doi.org/10.1523/JNEUROSCI.4515-09.2010

Moessner, R., Marshall, C. R., Sutcliffe, J. S., Skaug, J., Pinto, D., Vincent, J., Zwaigenbaum, L., Fernandez, B., Roberts, W., Szatmari, P., & Scherer, S. W. (2007). Contribution of SHANK3 mutations to autism spectrum disorder. *American Journal of Human Genetics*, *81*(6), 1289–1297. https://doi.org/10.1086/522590

Molyneaux, B. J., Arlotta, P., Menezes, J. R. L., & Macklis, J. D. (2007). Neuronal subtype specification in the cerebral cortex. *Nature Reviews Neuroscience 2007 8:6*, *8*(6), 427–437. https://doi.org/10.1038/nrn2151

Moreno-Jiménez, E. P., Terreros-Roncal, J., Flor-García, M., Rábano, A., & Llorens-Martín, M. (2021). Evidences for Adult Hippocampal Neurogenesis in Humans.

Journal of Neuroscience, *41*(12), 2541–2553. https://doi.org/10.1523/JNEUROSCI.0675-20.2020

Morgan, J. I., Cohen, D. R., Hempstead, J. L., & Curran, T. (1987). Mapping Patterns of c-fos Expression in the Central Nervous System After Seizure. *Science*, *237*(4811), 192–197. https://doi.org/10.1126/SCIENCE.3037702

Nakatani, H., Martin, E., Hassani, H., Clavairoly, A., Maire, C. L., Viadieu, A., Kerninon, C., Delmasure, A., Frah, M., Weber, M., Nakafuku, M., Zalc, B., Thomas, J. L., Guillemot, F., Nait-Oumesmar, B., & Parras, C. (2013). Ascl1/Mash1 promotes brain oligodendrogenesis during myelination and remyelination. *The Journal of Neuroscience : The Official Journal of the Society for Neuroscience*, *33*(23), 9752–9768. https://doi.org/10.1523/JNEUROSCI.0805-13.2013

Nato, G., Caramello, A., Trova, S., Avataneo, V., Rolando, C., Taylor, V., Buffo, A., Peretto, P., & Luzzati, F. (2015). Striatal astrocytes produce neuroblasts in an excitotoxic model of Huntington's disease. *Development (Cambridge)*, *142*(5). https://doi.org/10.1242/dev.116657

Naviaux, R. K., Costanzi, E., Haas, M., & Verma, I. M. (1996). The pCL vector system: rapid production of helper-free, high-titer, recombinant retroviruses. *Journal of Virology*, *70*(8). https://doi.org/10.1128/jvi.70.8.5701-5705.1996

Nery, S., Fishell, G., & Corbin, J. G. (2002). The caudal ganglionic eminence is a source of distinct cortical and subcortical cell populations. *Nature Neuroscience*, *5*(12), 1279–1287. https://doi.org/10.1038/NN971

Nery, S., Wichterle, H., & Fishell, G. (2001). Sonic hedgehog contributes to oligodendrocyte specification in the mammalian forebrain. *Development*, *128*(4), 527–540. https://doi.org/10.1242/DEV.128.4.527

Nieto, M., Schuurmans, C., Britz, O., & Guillemot, F. (2001). Neural bHLH genes control the neuronal versus glial fate decision in cortical progenitors. *Neuron*, *29*(2), 401–413. https://doi.org/10.1016/S0896-6273(01)00214-8

Nigro, M. J., Hashikawa-Yamasaki, Y., & Rudy, B. (2018). Diversity and Connectivity of Layer 5 Somatostatin-Expressing Interneurons in the Mouse Barrel Cortex. *Journal of Neuroscience*, *38*(7), 1622–1633. https://doi.org/10.1523/JNEUROSCI.2415-17.2017

Niquille, M., Limoni, G., Markopoulos, F., Cadilhac, C., Prados, J., Holtmaat, A., & Dayer, A. (2018). Neurogliaform cortical interneurons derive from cells in the preoptic area. *ELife*, *7*. https://doi.org/10.7554/ELIFE.32017

Nishiyama, A., Komitova, M., Suzuki, R., & Zhu, X. (2009). Polydendrocytes (NG2 cells): Multifunctional cells with lineage plasticity. In *Nature Reviews Neuroscience* (Vol. 10, Issue 1). https://doi.org/10.1038/nrn2495

Niu, W., Zang, T., Smith, D. K., Vue, T. Y., Zou, Y., Bachoo, R., Johnson, J. E., & Zhang, C. L. (2015). SOX2 reprograms resident astrocytes into neural progenitors

in the adult brain. *Stem Cell Reports*, *4*(5), 780–794. https://doi.org/10.1016/j.stemcr.2015.03.006

Niu, W., Zang, T., Zou, Y., Fang, S., Smith, D. K., Bachoo, R., & Zhang, C. L. (2013). In vivo reprogramming of astrocytes to neuroblasts in the adult brain. *Nature Cell Biology 2013 15:10*, *15*(10), 1164–1175. https://doi.org/10.1038/ncb2843

Noctor, S. C., Martinez-Cerdeño, V., Ivic, L., & Kriegstein, A. R. (2004). Cortical neurons arise in symmetric and asymmetric division zones and migrate through specific phases. *Nature Neuroscience*, *7*(2), 136–144. https://doi.org/10.1038/NN1172

Noctor, S. C., Martínez-Cerdeño, V., & Kriegstein, A. R. (2008). Distinct behaviors of neural stem and progenitor cells underlie cortical neurogenesis. *The Journal of Comparative Neurology*, *508*(1), 28–44. https://doi.org/10.1002/CNE.21669

Nori, S., Okada, Y., Yasuda, A., Tsuji, O., Takahashi, Y., Kobayashi, Y., Fujiyoshi, K., Koike, M., Uchiyama, Y., Ikeda, E., Toyama, Y., Yamanaka, S., Nakamura, M., & Okano, H. (2011). Grafted human-induced pluripotent stem-cell-derived neurospheres promote motor functional recovery after spinal cord injury in mice. *Proceedings of the National Academy of Sciences of the United States of America*, *108*(40). https://doi.org/10.1073/pnas.1108077108

Okaty, B. W., Miller, M. N., Sugino, K., Hempel, C. M., & Nelson, S. B. (2009). Transcriptional and electrophysiological maturation of neocortical fast-spiking GABAergic interneurons. *Journal of Neuroscience*, *29*(21). https://doi.org/10.1523/JNEUROSCI.0105-09.2009

Olmos-Serrano, J. L., Paluszkiewicz, S. M., Martin, B. S., Kaufmann, W. E., Corbin, J. G., & Huntsman, M. M. (2010). Defective GABAergic neurotransmission and pharmacological rescue of neuronal hyperexcitability in the amygdala in a mouse model of fragile X syndrome. *The Journal of Neuroscience : The Official Journal of the Society for Neuroscience*, *30*(29), 9929–9938. https://doi.org/10.1523/JNEUROSCI.1714-10.2010

Orduz, D., Benamer, N., Ortolani, D., Coppola, E., Vigier, L., Pierani, A., & Angulo, M. C. (2019). Developmental cell death regulates lineage-related interneuron-oligodendroglia functional clusters and oligodendrocyte homeostasis. *Nature Communications*, *10*(1). https://doi.org/10.1038/s41467-019-11904-4

Orduz, D., Maldonado, P. P., Balia, M., Vélez-Fort, M., de Sars, V., Yanagawa, Y., Emiliani, V., & Angulo, M. C. (2015). Interneurons and oligodendrocyte progenitors form a structured synaptic network in the developing neocortex. *ELife*, *4*(4), 1–53. https://doi.org/10.7554/ELIFE.06953

Palmer, T. D., Takahashi, J., & Gage, F. H. (1997). The adult rat hippocampus contains primordial neural stem cells. *Molecular and Cellular Neurosciences*, *8*(6), 389–404. https://doi.org/10.1006/MCNE.1996.0595

Pan-Vazquez, A., Wefelmeyer, W., Gonzalez Sabater, V., Neves, G., & Burrone, J. (2020). Activity-Dependent Plasticity of Axo-axonic Synapses at the Axon Initial

Segment. *Neuron*, *106*(2), 265-276.e6. https://doi.org/10.1016/J.NEURON.2020.01.037

Paolicelli, R. C., Bolasco, G., Pagani, F., Maggi, L., Scianni, M., Panzanelli, P., Giustetto, M., Ferreira, T. A., Guiducci, E., Dumas, L., Ragozzino, D., & Gross, C. T. (2011). Synaptic pruning by microglia is necessary for normal brain development. *Science (New York, N.Y.)*, *333*(6048), 1456–1458. https://doi.org/10.1126/SCIENCE.1202529

Paredes, M. F., Sorrells, S. F., Cebrian-Silla, A., Sandoval, K., Qi, D., Kelley, K. W., James, D., Mayer, S., Chang, J., Auguste, K. I., Chang, E. F., Gutierrez Martin, A. J., Kriegstein, A. R., Mathern, G. W., Oldham, M. C., Huang, E. J., Garcia-Verdugo, J. M., Yang, Z., & Alvarez-Buylla, A. (2018). Does Adult Neurogenesis Persist in the Human Hippocampus? *Cell Stem Cell*, *23*(6), 780. https://doi.org/10.1016/J.STEM.2018.11.006

Parras, C. M., Galli, R., Britz, O., Soares, S., Galichet, C., Battiste, J., Johnson, J. E., Nakafaku, M., Vescovi, A., & Guillemot, F. (2004). Mash1 specifies neurons and oligodendrocytes in the postnatal brain. *The EMBO Journal*, *23*(22), 4495–4505. https://doi.org/10.1038/SJ.EMBOJ.7600447

Parras, C. M., Hunt, C., Sugimori, M., Nakafuku, M., Rowitch, D., & Guillemot, F. (2007). The proneural gene Mash1 specifies an early population of telencephalic oligodendrocytes. *The Journal of Neuroscience : The Official Journal of the Society for Neuroscience*, *27*(16), 4233–4242. https://doi.org/10.1523/JNEUROSCI.0126-07.2007

Peça, J., Feliciano, C., Ting, J. T., Wang, W., Wells, M. F., Venkatraman, T. N., Lascola, C. D., Fu, Z., & Feng, G. (2011). Shank3 mutant mice display autistic-like behaviours and striatal dysfunction. *Nature*, *472*(7344), 437–442. https://doi.org/10.1038/NATURE09965

Pedram, A., Razandi, M., Hu, R. M., & Levin, E. R. (1998). Astrocyte progression from G1 to S phase of the cell cycle depends upon multiple protein interaction. *Journal of Biological Chemistry*, *273*(22). https://doi.org/10.1074/jbc.273.22.13966

Peel, A. L., & Klein, R. L. (2000). Adeno-associated virus vectors: activity and applications in the CNS. *Journal of Neuroscience Methods*, *98*(2), 95–104. https://doi.org/10.1016/S0165-0270(00)00183-7

Pereira, M., Birtele, M., Shrigley, S., Benitez, J. A., Hedlund, E., Parmar, M., & Ottosson, D. R. (2017). Direct Reprogramming of Resident NG2 Glia into Neurons with Properties of Fast-Spiking Parvalbumin-Containing Interneurons. *Stem Cell Reports*, *9*(3). https://doi.org/10.1016/j.stemcr.2017.07.023

Petryniak, M. A., Potter, G. B., Rowitch, D. H., & Rubenstein, J. L. R. (2007). Dlx1 and Dlx2 control neuronal versus oligodendroglial cell fate acquisition in the developing forebrain. *Neuron*, *55*(3), 417. https://doi.org/10.1016/J.NEURON.2007.06.036

Pilz, G. A., Shitamukai, A., Reillo, I., Pacary, E., Schwausch, J., Stahl, R., Ninkovic, J., Snippert, H. J., Clevers, H., Godinho, L., Guillemot, F., Borrell, V., Matsuzaki, F., & Götz, M. (2013). Amplification of progenitors in the mammalian telencephalon includes a new radial glial cell type. *Nature Communications 2013 4:1*, *4*(1), 1–11. https://doi.org/10.1038/ncomms3125

Pla, R., Stanco, A., Howard, M. A., Rubin, A. N., Vogt, D., Mortimer, N., Cobos, I., Potter, G. B., Lindtner, S., Price, J. D., Nord, A. S., Visel, A., Schreiner, C. E., Baraban, S. C., Rowitch, D. H., & Rubenstein, J. L. R. (2018). Dlx1 and Dlx2 Promote Interneuron GABA Synthesis, Synaptogenesis, and Dendritogenesis. *Cerebral Cortex (New York, NY)*, *28*(11), 3797. https://doi.org/10.1093/CERCOR/BHX241

Poitras, L., Ghanem, N., Hatch, G., & Ekker, M. (2007). The proneural determinant MASH1 regulates forebrain Dlx1/2expression through the I12b intergenic enhancer. *Development*, *134*(9), 1755–1765. https://doi.org/10.1242/DEV.02845

Polleux, F., Whitford, K. L., Dijkhuizen, P. A., Vitalis, T., & Ghosh, A. (2002). Control of cortical interneuron migration by neurotrophins and PI3-kinase signaling. *Development (Cambridge, England)*, *129*(13), 3147–3160. https://doi.org/10.1242/DEV.129.13.3147

Pringle, N. P., & Richardson, W. D. (1993). A singularity of PDGF alpha-receptor expression in the dorsoventral axis of the neural tube may define the origin of the oligodendrocyte lineage. *Development (Cambridge, England)*, *117*(2), 525–533. https://doi.org/10.1242/DEV.117.2.525

Priya, R., Paredes, M. F., Karayannis, T., Yusuf, N., Liu, X., Jaglin, X., Graef, I., Alvarez-Buylla, A., & Fishell, G. (2018). Activity Regulates Cell Death within Cortical Interneurons through a Calcineurin-Dependent Mechanism. *Cell Reports*, *22*(7), 1695–1709. https://doi.org/10.1016/J.CELREP.2018.01.007

Prönneke, A., Scheuer, B., Wagener, R. J., Möck, M., Witte, M., & Staiger, J. F. (2015). Characterizing VIP Neurons in the Barrel Cortex of VIPcre/tdTomato Mice Reveals Layer-Specific Differences. *Cerebral Cortex*, *25*(12), 4854–4868. https://doi.org/10.1093/CERCOR/BHV202

Puls, B., Ding, Y., Zhang, F., Pan, M., Lei, Z., Pei, Z., Jiang, M., Bai, Y., Forsyth, C., Metzger, M., Rana, T., Zhang, L., Ding, X., Keefe, M., Cai, A., Redilla, A., Lai, M., He, K., Li, H., & Chen, G. (2020). Regeneration of Functional Neurons After Spinal Cord Injury via in situ NeuroD1-Mediated Astrocyte-to-Neuron Conversion. *Frontiers in Cell and Developmental Biology*, *8*. https://doi.org/10.3389/FCELL.2020.591883

Qian, H., Kang, X., Hu, J., Zhang, D., Liang, Z., Meng, F., Zhang, X., Xue, Y., Maimon, R., Dowdy, S. F., Devaraj, N. K., Zhou, Z., Mobley, W. C., Cleveland, D. W., & Fu, X. D. (2020). Reversing a model of Parkinson's disease with in situ converted nigral neurons. *Nature*, *582*(7813). https://doi.org/10.1038/s41586-020-2388-4

Quan, X. J., Yuan, L., Tiberi, L., Claeys, A., De Geest, N., Yan, J., Van Der Kant, R., Xie, W. R., Klisch, T. J., Shymkowitz, J., Rousseau, F., Bollen, M., Beullens, M.,

Zoghbi, H. Y., Vanderhaeghen, P., & Hassan, B. A. (2016). Post-translational Control of the Temporal Dynamics of Transcription Factor Activity Regulates Neurogenesis. *Cell*, *164*(3), 460–475. https://doi.org/10.1016/J.CELL.2015.12.048

Rakic, P. (1974). Neurons in rhesus monkey visual cortex: systematic relation between time of origin and eventual disposition. *Science (New York, N.Y.)*, *183*(4123), 425–427. https://doi.org/10.1126/SCIENCE.183.4123.425

Ransdell, J. L., Faust, T. B., & Schulz, D. J. (2010). Correlated Levels of mRNA and Soma Size in Single Identified Neurons: Evidence for Compartment-specific Regulation of Gene Expression. *Frontiers in Molecular Neuroscience*, *3*(NOV). https://doi.org/10.3389/FNMOL.2010.00116

Rao, Y., Du, S., Yang, B., Wang, Y., Li, Y., Li, R., Zhou, T., Du, X., He, Y., Wang, Y., Zhou, X., Yuan, T. F., Mao, Y., & Peng, B. (2021). NeuroD1 induces microglial apoptosis and cannot induce microglia-to-neuron cross-lineage reprogramming. *Neuron*, *109*(24), 4094-4108.e5. https://doi.org/10.1016/j.neuron.2021.11.008

Raposo, A. A. S. F., Vasconcelos, F. F., Drechsel, D., Marie, C., Johnston, C., Dolle, D., Bithell, A., Gillotin, S., van den Berg, D. L. C., Ettwiller, L., Flicek, P., Crawford, G. E., Parras, C. M., Berninger, B., Buckley, N. J., Guillemot, F., & Castro, D. S. (2015). Ascl1 coordinately regulates gene expression and the chromatin landscape during neurogenesis. *Cell Reports*, *10*(9). https://doi.org/10.1016/j.celrep.2015.02.025

Reillo, I., De Juan Romero, C., García-Cabezas, M. Á., & Borrell, V. (2011). A role for intermediate radial glia in the tangential expansion of the mammalian cerebral cortex. *Cerebral Cortex (New York, N.Y. : 1991)*, *21*(7), 1674–1694. https://doi.org/10.1093/CERCOR/BHQ238

Reynolds, B. A., & Weiss, S. (1992). Generation of Neurons and Astrocytes from Isolated Cells of the Adult Mammalian Central Nervous System. *Science*, *255*(5052), 1707–1710. https://doi.org/10.1126/SCIENCE.1553558

Richards, L. J., Kilpatrick, T. J., & Bartlett, P. F. (1992). De novo generation of neuronal cells from the adult mouse brain. *Proceedings of the National Academy of Sciences of the United States of America*, *89*(18), 8591–8595. https://doi.org/10.1073/PNAS.89.18.8591

Ridder, K., Keller, S., Dams, M., Rupp, A. K., Schlaudraff, J., Del Turco, D., Starmann, J., Macas, J., Karpova, D., Devraj, K., Depboylu, C., Landfried, B., Arnold, B., Plate, K. H., Höglinger, G., Sültmann, H., Altevogt, P., & Momma, S. (2014). Extracellular Vesicle-Mediated Transfer of Genetic Information between the Hematopoietic System and the Brain in Response to Inflammation. *PLoS Biology*, *12*(6). https://doi.org/10.1371/journal.pbio.1001874

Rivetti Di Val Cervo, P., Romanov, R. A., Spigolon, G., Masini, D., Martín-Montañez, E., Toledo, E. M., La Manno, G., Feyder, M., Pifl, C., Ng, Y. H., Sánchez, S. P., Linnarsson, S., Wernig, M., Harkany, T., Fisone, G., & Arenas, E. (2017). Induction of functional dopamine neurons from human astrocytes in vitro and

mouse astrocytes in a Parkinson's disease model. *Nature Biotechnology*, *35*(5). https://doi.org/10.1038/nbt.3835

Robel, S., Berninger, B., & Götz, M. (2011). The stem cell potential of glia: lessons from reactive gliosis. *Nature Reviews Neuroscience 2011 12:2*, *12*(2), 88–104. https://doi.org/10.1038/nrn2978

Roe, T., Reynolds, T. C., Yu, G., & Brown, P. O. (1993). Integration of murine leukemia virus DNA depends on mitosis. *The EMBO Journal*, *12*(5). https://doi.org/10.1002/j.1460-2075.1993.tb05858.x

Roth, B. L. (2016). DREADDs for Neuroscientists. In *Neuron* (Vol. 89, Issue 4). https://doi.org/10.1016/j.neuron.2016.01.040

Rubin, A. N., Alfonsi, F., Humphreys, M. P., Choi, C. K. P., Rocha, S. F., & Kessaris, N. (2010). The germinal zones of the basal ganglia but not the septum generate GABAergic interneurons for the cortex. *Journal of Neuroscience*, *30*(36). https://doi.org/10.1523/JNEUROSCI.6178-09.2010

Rudy, B., & McBain, C. J. (2001). Kv3 channels: Voltage-gated K+ channels designed for high-frequency repetitive firing. In *Trends in Neurosciences* (Vol. 24, Issue 9). https://doi.org/10.1016/S0166-2236(00)01892-0

Russo, G. L. (2019). *Unraveling and overcoming hurdles in direct neuronal reprogramming*.

Rymar, V. V., & Sadikot, A. F. (2007). Laminar fate of cortical GABAergic interneurons is dependent on both birthdate and phenotype. *Journal of Comparative Neurology*, *501*(3), 369–380. https://doi.org/10.1002/CNE.21250

Sagar, S. M., Sharp, F. R., & Curran, T. (1988). Expression of c-fos Protein in Brain: Metabolic Mapping at the Cellular Level. *Science*, *240*(4857), 1328–1331. https://doi.org/10.1126/SCIENCE.3131879

Saino-Saito, S., Berlin, R., & Baker, H. (2003). Dlx-1 and Dlx-2 expression in the adult mouse brain: Relationship to dopaminergic phenotypic regulation. *Journal of Comparative Neurology*, *461*(1). https://doi.org/10.1002/cne.10611

Sánchez-Alcañiz, J. A., Haege, S., Mueller, W., Pla, R., Mackay, F., Schulz, S., López-Bendito, G., Stumm, R., & Marín, O. (2011). Cxcr7 Controls Neuronal Migration by Regulating Chemokine Responsiveness. *Neuron*, *69*(1). https://doi.org/10.1016/j.neuron.2010.12.006

Schafer, D. P., Lehrman, E. K., Kautzman, A. G., Koyama, R., Mardinly, A. R., Yamasaki, R., Ransohoff, R. M., Greenberg, M. E., Barres, B. A., & Stevens, B. (2012). Microglia sculpt postnatal neural circuits in an activity and complement-dependent manner. *Neuron*, *74*(4), 691–705. https://doi.org/10.1016/J.NEURON.2012.03.026

Schuman, B., Machold, R. P., Hashikawa, Y., Fuzik, J., Fishell, G. J., & Rudy, B. (2019). Four unique interneuron populations reside in neocortical layer 1. *Journal of Neuroscience*, *39*(1). https://doi.org/10.1523/JNEUROSCI.1613-18.2018

Schuurmans, C., & Guillemot, F. (2002). Molecular mechanisms underlying cell fate specification in the developing telencephalon. *Current Opinion in Neurobiology*, *12*(1), 26–34. https://doi.org/10.1016/S0959-4388(02)00286-6

Selby, L., Zhang, C., & Sun, Q. Q. (2007). Major defects in neocortical GABAergic inhibitory circuits in mice lacking the fragile X mental retardation protein. *Neuroscience Letters*, *412*(3), 227–232. https://doi.org/10.1016/J.NEULET.2006.11.062

Shakiba, N., Fahmy, A., Jayakumaran, G., McGibbon, S., David, L., Trcka, D., Elbaz, J., Puri, M. C., Nagy, A., van der Kooy, D., Goyal, S., Wrana, J. L., & Zandstra, P. W. (2019). Cell competition during reprogramming gives rise to dominant clones. *Science*, *364*(6438). https://doi.org/10.1126/science.aan0925

Simon, C., Götz, M., & Dimou, L. (2011). Progenitors in the adult cerebral cortex: cell cycle properties and regulation by physiological stimuli and injury. *Glia*, *59*(6), 869–881. https://doi.org/10.1002/GLIA.21156

Singh, P. B., & Zhakupova, A. (2022). Age reprogramming: cell rejuvenation by partial reprogramming. *Development (Cambridge)*, *149*(22). https://doi.org/10.1242/DEV.200755/281768

Sohal, V. S., Zhang, F., Yizhar, O., & Deisseroth, K. (2009). Parvalbumin neurons and gamma rhythms enhance cortical circuit performance. *Nature 2009 459:7247*, *459*(7247), 698–702. https://doi.org/10.1038/nature07991

Sommeijer, J. P., & Levelt, C. N. (2012). Synaptotagmin-2 is a reliable marker for parvalbumin positive inhibitory boutons in the mouse visual cortex. *PLoS ONE*, *7*(4). https://doi.org/10.1371/journal.pone.0035323

Somogyi, P. (1977). A specific “axo-axonal” interneuron in the visual cortex of the rat. *Brain Research*, *136*(2), 345–350. https://doi.org/10.1016/0006-8993(77)90808-3

Somogyi, P., Freund, T. F., & Cowey, A. (1982). The axo-axonic interneuron in the cerebral cortex of the rat, cat and monkey. *Neuroscience*, *7*(11), 2577–2607. https://doi.org/10.1016/0306-4522(82)90086-0

Sorrells, S. F., Paredes, M. F., Cebrian-Silla, A., Sandoval, K., Qi, D., Kelley, K. W., James, D., Mayer, S., Chang, J., Auguste, K. I., Chang, E. F., Gutierrez, A. J., Kriegstein, A. R., Mathern, G. W., Oldham, M. C., Huang, E. J., Garcia-Verdugo, J. M., Yang, Z., & Alvarez-Buylla, A. (2018). Human hippocampal neurogenesis drops sharply in children to undetectable levels in adults. *Nature 2018 555:7696*, *555*(7696), 377–381. https://doi.org/10.1038/nature25975

Sousa, V. H., Miyoshi, G., Hjerling-Leffler, J., Karayannis, T., & Fishell, G. (2009). Characterization of Nkx6-2-derived neocortical interneuron lineages. *Cerebral Cortex*, *19*(SUPPL. 1). https://doi.org/10.1093/cercor/bhp038

Southwell, D. G., Paredes, M. F., Galvao, R. P., Jones, D. L., Froemke, R. C., Sebe, J. Y., Alfaro-Cervello, C., Tang, Y., Garcia-Verdugo, J. M., Rubenstein, J. L., Baraban, S. C., & Alvarez-Buylla, A. (2012). Intrinsically determined cell death of

developing cortical interneurons. *Nature 2012 491:7422*, *491*(7422), 109–113. https://doi.org/10.1038/nature11523

Spassky, N., Goujet-Zalc, C., Parmantier, E., Olivier, C., Martinez, S., Ivanova, A., Ikenaka, K., Macklin, W., Cerruti, I., Zalc, B., & Thomas, J. L. (1998). Multiple restricted origin of oligodendrocytes. *The Journal of Neuroscience : The Official Journal of the Society for Neuroscience*, *18*(20), 8331–8343. https://doi.org/10.1523/JNEUROSCI.18-20-08331.1998

Spencer, D. D., Robbins, R. J., Naftolin, F., Marek, K. L., Vollmer, T., Leranth, C., Roth, R. H., Price, L. H., Gjedde, A., Bunney, B. S., Sass, K. J., Elsworth, J. D., Kier, E. L., Makuch, R., Hoffer, P. B., & Redmond, D. E. (1992). Unilateral transplantation of human fetal mesencephalic tissue into the caudate nucleus of patients with Parkinson's disease. *The New England Journal of Medicine*, *327*(22), 1541–1548. https://doi.org/10.1056/NEJM199211263272201

Spiegel, I., Mardinly, A. R., Gabel, H. W., Bazinet, J. E., Couch, C. H., Tzeng, C. P., Harmin, D. A., & Greenberg, M. E. (2014). Npas4 regulates excitatory-inhibitory balance within neural circuits through cell-type-specific gene programs. *Cell*, *157*(5), 1216–1229. https://doi.org/10.1016/J.CELL.2014.03.058

Srinivasan, R., Lu, T. Y., Chai, H., Xu, J., Huang, B. S., Golshani, P., Coppola, G., & Khakh, B. S. (2016). New Transgenic Mouse Lines for Selectively Targeting Astrocytes and Studying Calcium Signals in Astrocyte Processes In Situ and In Vivo. *Neuron*, *92*(6), 1181–1195. https://doi.org/10.1016/j.neuron.2016.11.030

Stevens, B., Allen, N. J., Vazquez, L. E., Howell, G. R., Christopherson, K. S., Nouri, N., Micheva, K. D., Mehalow, A. K., Huberman, A. D., Stafford, B., Sher, A., Litke, A. M. M., Lambris, J. D., Smith, S. J., John, S. W. M., & Barres, B. A. (2007). The classical complement cascade mediates CNS synapse elimination. *Cell*, *131*(6), 1164–1178. https://doi.org/10.1016/J.CELL.2007.10.036

Stolt, C. C., Lommes, P., Sock, E., Chaboissier, M. C., Schedl, A., & Wegner, M. (2003). The Sox9 transcription factor determines glial fate choice in the developing spinal cord. *Genes and Development*, *17*(13). https://doi.org/10.1101/gad.259003

Stumm, R. K., Zhou, C., Ara, T., Lazarini, F., Dubois-Dalcq, M., Nagasawa, T., Höllt, V., & Schulz, S. (2003). CXCR4 regulates interneuron migration in the developing neocortex. *Journal of Neuroscience*, *23*(12). https://doi.org/10.1523/jneurosci.23-12-05123.2003

Su, M., Hu, H., Lee, Y., D'Azzo, A., Messing, A., & Brenner, M. (2004). Expression specificity of GFAP transgenes. *Neurochemical Research*, *29*(11 SPEC. ISS.). https://doi.org/10.1007/s11064-004-6881-1

Sugiyama, S., di Nardo, A. A., Aizawa, S., Matsuo, I., Volovitch, M., Prochiantz, A., & Hensch, T. K. (2008). Experience-Dependent Transfer of Otx2 Homeoprotein into the Visual Cortex Activates Postnatal Plasticity. *Cell*, *134*(3). https://doi.org/10.1016/j.cell.2008.05.054

Sun, T., Pringle, N. P., Hardy, A. P., Richardson, W. D., & Smith, H. K. (1998). Pax6 influences the time and site of origin of glial precursors in the ventral neural tube. *Molecular and Cellular Neurosciences*, *12*(4–5), 228–239. https://doi.org/10.1006/MCNE.1998.0711

Sussel, L., Marin, O., Kimura, S., & Rubenstein, J. L. R. (1999). Loss of Nkx2.1 homeobox gene function results in a ventral to dorsal molecular respecification within the basal telencephalon: evidence for a transformation of the pallidum into the striatum. *Development*, *126*(15), 3359–3370. https://doi.org/10.1242/DEV.126.15.3359

Swinnen, N., Smolders, S., Avila, A., Notelaers, K., Paesen, R., Ameloot, M., Brône, B., Legendre, P., & Rigo, J. M. (2013). Complex invasion pattern of the cerebral cortex bymicroglial cells during development of the mouse embryo. *Glia*, *61*(2), 150–163. https://doi.org/10.1002/GLIA.22421

Szymczak, A. L., & Vignali, D. A. A. (2005). Development of 2A peptide-based strategies in the design of multicistronic vectors. *Expert Opinion on Biological Therapy*, *5*(5), 627–638. https://doi.org/10.1517/14712598.5.5.627

Takahashi, K., & Yamanaka, S. (2006). Induction of Pluripotent Stem Cells from Mouse Embryonic and Adult Fibroblast Cultures by Defined Factors. *Cell*, *126*(4). https://doi.org/10.1016/j.cell.2006.07.024

Tang, Y., Wu, Q., Gao, M., Ryu, E., Pei, Z., Kissinger, S. T., Chen, Y., Rao, A. K., Xiang, Z., Wang, T., Li, W., Chen, G., & Chubykin, A. A. (2021). Restoration of Visual Function and Cortical Connectivity After Ischemic Injury Through NeuroD1-Mediated Gene Therapy. *Frontiers in Cell and Developmental Biology*, *9*. https://doi.org/10.3389/FCELL.2021.720078

Taniguchi, H., Lu, J., & Huang, Z. J. (2013). The spatial and temporal origin of chandelier cells in mouse neocortex. *Science*, *339*(6115), 70–74. https://doi.org/10.1126/SCIENCE.1227622/SUPPL_FILE/TANIGUCHI.SM.PDF

Tapscott, S. J., Davis, R. L., Thayer, M. J., Cheng, P. F., Weintraub, H., & Lassar, A. B. (1988). MyoD1: A nuclear phosphoprotein requiring a Myc homology region to convert fibroblasts to myoblasts. *Science*, *242*(4877). https://doi.org/10.1126/science.3175662

Tasic, B., Menon, V., Nguyen, T. N., Kim, T. K., Jarsky, T., Yao, Z., Levi, B., Gray, L. T., Sorensen, S. A., Dolbeare, T., Bertagnolli, D., Goldy, J., Shapovalova, N., Parry, S., Lee, C., Smith, K., Bernard, A., Madisen, L., Sunkin, S. M., … Zeng, H. (2016). Adult mouse cortical cell taxonomy revealed by single cell transcriptomics. *Nature Neuroscience*, *19*(2). https://doi.org/10.1038/nn.4216

Tasic, B., Yao, Z., Graybuck, L. T., Smith, K. A., Nguyen, T. N., Bertagnolli, D., Goldy, J., Garren, E., Economo, M. N., Viswanathan, S., Penn, O., Bakken, T., Menon, V., Miller, J., Fong, O., Hirokawa, K. E., Lathia, K., Rimorin, C., Tieu, M., … Zeng, H. (2018). Shared and distinct transcriptomic cell types across neocortical areas. *Nature*, *563*(7729), 72. https://doi.org/10.1038/S41586-018-0654-5

Tekki-Kessaris, N., Woodruff, R., Hall, A. C., Gaffield, W., Kimura, S., Stiles, C. D., Rowitch, D. H., & Richardson, W. D. (2001). Hedgehog-dependent oligodendrocyte lineage specification in the telencephalon. *Development (Cambridge, England)*, *128*(13), 2545–2554. https://doi.org/10.1242/DEV.128.13.2545

Tiveron, M. C., Rossel, M., Moepps, B., Yong, L. Z., Seidenfaden, R., Favor, J., König, N., & Cremer, H. (2006). Molecular interaction between projection neuron precursors and invading interneurons via stromal-derived factor 1 (CXCL12)/CXCR4 signaling in the cortical subventricular zone/intermediate zone. *Journal of Neuroscience*, *26*(51). https://doi.org/10.1523/JNEUROSCI.4162-06.2006

Torper, O., Ottosson, D. R., Pereira, M., Lau, S., Cardoso, T., Grealish, S., & Parmar, M. (2015). InVivo Reprogramming of Striatal NG2 Glia into Functional Neurons that Integrate into Local Host Circuitry. *Cell Reports*, *12*(3). https://doi.org/10.1016/j.celrep.2015.06.040

Torper, O., Pfisterer, U., Wolf, D. A., Pereira, M., Lau, S., Jakobsson, J., Björklund, A., Grealish, S., & Parmar, M. (2013). Generation of induced neurons via direct conversion in vivo. *Proceedings of the National Academy of Sciences of the United States of America*, *110*(17). https://doi.org/10.1073/pnas.1303829110

Tosches, M. A., Yamawaki, T. M., Naumann, R. K., Jacobi, A. A., Tushev, G., & Laurent, G. (2018). Evolution of pallium, hippocampus, and cortical cell types revealed by single-cell transcriptomics in reptiles. *Science*, *360*(6391), 881–888. https://doi.org/10.1126/SCIENCE.AAR4237/SUPPL_FILE/AAR4237_TOSCHES_SM.PDF

Tremblay, R., Lee, S., & Rudy, B. (2016). GABAergic Interneurons in the Neocortex: From Cellular Properties to Circuits. In *Neuron* (Vol. 91, Issue 2). https://doi.org/10.1016/j.neuron.2016.06.033

Tsai, H. H., Niu, J., Munji, R., Davalos, D., Chang, J., Zhang, H., Tien, A. C., Kuo, C. J., Chan, J. R., Daneman, R., & Fancy, S. P. J. (2016). Oligodendrocyte precursors migrate along vasculature in the developing nervous system. *Science*, *351*(6271), 379–384. https://doi.org/10.1126/SCIENCE.AAD3839/SUPPL_FILE/TSAI.SM.PDF

Urbán, N., Van Den Berg, D. L. C., Forget, A., Andersen, J., Demmers, J. A. A., Hunt, C., Ayrault, O., & Guillemot, F. (2016). Return to Quiescence of mouse neural stem cells by degradation of a proactivation protein. *Science*, *353*(6296), 292–295. https://doi.org/10.1126/SCIENCE.AAF4802/SUPPL_FILE/URBAN-SM.PDF

Vanlandewijck, M., He, L., Mäe, M. A., Andrae, J., Ando, K., Del Gaudio, F., Nahar, K., Lebouvier, T., Laviña, B., Gouveia, L., Sun, Y., Raschperger, E., Räsänen, M., Zarb, Y., Mochizuki, N., Keller, A., Lendahl, U., & Betsholtz, C. (2018). A molecular atlas of cell types and zonation in the brain vasculature. *Nature*, *554*(7693), 475–480. https://doi.org/10.1038/NATURE25739

Velychko, S., Kang, K., Kim, S. M., Kwak, T. H., Kim, K. P., Park, C., Hong, K., Chung, C. H., Hyun, J. K., MacCarthy, C. M., Wu, G., Schöler, H. R., & Han, D. W. (2019).

Fusion of Reprogramming Factors Alters the Trajectory of Somatic Lineage Conversion. *Cell Reports*, *27*(1). https://doi.org/10.1016/j.celrep.2019.03.023

Verney, C., Monier, A., Fallet-Bianco, C., & Gressens, P. (2010). Early microglial colonization of the human forebrain and possible involvement in periventricular white-matter injury of preterm infants. *Journal of Anatomy*, *217*(4), 436–448. https://doi.org/10.1111/J.1469-7580.2010.01245.X

Vignoles, R., Lentini, C., d'Orange, M., & Heinrich, C. (2019). Direct Lineage Reprogramming for Brain Repair: Breakthroughs and Challenges. In *Trends in Molecular Medicine* (Vol. 25, Issue 10). https://doi.org/10.1016/j.molmed.2019.06.006

Vogt, D., Hunt, R. F., Mandal, S., Sandberg, M., Silberberg, S. N., Nagasawa, T., Yang, Z., Baraban, S. C., & Rubenstein, J. L. R. (2014). Lhx6 directly regulates Arx and CXCR7 to determine cortical interneuron fate and laminar position. *Neuron*, *82*(2), 350–364. https://doi.org/10.1016/J.NEURON.2014.02.030

Vong, L., Ye, C., Yang, Z., Choi, B., Chua, S., & Lowell, B. B. (2011). Leptin action on GABAergic neurons prevents obesity and reduces inhibitory tone to POMC neurons. *Neuron*, *71*(1), 142–154. https://doi.org/10.1016/J.NEURON.2011.05.028

Waddington, C. H. (1957). The Strategy of genes. *The Strategy of Genes*.

Walker, F., Möck, M., Feyerabend, M., Guy, J., Wagener, R. J., Schubert, D., Staiger, J. F., & Witte, M. (2016). Parvalbumin- and vasoactive intestinal polypeptide-expressing neocortical interneurons impose differential inhibition on Martinotti cells. *Nature Communications 2016 7:1*, *7*(1), 1–8. https://doi.org/10.1038/ncomms13664

Wamsley, B., & Fishell, G. (2017). Genetic and activity-dependent mechanisms underlying interneuron diversity. *Nature Reviews Neuroscience 2017 18:5*, *18*(5), 299–309. https://doi.org/10.1038/nrn.2017.30

Wang, J., Song, H. R., Guo, M. N., Ma, S. F., Yun, Q., Liu, W. J., Hu, Y. M., & Zhu, Y. Q. (2020). PGC-1α regulate critical period plasticity via gene × environment interaction in the developmental trajectory to schizophrenia. *Biochemical and Biophysical Research Communications*, *525*(4), 989–996. https://doi.org/10.1016/J.BBRC.2020.03.030

Wang, L. L., Serrano, C., Zhong, X., Ma, S., Zou, Y., & Zhang, C. L. (2021a). Revisiting astrocyte to neuron conversion with lineage tracing in vivo. *Cell*, *184*(21), 5465-5481.e16. https://doi.org/10.1016/j.cell.2021.09.005

Wang, L. L., Serrano, C., Zhong, X., Ma, S., Zou, Y., & Zhang, C. L. (2021b). Revisiting astrocyte to neuron conversion with lineage tracing in vivo. *Cell*, *184*(21). https://doi.org/10.1016/j.cell.2021.09.005

Wang, T., Liao, J. C., Wang, X., Wang, Q. S., Wan, K. Y., Yang, Y. Y., He, Q., Zhang, J. X., Chen, G., & Li, W. (2022). Unexpected BrdU inhibition on astrocyte-to-

neuron conversion. *Neural Regeneration Research*, *17*(7), 1526–1534. https://doi.org/10.4103/1673-5374.325747

Wang, Y., Li, G., Stanco, A., Long, J. E., Crawford, D., Potter, G. B., Pleasure, S. J., Behrens, T., & Rubenstein, J. L. R. (2011). CXCR4 and CXCR7 Have Distinct Functions in Regulating Interneuron Migration. *Neuron*, *69*(1). https://doi.org/10.1016/j.neuron.2010.12.005

Wang, Y., Su, H. H., Yang, Y., Hu, Y., Zhang, L., Blancafort, P., & Huang, L. (2013). Systemic delivery of modified mRNA encoding herpes simplex virus 1 thymidine kinase for targeted cancer gene therapy. *Molecular Therapy*, *21*(2). https://doi.org/10.1038/mt.2012.250

Wichterle, H., Garcia-Verdugo, J. M., Herrera, D. G., & Alvarez-Buylla, A. (1999). Young neurons from medial ganglionic eminence disperse in adult and embryonic brain. *Nature Neuroscience*, *2*(5). https://doi.org/10.1038/8131

Wichterle, H., Turnbull, D. H., Nery, S., Fishell, G., & Alvarez-Buylla, A. (2001). In utero fate mapping reveals distinct migratory pathways and fates of neurons born in the mammalian basal forebrain. *Development*, *128*(19). https://doi.org/10.1242/dev.128.19.3759

Wong, F. K., Bercsenyi, K., Sreenivasan, V., Portalés, A., Fernández-Otero, M., & Marín, O. (2018). Pyramidal cell regulation of interneuron survival sculpts cortical networks. *Nature*, *557*(7707), 668–673. https://doi.org/10.1038/S41586-018-0139-6

Wood, K. C., Blackwell, J. M., & Geffen, M. N. (2017). Cortical inhibitory interneurons control sensory processing. In *Current Opinion in Neurobiology* (Vol. 46). https://doi.org/10.1016/j.conb.2017.08.018

Wu, Z., Parry, M., Hou, X. Y., Liu, M. H., Wang, H., Cain, R., Pei, Z. F., Chen, Y. C., Guo, Z. Y., Abhijeet, S., & Chen, G. (2020). Gene therapy conversion of striatal astrocytes into GABAergic neurons in mouse models of Huntington's disease. *Nature Communications*, *11*(1). https://doi.org/10.1038/S41467-020-14855-3

Wylie, L. A., Hardwick, L. J. A., Papkovskaia, T. D., Thiele, C. J., & Philpott, A. (2015). Ascl1 phospho-status regulates neuronal differentiation in a Xenopus developmental model of neuroblastoma. *DMM Disease Models and Mechanisms*, *8*(5), 429–441. https://doi.org/10.1242/DMM.018630/257056/AM/ASCL1-PHOSPHO-STATUS-REGULATES-NEURONAL

Xie, Y., Hou, W., Song, X., Yu, Y., Huang, J., Sun, X., Kang, R., & Tang, D. (2016). Ferroptosis: process and function. *Cell Death & Differentiation 2016 23:3*, *23*(3), 369–379. https://doi.org/10.1038/cdd.2015.158

Xing, Y. L., Poh, J., Chuang, B. H. A., Kilpatrick, T. J., Osanai, Y., & Merson, T. D. (2023). *High-efficiency pharmacogenetic ablation of oligodendrocyte progenitor cells in the adult mouse CNS*. https://doi.org/10.1016/j.crmeth.2023.100414

Xu, H., Jeong, H. Y., Tremblay, R., & Rudy, B. (2013). Neocortical Somatostatin-expressing GABAergic Interneurons Disinhibit the Thalamorecipient Layer 4. *Neuron*, *77*(1), 155. https://doi.org/10.1016/J.NEURON.2012.11.004

Yamashita, T., Ninomiya, M., Acosta, P. H., García-Verdugo, J. M., Sunabori, T., Sakaguchi, M., Adachi, K., Kojima, T., Hirota, Y., Kawase, T., Araki, N., Abe, K., Okano, H., & Sawamoto, K. (2006). Subventricular zone-derived neuroblasts migrate and differentiate into mature neurons in the post-stroke adult striatum. *The Journal of Neuroscience : The Official Journal of the Society for Neuroscience*, *26*(24), 6627–6636. https://doi.org/10.1523/JNEUROSCI.0149-06.2006

Yang, J.-L., Fan, H., Fu, F.-F., Guo, B.-L., Huang, Y., Sun, L., Wang, W.-T., Xing, J.-L., Hu, X.-T., Ding, Y.-Q., Zhang, K., Hu, Y.-Z., & Wang, Y.-Z. (2023). Transient neurogenesis in ischemic cortex from Sox2 $^{+}$ astrocytes. *Neural Regeneration Research*, *18*(7), 1521. https://doi.org/10.4103/1673-5374.357910

Ye, Z., Mostajo-Radji, M. A., Brown, J. R., Rouaux, C., Tomassy, G. S., Hensch, T. K., & Arlotta, P. (2015). Instructing Perisomatic Inhibition by Direct Lineage Reprogramming of Neocortical Projection Neurons. *Neuron*, *88*(3). https://doi.org/10.1016/j.neuron.2015.10.006

Yin, J. C., Zhang, L., Ma, N. X., Wang, Y., Lee, G., Hou, X. Y., Lei, Z. F., Zhang, F. Y., Dong, F. P., Wu, G. Y., & Chen, G. (2019). Chemical Conversion of Human Fetal Astrocytes into Neurons through Modulation of Multiple Signaling Pathways. *Stem Cell Reports*, *12*(3), 488–501. https://doi.org/10.1016/J.STEMCR.2019.01.003

Yoon, Y., Kim, H. S., Hong, C. P., Li, E., Jeon, I., Park, H. J., Lee, N., Pei, Z., & Song, J. (2020). Neural Transplants From Human Induced Pluripotent Stem Cells Rescue the Pathology and Behavioral Defects in a Rodent Model of Huntington's Disease. *Frontiers in Neuroscience*, *14*. https://doi.org/10.3389/fnins.2020.558204

Zehnder, T., Petrelli, F., Romanos, J., de Oliveira Figueiredo, E. C., Lewis, T. L., Déglon, N., Polleux, F., Santello, M., & Bezzi, P. (2021). Mitochondrial biogenesis in developing astrocytes regulates astrocyte maturation and synapse formation. *Cell Reports*, *35*(2). https://doi.org/10.1016/j.celrep.2021.108952

Zeisel, A., M̂oz-Manchado, A. B., Codeluppi, S., Lönnerberg, P., Manno, G. La, Juréus, A., Marques, S., Munguba, H., He, L., Betsholtz, C., Rolny, C., Castelo-Branco, G., Hjerling-Leffler, J., & Linnarsson, S. (2015). Cell types in the mouse cortex and hippocampus revealed by single-cell RNA-seq. *Science*, *347*(6226). https://doi.org/10.1126/science.aaa1934

Zhang, L., Lei, Z., Guo, Z., Pei, Z., Chen, Y., Zhang, F., Cai, A., Mok, G., Lee, G., Swaminathan, V., Wang, F., Bai, Y., & Chen, G. (2020). Development of Neuroregenerative Gene Therapy to Reverse Glial Scar Tissue Back to Neuron-Enriched Tissue. *Frontiers in Cellular Neuroscience*, *14*. https://doi.org/10.3389/FNCEL.2020.594170

Zhang, L., Yin, J.-C., Yeh, H., Jin, P., Wu, G.-Y., & Correspondence, C. (2015). Small Molecules Efficiently Reprogram Human Astroglial Cells into Functional Neurons

Human astrocyte-converted neurons can integrate into mouse brain in vivo In Brief. *Stem Cell*, *17*.

Zhang, M., Eichhorn, S. W., Zingg, B., Yao, Z., Cotter, K., Zeng, H., Dong, H., & Zhuang, X. (2021). Spatially resolved cell atlas of the mouse primary motor cortex by MERFISH. *Nature*, *598*(7879). https://doi.org/10.1038/s41586-021-03705-x

Zhang, Y., Li, B., Cananzi, S., Han, C., Wang, L. L., Zou, Y., Fu, Y. X., Hon, G. C., & Zhang, C. L. (2022). A single factor elicits multilineage reprogramming of astrocytes in the adult mouse striatum. *Proceedings of the National Academy of Sciences of the United States of America*, *119*(11), e2107339119. https://doi.org/10.1073/PNAS.2107339119/SUPPL_FILE/PNAS.2107339119.SD04.XLSX

Zhao, M., Momma, S., Delfani, K., Carlén, M., Cassidy, R. M., Johansson, C. B., Brismar, H., Shupliakov, O., Frisén, J., & Janson, A. M. (2003). Evidence for neurogenesis in the adult mammalian substantia nigra. *Proceedings of the National Academy of Sciences of the United States of America*, *100*(13), 7925–7930. https://doi.org/10.1073/PNAS.1131955100

Zhu, X., Hill, R. A., Dietrich, D., Komitova, M., Suzuki, R., & Nishiyama, A. (2011). Age-dependent fate and lineage restriction of single NG2 cells. *Development*, *138*(4), 745–753. https://doi.org/10.1242/DEV.047951

Zywitza, V., Misios, A., Bunatyan, L., Willnow, T. E., & Rajewsky, N. (2018). Single-Cell Transcriptomics Characterizes Cell Types in the Subventricular Zone and Uncovers Molecular Defects Impairing Adult Neurogenesis. *Cell Reports*, *25*(9), 2457-2469.e8. https://doi.org/10.1016/J.CELREP.2018.11.003